SEDIMENTARY STRUCTURAL INDICATORS OF ARCTIC TERRESTRIAL AND AQUATIC PROCESSES

by

KRYSTOPHER JOHN CHUTKO

A thesis submitted to the Department of Geography

in conformity with the requirements for

the degree of Doctor of Philosophy

Queen's University

Kingston, Ontario, Canada

May 2008

ISBN: 978-0-494-38509-8

ABSTRACT

Annually and subannually laminated lacustrine sediments potentially contain a wide range of information that can be interpreted for paleoenvironmental reconstructions. These laminae are produced by the physical and biological processes that operate in the lake and in the surrounding terrestrial environment. However, identification of the influences that control laminae production may not be straightforward, and other processes may subtly influence the overall depositional sequence. This thesis examines two different depositional environments on Colin Archer Peninsula, Devon Island, Canada, with the objective of identifying the factors that influence subannual sediment deposition and how the resultant sedimentary structures can be used as indicators of paleoenvironmental conditions.

In proglacial Lake R, clastic sediment deposition is controlled primarily by subannual meteorological conditions. Periods of positive air temperature or large rainfall events produce discernable laminae that, when combined, form a varve sequence. However, overarching geomorphic controls influence the delivery of sediment to the lake and may reduce or enhance the hydrometeorological signal contained in the varves.

An additional influence for calibration of the varve record to meteorological observations is the role that melt season thermal inversions have on temperature extrapolation in the High Arctic. Meteorological stations at sea level may not be representative of the surrounding region, thereby reducing the accuracy of vertical temperature estimation. Investigation of the inversions in the central

Canadian High Arctic demonstrated that melt season inversions are common and increased inversion frequency may potentially have influenced enhanced glacial melt since the late 1980s, with implications for proglacial lake sediment transport and deposition.

In coastal Lake J, late Holocene sediments record a relatively unusual accumulation of microbially induced sedimentary structures (MISS). Such a record has not been previously described in the circum-Arctic, although they are known to exist elsewhere. These sediments are produced by the interaction between clastic sedimentation and cyanobacterial growth and production. Although chronological constraint could not be assigned with certainty to the record, statistical study of the laminated sequence suggested a dominant pattern that is plausibly annual. A heuristic model of annual sediment accumulation was developed in order to explore the potential for quasi-annual paleoenvironmental interpretations.

CO-AUTHORSHIP

This thesis conforms to the Manuscript Format as outlined by the School of Graduate Studies and Research. Each chapter has been written in the form of the publication in which it was submitted and contains its own literature cited. Scott Lamoureux, my thesis supervisor, is co-author on all chapters. All field and laboratory work was conducted by myself with the assistance of others noted in the acknowledgements section of each chapter. As all of the chapters in this thesis are referred to as “Chutko and Lamoureux, 2008” or “Chutko and Lamoureux, in preparation”, each “Chutko and Lamoureux” reference is followed by square brackets [ ] enclosing the chapter number.

Chapter 2 was co-authored by Scott Lamoureux. I conducted the field and laboratory work, the data analysis, drafted all the figures and tables, and was the primary author of the manuscript. This chapter has been published separately.

[2] Chutko, K.J. and S.F. Lamoureux. 2008. Identification of coherent links between interannual sedimentary structures and daily meteorological observations in Arctic proglacial lacustrine varves: potentials and limitations. *Canadian Journal of Earth Sciences*, **45**: 1-13.

Chapter 3 was co-authored by Scott Lamoureux. I performed the data analysis, drafted all the figures and tables, and was the primary author of the manuscript.

A version of this chapter has been accepted for publication and is currently in press.

[3] Chutko, K.J. and S.F. Lamoureux. In press. The influence of low-level thermal inversions on estimated melt season characteristics in the central Canadian Arctic. *International Journal of Climatology*.

Chapter 4 was co-authored by Scott Lamoureux. I conducted the field and laboratory work, the data analysis, drafted all the figures and tables, and was the primary author of the manuscript. This chapter is in preparation for publication.

[4] Chutko, K.J. and S.F. Lamoureux. Late Holocene biolaminated sedimentation in a coastal Arctic lake.

Chapter 5 was co-authored by Scott Lamoureux. I conducted the field and laboratory work, the data analysis, drafted all the figures and tables, and was the primary author of the manuscript. This chapter is in preparation for publication.

[5] Chutko, K.J. and S.F. Lamoureux. Lacustrine biolaminated sediments from a High Arctic freshwater lake.

ACKNOWLEDGEMENTS

Science is not carried out in a vacuum. From start to finish, I have received tremendous support and encouragement from many individuals. I have certainly forgotten some of the names I have encountered throughout this research, although I will try my best to summarize their involvement.

First and foremost, I would like to thank my supervisor Scott Lamoureux. His enthusiasm for the project kept it going forward when it was faced with numerous roadblocks. Armed with an incredible passion for research, Scott was able to convince me that making thin sections could be fun, or that it might be worthwhile to pick up a biology book or ten. He also stressed the importance of putting the work out in public, so that others who knew more than we did could give the project a nudge in the right direction.

Also, I would like to thank the committee members, whose comments and suggestions are greatly appreciated.

Throughout this research, I have worked with or been assisted by a number of people in several organizations and institutions. My fellow students in the Environmental Variability and Extremes Laboratory were a tremendous support in both the lab and the field. J. Cockburn and D. Fortin kept things moving in the Arctic despite the bears, cliffs and weather. My adventure in microbiology would not have been successful without the help of J. Tomkins.

I am indebted to the technicians and personnel who accommodated me and helped set up and run various analytical equipment, including F. Ginn, C. Grooms and L. Cameron (Dept. of Biology, Queen's University), M. Gorton and

G. Kretschmann (Dept. of Geology, University of Toronto), M. Bollen (Radiology Section, Kingston General Hospital), C. Cooney (Dept. of Mechanical and Materials Engineering, Queen's University), and K. Schultes (Dept. of Biology, McMaster University).

Of course, this work would not have been successful without the support of the Polar Continental Shelf Project and all of the staff in Resolute. Also, the Nunavut Research Institute and the community of Grise Fiord supported the work on Devon Island. The staff of the Department of Geography at Queen's provided superb support, technical and administrative, throughout this work.

Countless others offered suggestions or comments along the way. M. Sharp provided valuable insights on ice-temperature relationships. C. Omelon and R. Hunter were able to shed some light on preparing samples for electron microscopy. D. McDonald demonstrated the importance of properly prepared unit symbology.

Most importantly, I would like to thank my family, not only for their support in this endeavor but in all previous ones. I share my success with Amanda, who has supported me through everything.

STATEMENT OF ORIGINALITY

I hereby certify that all of the work described within this thesis is the original work of the author. Any published (or unpublished) ideas and/or techniques from the work of others are fully acknowledged in accordance with standard referencing practices.

Krystopher J. Chutko

May, 2008

TABLE OF CONTENTS

LIST OF TABLES

LIST OF FIGURES

Chapter 5.

GLOSSARY

Extracellular polymeric substances (EPS)

Compounds secreted by microorganisms, mostly composed of polysaccharides. EPS is an important component of microbial biofilms.

Melt event

A continuous period of positive air temperature, which can be defined with a duration (days) and intensity (°C). The term does not imply that snow and/or ice melt occurs during this period, or that snow and/or ice melt is restricted to this period.

Melt event duration

The length of time (days) that daily mean air temperature is continuously positive.

Melt event intensity

The mean air temperature (°C) of the melt event.

Melt event magnitude

The product of the melt event duration (days) and melt event intensity (°C). The magnitude is measured in melting degree-days (MDD).

Melt season

The period of time (days) between the first and last incidence of positive daily mean air temperature. The melt season may contain a single melt event, or it may be composed of several melt events separated by periods of below zero temperatures.

Microbially induced sedimentary structure (MISS)

A category of primary sedimentary structures that are produced by the syndepositional influence of cyanobacterial mats and biofilms on erosion, deposition and deformation of sediments.

Shallow lapse rate

Vertical lapse rates that are positive or relatively slightly negative. The term implies an increase in air temperature with altitude, or a decrease in air temperature with altitude that is less than a typically observed value.

Steep lapse rate

Vertical lapse rates that are strongly negative. The term implies a decrease in air temperature with altitude that is equal to or greater than a typically observed value.

Subannual sedimentary structure

Sedimentary laminae that are produced by physical, chemical or biological processes operating on short time scales (e.g., diurnal, event, seasonal). Sequences of subannual structures may form the larger varve.

Thermal inversion

An incidence of positive vertical lapse rate, where temperature increases with altitude.

Varve

A demonstrably annual sedimentary deposit, produced by seasonal fluctuations of physical, chemical, or biological processes. Varves are a valuable tool in paleoenvironmental reconstruction, as the implied

seasonal rhythmicity provides an annual, or subannual, temporal resolution.

CHAPTER 1

INTRODUCTION

Lacustrine sediments have long been used as a means of deducing past environmental changes, particularly those that occurred in the lake and the surrounding watershed (Gilbert, 2003a; Pienitz *et al*., 2004). The composition of the sediment is determined by physical, chemical, and biological process in the lake and basin, which in turn are controlled by complex interactions between climate, hydrology, biology, geomorphology, and geology (Gilbert, 2003a). Laminated sediments add another dimension to the potential information these lake records contain. Sedimentary laminae are produced by changes in the factors that control sedimentation, and in many cases reflect different forms of environmental perturbation (Sturm, 1979). In strongly seasonal environments, such as the High Arctic, laminated sediment structures derive in large part from the annual cycle of activation and cessation of the hydrologic system, which may impart an annual signature in the sediment (Gilbert, 2003b).

Where present, annually laminated lacustrine sediments (varves) can be used to develop high resolution paleoenvironmental reconstructions (e.g., Gilbert, 1975; Leonard, 1985; Desloges and Gilbert, 1994; Leemann and Niessen, 1994; Lamoureux and Bradley, 1996; Moore et al., 2001; Tomkins and Lamoureux, 2005). The temporal resolution of the sediment record may be refined further by the identification of subannual laminae. These laminae may record discrete environmental events, such as aeolian sedimentation (Lamoureux *et al*., 2002),

large rainfall events (Lamoureux, 2000), winter storms (Shaw *et al*., 1978) or summer melting degree-days (Hambley and Lamoureux, 2006).

However, the development of paleoenvironmental reconstructions from lacustrine sediments is complicated by the interactions between the physical, chemical and biological controls on lake sedimentation. Hodder *et al*. (2007) demonstrated that causal relationships, such as varve thickness relating to summer temperature, are not as straightforward as often assumed, and that an understanding of all the influences on sediment production, transport, and deposition are necessary. Unfortunately, such intensive, watershed-scale monitoring is rarely, if ever, performed (e.g., Braun *et al*., 2000; Cockburn and Lamoureux, in press), and the sediment record is necessarily interpreted as a generalization of the environmental controls.

This work investigates the nature of annually and subannually laminated sedimentary structures with a goal towards understanding the controls on the formation of these laminae. Two lakes on Colin Archer Peninsula (Fig. 1), one glacial and the other non-glacial, reveal substantially different sediment types and accumulation controls. In glacial Lake R, minerogenic sediment accumulation was derived from snow/ice melt and rainfall induced transport, while geomorphic influences controlled the rate of deposition on an annual basis. Conversely, non-glacial Lake J contained a record of Holocene post-glacial emergence, and the ~5000 year lacustrine component recorded an accumulation of microbially induced sedimentary structures. Despite the different accumulation of sediment in these two lakes, the laminated structures provided useful information for improved understanding of terrestrial and aquatic processes which influenced

sediment accumulation, and ultimately the development of more refined paleoenvironmental interpretations from such records.

Glacial lake sedimentation

Glacial lakes can receive significant amounts of meltwater and sediment (Lemmen *et al*., 1988). Due to the strongly seasonal nature of glacial environments, particularly those in the High Arctic, rhythmic deposits, including varves, are characteristic of glacial lake sediments (Smith and Ashley, 1985). Several processes, including underflows, slump-generated currents, and diurnal discharge fluctuations can lead to the formation of laminated sediments (Smith and Ashley, 1985). Østrem and Olsen (1987) showed that proglacial sediment deposition was positively related to water discharge. In arid environments, such as the High Arctic, the radiation budget is an important control on meltwater generation, and hence, meltwater discharge (Smith *et al*., 2004). Additionally, summer precipitation influences sediment deposition, although in a much more infrequent manner. However, rainfall must be of a significant magnitude in order to generate runoff and sediment transport, and ultimately deposition in the lake (Lamoureux, 2000). The contribution of these rainfall events to varve thickness may be significant (Østrem and Olsen, 1987; Lamoureux, 2000).

Chapter 2 identifies varved sediments from proglacial Lake R and uses the daily meteorological record from Resolute, Nunavut, adjusted for local elevation, to demonstrate that the subannual laminae were derived from sub-seasonal temperature fluctuations and large rainfall events. However, geomorphic factors

also influenced sediment deposition in the basin and acted to perturb the climate signal contained in the sediment record.

A further complication to the development of paleoenvironmental reconstructions in the High Arctic is the paucity of reliable, continuous weather monitoring stations on which the varve-meteorology relationship is built. Typically, High Arctic weather stations are located in communities near sea-level, which may not be regionally representative, particularly in the central and eastern Arctic which is dominated by plateau and alpine topography. Vertical temperature extrapolation is necessary in these environments and is often carried out in a simplified manner (e.g., Legates and Willmott, 1990; Glover, 1999; Braithwaite *et al*., 2006). However, vertical lapse rates are highly variable (Marshall *et al*., 2007) and summer thermal inversions can contribute significantly to positive temperatures at the elevation of low-level plateau ice caps. Chapter 3 examines the temporal trends of vertical lapse rates and suggests that inversions play a role in enhanced glacial melt observed in the High Arctic, which may also influence sediment delivery and deposition in proglacial lake basins.

Microbially induced sedimentary structures

Microbially induced sedimentary structures (MISS) are a classification of laminated sediments that are produced by the interaction between clastic sedimentation and microbial production (Noffke *et al*., 2001). Most notably, stromatolites are the lithified remains of MISS, and environments that contain microbial mat growth are considered to be modern or unlithified stromatolites (Parker *et al*., 1981; Reid *et al*., 2000). Stromatolites are the only biogenic

sedimentary structures that range in age from the early Archean to modern time, and therefore are critical geologic features in the investigation of early life on Earth (Pratt, 2003). Therefore, microbial mats may serve as contemporary analogs for stromatolites, and understanding the accumulation record of these modern environments has the potential to aid the investigation of ancient life.

MISS are produced primarily by photoautotropic prokaryotes, most notably cyanobacteria (Noffke *et al*., 2001). By the excretion of extracellular polymeric substances (EPS), cyanobacteria are able to move through sediment that accumulates to maintain an optimal position for the receipt of sunlight, their primary source of energy, and form extensive benthic mat and biofilm layers. By doing so, they leave discernable structures in the sediment, composed of cyanobacteria and biofilm residues (Noffke *et al*., 2001).

Many cyanobacteria exhibit high tolerances to a wide range of environmental factors, including temperature, light intensity, and nutrient supply (Vincent, 2000), and therefore are observed to occur in a wide range of environments, from tropical to polar sites (Pierson, 1992). In Antarctica, many of the Dry Valleys lakes support benthic microbial mat communities from which Holocene sedimentation history has been characterized, although the MISS have been treated in an indirect way (Wagner *et al*., 2006). However, in the High Arctic, microbial mat research has focused primarily on contemporary biogeochemical processes that operate at the mat-water interface (e.g., Vézina and Vincent, 1997), and no identification and documentation of long term microbial sedimentology exists. Despite the potential of MISS to contain records

of high resolution paleoenvironmental change, no research has been carried out to date.

The absence of paleoenvironmental interpretations from MISS records is potentially attributed to the complex microbial mat accumulation patterns, the lack of a thorough understanding of the controls on MISS formation and controlling factors, and an overall shortage of research that seeks to integrate contemporary sedimentology and microbiology. Chapters 4 and 5 examine a MISS record in a sedimentological and stratigraphic context, respectively, in an effort to assess the potential for developing paleoenvironmental interpretations from these complex records. A number of key issues encountered during this study (e.g., chronological, methodological) illustrate the overall challenges inherent in this subject of research. However, by application of statistical and time series analyses to the record, along with a physically plausible heuristic model to the sediment record, a chronological interpretation was developed and assessed, and potential controls over laminae formation were identified.

Thesis objectives

The primary objective of this research was to further knowledge of the formative controls on subannual sedimentary structures, both clastic and biogenic. By examining the compositional characteristics of the laminae, potential physical and/or biological controls can be attributed to each. This work also investigates the development of annually laminated (varved) sediments.

Two key questions addressed were:

1. *How does the combination of subannual processes contribute to overall varve formation?*
2. *Can a hypothesized complex annual accumulation model be used to develop a varve chronology?*

A variety of terrestrial and aquatic processes are reflected in the laminated sediments found on Colin Archer Peninsula, Devon Island. Therefore, they potentially contain paleoenvironmental information that can be used to reconstruct past local and regional environmental conditions. However, understanding the processes and how they interact and contribute to lamina and/or varve formation is critical to the development of those reconstructions.

References

Braithwaite, R.J., Raper, S.C.B. and K. Chutko. 2006. Accumulation at the equilibrium-line of glaciers inferred from a degree-day model and tested against field observations. *Annals of Glaciology*, **43**: 329-334.

Braun, C., Hardy, D.R., Bradley, R.B. and M.J. Retelle. 2000. Streamflow and suspended sediment transfer to Lake Sophia, Cornwallis Island, Nunavut, Canada. *Arctic, Antarctic, and Alpine Research*, **32**: 456-465.

Cockburn, J.M.H. and S.F. Lamoureux. In press. Hydroclimate controls over seasonal sediment yield in two adjacent High Arctic watersheds. *Hydrological Processes*,.

Desloges, J.R. and R. Gilbert. 1994. Sediment source and hydroclimatic inferences from glacial lake sediment: the postglacial sedimentary record of Lillooet Lake, British Columbia. *Journal of Hydrology*, **159**: 375-393.

Gilbert, R. 1975. Sedimentation in Lillooet Lake, British Columbia. *Canadian Journal of Earth Sciences*, **12**: 1697-1711.

Gilbert, R. 2003a. Lacustrine sedimentation. *In:* Middleton, G.V. (ed.). *Encyclopedia of Sedimentology and Sedimentary Rocks*. Kluwer AP, Dordrecht: 404-408.

Gilbert, R. 2003b. Varves. *In:* Middleton, G.V. (ed.). *Encyclopedia of Sedimentology and Sedimentary Rocks*. Kluwer AP, Dordrecht: 764-766.

Glover, R.W. 1999. Influence of spatial resolution and treatment of orography on GCM estimates of the surface mass balance of the Greenland Ice Sheet. *Journal of Climate*, **12**: 551-563.

Hambley, G.W. and S.F. Lamoureux. 2006. Recent summer climate recorded in complex varved sediments, Nicolay Lake, Cornwall Island, Nunavut, Canada. *Journal of Paleolimnology*, **35**: 629-640.

Hodder, K.R., Gilbert, R. and J.R. Desloges. 2007. Glaciolacustrine varved sediment as an alpine hydroclimatic proxy. *Journal of Paleolimnology*, **38**: 365-394.

Lamoureux, S.F. 2000. Five centuries of interannual sediment yield and rainfall-induced erosion in the Canadian High Arctic recorded in lacustrine varves. *Water Resources Research*, **36**: 309-318.

Lamoureux, S.F. and R.S. Bradley. 1996. A late Holocene varved sediment record of environmental change from northern Ellesmere Island, Canada. *Journal of Paleolimnology*, **16**: 239-255.

Lamoureux, S.F., Gilbert, R. and T. Lewis. 2002. Lacustrine sedimentary environments in High Arctic proglacial Bear Lake, Devon Island, Nunavut, Canada. *Arctic, Antarctic, and Alpine Research*, **34**: 130-141.

Leemann, A. and F. Niessen. 1994. Varve formation and the climatic record in an Alpine proglacial lake: calibrating annually-laminated sediments against hydrological and meteorological data. *The Holocene*, **4**: 1-8.

Legates, D.R. and C.J. Willmott. 1990. Mean seasonal and spatial variability in global surface air temperature. *Theoretical and Applied Climatology*, **41**: 11-21.

Lemmen, D.S., Gilbert, R. Smol, J.P. and R.I. Hall. 1988. Holocene sedimentation in glacial Lake Tasikutaaq, Baffin Island. *Canadian Journal of Earth Sciences*, **25**: 810-823.

Leonard, E.M. 1985. Glaciological and climatic controls on lake sedimentation, Canadian Rocky Mountains. *Zeitschrift für Gletscherkunde und Glazialgeologie*, **21**: 35-42.

Marshall S.J., Sharp M.J., Burgess D.O. and F.S. Anslow. 2007. Near-surface temperature lapse rates on the Prince of Wales Icefield, Ellesmere Island, Canada: implications for regional downscaling of temperature. *International Journal of Climatology*, **27**: 385-398.

Moore, J.J., Hughen, K.A., Miller, G.J. and J.T. Overpeck. 2001. Little Ice Age recorded in summer temperature reconstruction from varved sediments of Donard Lake, Baffin Island, Canada. *Journal of Paleolimnology*, **25**: 503-517.

Noffke, N., Gerdes, G., Klenke, T., Krumbein, W.E. 2001. Microbially induced sedimentary structures – a new category within the classification of primary sedimentary structures. *Journal of Sedimentary Research*, **71**: 649-656.

Østrem, G. and H.C. Olsen. 1987. Sedimentation in a glacier lake. *Geografiska Annaler*, **69A**: 123-138.

Parker, B.C., Simmons Jr., G.M., Love, F.G., Wharton, R.A. and K.G. Seaburg. 1981. Modern stromatolites in Antarctic Dry Valley lakes. *Bioscience*, **31**: 656-661.

Pienitz, R., Douglas, M.S.V. and J.P. Smol (eds.). 2004. *Long-term Environmental Change in Arctic and Antarctic Lakes*. Developments in Paleoenvironmental Research, Volume 8. Kluwer AP, Dordrecht.

Pierson, B.K. 1992. Modern mat-building microbial communities: A key to the interpretation of Proterozoic stromatolitic communities - Introduction. *In*: Schopf, J.W. and C. Klein (eds.). *The Paleozoic Biosphere: A Multidisciplinary Study*. Cambridge UP, Cambridge: 247-251.

Pratt, B.R. 2003. Stromatolites. *In*: Middleton, G.V. (ed.). *Encyclopedia of Sedimentology and Sedimentary Rocks*. Kluwer AP, Dordrecht: 688-690.

Reid, R.P., Visscher, P.T., Decho, A.W., Stolz, J.F., Bebout, B.M., Dupraz, C., Macintyre, I.G., Paerl, H.W., Pinckney, J.L., Prufert-Bebout, L., Steppe, T.F. and D.J. DesMarais. 2000. The role of microbes in accretion, lamination and early lithification of modern marine stromatolites. *Nature*, **406**: 989-992.

Shaw, J., Gilbert, R. and J.J.J. Archer. 1978. Proglacial lacustrine sedimentation during winter. *Arctic and Alpine Research*, **10**: 689-699.

Smith, N.D. and G.M. Ashley. 1985. Proglacial lacustrine environment. *In*: Ashley, G.M., Shaw, J. and N.D. Smith (eds.). *Glacial Sedimentary Environments*. SEPM Short Course No. 16: 135-215.

Smith Jr., S.V., Bradley, R.S. and M.B. Abbott. 2004. A 300 yr record of environmental change from Lake Tuborg, Ellesmere Island, Nunavut, Canada. *Journal of Paleolimnology*, **32**: 137-148.

Sturm, M. 1979. Origin and composition of clastic varves. *In*: Schlüchter, C. (ed.). *Moraines and Varves: Origin/Genesis/Classification*. A.A. Balkema, Rotterdam: 281-285.

Tomkins, J.D. and S.F. Lamoureux. 2005. Multiple hydroclimatic controls over recent sedimentation in proglacial Mirror Lake, southern Selwyn

Mountains, Northwest Territories. *Canadian Journal of Earth Sciences*, **42**: 1589-1599.

Vézina, S. and W.F. Vincent. 1997. Arctic cyanobacteria and limnological properties of their environment: Bylot Island, Northwest Territories, Canada (73°N, 80°W). *Polar Biology*, **17**: 523-534.

Vincent, W.F. 2000. Cyanobacterial dominance in the polar regions. *In*: Whitton, B.A. and M. Potts (eds.). *The ecology of cyanobacteria*. Kluwer AP, Dordrecht: 321-340.

Wagner, B., Melles, M., Doran, P.T., Kenig, F., Forman, S.L., Pierau, R. and P. Allen. 2006. Glacial and postglacial sedimentation in the Fryxell basin, Taylor Valley, southern Victoria Land, Antarctica. *Palaeogeography, Palaeoclimatology, Palaeoecology*, **241**: 320-337.

Figure Captions

Figure 1. A) Study site on Colin Archer Peninsula, Devon Island, Nunavut Canada, showing the location of the Hamlet of Resolute (R) and the Devon Ice Cap (DIC). B) Archer River valley, showing the location of the two study lakes, Lake R and Lake J.

Figure 1.

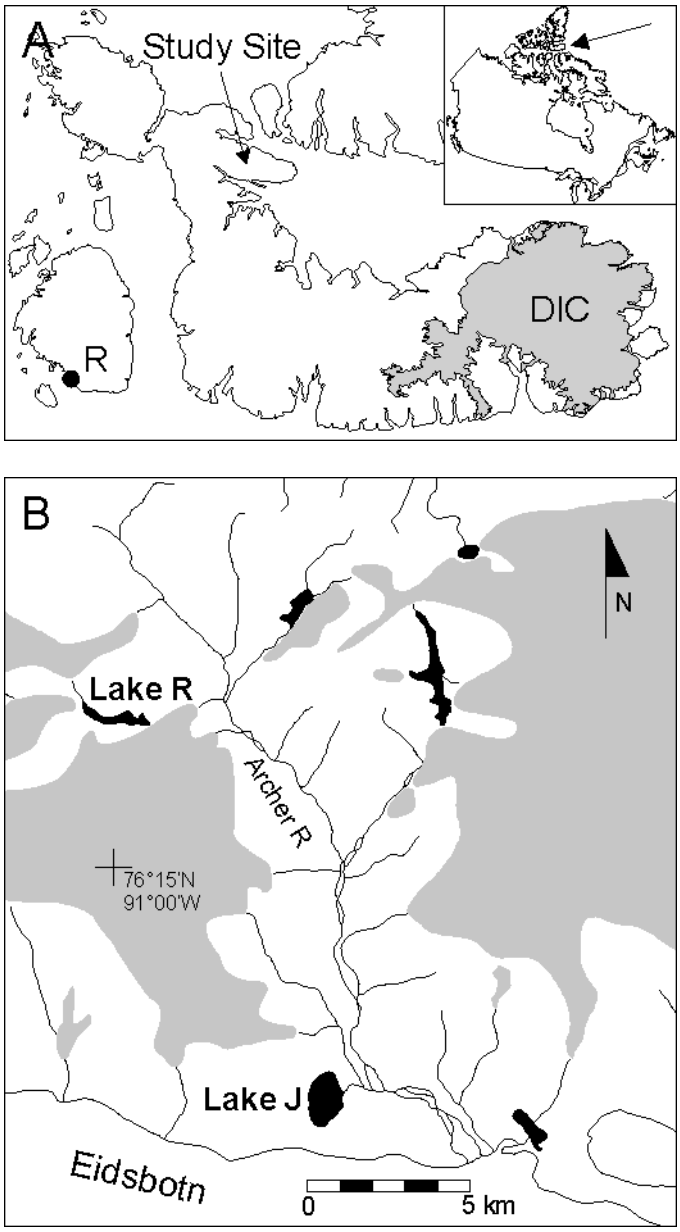
A
Study Site
DIC
R
B
N
Lake R
Archer R
76°15'N
91°00'W
Lake J
Eidsbotn
0
5 km

CHAPTER 2

IDENTIFICATION OF COHERENT LINKS BETWEEN INTERANNUAL SEDIMENTARY STRUCTURES AND DAILY METEOROLOGICAL OBSERVATIONS IN ARCTIC PROGLACIAL LACUSTRINE VARVES: POTENTIALS AND LIMITATIONS

KRYSTOPHER J. CHUTKO AND SCOTT F. LAMOUREUX

This chapter has been published separately:
Chutko, K.J. and S.F. Lamoureux. 2008. Identification of coherent links between interannual sedimentary structures and daily meteorological observations in Arctic proglacial lacustrine varves: potentials and limitations. *Canadian Journal of Earth Sciences*, **45**: 1-13.

Abstract

Proglacial lacustrine sediments from High Arctic Lake R (76°17.9' N 90°59.3' W, unofficial name) are shown to be annually laminated (varved) and contain a variety of subannual structures. The formation of the subannual structures (and overall varve) was controlled by a combination of meteorologic (temperature and rainfall) and geomorphic factors. Using a training set of the ten thickest varves in the 38-year sedimentary record, a heuristic model was developed to link subannual structures with regional meteorological conditions. Within the training set, significant correlations were shown between subannual structure thickness and the magnitude of the corresponding melt event, defined as a period of continuously positive temperature. However, these correlations deteriorated as the varves progressively thinned, and several varves exhibited no relationship between their subannual structures and respective meteorological conditions. Grain size analyses showed that the thin varves were significantly finer than the thick varves, and are inferred to reflect changed sediment inflow patterns that altered deposition and reduced the fidelity of the model. Despite these complexities, this study identified the potential to produce long term, subannual reconstructions of weather conditions. Model results revealed the limitations of simple varve-meteorology relationships, as well as identified necessary environmental and sampling conditions required to produce a more robust model for future applications.

Introduction

Early observations of annually laminated sediments (varves) were made in the late 19th and early 20th century by de Geer (1912). Identification of these sediments was originally restricted to glaciolacustrine environments, where strongly seasonal depositional patterns yielded a couplet of laminae within a given year (de Geer 1912). By the second half of the century, varved sediments were observed in a number of different lacustrine and marine settings (Sturm 1979; O'Sullivan 1983). Also, with more detailed sedimentological studies, an increased complexity of the sediments was observed (Petterson et al. 1993; Gilbert 2003a). Varved sediments are especially valuable in the development of paleoenvironmental reconstructions, largely due to their high temporal resolution and their close linkages with local climatic and hydrologic systems (e.g., Gilbert 1975; Leonard 1985; Desloges and Gilbert 1994; Leemann and Niessen 1994; Lamoureux and Bradley 1996; Moore et al. 2001; Tomkins and Lamoureux 2005).

Few studies have examined the potential information contained within the subannual record of varved sediments (e.g., Lamoureux 2000; Gilbert 2003b; Hambley and Lamoureux 2006). Similar to annual structures, subannual sedimentary units are produced by different environmental conditions that drive sediment delivery to the lake basin (Sturm 1979). In Arctic watersheds, the dominant source of hydrologic energy is snow ablation driven by melt energy derived from positive air temperatures (Hardy 1996), but this can be restricted by available snow water equivalence in the watershed (Forbes and Lamoureux 2005). However, in glacierized catchments, ice and permanent snow cover

provide an additional supply of meltwater (Marsh and Woo 1981). In this case, sediment transport is closely related to water discharge (Lawson 1993), and is therefore also to melt energy, though likely in a non-linear fashion (Hardy 1996).

Subannual laminae have been attributed to a variety of environmental factors. Lamoureux et al. (2002) described the discrete deposition of aeolian sediments emplaced on lake ice as a result of winter storminess and subsequently sedimented to the lake floor during the summer. Lamoureux (2000) identified subannual rhythmites as being formed by large rainfall events during periods of higher runoff ratios. Snowcover, evaporation, and storage in the active layer all act to reduce the total runoff from these events, though in favourable conditions runoff will be enhanced and sediment transport and deposition will occur. Hambley and Lamoureux (2006) showed that the basal rhythmite in each varve from non-glacierized Nicolay Lake (Cornwall Island, Nunavut) was significantly correlated to summer melting degree-days (MDD), and isolation of the rhythmites produced a significant correlation with regional climatic conditions.

The role of precipitation, particularly summer rainfall, is less clear. Leemann and Niessen (1994) identified the importance of 'primary' and 'secondary' controls on seasonal lake sedimentation in the Alps. In their study, the strong correlation between summer temperature and varve thickness was compromised by the incidence of summer precipitation, and the proportion of glacial cover in the basin acts to control the relative importance of summer temperature and precipitation, with a positive relationship between glacial coverage and the relative importance of the temperature control (Desloges and Gilbert 1994). In Arctic environments, where positive temperatures exist for only

a short period each year, and thick snow cover persists often into the mid-summer, summer rainfall must be of considerable magnitude before any significant transport of sediment can be observed in the sedimentary record (Hardy 1996; Lamoureux 2000).

The potential environmental proxy record(s) contained within a varve sequence vary from simple to complex in origin. Hodder et al. (2007) summarized a wide range of research that identified links between various sedimentary and climatic indices. In most cases, the sedimentary index used was overall varve thickness. However, the complex interactions between meteorology, hydrology, and geomorphology which produce subannual laminae suggest that an individual varve thickness need not reflect a single climatic variable, thus producing poor correlation coefficients in many studies.

This paper presents a systematic approach to investigate and correlate subannual sedimentary structures with a regional meteorological record for a High Arctic glacial watershed. The objectives of this work were to: a) identify and characterize subannual sedimentary structures as to their potential deposition mechanisms; b) produce a method by which individual varves could be systematically broken down into their sedimentary structural components; and c) establish links between the interannual sedimentary and meteorologic records.

Study site

The Archer River basin (~250 km^2) is located on the Colin Archer Peninsula, northwest Devon Island, Nunavut (Fig. 1A). The peninsula contains four separate ice fields, with their size and elevation increasing from west to east.

The headwaters of the Archer River are fed by three of the four icefields, and ice-dammed lakes can be found on both of the main river branches. An unnamed lake, located on the western side of the basin (76° 17.9' N 90° 59.3' W; 300 m asl), is the focus of this work and is henceforth given the unofficial name, Lake R. The site is approximately 200 km NNE and 225 km W of the communities of Resolute and Grise Fiord, Nunavut, respectively (Fig. 1). The bedrock geology of the site is mid-Devonian limestone of the Douro Formation, and is described more completely by Mayr et al. (1998). The entire region was glaciated during the Late Wisconsinan and ice retreat and exposure of the land began in the early Holocene (Dyke 1999). The marine limit at Colin Archer Peninsula is 120 m asl and dated at ca. 9.3-ka BP (Dyke 1998). Little is known about Holocene conditions in the region, but temperatures appear to have peaked in the early Holocene and cooled after ca. 4-ka BP (Bradley 1990; Koerner and Fisher 1990).

Lake R is 2.2 km long and has an area of 5.4 ha (Fig. 1C). Exposed raised lacustrine deltaic deposits occur along the northwestern edge of the lake, and likely are the result of partial drainage due to changed ice dam conditions. The lake drains through a gorge between a bedrock slope and the icecap for approximately 1.5 km before joining the western branch of the Archer River. The principal inflow to the lake is a small stream draining a snowfield in the northwestern part of the basin. However, in the eastern end, drainage from the icefield likely contributes the primary source of water and sediment to the lake. Air photographs from 1958 show the complete loss of lake ice in late summer.

Methodology

Field and laboratory work

Fieldwork was carried out primarily in late May 2005. Bathymetry and sediment cores were obtained through holes augered in the ice (thickness > 2 m). Depths were obtained with a Humminbird echo sounder (0.3 m accuracy) and located with a Garmin GPS receiver. Surface cores of the lake bottom sediments were obtained using an Aquatics Research Instruments gravity corer from depths of 18 to 31 m. This study is based on surface cores R1-05 and R2-05, which were recovered from the eastern end of the lake in 31 m of water and returned to the laboratory unfrozen. The cores were split length-wise, exposed faces cleaned and one half of each core was archived. Sediment slabs (7 x 2 x 0.5 cm) were extracted for thin section preparation. The slabs were dehydrated using repeated acetone exchanges and impregnated with a single application of Spurr's low viscosity epoxy resin under low vacuum (Lamoureux 1994). The cured sediment slabs were prepared as thin sections using standard methods. The finished thin sections were then scanned at 2400 dpi and transferred to imaging software. The images were assembled in stratigraphic order and adjacent images were correlated using prominent sedimentary features. Both authors measured laminae five times independently in order to produce an objective and reproducible analysis. Grain size analysis of the cores was performed on a Beckman Coulter LS200 laser diffraction particle size analyzer. Samples were pretreated in 30% H_2O_2 for two weeks to remove organic matter and sodium hexametaphosphate was added as a dispersant. During the analysis, samples

were sonicated for 60 seconds and then analyzed with sonication three successive times for 60 seconds each.

Meteorological data

Historical temperature and precipitation data from Resolute, Nunavut, were obtained from Environment Canada. Temperature was recorded at the field site from June 1 2004 to May 15 2005 with an Onset HOBO temperature probe and data logger at ~80 m asl and ~10 km SSE of Lake R at 15 minute intervals. When compared to the Resolute temperature record for the same period, a strong correlation was observed (r^2 = 0.956, n = 8354, p < 0.001). Likewise, when the Resolute record was compared to temperature recorded by Marsh and Woo (1981) at a nearby catchment, similar patterns and magnitudes were observed during both 1979 and 1980. These comparisons provided justification for the use of the Resolute record as a source of long term weather data at this location.

Due to the settlement pattern in the Arctic, most long term weather records are obtained from monitoring stations at or near sea level (e.g., Resolute) and were therefore manipulated to account for altitude and other local temperature effects. Atkinson and Gajewski (2002), based on analyses of data from across the Canadian Arctic, suggested that a vertical lapse rate can be calculated using temperature readings from rawinsonde ascents to account for the altitudinal difference. For this study, data from the Resolute upper air station were extracted for a 14-day period (July 1 –14) for each year from 1961 to 2003. These data yielded a range of annual mean lapse rates between –3.6 and –5.5

°C·km^{-1}. Atkinson and Gajewski (2002) also identified a 3.0 °C reduction of mean temperature due to icefield proximity. Since the study site for this work is located at an elevation of ~300 m asl and immediately adjacent to an icefield, a reduction of between 4.07 and 4.66 °C (3.0 °C summed with the mean lapse rate calculated for each year) was applied to the recorded Resolute daily temperature data.

The temperature data were further organized to identify periods of melting degree-days (MDD), hereafter termed 'melt events'. Using the adjusted daily Resolute temperature data, intervals of continuous MDD were grouped together and a duration (measured in days) and an intensity (the mean temperature of the period) were identified (Fig. 2). Similarly, the total MDD for the melt event is referred to here as the 'event magnitude'. Melt events were distinguished by intervals of time when the daily mean temperature was below 0 °C and no MDD were recorded.

For the purposes of this study, only rainfall was considered, as summer snowfall was expected to yield a much smaller input of water and is also released as runoff in a more diffuse manner than rainfall. Rainfall totals recorded at Resolute (1961-2003) were comparatively low, with a range from 24.6 to 131.0 mm·a^{-1}. Daily amounts range from 0.2 to 20.8 mm (trace amounts, < 0.2 mm·d^{-1}, were omitted), with a mean of 23.6% of the annual rainfall occurring in a single day each year. Large events are rare but may be a significant source of sediment transport energy (e.g., Cogley and McCann 1976; Lamoureux 2000). The spatial variability of precipitation across the Arctic is a potential source of uncertainty, largely due to the paucity of long weather records across the region.

Therefore, the Resolute precipitation record was used in this study as a source of timing and relative magnitude of the events, not for the absolute quantity of precipitation.

Results

Sedimentology and chronology

The Lake R cores were composed entirely of rhythmically laminated clastic sediments. In thin section, the rhythmites were composed of graded silt units capped by a thin clay lamina. The rhythmic units ranged in thickness from 0.56 to 15 mm. Multiple silt rhythmites were found in 37 of 42 silt-clay units, with as many as 19 silt rhythmites within a single unit. Individual silt rhythmites ranged in thickness from 0.56 to 2 mm and all units exhibited conformable contacts. Based on the clearly defined rhythmicity of the sediments and the strong seasonality of the regional hydrometeorological regime, the Lake R silt-clay units were interpreted as varves. Independent dating of the R1-05 core with ^{137}Cs supported the hypothesis that the rhythmites were varves (Fig. 3).

The Lake R varve chronology was constructed from two cores (Fig. 3). Core R1-05 (22.6 cm) contained varves from 1959 to 2000 and core R2-05 (16.3 cm) contained varves from 1963 to 2003. Disturbance associated with transport of the cores precluded a complete chronology from R1-05. Correlation of the two cores was accomplished by comparing consistent varve structures and identification of a coarse grained (D_{50} >100 μm) bed in both cores. The varve chronology indicates that this layer was deposited in 1962 (Fig. 3).

Subannual structures mark identifiable changes in sediment properties within a varve and the formation of each can be considered to be dependent on the particular environmental conditions at the time of deposition (Sturm 1979; Desloges and Gilbert 1994; Lamoureux 2000). In order to assess depositional controls, a generalized classification scheme was applied to consistently define the variety of structures (Table 1). In general, each complex varve was composed of a fine silt basal unit overlain by one or more graded silt units, followed in some years by one or more coarser-grained units, and capped with a unit of well-sorted fine clay (Fig. 4). Deviations from this pattern included clay caps interrupted with coarse material (e.g., Shaw et al. 1978) and rhythmic silt micro-units (Fig. 4).

Characteristics of melt and rainfall events

Large variations occurred in the size and duration of the melt events at Resolute on both inter- and intra-annual scales. The distributions of event intensity and duration showed a preponderance of short-lived (< 2 days) or low intensity (< 1 °C) events, which collectively made up 59% of all melt events between 1961-2003. Low magnitude (< 5 MDD) events composed 66% of all melt events during this period while large events (> 30 MDD) were rare (3% of all melt events) and had a mean duration of 13 days (Fig. 5). The distribution of melt events within a given year showed little to no pattern. Although the events all occurred within the short arctic summer (June – August), the annual maximum and minimum events occurred at any time during that period.

Rainfall occurred mainly as drizzle or light rain (Fig. 5). Between 1961 and 2000 there were 896 days with rain (> 0.2 $mm \cdot d^{-1}$) at Resolute, with 76% of these days yielding less than 3 $mm \cdot d^{-1}$. Large rainfall events (> 7.5 $mm \cdot d^{-1}$, Cook 1967; Lamoureux 2000) were rare (6.9%). In terms of sediment transport, late season rainfall (August/September) was expected to play a potentially important role due to the increased prevalence of thawed sediments and well-developed channel systems (Gurnell et al. 1994). Of the 62 large rainfall events recorded, 39 (63%) occurred as late season events.

Influence of meteorology on sedimentary structure

Correlation between Lake R total varve thickness and annual melting degree-days recorded at Resolute was weak and insignificant (r^2 = 0.09), as were correlations with monthly melting degree-days (June: r^2 = 0.09; July: r^2 = 0.14; August: r^2 = 0.01). Similarly, correlations between varve thickness and summer total rainfall (r^2 = 0.00) and winter (September – May) snowfall (r^2 = 0.02) were poor. Therefore, the total varve record provided little information on climatic conditions in this catchment (e.g., Desloges and Gilbert 1994; Leemann and Niessen 1994; Tomkins and Lamoureux 2005; Hambley and Lamoureux 2006). This contrasts with previous studies that have demonstrated significant associations between total varve thickness and meteorological controls in glacierized catchments (Hardy et al. 1996; Moore et al. 2001; Lamoureux and Gilbert 2004), although in these cases, the varves were not identified to explicitly contain subannual laminae.

Heuristic model for comparison of sedimentary units and meteorological events

In order to objectively define the linkages between the melt events and the subannual sedimentary units, several heuristics were developed. These were developed with the ten thickest varves as a training set for the remainder of the series. The heuristic rules were used to identify physically plausible approaches to link inferred meteorological events to sedimentary units, as there were substantially more melt events than sedimentary units. The rules were defined as:

1) melt events less than 1 MDD did not create subannual sedimentary units;
2) melt events separated by 4 or more days formed separate subannual sedimentary units;
3) melt events separated by less than 4 days were:
    a. combined if the first melt event was larger than subsequent melt events, or
    b. separated if a melt event was larger than the preceding melt event;
4) unusually coarse units were derived from large (> 7.5 $mm \cdot d^{-1}$) rainfall events;
5) high-frequency micro-laminae were produced by complex hydrologic and geomorphic influences.

Rule 1 identified an inferred minimum energy threshold for melt-induced subannual units based on the training set of the ten thickest varves. Rule 2 addressed the potential for the reduction or interruption of meltwater discharge and sediment delivery between melt events. The value of four days represents the end of the estimated lag-time between meteorological forcing and runoff-

induced sediment deposition, and was derived from the correlation between the meteorological record and subannual sedimentary structures. The separation of sedimentary events would be caused by reduced sediment inflow and inflow competence characterized in the varve record by finer grain size (e.g., Sturm 1979). Rule 3 was intended to systematically treat the complex behaviour of the sediment transport system between multiple melt events separated by time gaps less than four days. In these cases, the separation between the melt events was inferred to be insufficient to create separate sedimentary units. Further, given the likelihood that stream discharge and sediment grain size were unlikely to be greater if a smaller melt event immediately followed a larger event, the latter was added to the MDD of the initial event, and therefore, would produce a single sedimentary unit for the two (or more) melt events (Rule 3a). During the opposite situation, where a smaller melt event was followed by a larger event, there were two sedimentary units created due to the inferred increase in discharge and inflow competence that would result in a transition from fine to coarse sediment in the lacustrine record (Rule 3b). Rule 4 applied to cases where sedimentary structures were unusually uniform and coarse. These characteristics suggested a sedimentary response to large rainfall events, typically in August and September (e.g., Desloges and Gilbert 1994; Leemann and Niessen 1994; Lamoureux 2000; Cockburn and Lamoureux 2007). Rainfall-induced sediment transport was expected to be potentially more energetic and therefore increase stream competence above that which is generated by snow and ice melt. Additionally, rainfall-induced runoff would access sediment supplies on the landscape surface, often during the late season when the landscape is thawed

and stream channels have minimal snow to protect bed materials from erosion (Lamoureux 2000). Finally, Rule 5 identified the unusual deposition pattern that only applied to the 1963 and 1982 varves, where a large number of micro-rhythmites occurred without any apparent hydroclimatic correlation.

Application of the heuristics to the Lake R subannual structures provided a means to assign each sedimentary unit a hydroclimatic source. Figures 2 and 6 illustrate the assignment of melt and rainfall events to the associated subannual sedimentary units for the 2000 varve. Superposition was applied to assign relative timing to the sedimentary units, although the absolute subannual timescale cannot be further interpreted from the sediments. Further, in an arctic watershed such as Lake R, it can be reasonably expected that sediment deposition occurred within the summer melt period. During 1979 and 1980, runoff in several nearby catchments began in late June and ceased by mid-August (Marsh and Woo 1981).

Melt-induced units

The most common sedimentary units in the Lake R varves contained normally graded silts with well-defined contacts and intermediate coarseness between the clay cap and the inferred rainfall-induced units. These structures were interpreted to be associated with melt season runoff events. Application of the heuristics 1-3 to the training set of ten years indicated a strong and significant relationship ($r^2 = 0.637$; $n = 45$; $p < 0.01$) between the magnitude of the melt events and the thickness of the respectively assigned subannual unit (Fig. 7). Two outliers substantially reduced the coefficient of determination for this

relationship. Inferred melt units in 1991 (1.8 mm) and 1972 (1.9 mm) were assigned to melt events of 61.8 and 6.6 MDD, respectively, with the 1972 event being the combination of two events (Rule 3a). The predicted under-deposition of the 1991 melt unit and the over-deposition of the 1972 melt unit are potentially explained by variations in the proximal-distal relationship of the coring site relative to the inflow (see below). Non-linear (power, quadratic, cubic) regressions improved the strength of the relationship somewhat, though the asymptotic behaviour of these relationships could not be justified based on the available observations.

Rainfall-induced units

The coarsest of the sedimentary units inferred to be associated with rainfall-induced discharge commonly occurred near the top of the varve and indicated late season deposition. Sharp contacts between the melt- and rainfall-induced structures facilitated identification of the units. While the rainfall interpretation has been demonstrated in a number of contexts (Østrem and Olsen 1987; Leemann and Niessen 1994; Lamoureux 2000; Gilbert 2003b; Cockburn and Lamoureux 2007), the sedimentary interpretation is equivocal, and could also arise from slumps unrelated to rainfall events (Hambley and Lamoureux 2006). Notwithstanding these uncertainties, in this study, the coarse units mark a significant increase in the competence of the lake inflow that is likely caused by large, late-season (August and September) rainfall events, as melt events were uncommon and of low magnitude. Early season rainfall units were less common, and occurred only twice in the training set. These results are consistent with a

similar study based on 30 years of meteorological and varve sedimentology, where only one major early season rainfall event generated a sedimentary deposit (Lamoureux 2000). Since rainfall values must be interpreted with caution due to the inherent spatial variability in precipitation, correlations between rainfall amount and unit thickness were not carried out for this study. However, the observed relationship (r^2 = 0.81; n = 8; p < 0.05) between the number of identified rainfall units and the number of large (> 7.5 $mm \cdot d^{-1}$) rainfall events suggests that this approach worked well (Fig. 8). In the instance where seven rainfall events occurred (1994), the number of sedimentary events inferred to be rainfall-induced was only four. This may be explained by the presence of an early season large rainfall event and three large rainfall events which occurred within a 10-day time span.

Fine basal unit

The fine basal unit was the first unit of each varve, deposited directly above the clay cap from the previous year. Other than the clay cap, the basal unit was the finest-grained of all subannual sedimentary units. These subannual units stratigraphically preceded the initial melt event, and therefore likely represent some form of early melt season, low energy fluvial transport. The melt events discussed in the previous section were created based on mean daily temperatures, although the possibility exists that the maximum daily temperature was above 0°C while the mean daily temperature was below zero. These conditions are common during initial snow melt in the Arctic (Woo 1983). This would allow for some limited melt to occur prior to the melt events described

above. Similarly, the fine basal unit could represent a distinction between nival and glacial melt regimes. In glacial systems, nival precedes glacial melt, and the expected intensity of each melt regime is consistent with the observed sedimentary characteristics of the units.

Using the training set of the ten thickest varves, the total MDD were calculated for the condition that the maximum daily temperature was above 0°C but the mean daily temperature was below 0°C for all days before the first melt event. For these 10 years, a mean of 5.5 days fit this condition, and a mean of 6.8 MDD were recorded. When compared to the thickness of the basal unit for the respective years, an r^2 = 0.62 (mean thickness = 0.3 mm, n = 10, p < 0.01) was observed (Fig. 9). These results suggest that the fine basal layer was created by low-intensity melt prior to the onset of the main melt season. Snowmelt events occur from early June and into the early half of July and likely precede glacial meltwater generation (Woo 1983). These results are consistent with other sediment-snow melt studies (e.g., Hardy et al. 1996; Hughen et al. 2000; Francus et al. 2002) and closely resemble similar findings by Hambley and Lamoureux (2006) where initial annual sedimentation units were significantly correlated with melt season energy.

Clay caps

The clay cap represents the last depositional phase of the year and is likely indicative of flocculation and suspension settling of fine particles after the melt season and during winter (e.g., Sturm 1979). Especially at high latitudes, the prolonged and severe winter results in full cessation of hydrologic and

sedimentary inputs and thick lake ice cover. These conditions allow for the progressive deposition of grains that remain in suspension in the water column during the summer (Gilbert 2003b).

In the Lake R training set record, six varves contained a clay cap interrupted by a coarser layer. It is likely that the interruptions were caused by either subaqueous slumps or increased runoff in late summer (e.g., Shaw et al. 1978; Hambley and Lamoureux 2006). In the case of increased late summer runoff, the onset of clay cap deposition prior to the interruption indicates that a substantial amount of time had passed after the main melt season. Most interrupted clay caps in Lake R were associated with large (8.6 – 15.6 $mm \cdot d^{-1}$) late season rainfall events that occurred at least 15 days after the last melt event. Based on Stoke's Law, this interval would represent sufficient time for appreciable accumulation of fine silt and clay to form the initial clay cap (Gilbert 2003a). In years where the clay cap was interrupted, late season rainfall events greater than 8.6 $mm \cdot d^{-1}$ substantially increased sediment delivery to the lake. Alternatively, large rainfall events (7.5 – 11.2 $mm \cdot d^{-1}$) that occurred too soon after the melt period (< 12 days) did not appear to provide sufficient time for the initial deposition of the clay cap.

An exception to this interpretation was the 1998 varve. The interruption observed in this varve was composed of unusually coarse grains (> 100 μm). An intense rainfall event (12.6 mm) occurred late in the year, although only five days after the last melt event. However, the coarse sediments contained in this unit suggest that it was potentially caused by a subaqueous slump. A similar unit

appeared in the 1962 varve, although it occurred earlier in the season and not as an interrupted clay cap.

Rhythmic silt micro-units

In two varves (1963, 1982; Fig. 4), unusual laminae were produced which appeared as series of thin (< 0.25 mm) rhythmic structures. In most respects, they were similar to proximal silt rhythmites presented by Lamoureux (1999a) in Nicolay Lake, which were suggested to have formed by diurnal deposition events. In Lake R, the units occurred early in their respective varve, suggestive that they were a response to the nival melt system, as opposed to the ice melt and rainfall dominated system later in the melt season. Their comparatively narrow range of grain size and abundance suggest that these units were derived from short time scale (e.g., diurnal) variations in the hydrologic system, though identification of the units as melt-induced sedimentary units could not be made through correlation with the daily temperature record. The diurnal temperature ranges in 1963 and 1982 were not unusual compared to the 1961-2003 record. While the potential causes of the formation of these units can be speculated on, we suggest here that these sedimentary structures represent a complex combination of short term hydrologic and geomorphic controls on varve deposition that occur infrequently in the basin.

The entire recent varve record

Using the relationships established above, we evaluated the heuristic model using the observed subannual structures in the varves not included in the training set. We applied the regression equation as determined for the training

set melt events to the next ten thickest varves (the test set) in the Lake R sediments in order to test whether the model could accurately predict the number and magnitude of the melt events based on the interpretation and measurement of the subannual units in those varves. In three cases within the test set, substantial differences were observed between the subannual structures and the meteorological record, such that sedimentary units and meteorological events could not be reconciled. For the remainder of the test set, the prediction of the total number of melt events was comparable to the observed number of events in the meteorological record (predicted 35, observed 34), though we were not able to accurately predict the magnitude of those events on a consistent basis. For 11 observed melt events less than 5 MDD, we predicted a mean MDD 55.4% greater than the observed. For 9 observed melt events between 5 and 10 MDD, we predicted a mean MDD 3.8% greater than the observed. For 14 observed melt events greater than 10 MDD, we predicted a mean MDD 69.5% less than the observed. Overall, the relationship between the predicted and observed melt event magnitudes yielded an $r^2 = 0.224$ ($n = 34$, $p < 0.01$).

For the remaining 18 varves in the Lake R sediments, a further weakening of the relationship was observed, and an increasing disassociation existed between the predicted and observed number of melt events per year, with more subannual units being predicted by the meteorological record than observed in the sediments. Likewise, a greater underestimation between predicted and observed subannual unit thickness was seen. The loss of coherency between the varve thickness and meteorological record was best illustrated when the thinnest varves were examined, particularly the 1971 and 1986 varves. The 1971

varve (Fig. 4B) was 0.94 mm thick and composed of three subannual units: a basal unit (0.31 mm), an inferred melt unit (0.30 mm) and a clay cap. The varve was ranked as the 36th thickest varve in the 8th largest year of cumulative MDD (of 38 years available, Table 2). However, the heuristic model suggested that there would be three melt-induced units and one rainfall-induced unit that year. Similarly, the 1986 varve measured 0.99 mm thick (34th thickest) and was composed of three subannual units which would be interpreted the same as those in the 1971 varve. The meteorological record, however, suggested that no melt- and rainfall-induced sedimentary events should have formed, as no melt event exceeded 1.0 MDD and there were no large rainfall events. In fact, 1986 had the lowest cumulative MDD in the study period. Although these years experienced considerably different meteorological conditions, the sedimentary record suggested similar runoff and sediment delivery.

In order to address the potential cause(s) of the reduced fidelity of the model, we examined the grain size distributions of the sediment for individual years. Millimetre-scale sampling was carried out on core R1-05 (n = 234) and annual units were identified using the depth-age model. Ranking the varve record by thickness allowed for the comparison of particle size data for the 10 thickest years and the 10 thinnest years between 1963 and 2000 (Table 2, Fig. 10). This analysis was also performed for the 10 warmest and 10 coldest (based on total MDD) years in the study period. The results of the particle size analysis showed no significant difference in the median grain size between the coldest (D_{50} = 9.9 μm) and warmest (D_{50} = 9.7 μm) years. However, the thickest varves (D_{50} = 11.1 μm) were composed of significantly coarser grains than the thinnest

varves (D_{50} = 8.5 μm). Furthermore, we separated the thinnest varves into varves that should have been thin based on model estimates of the meteorological record (e.g., low MDD, rainfall, or early melt) and varves that were thin despite meteorological conditions that favoured a thick deposit (e.g., 1971). Additionally, we identified varves that were thick despite meteorological conditions that suggested a thin deposit. These divisions were based on a ranking system, where a large difference between the varve thickness rank and the MDD rank identified 10 'unusual' varves (Table 2). Again, a significant median size difference was observed between the varves that were thinner-than-expected (D_{50} = 9.4 μm) and those that were thicker-than-expected (D_{50} = 11.8 μm). All significant differences were tested using a Mann-Whitney nonparametric test (α = 0.05).

Discussion

Subannual rhythmites as an indication of weather events

The relatively thick Lake R varves were formed by a number of weather-induced mechanisms that imprinted a discernable signature as a subannual sedimentary record. The formation of the subannual units was controlled by i) available melt energy driven by estimated positive air temperatures, ii) major rainfall events, and iii) uncommon events not clearly related to meteorology. In the majority of years, melt-induced units comprised the bulk of the varve structure and mass accumulation, although rainfall events, especially late-season events, contributed notably to their overall thickness. Based on this analysis, structures

generated by factors unrelated to weather conditions were rare, but were visually distinct.

After subdivision of the varves into individual sedimentary structures, it was apparent why the correlations between seasonal weather variables (cumulative MDD, rainfall) and total varve thickness yielded poor results in this environment. The Lake R varves were composed of a complex combination of weather variables which all acted to form the cumulative varve structure (e.g., Leemann and Niessen 1994; Gilbert 2003b; Hambley and Lamoureux 2006). These results showed that three primary meteorological controls contributed to overall varve development: 1) early season snowpack melt that occurred during the initial period of positive temperatures in the year; 2) major melt events (> 1 MDD) throughout the summer months (June, July, and August); and 3) large (> 7.5 $mm \cdot d^{-1}$) rainfall events that increased inflow competence and sediment transport, primarily in the latter portion of the summer. Together, these results show that sediment transport was not restricted to a short period of intense runoff usually attributed to the spring snowmelt (e.g., Hardy 1996) and demonstrate the role of continued meltwater production by the glacier (e.g., Marsh and Woo 1981; Lawson 1993; Gilbert 2003b).

The timing of a precipitation event was important when considering the hydrological implications of water input. Early season (May and June) rain is likely to fall onto snowcover. Although exceptional rainfall events on snowcover can generate a considerable hydrological response (e.g., Church 1972), at low intensities, rain-on-snow events mute the overall impact of the rainfall by effectively reducing the overall hydrological (and consequently sedimentological)

impacts (Lewkowicz and Young 1990). Therefore these early events can be typically considered to be of minor importance (Lamoureux 2000). Conversely, late season rainfall is rapidly channelized and increases associated sediment transport (Cowan et al. 1988). Thaw of channel and adjacent land surfaces provides increased erodible sediment in the late season, and further enhances the potential impact of rainfall erosion and increased stream discharge. These events can be considered significant contributors to sediment delivery in the High Arctic (Cogley and McCann 1976; Lamoureux 2000).

When the model was applied to the remainder of the Lake R varve record, a progressive deterioration of the relationship between subannual unit thickness and the meteorological record was observed. In some cases, these poor correlations reiterate important cautions regarding the use of laminated sediments in paleoenvironmental reconstruction (e.g., Lamoureux 1999b; Braun et al. 2000; Hambley and Lamoureux 2006; Hodder et al. 2007). Sediment deposition patterns have been observed to periodically change due to variable sediment routing, leading to changes in the proximal-distal relationship at a single site (e.g., Lamoureux 1999b). At Lake R, particle size analysis from a single core showed that sediment in thin varves was finer and less variable than sediment in thick varves. The fine, more uniform sediment is consistent with a more distal depositional position, whereas the coarse sediment with high variance is consistent with a relatively proximal depositional site. Similarly, the inferred proximal-distal changes in grain size properties would be paralleled by distal thinning (Smith 1978) and represent a likely explanation for the thinner varves in the Lake R sediments.

We hypothesize that these particle size differences were derived from changes in the routing of sediment inflow to the lake (e.g., Lamoureux 1999b). Year-to-year variation in the routing of sediment-laden water from the ice cap could either direct the main sediment plume at or away from the R1-05 coring site, ultimately leading to the variation in composition of the deposited material. Furthermore, the lack of difference between deposited particle sizes during warm and cold years suggest that the causal mechanism is not climatic (cf. Francus et al. 2002). In the case of Lake R, results suggest that geomorphic processes impacted a substantial portion of varve deposition. The depositional environment at R1-05 was selected due to its perceived optimal location (deepest water, adjacent to the major inflow). However, the observed differences in grain size at a fixed location in the lake suggest that sediment delivery conditions changed and potentially altered the baseline controls between melt energy and sediment delivery. This limited the ability of the model to predict meteorological conditions based on the interpretation of subannual sedimentary structures to the units that were inferred to receive the most direct input of sediment from the main glacial inflow (i.e., the thickest varves).

The observed Lake R grain size results suggest that the model developed here worked best when a proximal depositional regime was dominant, where the associations between meteorology, inflow, and deposition could be expected to be most closely connected. However, as observed at Lake R, these conditions are not necessarily temporally static. Potential subtle changes in hydrology, meteorology and/or geomorphology may lead to variable routing of sediment through the lake, thus leading to no single coring site containing an optimal

sedimentary record. Such spatial variability of sediment deposition has been identified in both proglacial (Lewis et al. 2002; Lamoureux and Gilbert 2004; Schiefer 2006) and non-glacial (Lamoureux 1999b) environments, and raises concerns regarding the nature of the environmental signal contained within sedimentary records.

Although the Lake R record is affected by non-stationary catchment and lake conditions, and the resultant linkages between the subannual and meteorological records are inconsistent, the potential for such a model has been demonstrated by these results. Where available, subannual sedimentary records from a number of different environments (alpine/glacial: Leemann and Niessen 1994; Cockburn and Lamoureux 2007; Arctic/non-glacial: Hambley and Lamoureux 2006; Arctic/glacial: this study) have been used to identify the relative occurrence and/or importance of hydrometeorologic and geomorphic processes in lacustrine depositional environments. At Lake R, when sedimentation rates were highest and geomorphic controls were likely minimal, the subannual units provided a detailed record of prevailing weather conditions in the region. The failure to predict the meteorological conditions beyond the 10-varve training set does not render the model unsuccessful. Instead, it illuminates the necessary environmental conditions and sampling strategies required to produce an optimal sediment record on which to test the model. Also, the short record recovered from Lake R precludes a long term reconstruction of seasonal weather conditions. Though compaction of the sediments at greater depths is known to occur, the structures in the sediment remain intact, including the presence of subannual structures (Petterson et al. 1993), and would allow for decadal to

centennial length subannual meteorological reconstructions where such records could be recovered.

Importantly though, this work further illustrates past and present concerns regarding the environmental signal that may be contained within lacustrine varves. Hodder et al. (2007) discussed at length the shortcomings of studies that relied on simple varve couplets as paleoenvironmental proxies, and cited examples of previous studies where simple relationships were used to link the hydroclimatic system to varved sediments. Results presented here show that the Lake R varves are a composite of several meteorological factors as well as non-stationary geomorphic factors. Outside of the relatively simple High Arctic environment (e.g., temperate alpine), increased environmental complexity may serve to further render the simple varve-meteorology relationships as inadequate.

Conclusions

Deposition of complex varves in a small Arctic proglacial lake was shown to be controlled by short-lived regional weather conditions. Inferred melt- and major rainfall-induced sedimentary units corresponded to melt and rainfall events derived from an elevation-adjusted weather record from a station located 200 km away. Other subannual units, such as thin basal laminae and interrupted clay caps were controlled by early melt season temperature and late season rainfall, respectively. Geomorphic influences were hypothesized to affect sediment deposition on both subannual and annual scales. Silt micro-laminae (< 0.25 mm thick) did not correspond with the meteorological record, and were interpreted as geomorphically-influenced sedimentation or sub-synoptic weather controls. More

importantly, thin varves were identified as sedimentologically distinct from the thicker varves used to develop the varve-meteorology model, and suggested that variable sediment routing into the lake generated thinner varves and precluded the identification of meteorological events in the subannual structures in some years. These results identified the potential for producing long term, high resolution reconstructions of subannual weather conditions. Though the Lake R sediment did not provide a record beyond the instrumental period in the Arctic, the potential to perform such a reconstruction has been demonstrated. Model limitations illuminate the necessary environmental and sampling conditions required to produce a more robust model for future applications.

Acknowledgements

This work was supported by ArcticNet, a Network of Centres of Excellence of Canada, and a Natural Sciences and Engineering Research Council of Canada Discovery Grant to S.F.L. and Northern Scientific Training Program and Queen's University Graduate Dean's Travel grants to K.J.C. The Polar Continental Shelf Project, Natural Resources Canada, provided logistical field support. This research was supported by Nunavut Research Institute Scientific Research License 0200406R-M. Field assistance from J. Cockburn and D. Fortin is greatly acknowledged. Formal reviews of the manuscript by C. Hillaire-Marcel, J. Ridge and an anonymous reviewer are appreciated. This is Polar Continental Shelf Project (PCSP) contribution 025-07.

References

Atkinson, D.E., and Gajewski, K. 2002. High-resolution estimation of summer surface air temperature in the Canadian Arctic Archipelago. Journal of Climate, **15**: 3601-3614.

Bradley, R.S. 1990. Holocene paleoclimatology of the Queen Elizabeth Islands, Canadian High Arctic. Quaternary Science Reviews, **9**: 365-384.

Braun, C., Hardy, D.R., Bradley, R.S., and Retelle, M.J. 2000. Streamflow and suspended sediment transfer to Lake Sophia, Cornwallis Island, Nunavut, Canada. Arctic, Antarctic, and Alpine Research, **32**: 456-465.

Church, M.A. 1972. Baffin Island Sandurs: A Study of Arctic Fluvial Processes. Geological Survey of Canada Bulletin 216.

Cockburn, J.M.H., and Lamoureux, S.F. 2007. Century-scale variability in late-summer rainfall events recorded over seven centuries in subannually laminated lacustrine sediments, White Pass, British Columbia. Quaternary Research, **67**: 193-203.

Cogley, J.G., and McCann, S.B. 1976. An exceptional storm and its effects in the Canadian High Arctic. Arctic and Alpine Research, **8**: 105-110.

Cook, F.A. 1967. Fluvial processes in the High Arctic. Geographical Bulletin, **9**: 262-268.

Cowan, E.A., Powell, R.D., and Smith, N.D. 1988. Rainstorm-induced event sedimentation at the tidewater front of a temperate glacier. Geology, **16**: 409-412.

de Geer, G. 1912. A geochronology of the last 12,000 years. *In* Proceedings of the 1910 International Geological Congress, Stockholm, Sweden, pp. 241-253.

Desloges, J.R., and Gilbert, R. 1994. Sediment source and hydroclimatic inferences from glacial lake sediment: the postglacial sedimentary record of Lillooet Lake, British Columbia. Journal of Hydrology, **159**: 375-393.

Dyke, A.S. 1998. Holocene delevelling of Devon Island, Arctic Canada: implications for ice sheet geometry and crustal response. Canadian Journal of Earth Sciences, **35**: 885-904.

Dyke, A.S. 1999. Last glacial maximum and deglaciation of Devon Island, arctic Canada: support for an Innuitian Ice Sheet. Quaternary Science Reviews, **18**: 393-420.

Forbes, A.C., and Lamoureux, S.F. 2005. Climatic controls on streamflow and suspended sediment transport in three large Middle Arctic catchments, Boothia Peninsula, Nunavut, Canada. Arctic, Antarctic, and Alpine Research, **37**: 304-315.

Francus, P., Bradley, R.S., Abbott, M.B., Patridge, W., and Keimig, F. 2002. Paleoclimate studies of minerogenic sediments using annually resolved textural parameters. Geophysical Research Letters, **29**: 1998-2001.

Gilbert, R. 1975. Sedimentation in Lillooet Lake, British Columbia. Canadian Journal of Earth Sciences, **12**: 1697-1711.

Gilbert, R. 2003a. Varves. *In* Encyclopedia of Sedimentology and Sedimentary Rocks. *Edited by* G.V. Middleton. Kluwer Academic Publishers, Dordrecht, Netherlands, pp 764-766.

Gilbert, R. 2003b. Lacustrine sedimentation. *In* Encyclopedia of Sedimentology and Sedimentary Rocks. *Edited by* G.V. Middleton. Kluwer Academic Publishers, Dordrecht, Netherlands, pp 404-408.

Gurnell, A.M., Hodson, A., Clark, M.J., Bogen, J., Hagen, J.O., and Tranter, M. 1994. Water and sediment discharge from glacier basins: an arctic and alpine comparison. IAHS Publication No. **224**: 325-334.

Hambley, G.W., and Lamoureux, S.F. 2006. Recent summer climate recorded in complex varved sediments, Nicolay Lake, Cornwall Island, Nunavut, Canada. Journal of Paleolimnology, **35**: 629-640.

Hardy, D.R. 1996. Climatic influences on streamflow and sediment flux into Lake C2, northern Ellesmere Island, Canada. Journal of Paleolimnology, **16**: 133-149.

Hardy, D.R., Bradley, R.S., and Zolitschka, B. 1996. The climatic signal in varved sediments from Lake C2, northern Ellesmere Island, Canada. Journal of Paleolimnology, **16**: 227-238.

Hodder, K.R., Gilbert, R., and Desloges, J.R. 2007. Glaciolacustrine varved sediment as an alpine hydroclimatic proxy. Journal of Paleolimnology, **38**: 365-394.

Hughen, K.A., Overpeck, J.T., and Anderson, R.F. 2000. Recent warming in a 500-year palaeotemperature record from varved sediments, Upper Soper Lake, Baffin Island, Canada. The Holocene, **10**: 9-19.

Koerner, R.M., and Fisher, D.A. 1990. A record of Holocene summer climate from a Canadian High Arctic ice core. Nature, **343**: 630-631.

Lamoureux, S.F. 1994. Embedding unfrozen lake sediments for thin section preparation. Journal of Paleolimnology, **10**: 141-146.

Lamoureux, S.F. 1999a. Catchment and lake controls over the formation of varves in monomictic Nicolay Lake, Cornwall Island, Nunavut. Canadian Journal of Earth Sciences, **36**: 1533-1546.

Lamoureux, S.F. 1999b. Spatial and interannual variations in sedimentation patterns recorded in nonglacial varved sediments from the Canadian High Arctic. Journal of Paleolimnology, **21**: 73-84.

Lamoureux, S.F. 2000. Five centuries of interannual sediment yield and rainfall-induced erosion in the Canadian High Arctic recorded in lacustrine varves. Water Resources Research, **36**: 309-318.

Lamoureux, S.F., and Bradley, R.S. 1996. A late Holocene varved sediment record of environmental change from northern Ellesmere Island, Canada. Journal of Paleolimnology, **16**: 239-255.

Lamoureux, S.F., and Gilbert, R. 2004. A 750-yr record of autumn snowfall and temperature variability and winter storminess recorded in the varved sediments of Bear Lake, Devon Island, Arctic Canada. Quaternary Research, **61**: 134-147.

Lamoureux, S.F., Gilbert, R., and Lewis, T. 2002. Lacustrine sedimentary environments in High Arctic proglacial Bear Lake, Devon Island, Nunavut, Canada. Arctic, Antarctic, and Alpine Research, **34**: 130-141.

Lawson, D.E. 1993. Glaciohydrologic and glaciohydraulic effects on runoff and sediment yield in glacierized basins. U.S. Army Cold Regions Research and Engineering Laboratory Monograph 93-02.

Leemann, A., and Niessen, F. 1994. Varve formation and the climatic record in an Alpine proglacial lake: calibrating annually-laminated sediments against hydrological and meteorological data. The Holocene, **4**: 1-8.

Leonard, E.M. 1985. Glaciological and climatic controls on lake sedimentation, Canadian Rocky Mountains. Zeitschrift für Gletscherkunde und Glazialgeologie, **21**: 35-42.

Lewis, T., Gilbert, R., and Lamoureux, S.F. 2002. Spatial and temporal changes in sedimentary processes at proglacial Bear Lake, Devon Island, Nunavut, Canada. Arctic, Antarctic, and Alpine Research, **34**: 119-129.

Lewkowicz, A.G., and Young, K.L. 1990. Hydrology of a perennial snowbank in the continuous permafrost zone, Melville Island, Canada. Geografiska Annaler, **72A**: 13-21.

Marsh, P., and Woo, M.-K. 1981. Snowmelt, glacier melt and high arctic streamflow regimes. Canadian Journal of Earth Sciences, **18**: 1380-1384.

Mayr, U., de Freitas, T., and Beauchamp, B. 1998. The Geology of Devon Island North of 76°, Canadian Arctic Archipelago. Geological Survey of Canada Bulletin 526.

Moore, J.J., Hughen, K.A., Miller, G.J., and Overpeck, J.T. 2001. Little Ice Age recorded in summer temperature reconstruction from varved sediments of Donard Lake, Baffin Island, Canada. Journal of Paleolimnology, **25**: 503-517.

Østrem, G., and Olsen, H.C. 1987. Sedimentation in a glacier lake. Geografiska Annaler, **69A**: 123-138.

O'Sullivan, P.E. 1983. Annually-laminated lake sediments and the study of Quaternary environmental changes – a review. Quaternary Science Reviews, **1**: 245-313.

Petterson, G., Renberg, I., Geladi, P., Lindberg, A., and Lindgren, F. 1993. Spatial uniformity of sediment accumulation in varved lake sediments in northern Sweden. Journal of Paleolimnology, **9**: 195-208.

Schiefer, E. 2006. Depositional regimes and areal continuity of sedimentation in a montane lake basin, British Columbia, Canada. Journal of Paleolimnology, **35**: 617-628.

Shaw, J., Gilbert, R., and Archer, J.J.J. 1978. Proglacial lacustrine sedimentation during winter. Arctic and Alpine Research, **10**: 689-699.

Smith, N.D. 1978. Sedimentation processes and patterns in a glacier-fed lake with low sediment input. Canadian Journal of Earth Sciences, **15**: 741-756.

Sturm, M. 1979. Origin and composition of clastic varves. *In* Moraines and Varves: Origin/Genesis/Classification. *Edited by* C. Schlüchter. A.A. Balkema, Rotterdam, Netherlands, pp. 281-285.

Tomkins, J.D., and Lamoureux, S.F. 2005. Multiple hydroclimatic controls over recent sedimentation in proglacial Mirror Lake, southern Selwyn Mountains, Northwest Territories. Canadian Journal of Earth Sciences, **42**: 1589-1599.

Woo, M.-K. 1983. Hydrology of a drainage basin in the Canadian High Arctic. Annals of the Association of American Geographers, **73**: 577-596.

Table 1. Sedimentary criteria used to identify and classify subannual laminae (after Cockburn and Lamoureux, 2007).

Classification	Hypothesized hydroclimatic influence	Sedimentary characteristics
Fine basal unit	Melt induced	Fine grained, usually thin structure at the base of the varve
Graded silt units	Melt induced	Common sedimentary unit, fine grain size, consistent normal (upward) grading
Coarse silt units	Rainfall induced	Thin, coarse unit, minimal grading, contain detrital organic material
Interrupted clay caps	Rainfall induced	Thin separation between clay deposits, contain detrital organic material
High-frequency micro units	Unknown, potentially diurnal hydrological variability	Thin (< 0.25 mm) and repeating units with little internal structure

Table 2. Varve thickness and cumulative melting degree-day ranks, where 1 was thickest/warmest and 38 was thinnest/coldest. The difference in rank was used to identify years where varve deposition was thicker/thinner than expected based on the corresponding melt energy availability. The top five of each type are shown.

	Year	Varve Thickness Rank	MDD Rank	Difference
Thicker-than-expected	1972	8	35	-27
	1967	12	37	-25
	1964	15	36	-21
	1963	3	23	-20
	1985	6	21	-15
Thinner-than-expected	1987	21	6	+15
	1969	27	11	+16
	1988	17	1	+16
	1971	34	8	+26
	1973	37	5	+32

Figure Captions

Figure 1. Locations of Colin Archer Peninsula, Devon Island (A) and the Archer River basin (B). Devon Ice Cap (DIC) and Resolute (R) are identified. Permanent ice is identified in gray, lakes in black. Bathymetry and coring sites in Lake R (C).

Figure 2. Melt and rainfall event diagram for 2000. The numbers correspond to the sediment image in Fig. 6. Section 1 corresponds to the minor melt period prior to the main melt season. Sections 4, 9 and 11 are colder periods of reduced or no melt and correspond with deposition of fine grains and the clay cap. The unadjusted Resolute temperature record is shown on the bold solid line. The 4.34 °C adjustment for 2000 is identified.

Figure 3. Varve thickness series from Lake R for cores R1-05 and R2-05. Stars along the x-axis indicate the years used in the training set. Inset shows ^{137}Cs profile (bars) and estimated varve depth-age (dots) from R1-05. The 1963 bomb peak is identified by the vertical line.

Figure 4. Scanned images (2400 dpi) of selected thin section areas from core R1-05. Image A shows a period of high sedimentation from 1981 to 1985 (bottom to top; white boxes distinguish the varves). Note the interrupted clay caps in 1981 and 1985 (arrows). The non-climatic silt micro-rhythmites deposited in 1982 are identified by the centre box. Panel B shows a period of reduced sedimentation from 1964 to 1973 (bottom to top). Note the presence of thin and generally simple varves.

Figure 5. Melt event magnitude and rainfall frequency distributions from Resolute weather station, 1961-2003.

Figure 6. Thin section scan (2400 dpi) of the 2000 varve from core R1-05 with the identification of subannual units. B = fine basal unit, M = melt-induced units, R = rainfall-induced units, C = clay deposition during prolonged cold periods. The adjacent numbers correspond to the 2000 melt and rainfall event diagram in Fig. 2. The vertical scale bar is 1 mm.

Figure 7. Relationship between observed melting degree-days and subannual unit thickness for eight training set years (1963 and 1982 are omitted due to the inferred non-climatic induced units). MDD based on Resolute temperature record, 1961-2003.

Figure 8. Comparison of the observed number of large (> 7.5 $mm \cdot d^{-1}$) rainfall events (recorded at Resolute, 1961-2003) to the number of large rainfall events predicted from the occurrence of coarse subannual units in the training set years. (n = 8, there is overlap of data points).

Figure 9. Comparison between the basal subannual unit thickness and calculated melting degree-days during the early-season, minor melt period. MDD based on Resolute temperature record, 1961-2003.

Figure 10. Median grain size frequency distributions between A) the 10 thickest and 10 thinnest varves, B) the 10 warmest and 10 coldest years between 1961 and 2000 at Resolute, and C) the 5 most thicker-than-expected and 5 most thinner-than-expected varves, based on estimates generated from the respective meteorological melt season data.

Figure 1.

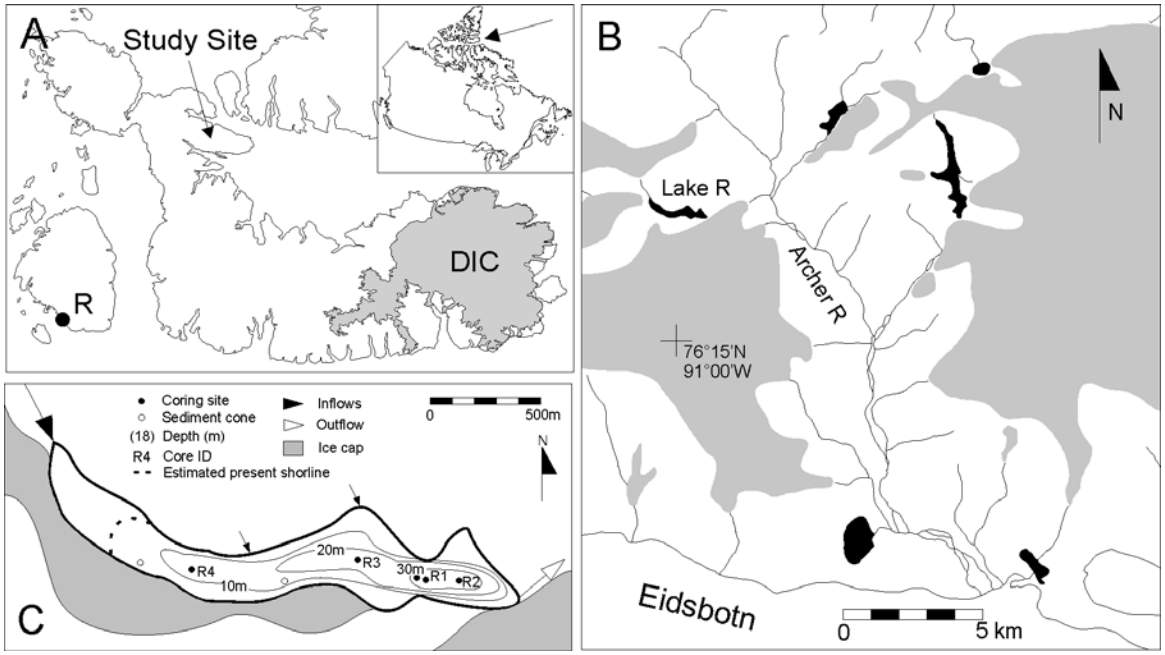
A
Study Site
DIC
R
B
N
Lake R
Archer R
76°15'N
91°00'W
Eidsbotn
0
5 km
C
Coring site
Sediment cone
(18) Depth (m)
R4 Core ID
Estimated present shorline
Inflows
Outflow
Ice cap
0
500m
N
20m
30m
10m
R4
R3
R1
R2

Figure 2.

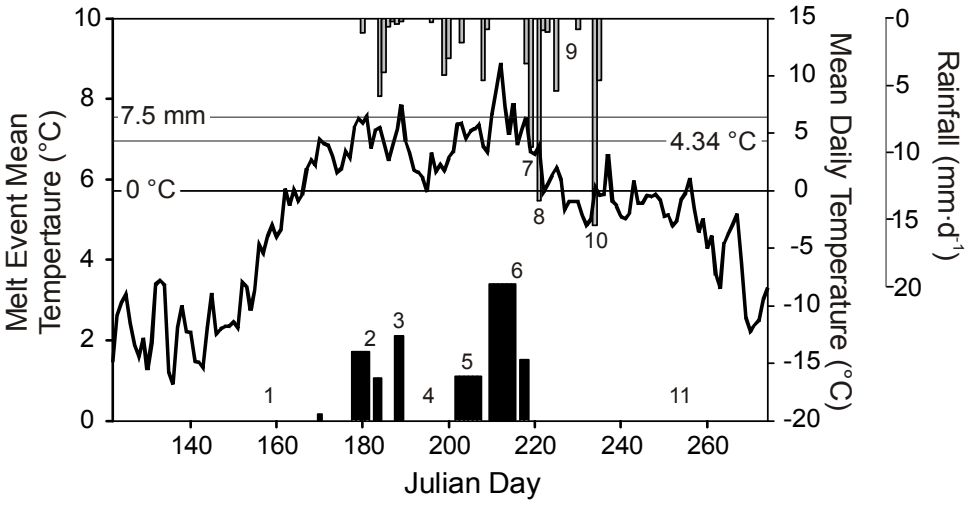
Melt Event Mean Tempertaure (°C)
Mean Daily Temperature (°C)
Rainfall (mm·d-1)
Julian Day
7.5 mm
4.34 °C
0 °C
1
2
3
4
5
6
7
8
9
10
11

Figure 3.

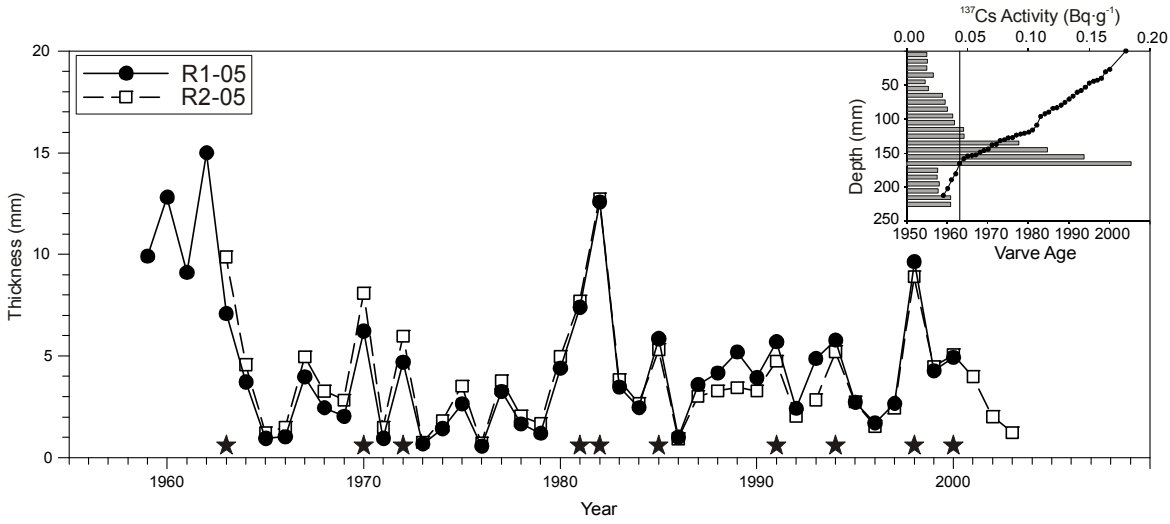
R1-05
R2-05
Thickness (mm)
Year
1960
1970
1980
1990
2000
0
5
10
15
20
^{137}Cs Activity (Bq·g^{-1})
0.00
0.05
0.10
0.15
0.20
Depth (mm)
50
100
150
200
250
1950 1960 1970 1980 1990 2000
Varve Age

Figure 4.

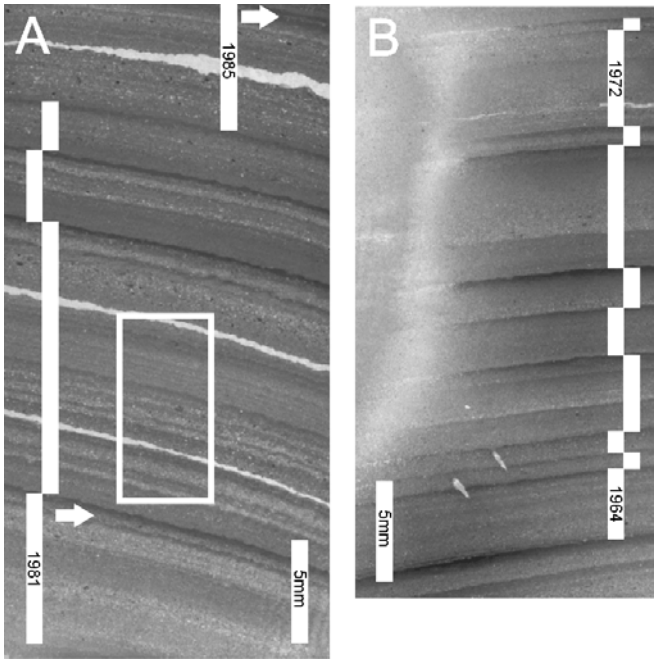

Figure 5.

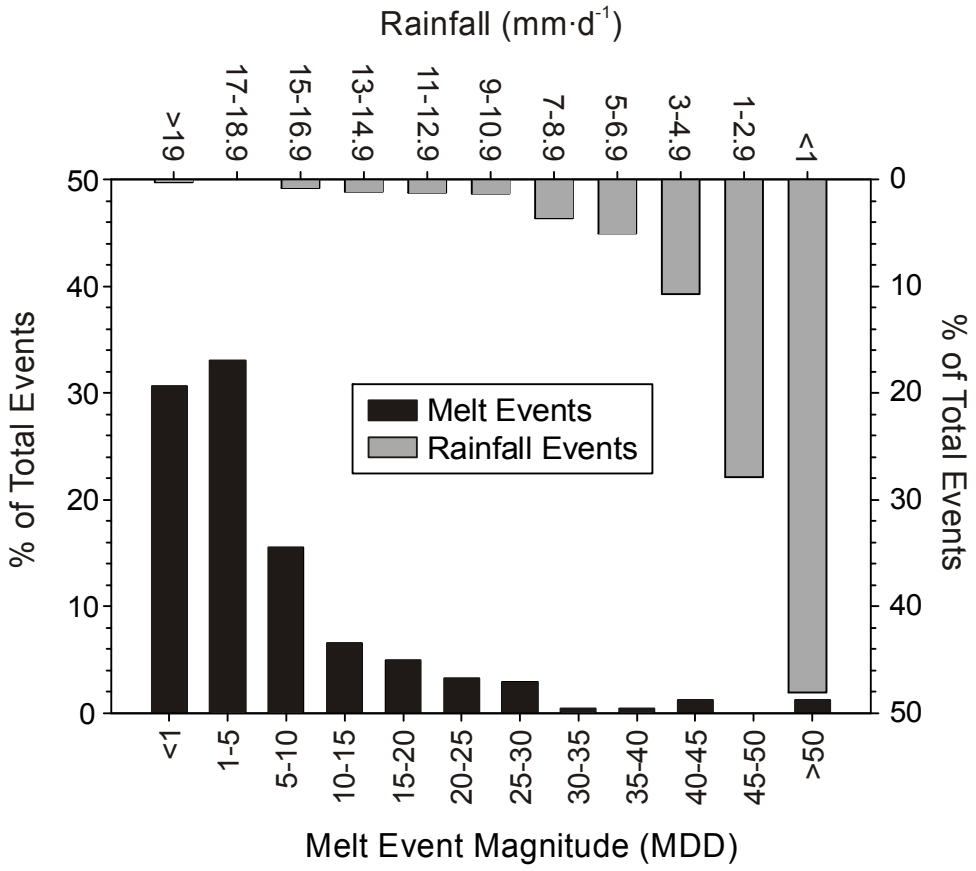
Rainfall (mm·d-1)
>19
17-18.9
15-16.9
13-14.9
11-12.9
9-10.9
7-8.9
5-6.9
3-4.9
1-2.9
<1
% of Total Events
Melt Events
Rainfall Events
<1
1-5
5-10
10-15
15-20
20-25
25-30
30-35
35-40
40-45
45-50
>50
Melt Event Magnitude (MDD)

Figure 6.

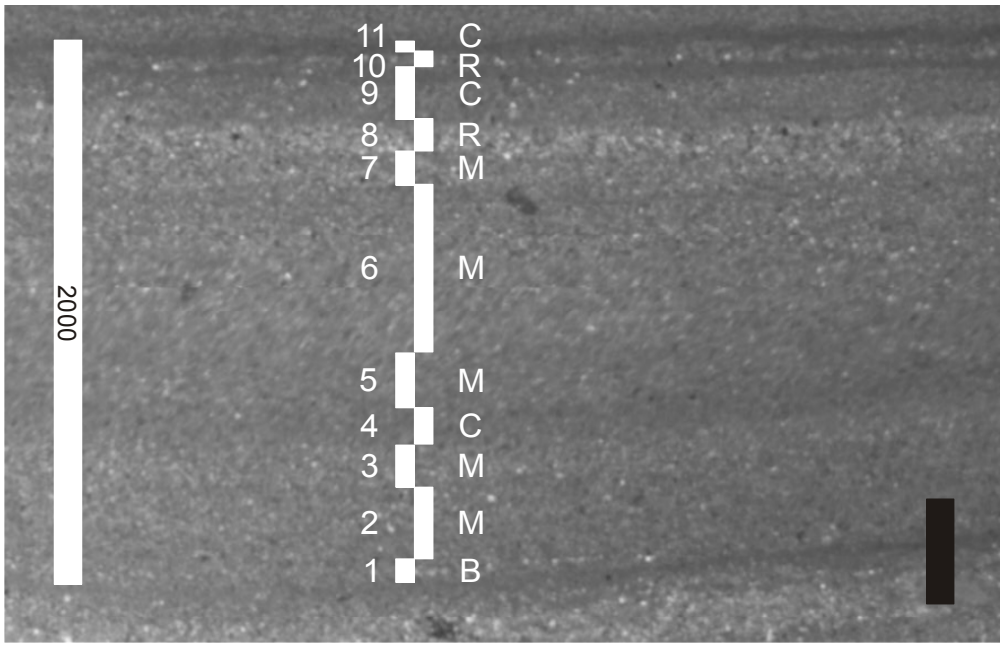

Figure 7.

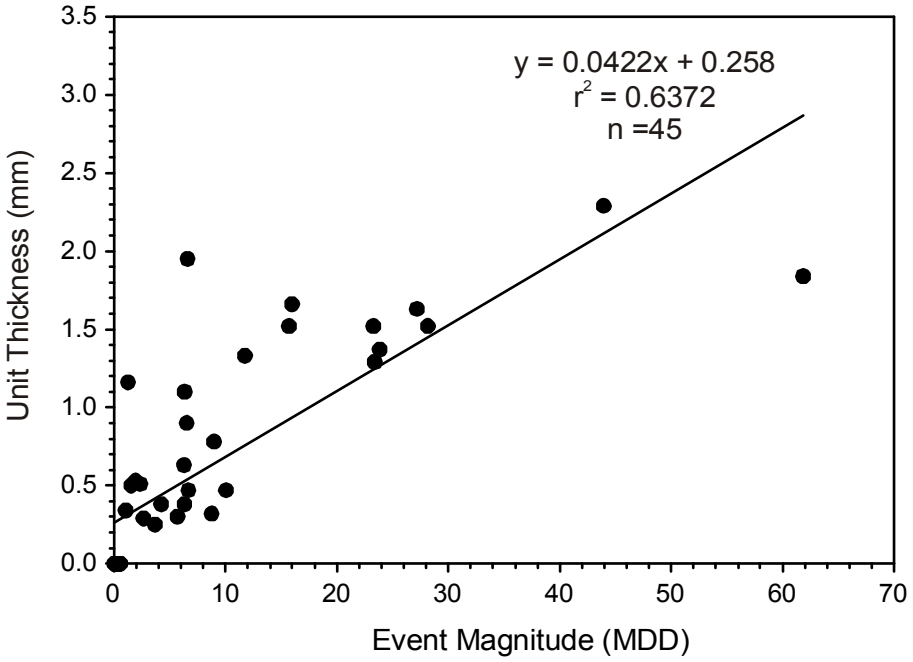
y = 0.0422x + 0.258
r2 = 0.6372
n =45
Unit Thickness (mm)
Event Magnitude (MDD)
0.0
0.5
1.0
1.5
2.0
2.5
3.0
3.5
0
10
20
30
40
50
60
70

Figure 8.

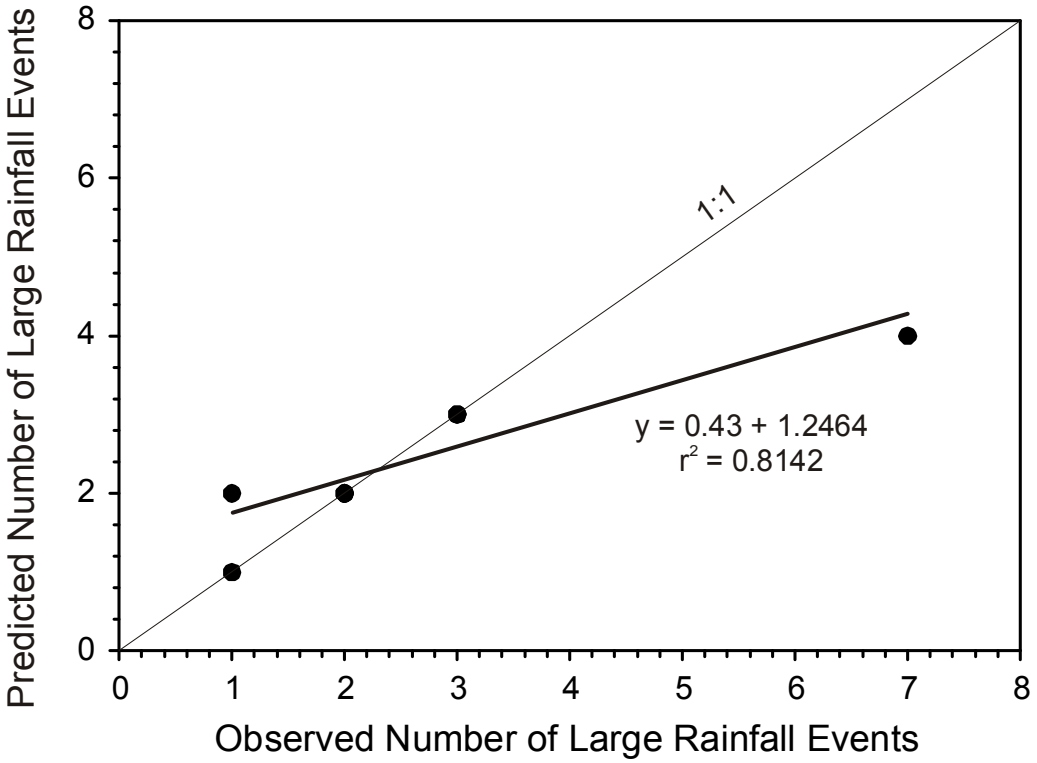
Predicted Number of Large Rainfall Events
Observed Number of Large Rainfall Events
1:1
y = 0.43 + 1.2464
r2 = 0.8142
0
2
4
6
8
0
1
2
3
4
5
6
7
8

Figure 9.

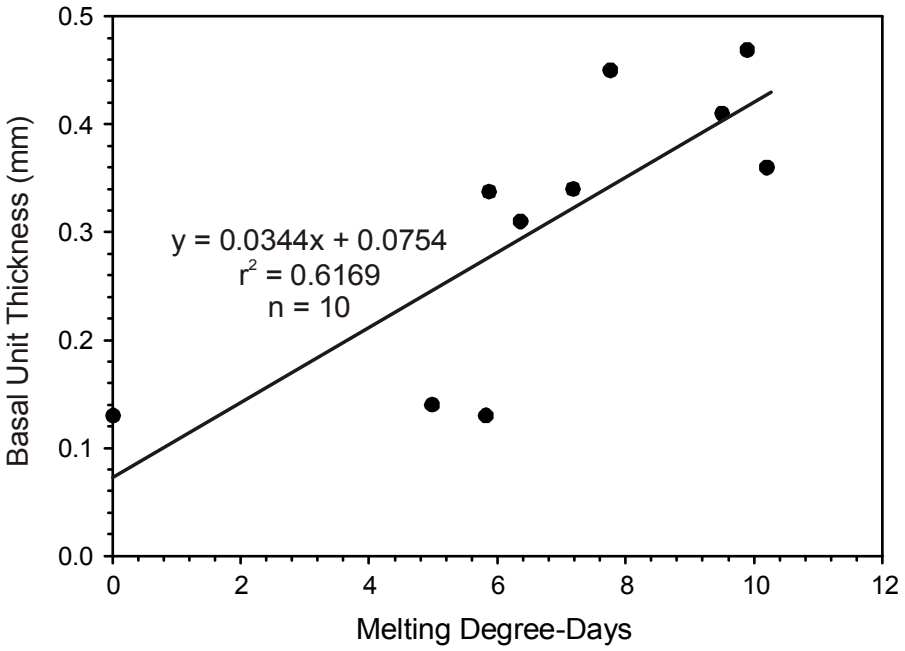
Basal Unit Thickness (mm)
0.0
0.1
0.2
0.3
0.4
0.5
0
2
4
6
8
10
12
Melting Degree-Days
y = 0.0344x + 0.0754
r2 = 0.6169
n = 10

Figure 10.

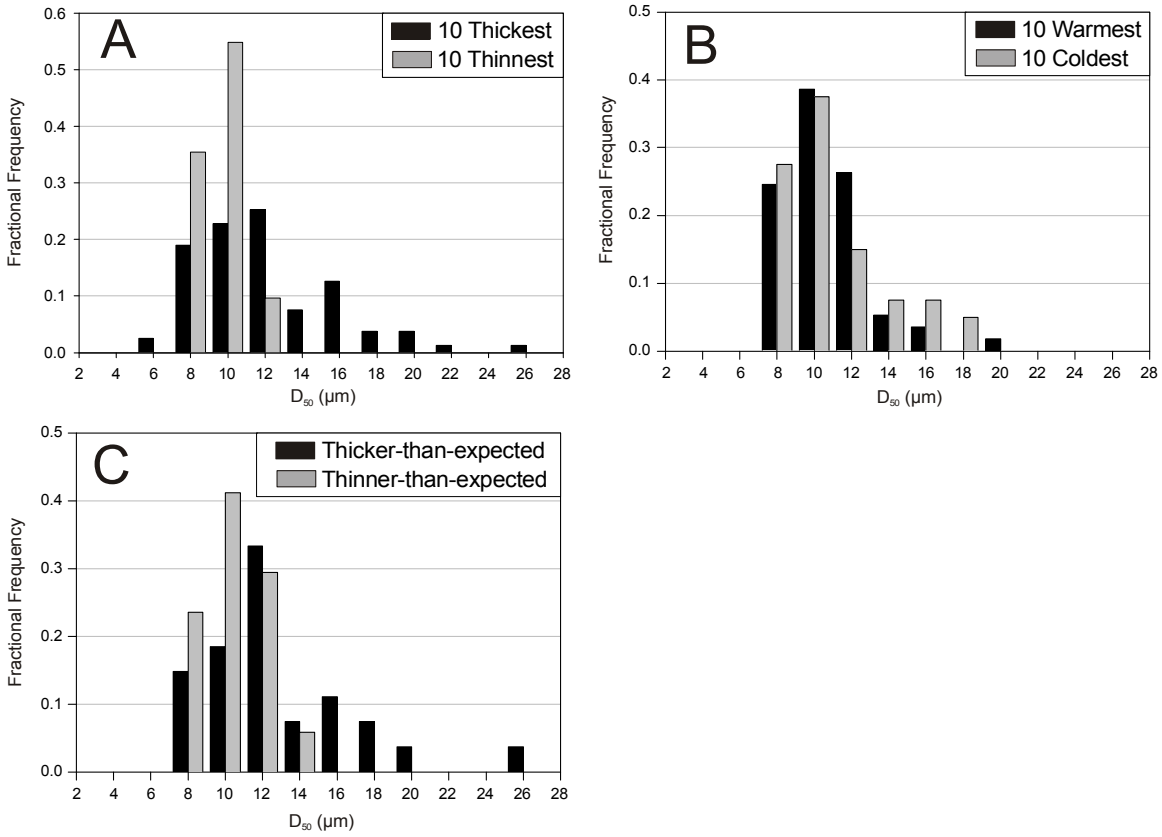
A
10 Thickest
10 Thinnest
Fractional Frequency
D_{50} (μm)
B
10 Warmest
10 Coldest
Fractional Frequency
D_{50} (μm)
C
Thicker-than-expected
Thinner-than-expected
Fractional Frequency
D_{50} (μm)

CHAPTER 3

THE INFLUENCE OF LOW-LEVEL THERMAL INVERSIONS ON ESTIMATED MELT SEASON CHARACTERISTICS IN THE CENTRAL CANADIAN ARCTIC

KRYSTOPHER J. CHUTKO AND SCOTT F. LAMOUREUX

A version of this chapter has been accepted for publication and is currently in press.
Chutko, K.J. and S.F. Lamoureux. In press. The influence of low-level thermal inversions on estimated melt season characteristics in the central Canadian Arctic. *International Journal of Climatology*.

Abstract

Daily vertical temperature gradients were examined in order to infer melt event characteristics at an elevation relevant to basin-scale snow and plateau ice melt studies in the Canadian Arctic. Surface and upper-air temperature data from Resolute, Cornwallis Island, were used to estimate vertical lapse rates up to 300 m asl, and to identify the presence of inversions at that altitude. Lapse rates varied throughout the melt season and were substantially less than typically published generalized values. Thermal inversions were more frequent during the melt season than in the periods immediately before and after, and suggested a strong control on intraseasonal temperature patterns. In July, the period of maximum temperature in the High Arctic, inversion frequency was highest and closely related to calculated melting degree-days. Results showed that increased summer mean temperature resulted in a substantial lengthening of estimated melt events, as opposed to increased event intensity. Increased inversion frequency leading to shallower vertical lapse rates since the late 1980s is speculated to be the result of synoptic scale climate patterns, and is potentially an important meteorological mechanism for enhanced glacial melt since the late 1980s.

1. Introduction

Accurate modelling of glacier mass balance is of increasing concern in light of predictions that future climate warming will be most significant at high latitudes, particularly in the northern hemisphere (Johannessen *et al*., 2004; IPCC, 2007). Meltwater produced as a result of this warming is expected to be a significant contributor to eustatic sea level rise, and the contribution from small ice caps and glaciers may be important (Meier, 1984; Raper and Braithwaite, 2006; IPCC, 2007). The Canadian High Arctic contains the largest area of land ice in the world outside of Greenland and Antarctica, and therefore may play a crucial role in future sea level rise (Gardner and Sharp, 2007). Long term (> 30 years) direct measurement of glacier ablation through mass balance measurements has been performed on only four ice masses in the Canadian Arctic (Koerner, 2002), therefore melt models are an important tool for quantifying total ice melt in the region.

Observations of global glacier mass balance suggest that, with few exceptions, small glaciers and ice caps have been shrinking since at least the early 1960s (Dyurgerov and Meier, 2005). However, since the early 1990s, the rate of glacier mass losses has increased, and the contribution to sea level rise has nearly doubled the mean 1961-2003 rate (Dyurgerov and Meier, 2005). Increased glacier melt has been witnessed in the Canadian Arctic as well (Dyurgerov and McCabe, 2006). Glaciers are considered good indicators of climate change as their growth and decay is sensitive to fluctuations in temperature and precipitation conditions (Cogley *et al*., 1995). The widespread

mass loss from glaciers is among the most visible forms of global climate change in the Canadian Arctic.

Glacial melt in polar regions is strongly related to the duration of the ablation season (Kuhn, 1984). In the Canadian Arctic, the 2000 to 2004 melt season durations were closely related to pressure-related variability of near-surface temperature, and the annual mean melt season duration was positively correlated with the July 500 hPa height, such that high pressure years yielded increased glacier melt at higher elevations (Wang *et al*., 2004). Furthermore, Wang *et al*. (2004) showed that an inverse relationship existed between melt season duration at high and low elevations, and that this could be explained by variations in the vertical gradient of surface air temperatures. Gardner and Sharp (2007) extend these observations over the 1960-2003 period, and show that the variations in the 500 hPa height were driven by the position of the circumpolar vortex.

Estimating air temperature is necessary for many scientific studies, particularly in regions where observational data are sparse, such as the Canadian High Arctic. However, long term Arctic weather monitoring has been carried out in coastal communities that lie at or close to sea level, and therefore may not be climatically representative of the larger region, notably for higher elevation plateau or mountain regions common in the central and eastern Canadian Arctic (Hardy, 1996). Spatial estimation of weather conditions is often accomplished through either extrapolation of temperature from meteorological stations or interpolation of temperature from reanalyzed climatologies or climate models, often with a resolution greater than 10 km^2 (Marshall *et al*., 2007).

Vertical temperature gradients are high and can vary greatly, although they are generally treated with a constant lapse rate of –6 to –8 °C·km^{-1} (e.g., Legates and Willmott, 1990; Walland and Simmonds, 1996; Glover, 1999) that represents a typical moist adiabatic lapse rate (Seidel and Free, 2003).

The use of vertical lapse rates (VLRs) is a common practice throughout much of the modelling literature focused on snow and ice ablation, particularly in glacial environments. For example, Braithwaite *et al*. (2006) used seasonally-fixed VLRs ranging from –5.5 to –7.5 °C·km^{-1} to model winter mass balance at the equilibrium line of 180 glaciers. Marshall *et al*. (2007) identified strong seasonal variability of observed VLRs along a near-surface gradient on Prince of Wales Icefield, Ellesmere Island. Their results suggested that published VLRs were unsatisfactory and did not accurately model near-ice-surface thermal conditions, and that a seasonally fixed value missed the intrannual variability in snow and ice melt. In another study, ice ablation model sensitivity was closely linked to the selection of a vertical lapse rate in Antarctica (Braun and Hock, 2004). By applying a constant VLR of –6.0 °C·km^{-1}, their modelled ice ablation underestimated the observed ablation by one-third. Braun and Hock (2004) also demonstrated the need for seasonally variable VLRs in order to simulate the prevailing weather conditions within a given year.

This study examined the interannual influence that vertical lapse rates have on temperature conditions at the elevation of regional glacier ablation areas. Low altitude lapse rates were calculated from upper-air temperature records from a regionally-based continuous and long term weather monitoring station and used to estimate May through September mean daily temperature at the study

elevation. The objective of this work was to determine whether temporal (interannual and seasonal) variations of vertical lapse rates were reflected in estimates of yearly melt season characteristics and observed glacial melt trends in the Canadian Arctic.

2. Study site and methodology

2.1. Study site

Resolute, Cornwallis Island (74°43.2'N 94°59.4'W) is located in the central Canadian Arctic (Figure 1) and a continuous record of daily surface weather conditions has been maintained since October 1947. Few long term meteorological stations serve the region and none north of 72°N extend earlier than 1947. Similarly, continuous upper-air pressure and temperature data are limited to only a few stations, including Resolute where measurements began in 1961. Rawinsonde ascents are made twice daily at 0000Z and 1200Z (1800h and 0600h local), respectively. Raw upper-air data from 1961 to 2003 were obtained from the Meteorological Service of Canada, Environment Canada. Bradley (1975) demonstrated that the temperature record from Resolute was suitable for modelling glacier mass balance at a regional scale (e.g., Devon Ice Cap, ~350 km east).

Long term mass balance records have been maintained on four ice masses in the Canadian Arctic: White Glacier, Axel Heiberg Island, 1960-2005 (Cogley *et al*., 1996; Dyurgerov and Meier, 2005; WGMS, 2006), Devon Ice Cap, Devon Island, 1961-2001, Meighen Ice Cap, Meighen Island, 1960-2003, and Melville South Ice Cap, Melville Island, 1963-2003 (Koerner, 2002, Dyurgerov

and Meier, 2005) (Figure 1). All glacial mass balance analyses presented here used the period 1963-2001 for maximum record overlap.

An elevation of 300 m asl was chosen for this work as it represents an altitude band which is relevant in terms of watershed-scale snow modelling. Additionally, many glaciers and icefields in the region extend down to this elevation or lower, and therefore this elevation represents a key level of their respective ablation zones. For example, small and dynamic icefields on northern Devon, North Kent, and southwestern Ellesmere Islands extend to this elevation, while the larger Devon Ice Cap and Manson and Prince of Wales Icefields (eastern Ellesmere Island) extend to sea level (Koerner, 2002; Figure 1). Also, Bradley (1972) reported that low-level inversions in July commonly occurred between 65 and 500 m asl, suggesting that this elevation is highly susceptible to variable lapse rate conditions. Also, previous work has shown that the presence of inversions between sea level and 500 m asl (Marsh and Woo, 1981; Hardy, 1996) was an important control on snowmelt in the Canadian Arctic.

2.2. Terminology

Generally, air temperature decreases with elevation, and therefore the lapse rate is usually negative, and the referral to an increase or decrease in the lapse rate can become confusing. This work will follow the terminology used by Pepin and Losleben (2002), where a ‘steep’ lapse rate has a rapid decrease of temperature with elevation, and a ‘shallow’ lapse rate is a less negative or positive lapse rate (a thermal inversion). Inversion frequency is the ratio of days with a recorded inversion to the total number of days in the set.

Further, in order to describe the period of positive temperatures during the course of a year, we use the term ‘melt season’. This represents the length of time (measured in days) from the first day when mean daily temperature exceeded 0 °C to the last, including intervening periods of freezing conditions. The term is based solely on air temperature characteristics, and does not necessarily imply that ice melt occurs in, or is restricted to, this period. Similarly, the term ‘melt event’ is used here to represent a period of continuous positive mean daily temperature. Melt events are defined by their duration (days) and intensity (mean temperature, °C), with the product of these yielding the event magnitude (melting degree-days, MDD).

2.3. Estimating low-level inversion characteristics

Daily lapse rates were calculated using a linear trendline for each ascent from May 1 to Sep 30 of each year, and the mean value for the two daily ascents was used. The lapse rates were calculated using the temperature/elevation data recorded at the station elevation and the first measurement directly above 300 m asl. Station elevation was 66 m asl from 1961 through 1980, 40 m asl from 1981 to June 1999, and 46 m asl from July 1999 through 2003. Due to changes in the rawinsonde equipment, data from 1962 to 1980 were recorded at 50 mbar standard pressure heights, whereas from 1981 to 2003, the data were recorded at 25 mbar standard pressure heights and significant levels (depending on ambient pressure and wind conditions). Therefore, the range of altitudes at which the upper-air temperature data were collected varied considerably (typically comprised of a surface value, the first value above 300 m asl, and one

to three intervening measurements). The calculated daily lapse rate was applied to the respective mean daily surface temperature recorded at Resolute to estimate the temperature at 300 m asl. Daily thermal inversions were identified when the estimated temperature at 300 m asl was greater than that at the surface elevation.

In order to demonstrate the effect that consideration of variable lapse rates had on temperature estimates, calculations were also made using a lapse rate fixed at -6.0 °C·km^{-1}. Mean daily temperature at Resolute was modified with this lapse rate to estimate temperature at 300 m asl.

3. Results

3.1. Lapse rates

The mean daily lapse rate was –2.4 °C·km^{-1} over the 1961-2003 period. When a shorter spring/summer period (21 May – 23 September, see below) was considered, the mean daily lapse rate steepened to –2.8 °C·km^{-1} (Figure 2). Inversion frequencies were substantially lower than those reported for the winter period (Bradley *et al*., 1992), with typical frequencies of between 15 and 40% (Figure 2). A strong relationship between inversion frequency and calculated lapse rate (r^2 = 0.548, n = 42, p < 0.001) demonstrated the important role of inversions on estimated higher elevation temperatures, as opposed to merely shallow negative lapse rates.

Lapse rates were seen to vary systematically during the melt season, and were divided into five periods (Periods I – V; Figure 3). Inversions are common during the arctic winter (e.g., Bradley *et al*., 1992; Serreze *et al*., 1992), and were

observed to continue into mid-May (Period I), when inversion frequency is high (43%). However, since the mean daily surface temperature at Resolute during the first 20 days of May is –12.8 °C, the inversions did not lead to positive temperatures at 300 m asl at that time of the season. Mean lapse rates steepened (mean VLR = -2.96 °C·km^{-1}) during Period II as spring progressed, from mid-May to late June. In many cases, the relatively steep lapse rates prolonged negative temperatures during this time of year. Period III, during the main summer period (late-June – mid-August), experienced shallower lapse rates (mean VLR = -1.95 °C·km^{-1}), and was the primary period of positive temperatures and inferred melt conditions at 300 m asl. Lapse rates steepened (mean VLR = -3.69 °C·km^{-1}) again during Period IV in the late summer (mid-August – late-September). In years where shallow lapse rates or inversions occurred during this period, the melt season was prolonged. The onset of Period V and early winter conditions was characterized by shallower lapse rates (mean VLR = -2.36 °C·km^{-1}) at the end of September. Difference-of-means tests were performed to identify significant differences between the periods (Table 1). The transition dates were selected based on observed points of inflection in the data series and are listed in Table 1.

Vertical lapse rates varied temporally, both between and within years. Interannual variations suggested that VLRs demonstrate a quasi-decadal oscillation, being generally shallower in the 1970s and 1990s and steeper in the 1960s and 1980s (Figure 4). From 1989 to 2003, 10 of 15 years exhibited positive lapse rate anomalies, and substantial positive anomalies (>1.0 σ) occurred in six years. By comparison, in the previous 28 years only three years

exhibited anomalies >1.0 σ. Substantial negative anomalies (< -1.0 σ) occurred in 6 years from 1961-1988 and once from 1989 to 2003.

3.2. Temperature

Mean daily surface temperature at Resolute was –2.02 °C for May through September, 1961-2003. Estimated mean daily temperature at 300 m asl (May – September, 1961-2003) was –2.48 °C with an annual mean of 205.0 total melting degree-days (MDD). The shorter spring/summer period (May 21 – September 23) yielded a mean daily temperature at 300 m asl of –0.60 °C. The occurrence of positive mean daily temperature outside of the May 21 – September 23 period was rare (four out of 1204 days) and did not contribute substantially to the total annual MDD value.

When compared to estimates of temperature at 300 m asl produced by applying a –6 °C·km^{-1} fixed lapse rate, the importance of shallow lapse rates was apparent. Calculated mean increases of annual and July MDD were 68% and 55%, respectively. Additionally, the simulated mean melt season length increased from 70 to 88 days for the fixed and variable lapse rate calculations, respectively. The proportion of days with positive temperatures within the melt season was similar (66% and 68% for variable and fixed, respectively) between the two lapse rate methods.

To evaluate the difference in melt season characteristics between warm and cold years, we used the five coldest and five warmest (based on total MDD) years in the 1961-2003 record and examined the characteristics of the melt events for those years (Table 2). Results show that the mean daily temperature

(May – September) was 2.5 °C greater for the warm years compared to the cold years, and the former exhibited decreased frequency (-17%) and an increased duration (+56%) and intensity (+121%) of melt events (Figure 5). The decreased frequency was a function of a combination of smaller events that increased duration of the melt events overall.

Comparison between the pattern of melt events and the occurrence of thermal inversions suggested that the latter may also effectively determine the length of the melt season. In most years, the melt season was bracketed by extended periods with few or no inversions (e.g., Figure 6). From 1961-2003, inversion frequency during the melt season was 29.3% and 32.3% during July, while inversion frequency for the ten days immediately before and immediately after the melt season was 24.4% and 9.8%, respectively. These periods also experienced moderate negative temperatures (mean temperature = -4.5 °C), and it is possible that, if an inversion had occurred, these days would have experienced positive temperatures, and thus extended the duration of the melt season.

Correlation between inversion frequency and total melting degree-days was weak although significant (r^2 = 0.12, n = 43, p < 0.001). Observations of the timing of thermal inversions suggested that positive lapse rates were an important source of the estimated increased melt energy availability (Figure 6). Thermal inversions (VLR > 0) occurred sporadically throughout the melt season and were coincident with periods of positive temperatures (melt events). The linkage between thermal inversions and increased MDD was two-fold. First, the inversion raised pre-existing sea level positive temperatures to ultimately

increase the melt event intensity. Second, inversions increased slightly negative sea level temperatures above 0 ºC to effectively increase the duration of melt events, or to combine two or more events into one. Together, these acted to raise the overall magnitude of the estimated melt events and reduce the frequency of lower intensity events.

3.3. Glacier mass balance

Observations from Canadian Arctic ice masses show substantially increased rates of mass loss in the 1987-2001 period (Figure 7). The mean rate of mass loss increased from –0.07 $m_{swe} \cdot a^{-1}$ (1963-1986) to –0.20 $m_{swe} \cdot a^{-1}$ (1987-2001). Similarly, the period 1987-2001 exhibited only four years where standardized mass balance anomalies were positive compared to 20 in the 1963-1986 period (Gardner and Sharp, 2007). These changes appear to be mainly driven by increased summer ablation, as opposed to decreased winter accumulation, given that the net mass balance on the Devon Ice Cap was strongly correlated with the summer balance (r^2 = 0.974, n = 40, p < 0.001) and only weakly with the winter balance (r^2 = 0.060, n = 40, p < 0.05).

4. Discussion

4.1. Seasonally variable vertical lapse rates

The results from this study to estimate air temperature at low elevations reinforce concerns raised about the use of fixed lapse rates based on generalized conditions (e.g., Legates and Willmott, 1990; Walland and Simmonds, 1996; Glover, 1999; Braithwaite *et al*., 2006). Observational data in this study yielded

mean lapse rates that were substantially shallower than the typically applied -6 – -8 °C·km^{-1}. These results suggest the need for use of local, specific VLRs in studies where vertical temperature estimation is necessary. This builds on similar results by Braun and Hock (2004) and Marshall *et al*. (2007) where seasonal variations were identified to play important roles in influencing snow and ice melt. Fixed lapse rates would not be able to accurately estimate the rate of surface melt where temperature at higher elevations regularly fluctuates around the freezing point throughout the summer, and slight changes in temperature may substantially influence melt. Consideration of daily lapse rates potentially allows for more accurate modelling of temperature at higher elevations above meteorological data collected near sea level by factoring in rapid changes in the vertical temperature profile that are otherwise missed by less-rigourous methods of evaluation. These results also illustrated the important seasonal patterns in the central Canadian High Arctic, where lapse rates may shift significantly for extended periods of time, and that periodic thermal inversions play an important role in warmer surface temperatures at elevations above sea level.

The inclusion of these observations in snow/ice melt models may result in significantly higher rates of melt than otherwise estimated. Temperature index and degree-day models are based upon the known relationship between snow/ice melt and air temperature (Hock, 2003). Also, degree-day factors tend to be site specific, as variations in slope, aspect, and time of day can substantially affect the model parameters, and therefore typical degree-day factors are adequate for average conditions only (Hock, 2003). Degree-day factors are often obtained from optimization procedures in order to minimize discrepancies

between model results and observations, and an accurate evaluation of vertical lapse rates is important in this process (Braun and Hock, 2004). Application of these models typically use available air temperature data, potentially from a single site from which temperature is extrapolated across a given area (e.g., catchment, ice mass). Again, an understanding of vertical lapse rates, both their magnitude and temporal variation, is necessary in order to accurately determine snow and ice ablation.

While previous studies (e.g., Marshall *et al*., 2007) used locally measured vertical temperature profiles, this work used a regional weather station as a source of temperature data. Validation of the results presented in this study is prevented due to the lack of observational data at a specific location. However, this issue is a reality in a number of remote High Arctic studies, as site-specific data tends to be spatially and temporally restricted, which necessitates the use of weather data from the surrounding region (e.g., Bradley and Serreze, 1987; Hardy, 1996). Nonetheless, the importance of seasonally variable lapse rates in defining the melt season characteristics as reported here is consistent with previously published reports of the influence of variable lapse rates on surface ice melt (Braun and Hock, 2004; Marshall *et al*., 2007).

4.2. Annual characteristics of vertical lapse rates and melt events

Shallow vertical lapse rates, particularly the occurrence of thermal inversions, played critical roles and substantially defined the characteristics and timing of the inferred melt seasons at 300 m asl. Shallow lapse rates enhanced the magnitude and duration of melt events beyond that estimated with

generalized lapse rates. Furthermore, positive lapse rates (inversions) created new melt events from previously freezing conditions or combined several melt events into a single longer event. The timing of inversions was also influential in defining the beginning and end of the melt season. Onset of the melt season was delayed in many cases by extended periods of steeper (negative) lapse rates in the spring of most years (Figure 3). Similarly, the end of the melt season was marked by decreased inversion frequency and steeper lapse rates.

Melt event characteristics are strongly influenced by air temperature during the melt season. As the mean temperature increases, the duration of the melt event lengthens at a greater rate than the mean event intensity increases (Figure 5). These observations may also be applied to understand the impact of potential future climate warming in the arctic. The observed mean daily temperature increase between the five coldest and warmest years was 2.5 °C, while a 3 – 5 °C increase by 2090 has been projected for the Arctic (ACIA, 2004). A substantial lengthening of the melt season in a warmer future could potentially increase terrestrial snow and ice melt (Kuhn, 1984; Hooke et al., 1987), as well as sea ice melt, beyond that which is predicted by an increased summer mean temperature. These results suggest a wide range of changes to the melt season characteristics that need to be considered to accurately model the response of ice and snow melt to future climate changes.

In glacial environments, modification of near-surface temperatures as a result of the cooling effect of the ice surface has been demonstrated (Havens et al., 1965; Bradley and Serreze, 1987). Although this modification has not been considered here, it should be noted that a reduction of 3 °C (e.g., Havens et al.,

1965; Atkinson and Gajweski, 2000) results in a 64% decrease in the calculated average annual MDD. Bradley and Serreze (1987) suggest that the ice cooling factor is somewhat less than this. Regardless, this reduction strongly influences the characteristics of the melt season and events, although the influence of shallow lapse rates and inversions is not diminished (Chutko, unpublished data).

4.3. Trends in vertical lapse rates, 1961-2003

Since observations began at Resolute in 1961, the characteristics of vertical lapse rates in the central Canadian High Arctic can be divided into three distinct periods (Figure 2). From 1961-1974, lapse rates fluctuated around the long term (1961-2003) mean value of –2.8 °C·km^{-1}. From 1975-1988, lapse rates were consistently lower than the long term mean, while from 1989-2003, lapse rates were generally above the mean. We note that the distinction of these periods is coincident with known regime shifts in the Pacific Decadal Oscillation in 1976 (Mantua et al., 1997) and the North Atlantic Oscillation (Hurrell, 1995) and Arctic Oscillation in 1989 (Thompson and Wallace, 1998), as well as regime shifts in Arctic annual sea level pressures (Walsh et al., 1996) and Northern Hemisphere snow extent (Robinson and Frei, 2000) in 1987.

July is the warmest month in the Canadian High Arctic, and therefore it is expected that the temperature characteristics during the month are important for ice melt in the region (Bradley, 1975). Increased inversion frequency in July since 1988 is reflected as increased MDD estimated at 300 m asl (Figure 8). This suggests a greater potential for ice melt during this period than in prior years.

4.4. Synoptic controls over lapse rates and ice melt

The synoptic climatology of the Arctic is dominated by the circumpolar vortex, which is a product of Earth's rotation and the temperature differential between arctic and equatorial regions (Maxwell, 1980) and is present year round in the troposphere (Serreze and Barry, 2005). Alt (1978, 1979, 1987) showed that mass balance conditions for several ice masses in the Canadian Arctic were related to the shape and position of the circumpolar vortex. The vortex can be centered in the eastern (i.e., Siberia) or western (i.e., Ellesmere Island) hemispheres (Gardner and Sharp, 2007). When centered over northern Canada in summer, the vortex blocks northward moving warm air masses and maintains cooler surface air temperatures. However, when centered over Siberia, warm air masses can penetrate into the Canadian Arctic and lead to anomalously warm air temperatures (Alt, 1987; Gardner and Sharp, 2007).

Alt (1987) examined the synoptic conditions during the 1964 melt season in detail. This particular year was notable as a highly positive mass balance year for Arctic ice masses (Figure 7). Our analysis indicates that this year also experienced below mean inversion frequency (Figure 2). Alt's (1987) results described a number of storm tracks originating in the Arctic Ocean during July 1964, which moved southward over the Arctic Archipelago. This pattern resulted in colder than usual conditions in the Arctic, along with above normal summer snowfall. As the storms crossed over or near to Resolute, inversions were largely absent. Similarly, the early summer (June) of 1972 experienced persistent northwesterly winds (Alt, 1987) and initiation of the inferred melt season was delayed until June 28 (20 days later than the estimated mean start date). In the

preceeding three weeks, inversions were absent. These synoptic conditions were the result of the circumpolar vortex being positioned in the eastern hemisphere (Alt, 1987).

The incursion of warm air masses from the south is potentially one mechanism that causes thermal inversions. Maxwell (1980) described a thin layer of cold air which covers the landscape year round in the Arctic. As frontal systems move northward, they travel above this layer, leaving colder conditions at ground level and warmer conditions aloft (Maxwell, 1980). The timing of thermal inversions may therefore also be a surrogate indicator of warm air incursions into the region.

Gardner and Sharp (2007) reported a 40% decrease in the occurrence of the western-centered circumpolar vortex since 1987. We speculate that this shift in the circumpolar vortex increased the number of warm air incursions that led to increased inversion frequency, and ultimately, the enhanced surface melt in the 1987-2003 period reported by Gardner and Sharp (2007). These observations of synoptic changes were consistent with the results presented in this study and provide a possible mechanism to explain the temporal pattern of the VLR observations at Resolute. Regime shifts of arctic sea level pressure (Walsh *et al*., 1996) and northern hemisphere snow extent (Robinson and Frei, 2000) also occurred in the late 1980s and indicate the regional impact of the synoptic-scale climate shifts described by Gardner and Sharp (2007).

We speculate that the increased inversion frequency since the late 1980s, potentially caused by decreased prevalence of western hemisphere circumpolar vortex activity during the same period, resulted in summer temperatures at higher

elevations that are above those that would be inferred from sea level conditions, and provides a climatic mechanism to which the increased ice ablation can be attributed.

5. Conclusions

Variable vertical lapse rates were seen to have strong inter- and intra-annual influences on estimated temperature conditions at low elevations. Temperature was estimated at 300 m asl, an elevation relevant to watershed-scale snow and ice melt modelling. Seasonal variations suggested that thermal inversions were critical in defining the length of the melt season as well as the intensity and duration of individual melt events. Warmer summers experienced substantially more frequent thermal inversions and resultant longer periods of positive temperatures than cooler summers in the 1961-2003 period, and may continue to lengthen with the anticipated future climate change.

Interannual variations of vertical lapse rates appear to be closely related to synoptic scale changes of weather. We speculate that increased inversion frequency since the late 1980s is the result of increased warm air incursions into the High Arctic as a product of the relatively low incidence of a western hemisphere centered circumpolar vortex in the same time period. The increased inversion frequency also correlates well with the increased incidence of highly negative glacier mass balance observations in the Arctic. Therefore, we suggest that shallow lapse rates, especially thermal inversions, resulted in increased melting degree-days and hence explain a substantial proportion of the regime shift in glacier ablation and mass balance observed in the late 1980s.

Acknowledgements

This work was supported by ArcticNet, a Network of Centres of Excellence of Canada, a Natural Sciences and Engineering Research Council of Canada Discovery Grant to S.F.L. and Northern Scientific Training Program and Queen's University Graduate Travel grants to K.J.C. M. Sharp provided valuable comments and suggestions during the development of this work. Comments from two anonymous reviewers greatly improved the manuscript. This is PCSP contribution 028-07.

References

Alt, BT. 1978. Synoptic climate controls of mass balance variations on Devon Ice Cap. *Arctic and Alpine Research* **10**: 61-80.

Alt, BT. 1979. Investigation of summer synoptic climate controls on the mass balance of Meighen Ice Cap. *Atmosphere-Ocean* **17**: 181-199.

Alt, BT. 1987. Developing synoptic analogs for extreme mass balance conditions on Queen Elizabeth Island ice caps. *Journal of Climate and Applied Meteorology* **26**: 1605-1623.

Arctic Climate Impact Assessment (ACIA). 2004. *Impacts of a Warming Arctic*. Cambridge UP: Cambridge.

Atkinson DE, Gajewski K. 2002. High-resolution estimation of summer surface air temperature in the Canadian Arctic Archipelago. *Journal of Climate* **24**: 3601-3614.

Bradley RS. 1972. The problem of inversions in estimating the height of glaciation limits in Arctic regions. *Arctic and Alpine Research* **4**: 359-360.

Bradley RS. 1975. Equilibrium-line altitudes, mass balance, and July freezing-level heights in the Canadian High Arctic. *Journal of Glaciology* **14**: 267-274.

Bradley RS, Keimig FT, Diaz HF. 1992. Climatology of surface-based inversions in the North American Arctic. *Journal of Geophysical Research* **97**: 15699-15712.

Bradley RS, Serreze MC. 1987. Topoclimatic studies of a High Arctic plateau ice cap. *Journal of Glaciology* **33**: 149-158.

Braithwaite RJ, Raper SCB, Chutko K. 2006. Accumulation at the equilibrium-line of glaciers inferred from a degree-day model and tested against field observations. *Annals of Glaciology* **43**: 329-334.

Braun M, Hock R. 2004. Spatially distributed surface energy balance and ablation modelling on the ice cap of King George Island (Antarctica). *Global and Planetary Change* **42**: 45-58.

Cogley JG, Adams WP, Ecclestone MA, Jung-Rothenhäusler F, Ommanney CSL. 1995. *Mass Balance of Axel Heiberg Island Glaciers, 1960-1991: A Reassessment and Discussion*. Saskatoon, SK, Environment Canada, National Hydrological Reseach Institute. (NHRI Science Report No. 6.)

Cogley JG, Adams WP, Ecclestone MA, Jung-Rothenhäusler F, Ommanney CSL. 1996. Mass balance of White Glacier, Axel Heiberg Island, NWT, Canada, 1960-1991. *Journal of Glaciology* **42**: 548-563.

Dyurgerov MB, Meier MF. 2005. *Glaciers and the changing Earth system: a 2004 snapshot*. Occasional Paper No. 58. Institute of Arctic and Alpine Research, University of Colorado, Boulder.

Dyurgerov MB, McCabe GJ. 2006. Associations between accelerated glacier mass wastage and increased summer temperature in coastal regions. *Arctic, Antarctic, and Alpine Research* **38**: 190-197.

Gardner AS, Sharp M. 2007. Influence of the arctic circumpolar vortex on the mass balance of Canadian High Arctic glaciers. *Journal of Climate* **20**: 4586-4598.

Glover RW. 1999. Influence of spatial resolution and treatment of orography on GCM estimates of the surface mass balance of the Greenland Ice Sheet. *Journal of Climate* **12**: 551-563.

Hardy DR. 1996. Climatic influences on streamflow and sediment flux into Lake C2, northern Ellesmere Island, Canada. *Journal of Paleolimnology* **16**: 133-149.

Havens JM, Müller F, Wilmot GC. 1965. *Comparative meteorological survey and a short term heat balance study of the White Glacier, summer 1962*. Axel Heiberg Island Research Reports – Meteorology No. 4. McGill University, Montréal.

Hock R. 2003. Temperature index melt modelling in mountain areas. *Journal of Hydrology* **282**: 104-115.

Hooke RB, Johnson GW, Brugger KA, Hanson B, Holdsworth G. 1987. Changes in mass balance, velocity, and surface profile along a flow line on Barnes Ice Cap, 1970-1984. *Canadian Journal of Earth Sciences* **24**: 1550-1561.

Hurrell JW. 1995. Decadal trends in the North Atlantic Oscillation: regional temperatures and precipitation. *Science* **269**: 676-679.

Intergovernmental Panel on Climate Change (IPCC). 2007. *Climate Change 2007 – The Physical Science Basis*. Cambridge UP: Cambridge.

Johannessen OM, Bengtsson L, Miles MW, Kuzmina S, Semenov VA, Alekseev GV, Nagurnyi AP, Zakharov VF, Bobylev LP, Pettersson LH, Hasselmann K, Cattle HP. 2004. Arctic climate change: observed and modelled temperature and sea-ice variability. *Tellus* **56A**: 328-341.

Koerner RM. 2002. Glaciers of the High Arctic Islands. In *Glaciers of the Arctic Islands*. Williams RS, Ferrigno JG (eds.). United States Geological Survey Professional Paper 1386-J-1: J111-J146.

Kuhn M. 1984. Mass budget imbalances as criterion for a climatic classification of glaciers. *Geografiska Annaler* **66A**: 229-238.

Legates DR, Willmott CJ. 1990. Mean seasonal and spatial variability in global surface air temperature. *Theoretical and Applied Climatology* **41**: 11-21.

Mantua NJ, Hare SR, Zhang Y, Wallace JM, Francis RC. 1997. A Pacific interdecadal climate oscillation with impacts on salmon production. *Bulletin of the American Meteorological Society* **78**: 1069-1079.

Marsh P, Woo M-K. 1981. Snowmelt, glacier melt and high arctic streamflow regimes. *Canadian Journal of Earth Sciences* **18**: 1380-1384.

Marshall SJ, Sharp MJ, Burgess DO, Anslow FS. 2007. Near-surface-temperature lapse rates on the Prince of Wales Icefield, Ellesmere Island, Canada: implications for regional downscaling of temperature. *International Journal of Climatology* **27**: 385-398.

Maxwell JB. 1980. *The climate of the Canadian Arctic Islands and adjacent waters: Climatological Studies No. 30. Vol. 1*. Atmospheric Environmental Services, Environment Canada.

Meier MF. 1984. Contribution of small glaciers to global sea level. *Science* **226**: 1418-1421.

Pepin N, Losleben M. 2002. Climate change in the Colorado Rocky Mountains: free air versus surface temperature trends. *International Journal of Climatology* **22**: 311-329.

Raper SCB, Braithwaite RJ. 2006. Low sea level rise projections from mountain glaciers and ice caps under global warming. *Nature* **439**: 311-313.

Robinson DA, Frei A. 2000. Seasonal variability of northern hemisphere snow extent using visible satellite data. *Professional Geographer* **52**: 307-315.

Seidel DJ, Free M. 2003. Comparison of lower-tropospheric temperature climatologies and trends at low and high elevation radiosonde ascents. *Climatic Change* **59**: 53-74.

Serreze MC, Barry RG. 2005. *The Arctic Climate System*. Cambridge UP: Cambridge.

Serreze MC, Kahl JD, Schnell RC. 1992. Low-level temperature inversions of the Eurasian Arctic and comparisons with Soviet drifting station data. *Journal of Climate* **5**: 615-629.

Thompson DWJ, Wallace JW. 1998. The Arctic Oscillation signature in the wintertime geopotential height and temperature fields. *Geophysical Research Letters* **25**: 1297-1300.

Walland DJ, Simmonds I. 1996. Sub-grid-scale topography and the simulation of northern hemisphere snow cover. *International Journal of Climatology* **16**: 961-982.

Walsh JE, Chapman WL, Shy TL. 1996. Recent decrease of sea level pressure in the central Arctic. *Journal of Climate* **9**: 480-486.

Wang L, Sharp MJ, Rivard B, Marshall S, Burgess D. 2005. Melt season duration on Canadian Arctic ice caps, 2000-2004. *Geophysical Research Letters* **32**: L19502. DOI: 10.1029/2005GL023962.

World Glacier Monitoring Service (WGMS). 2006. *Glacier mass balance data 2003/2004 and 2004/2005* [online]. Available from *http://www.geo.unizh.ch/wgms/mbb/mbb9/sum05.html* [accessed June 13 2007].

Table 1. Results of difference-of-means tests for interannual periods of VLRs. All tests were performed with Student's *t*-distribution and assume unequal variances, an expected mean difference = 0, and $\alpha = 0.05$. Calculated *t*-statistics and *p*-values are shown in upper-right and lower-left portions of the table, respectively.

Period	I	II	III	IV	V
I	---	5.39	3.86	6.66	4.02
II	2.39×10^{-5}	---	-5.32	4.13	-1.58
III	9.72×10^{-4}	1.24×10^{-6}	---	12.04	1.14
IV	1.73×10^{-6}	1.18×10^{-4}	3.26×10^{-20}	---	-3.72
V	4.76×10^{-4}	0.149	0.291	7.41×10^{-3}	---

Table 2. Characteristics of the five coldest and five warmest (based on total MDD) years, 1961-2003. Results represent estimates of temperature conditions at 300 m asl. Mean daily temperature is for May 1 – September 30.

	Year	Mean Daily Temperature	Total MDD	Number of Melt Events
Warm conditions	1998	+0.7	382.5	7
	1962	-1.5	334.7	7
	1988	-1.5	298.2	5
	1973	-1.5	297.3	7
	2000	-2.2	282.8	13
Cold conditions	1976	-3.4	122.2	13
	1972	-4.5	108.3	7
	1967	-3.3	102.8	12
	1964	-3.4	98.5	8
	1986	-4.1	86.1	7

Figure Captions

Figure 1. The Canadian Arctic Archipelago, with the location of four ice masses referred to in this work: 1) Melville South Ice Cap; 2) Meighen Ice Cap; 3) White Glacier; 4) Devon Ice Cap. Resolute is identified by the black circle. The box identifies the location of minor icefields with ablation zones below 300 m asl.

Figure 2. Calculated mean vertical lapse rate and inversion frequency between surface and 300 m asl, 1961-2003. The values are for the May 21 – September 23 period only.

Figure 3. Mean daily vertical lapse rate, 1961-2003. Gray line is the mean daily lapse rate record, the black line is the 5-day unweighted mean. I: May 1 – May 20 (mean = 0.47 °C·km-1), II: May 21 – June 25 (mean = -2.96 °C·km^{-1}), III: June 26 – August 13 (mean = -1.95 °C·km^{-1}), IV: August 14 – September 23 (mean = -3.69 °C·km^{-1}), V: September 24 – September 30 (mean = -2.36 °C·km^{-1}). Period mean lapse rates are horizontal dashed lines.

Figure 4. Melt season vertical lapse rate anomalies, 1961-2003. Values are standardized to the 1961-2003 mean.

Figure 5. Observed changes of melt event characteristics between the warmest five years and the coldest five years in the 1961-2003 Resolute record. The observed estimated temperature increase was 2.5 °C. The calculations reflect estimated conditions at 300 m asl.

Figure 6. Melt season schematic for 1980 estimated at 300 m asl. Black bars indicate melt events and gray bars indicate inversions. Note the higher inversion frequency during the melt season as opposed to the periods before and after the melt season.

Figure 7. Inversion frequency and cumulative mass balance of four Canadian Arctic ice masses, 1963-2001. The increased rate of mass loss since the regime shift in 1987 (Gardner and Sharp, 2007) is indicated by the increased slope of the 1987-2001 mean line. Inversion frequency is distributed around the 1961-2003 mean value.

Figure 8. July inversion frequency and melting degree-day anomalies, 1961-2003.

Figure 1.

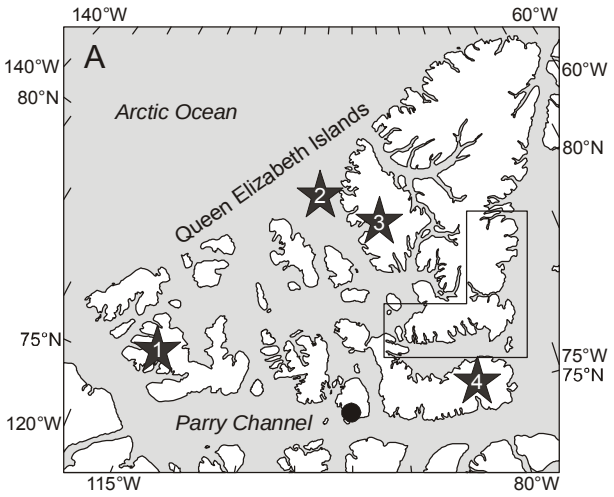
140°W
60°W
A
140°W
80°N
Arctic Ocean
Queen Elizabeth Islands
60°W
80°N
2
3
75°N
1
4
75°W
75°N
120°W
Parry Channel
115°W
80°W

Figure 2.

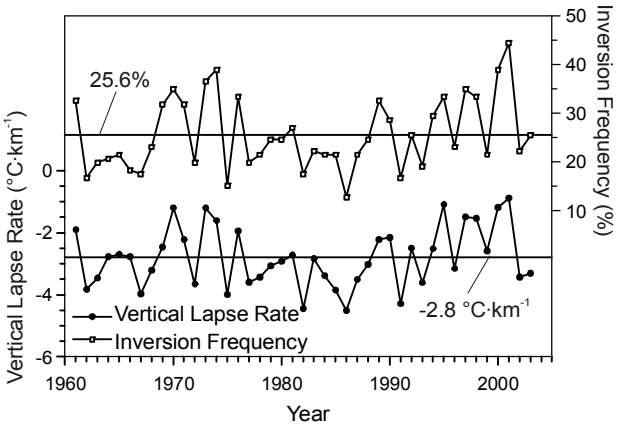
Vertical Lapse Rate (°C·km-1)
Inversion Frequency (%)
Year
25.6%
-2.8 °C·km-1
Vertical Lapse Rate
Inversion Frequency
50
40
30
20
10
0
-2
-4
-6
1960
1970
1980
1990
2000

Figure 3.

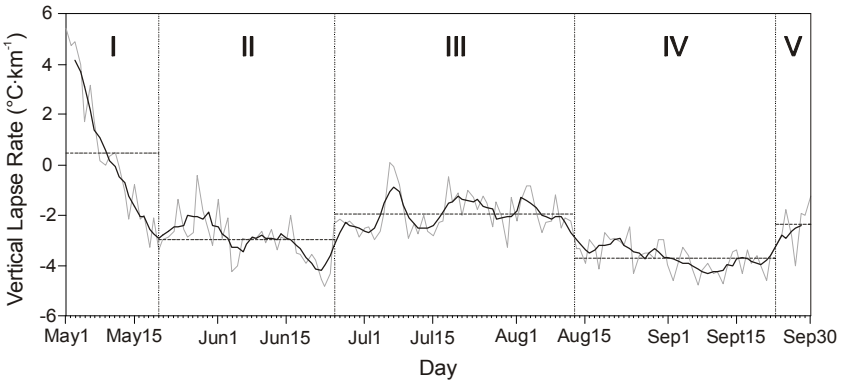
I
II
III
IV
V
Vertical Lapse Rate (°C·km-1)
6
4
2
0
-2
-4
-6
May1
May15
Jun1
Jun15
Jul1
Jul15
Aug1
Aug15
Sep1
Sept15
Sep30
Day

Figure 4.

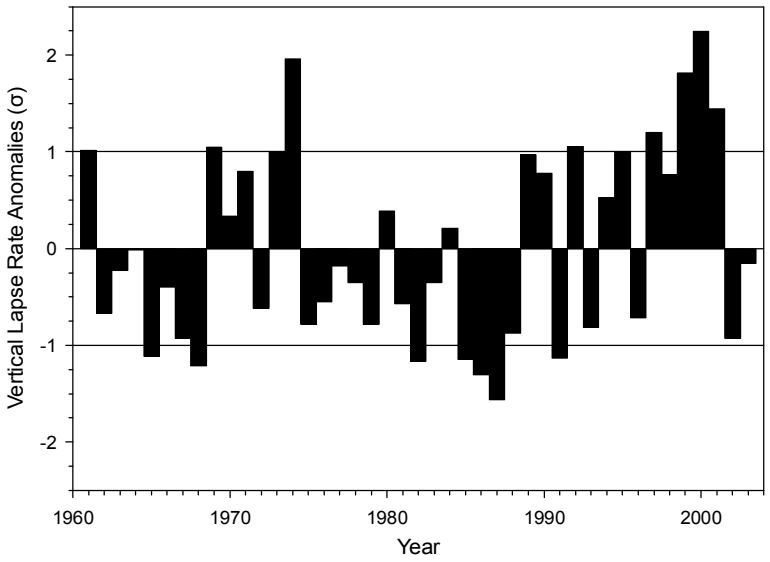
Vertical Lapse Rate Anomalies (σ)
2
1
0
-1
-2
1960
1970
1980
1990
2000
Year

Figure 5.

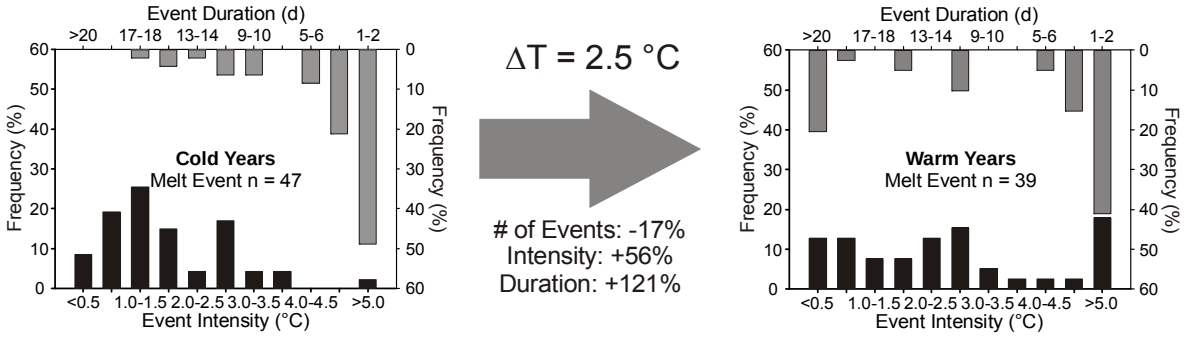
Event Duration (d)
>20
17-18
13-14
9-10
5-6
1-2
Frequency (%)
Cold Years
Melt Event n = 47
<0.5
1.0-1.5
2.0-2.5
3.0-3.5
4.0-4.5
>5.0
Event Intensity (°C)
ΔT = 2.5 °C
# of Events: -17%
Intensity: +56%
Duration: +121%
Warm Years
Melt Event n = 39

Figure 6.

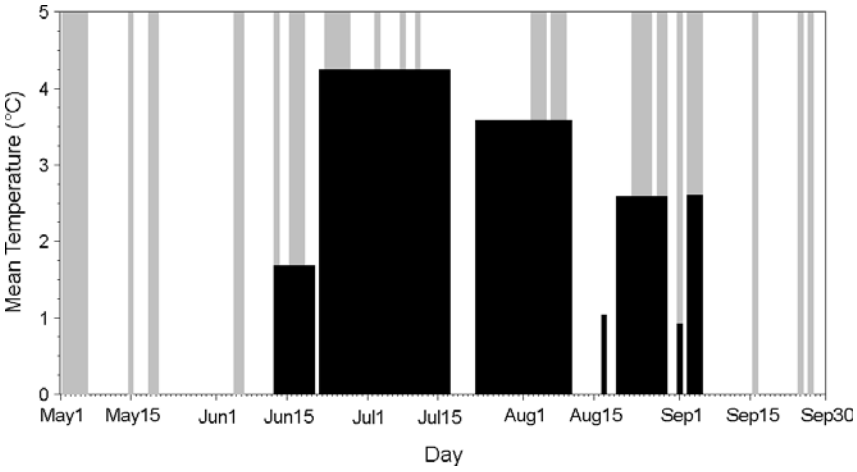
Mean Temperature (°C)
0
1
2
3
4
5
May1
May15
Jun1
Jun15
Jul1
Jul15
Aug1
Aug15
Sep1
Sep15
Sep30
Day

Figure 7.

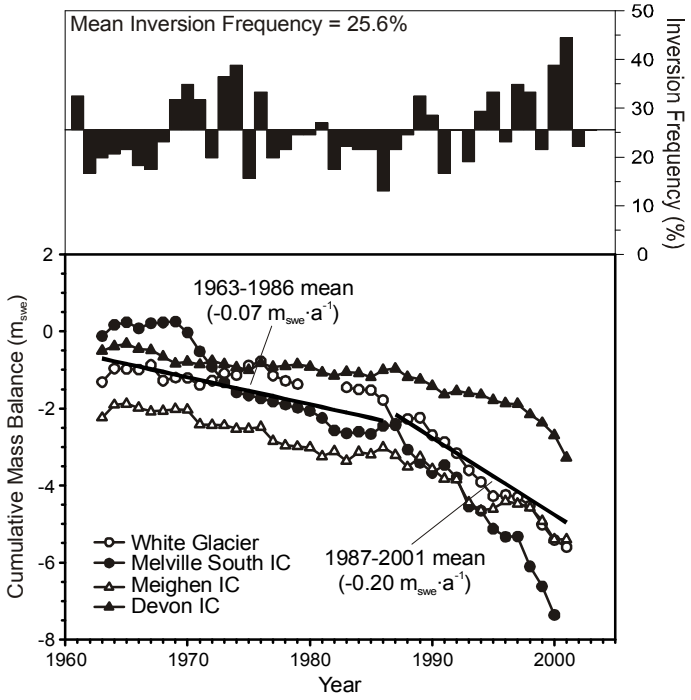
Mean Inversion Frequency = 25.6%
Inversion Frequency (%)
50
40
30
20
10
0
2
0
-2
-4
-6
-8
1963-1986 mean
(-0.07 m$_{swe}$·a^{-1})
1987-2001 mean
(-0.20 m$_{swe}$·a^{-1})
White Glacier
Melville South IC
Meighen IC
Devon IC
Cumulative Mass Balance (m$_{swe}$)
1960
1970
1980
1990
2000
Year

Figure 8.

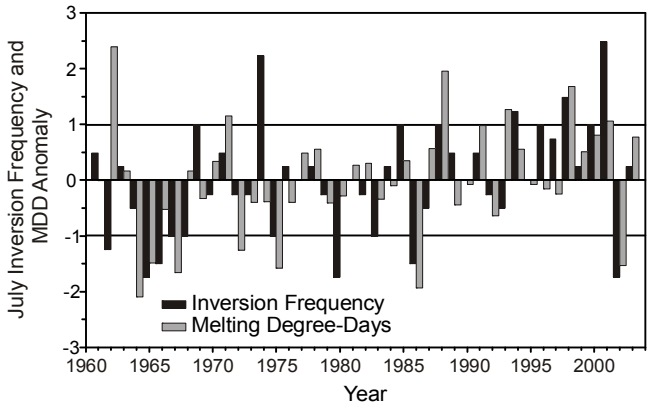
July Inversion Frequency and MDD Anomaly
3
2
1
0
-1
-2
-3
1960
1965
1970
1975
1980
1985
1990
1995
2000
Year
Inversion Frequency
Melting Degree-Days

CHAPTER 4

LATE HOLOCENE BIOLAMINATED SEDIMENTATION IN A COASTAL ARCTIC LAKE

KRYSTOPHER J. CHUTKO AND SCOTT F. LAMOUREUX

ABSTRACT

An unusual record of laminated organic and clastic sediments was recovered from a small coastal freshwater lake on the Colin Archer Peninsula, Devon Island. The sediment core was 3.98 m in length with a distinct transition to laminated sediments in the upper 2.25 m. Based on the inferred sedimentology and a radiocarbon date, this transition was interpreted to represent the post-glacial emergence of the lake from the marine environment *c*. 5.7-ka cal BP. Three sedimentary components were identified in the laminated record: clastic material composed dominantly of detrital carbonate sediments, and two types of organic matter. The organic components were distinguished based on colour, relative texture, and composition, and were inferred to represent distinct phases of microbial growth.

The typical sedimentary rhythmite was composed of three distinct units. The basal unit was normally graded silt that ranged in thickness from < 100 µm to > 5 mm. Clastic units were frequently overlain by multiple laminae composed of red-coloured organic material inferred to be cyanobacterial mats. Finally, a unit of featureless yellow organic matter of relatively consistent thickness (~ 100 µm) occurred. These units were interpreted to be organic residue and potentially extracellular polymeric substances. In most cases, conformable contacts between the units were observed.

Although the existence of annual rhythmicity could not be confirmed, the relatively simple arctic lacustrine depositional environment and the inferred strong seasonality of the three units suggested that these sediments may reveal a complex quasi-annual signal of clastic and organic sediment accumulation.

While known to exist in Antarctic lakes and a number of temperate and tropical settings, thick microbial accumulations have not been reported for Arctic lacustrine environments. The long record of biolaminated organic accumulation (*c*. 5000 years) from this lake provides a unique opportunity to understand the physical processes which may influence microbial growth in this environment.

INTRODUCTION

The evolution of arctic lakes is strongly controlled by the physical processes that occur in their surrounding landscapes (Van Hove *et al*., 2006). For coastal lakes, ongoing responses to deglaciation may be evident in the lake sediments, and such sedimentary sequences reveal continuous records of environmental conditions during marine and lacustrine phases (Retelle, 1986). However, the composition of the sediment may also be determined by chemical and biological influences in the lake and surrounding watershed and may be manifested as distinct autochthonous sedimentary structures (Gilbert 2003). Where it is possible to assign a timescale, these sedimentary structures can provide paleoenvironmental information, although most efforts have been directed towards clastic laminae (e.g., Gilbert, 1975; Leemann and Niessen, 1994; Lamoureux and Bradley, 1996; Tomkins and Lamoureux, 2005) or laminae composed of subfossils or chemical precipitates (e.g., Lotter, 1989; St. Jacques *et al*., in press).

Microbially induced sedimentary structures (MISS) are produced primarily by cyanobacterial films and mats (Noffke *et al*., 2001). Cyanobacteria are photoautotrophic prokaryotes and many species show phototactic behaviour and therefore can actively move to optimize their exposure to light (Noffke *et al*., 2001). By doing so, the cyanobacteria and their related extracellular polymeric substances (EPS) cover sediment particles in layers referred to as biofilms (Wilderer and Characklis, 1989; Paterson and Black, 2000). Under favourable conditions, biofilms grow to form thick organic layers called microbial mats (Krumbein, 1983). Actively growing/living microbial mats have been identified in

a wide range of aquatic settings, from tropical (Pierson, 1992) to under permanent lake ice cover in Antarctica (Parker *et al*., 1981; Simmons *et al*., 1993).

In the Canadian Arctic, contemporary cyanobacterial mats are found in several different terrestrial and aquatic environments, although their distribution and abundance has remained uncertain until recently (Vézina and Vincent, 1997). Queseda *et al*. (1999) and Bonilla *et al*. (2005) described the presence of mats in lakes, ponds and streams on several of the Canadian Arctic islands. These studies suggest that cyanobacterial assemblages compose a significant portion of the biomass in aquatic systems in polar regions (Vézina and Vincent, 1997).

MISS are produced through the interaction between clastic sedimentation and microbial growth (Noffke *et al*., 2001), and therefore potentially contain a record of clastic sediment delivery processes and benthic productivity. Despite this potential, little work related to the sedimentary record produced by cyanobacterial mats and biofilms has been carried out in polar regions. The majority of polar lacustrine mat research has focused on the sediment-water interface, primarily in describing the composition of the surface mats and their role(s) in contemporary biogeochemical processes (e.g., Wharton *et al*., 1993; Quesada *et al*., 1999; Bonilla *et al*., 2005; Vopel and Hawes, 2006). Longer sedimentary records have only been described from the Dry Valleys region of Antarctica (Parker *et al*., 1981; Vincent, 2000; Wagner *et al*., 2006).

The objective of this study was to document the Holocene sedimentary record recovered from a High Arctic coastal freshwater lake which contained a

record of marine and lacustrine sedimentation. The late Holocene portion of this sequence was inferred to be composed of microbially induced sedimentary structures. Detailed sedimentary, electron microscope and biogeochemical analyses were combined to assess the composition and environmental context for the MISS. To our knowledge, this work represents the first instance of documented MISS in the northern high latitudes and presents a framework for further analyses from other similar settings.

STUDY SITE & METHODOLOGY

Study Site

Lake J (unofficial name) is a shallow (z_{max} = 15 m), 140 ha lake located at 46 m above sea level (asl) on the south coast of the Colin Archer Peninsula, Devon Island, Canada (76° 11.4' N, 90° 46.4' W; Fig. 1). A prominent delta in the southwest corner of the lake suggests an inflow originating from the southern edge of a small icefield in the western half of the catchment, although aerial photography from 1958 shows that ice retreat has likely rendered this inflow to be currently minor and most inflows arise from the valley slopes around the lake. The lake drains eastward through a short channel into the Archer River. Inputs of water to the lake from the Archer River during times of flooding could not be confirmed during field visits. Electrical conductivity was measured with a calibrated YSI Model 30 conductivity meter and bottom water was 284 $\mu S \cdot cm^{-1}$, indicative of freshwater conditions.

The lake and catchment is underlain by mid-Devonian Douro Formation limestone (Mayr *et al*., 1998). The region was glaciated during the Late

Wisconsinan and post-glacial exposure of the land began in the early Holocene (Dyke, 1999). The peninsula is currently ~34% glaciated, primarily by low elevation plateau ice caps (< 700 m asl). Similar ice caps in the region have been classified as stagnant and likely originated during the last millenium (Koerner, 2002). Postglacial marine limit at Colin Archer Peninsula is ~120 m asl and dated at *c*. 9.3-ka BP (Dyke, 1999).

The mean July temperature at Resolute, the closest weather station, is 4.3 °C and mean annual rainfall and snowfall (September – August) are 54.8 mm and 97.0 cm (1948-2007), respectively. Runoff at a nearby catchment was characterized by Marsh and Woo (1981). Nival melt was initiated in late June or early July, shortly after the onset of positive temperatures. Peak discharge was reached within 11 days of initiation and declined through the summer as snowpack sources diminished. Lake ice was 2.2 m thick in May 2004 and likely lasts until July in most years. Aerial photography and satellite imagery shows the lake to be ice-free by late August in 1958 and 1974.

Field and laboratory methods

Sediment cores were recovered from Lake J in late May 2004 and 2005. Lake bathymetry and cores were obtained from the ice surface. Depths were obtained with a Humminbird echo sounder (0.3 m accuracy) and located with a Garmin GPS receiver (± 5 m). Surface sediment cores (max length = 37.5 cm) were obtained with Boyle (1995) and Aquatics Research Instruments gravity corers at 14 and 15 m depths. A vibracore (Smith, 1998) was obtained at 15 m

depth. All cores were maintained unfrozen and returned to the laboratory where they were split lengthwise, exposed faces cleaned, and one half archived.

Undisturbed and overlapped sediment slabs (7 x 2 x 0.5 cm) were extracted for thin section preparation. The slabs were dehydrated using repeated acetone exchanges and impregnated with a single application of Spurr's low viscosity epoxy resin under low vacuum (Lamoureux, 1994). The cured sediment slabs were prepared as 7 x 2 cm thin sections using standard methods. The finished thin sections were scanned at 2400 dpi and transferred to CorelDRAW software. The images were assembled in stratigraphic order and adjacent images were correlated using prominent sedimentary features. The process of dehydration using hygroscopic solvents (e.g., acetone, ethanol) leaches pigments from the sediment (e.g., Vézina and Vincent, 1997), and therefore, any reference to colours in the thin sections must reflect solvent exposure to some extent. However, the broad colour classifications used below are consistent between the pre- and post-acetone treated sediments.

Sediment organic matter and carbonate content were determined by loss-on-ignition (LOI) at 550 °C and 950 °C, respectively (Heiri *et al*., 2001). Samples for LOI were taken at 1 cm intervals above 2.4 m and at 8 cm intervals below 2.4 m. An error of ± 1.3% for LOI at 550 °C was determined on repeat samples and could be associated with the position of the sample in the furnace (Heiri *et al*., 2001).

Percent carbon, nitrogen and sulphur were determined with a Leco CNS-2000 analyzer. Dried samples were pretreated with 5 mL of 0.5M HCl for 24

hours, centrifuged and the supernatant removed with suction and repeated three times (Midwood and Boutton, 1998).

Grain size analysis of the cores was performed on a Beckman Coulter LS200 laser diffraction particle size analyzer. Samples were pretreated in repeated applications of 30% H_2O_2 for two weeks to remove organic matter (Mikutta *et al*., 2005) and sodium hexametaphosphate was added as a dispersant prior to analysis. Samples were sonicated for 60 seconds and then analyzed with sonication three successive times for 60 seconds each. Grain size analysis of the upper sediment appeared to be complicated due to the abundance of organic material and detrital carbonates forming resistant aggregates. This composition fouled the lenses of the laser diffraction system and required unusually frequent system cleaning between runs. Similar results were observed with sediments from several other Devon Island lakes (S. Lamoureux, unpublished data).

Scanning electron and environmental scanning electron microscopy was performed on a Jeol JSM-840 SEM (Queen's University) and an ElectroScan 2020 ESEM (McMaster University). Sediment samples were extracted from the core face into 8 mm diameter plastic molds and immersed in a 2.5% glutaraldehyde + 0.075% Ruthenium red stain ($Ru_3O_2(NH_3)_{14}Cl_6 \cdot 4H_2O$) solution for two hours. Samples were rinsed repeatedly in 0.2M HEPES buffer (pH 7.2) (Priester *et al*., 2007). Post-fixation in osmium tetroxide (OsO_4; two hours) did not discernibly improve the images. Sediment samples prepared for SEM were freeze-dried and pulse-coated in gold prior to imaging while sediments prepared for ESEM were imaged in their hydrated state. SEM and ESEM images were obtained at 10 and 20 kV, respectively.

A ^{14}C sample of detrital plant material was extracted from the core, cleaned with distilled water and kept frozen until delivery to the IsoTrace Laboratory, University of Toronto. The radiocarbon date was calibrated with IntCal04 (Reimer *et al*., 2004). Additional macro-organic material was not available for radiocarbon analysis. Samples for ^{210}Pb dating were oven-dried for 24 hours at 105°C and activity was measured with α-spectroscopy at MyCore Scientific Inc. (Deep River, Canada). Samples for ^{137}Cs were freeze-dried and ground and analyzed for 80 000 seconds with an ORTEC high-resolution gamma counting system (Department of Biology, Queen's University).

RESULTS

Sedimentology

The Lake J long core contained 3.98 m of sediment which could be divided into three primary facies (Fig. 4). Facies I (2.25 – 3.98 m) was composed of massive gray sediment which contained numerous marine macrofossils and coarse clasts. The transition to Facies II was marked by the onset of laminated sediment at 2.25 m. The laminae continued to 1.93 m and showed a distinct colour transition from gray to orange/brown at 1.99 m depth. A 2 mm unit of dark sediment separated Facies II and III. Facies III began at 1.91 m and extended to the top of the core and was composed of finely laminated orange-brown sediment. A 5 mm-thick homogeneous deposit of aquatic *Calliergon giganteum* (Arctic moss) occurred at 1.45 m depth, and represented the only deviation from

the physical characteristics of the facies. Thin section observations and other analyses were used to refine these facies further.

Facies I

Massive sediment composed primarily of silt dominated the lower record from 3.98 to 2.25m (Fig. 5A). Numerous dropstones (up to 6 cm diameter), bivalves of *Portlandia arctica*, a gastropod (*Buccinum sp.*), and foraminifers (*Elphidium sp.*) were found in this section of the core. Organic matter content was low (< 3.5 %LOI) and carbonate content (mean = 34%) was relatively high, although both variables showed no discernible trends throughout the facies (Fig. 6). Grain size analysis showed a greater proportion of sand sized (>62 µm) particles below 3.0 m than above, although the lowest portion (3.74 – 3.98 m) of the core was substantially finer (Fig. 6).

Facies II

Facies II sediments were identified by the onset of laminated sediment at 2.25 m. Initial laminae were thick (1.0 – 4.5 mm) and poorly defined with inconsistent contacts between the units (Fig. 5B). Above 2.22 m, the laminae became thinner (0.5 – 3.0 mm) and the contacts between units became sharp. The laminae became progressively thinner through this section and continued through the observed colour change at 1.99 m (Fig. 5C). The colour change reflected a gradation from sediments primarily composed of grey laminae to orange laminae. Micro-laminae (< 100 µm) began at 2.01 m and continued to 1.93 m. In total, 442 dark-light couplets were counted in this section. At 1.99 m,

the structure of the couplets changed from silt-clay units to clastic-organic units, relatively similar to those observed in Facies III. A 20 mm thick unit of massive dark sediment capped Facies II (Fig. 5D).

Particle size was finer than in the underlying facies and sand-sized grains were altogether absent (Fig. 6). Clay-sized material was similar to the unit below, although clay content increased above 1.97 m, coincident with the observed colour change. Similarly, organic matter content was low (<3%) until 1.99 m where it abruptly increased to ~6%. Carbonate content was relatively stable through the facies at ~27%.

Facies III

Orange/brown laminae were observed from 1.91 m to the sediment surface. The sedimentary contacts between the laminae varied, although they were clearer in the uppermost sediments. The preservation quality of the laminae in the vibracore (Fig. 5E) was somewhat less than that from the surface (gravity) cores (Fig. 5F), and suggests that disturbance due to vibration or transport affected the sediment. Alternatively, diagenetic alteration of the sediments rendered the deeper parts of the facies less well defined than those near the sediment surface. Regardless, correlation between the surface cores (from 2004 and 2005) and the vibracore was possible on the basis of distinct marker layers.

In thin section, the sediment was composed of three distinct types of laminae (Fig. 5F). First, normally graded clastic material (Type 1 sediment) formed units which varied substantially in thickness (< 100 µm to > 5 mm). In

many cases, scattered fine detrital organic matter was observed within the units. Second, laminae composed of red coloured material (Type 2 sediment) ranged in thickness from < 100 µm to 0.5 mm. Internal laminae were observed in many of these units and they appeared to be composed of lamina of uniform, non-granular material (Fig. 5G). The colour and structure of these units suggested that they were composed of organic matter. The Type 3 units were composed of homogenous and featureless lightly coloured material that ranged in thickness from < 100 µm to 1 mm. Many of these units contained isolated individual lithic grains within the uniform matrix (Fig. 5H). Sequences containing all three sediment types were most common, although deviations from the pattern frequently occurred, and included thick accumulations of the Type 3 sediments, missing laminae, and alternative sequences (Chutko and Lamoureux, in preparation [5]).

Detailed thin section investigation of the laminated structures did not reveal features typically described in Arctic lacustrine sediment records (e.g., Zolitschka, 1996; Lamoureux, 1999; Chutko and Lamoureux, 2008 [2]), and therefore further approaches to identifying the nature of the laminae were used. Due to the apparently complex organic-clastic stratigraphy observed (e.g., Fig. 5), investigations led to test the supposition that the organic sedimentary structures were produced by microbial activity. The organic units often exhibited a wavy or wrinkled profile typical of microbial mat accumulations (Schieber, 1999), and the presence of individual grains suspended in the matrix of the Type 3 sediments was potentially indicative of microbial grain separation (Noffke *et al*., 2001).

SEM and ESEM images revealed compositional differences between the clastic and organic sediment units. Clastic units were composed of silt-sized grains, with little evidence of organic matter (Fig. 7A/B). However, the organic units were dominated by the presence of fine filaments (Fig. 7C/D) and/or mucus (Fig. 7E/F) binding clastic grains. These observations revealed that the Facies III sediments were likely produced by a complex interaction between clastic sedimentation and microbial activity. Additional grain size analyses on samples divided into either Type 1 or combined Type 2/3 sediments revealed that Type 1 sediment was coarser and showed greater variability than the Type 2/3 sediment (Table 1).

In order to quantify the nature of the different sediment units in Facies III, specific depths in the surface cores were identified in thin section images and classified as either clastic or organic. Couplets (clastic-organic) or triplets (clastic-organic-clastic / organic-clastic-organic) were sampled from five sample intervals (total units sampled = 12) for organic and carbonate content analyses. Due to the relatively thin organic laminae, physical differentiation between the Type 2 and Type 3 sediments could not be made. Five sample intervals were selected based on visual distinctions observed in the thin section images. In all cases, the clastic units yielded significantly ($p < 0.005$) lower %OM and higher $\%CaCO_3$ values than the organic units (Table 1). Identification of significant differences was based on a one-tailed Student's *t*-test assuming equal variances (tested with *F*-test) with the null hypothesis that the composition of the two sediment types was not different.

Chronology

A sedimentary chronology was attempted with ^{210}Pb, ^{137}Cs and ^{14}C methods. Lead-210 analysis results were inconclusive, due to the overall low ^{210}Pb concentration observed in the region (Hermanson, 1990) and uncertainty in determining the supported ^{210}Pb levels (Fig. 2). Similarly, ^{137}Cs analysis of the surface cores yielded an erratic profile for the upper 10 cm. As ^{137}Cs is not readily adsorbed onto organic matter or onto the surface of clastic particles in the presence of high organic matter content (Dumat *et al*., 1997), this isotope may have remained mobile in the sediment pore water. Cesium-137 activity in the Lake J sediments was substantially lower (mean 0.0014 $Bq \cdot g^{-1}$) than those in clastic sediments in a nearby proglacial lake (mean 0.09 $Bq \cdot g^{-1}$; Chutko and Lamoureux, 2008 [2]). Finally, a single radiocarbon date was obtained on a *Salix arctica* (arctic willow) twig at 2.26 m core depth that yielded an uncalibrated date of 6800 ± 70 yr BP (5705 ± 50 cal yr BP). The absence of additional terrestrial macro-organic material and the presence of carbonate bedrock in the basin prevented further radiocarbon analyses (Abbott and Stafford, 1996).

Chronological constraint was also estimated by the Holocene post-glacial isostatic emergence of Lake J area. Dyke (1998) produced a relative sea level (RSL) curve for the Colin Archer Peninsula (Fig. 3), which suggests emergence of the lake at *c*. 6500 BP (uncalibrated years). Therefore, based on the sedimentology, it was expected that the upper 2.25 m of the core represented the past ~5700 years, most of which was as an isolated lacustrine basin. A more refined chronology could not be made based on the available evidence.

DISCUSSION

Holocene lake development

The sedimentary stratigraphy suggests three primary distinguishable deposition phases in Lake J through the Holocene (Fig. 4). The presence of dropstones, foraminfera and molluscs, along with the lack of laminated sediments in Facies I suggest an open marine coastal system. Dyke (1999) showed that ice persisted in the Eidsbotn fjord as recently as 8 – 8.5-ka BP, and the accumulation of coarse sediments and dropstones is interpreted as proximal glaciomarine deposition. Similar early Holocene postglacial sediment deposition in pre-emergent marine basins has been observed in the sediments from other High Arctic coastal lakes (e.g., Retelle, 1986; Lamoureux and Bradley, 1996; Lamoureux, 1999).

At approximately 5.7-ka cal BP, the onset of laminated sediments marks a transition from marine conditions to a more isolated basin where seasonal variations in sediment supply controlled deposition. The presence of laminated sediment and absence of sand and dropstones suggests a less energetic environment, due to initial isolation of the lake basin from the open coastal environment. Lake J is currently separated from the fjord by a low ridge ~70 m asl (~24 m above modern lake surface). This ridge would have emerged prior to the lake basin, effectively producing a more sheltered environment prior to and during initial emergence (King, 1991; Lamoureux, 1999). The fining of the laminae through the transitional section suggested progressive isolation of the basin, isolation from marine sediment supplies, and increased quiescence of the depositional environment.

The thin laminae observed between 2.25 and 1.93 m depth (Fig. 5C) could potentially represent annual units, although independent dating and confirmation of this inference cannot be made. If the laminae are indeed annual, then the number of couplets suggests that the transitional period lasted approximately 450 years. The composition of the laminae also reflected changing environmental conditions during this time. The transition from silt-clay couplets to organic-clastic couplets and concomitant increase in organic matter content suggests the onset of microbial activity in the lake basin. Directly above these laminae, the distinctive unit between Facies II and I and composed of dark sediment coincided with the prominent peak in sulphur (Fig. 6). The deposition of sulphur has been attributed elsewhere to reduced sulphate concentrations in the bottom waters, and likely the result of freshwater incursion to the lake (Berner, 1970; Berner, 1984; Retelle, 1986; Wagner *et al*., 2006). The presence of laminae and sulphur deposition suggests that these sediments indicate the transition from marine to freshwater lacustrine environmental conditions.

The current sedimentary environment was established sometime after 5.7-ka cal BP. The contemporary lacustrine environment is characterized by minimal sedimentary input and the development of a benthos that left discernable sedimentary structures. Laminated organic-clastic sediments have been deposited consistently from the time of inferred basin isolation to the present. Under high magnification, the organic component of the sediment appeared to be composed of filamentous and mucus-like material, inferred to be cyanobacteria and extracellular polymeric substances (EPS) (Fig. 7), the basis for microbial mat communities and similar to previously reported microbial mat deposits (Gerdes *et*

al., 1993; Laval *et al*., 2000; Rozanov, 2005). Although the marine-to-lacustrine lake evolution has been described in detail throughout the Arctic (e.g., Van Hove *et al*., 2006), the long period of microbially induced laminated sediment accumulation during the Holocene is unreported in the Arctic.

Biolaminated sediment

The inferred lacustrine section that contained 1.91 m of organic-clastic laminae is the most remarkable part of the Lake J record. The detailed laminated stratigraphy of the section is highly complex and is composed of three primary sediment types which occur in varying patterns (Fig. 5). Detailed analyses of such structures are not reported in the current literature, and there are few examples of the identification of MISS in polar sedimentary records (Parker *et al*., 1981; Simmons *et al*., 2003; Wagner *et al*., 2006).

The classification of the laminae as either clastic or organic was based on a combination of visual and compositional approaches. In thin section, the clastic and organic laminae were visually distinct, both in colour and texture. Clastic units (Fig. 7A/B) were composed of granular material and were similar to clastic sediments in a nearby proglacial lake and elsewhere on Devon Island (Lamoureux *et al*. 2002; Chutko and Lamoureux, 2008 [2]). Terrestrial organic remains were found in many of the clastic laminae, although they were irregularly distributed throughout and did not produce sedimentary structures.

The organic units in Lake J did not contain granular texture; the Type 2 sediment appeared gelatinous and was often finely laminated, while the Type 3 sediment was characterized by featureless, thin laminae. The colour of the

organic laminae also distinguished them from the clastic units. Compositionally, the clastic units exhibited less organic matter, higher carbonate content, and more variable grain size distribution than the organic units (Table 1).

These descriptions are consistent with previously reported microbial mat accumulations. Reid *et al*. (2000) described in detail the succession of microbial mat components during sedimentation and hiatal intervals. During periods of sedimentation, filamentous cyanobacteria bind to and move through the accumulating sediment to form a mat on the surface (Noffke *et al*., 2001). During extended periods without substantial sedimentation, a more mature community described as a "continuous sheet of amorphous exopolymer" formed (Reid *et al*., 2000). While the work of Reid *et al*. (2000) was based on modern marine stromatolites in tropical settings, these observations provide a framework to interpret the inferred organic succession in Lake J. We propose a succession of microbial community types as described by Reid *et al*. (2000) also occurs in Lake J and forms the Type 2 and Type 3 sediments. The finely laminated Type 2 sediment would represent a residual material from a pioneer cyanobacteria community and the featureless Type 3 sediment represent accumulation from a secondary EPS or biofilm community.

MISS origins and persistence in Lake J

Based on the Lake J sedimentary record, the MISS began to accumulate during isolation and freshening of the lake. Cyanobacteria, the primary producer of MISS, are ubiquitous in polar terrestrial and lacustrine environments but much less so in polar marine environments (Hawes, 1989; Vézina and Vincent, 1997).

Cyanobacteria are commonly found in snow, ice, soil, and rivers in addition to lakes in polar environments, and are considered to be primary colonizers (Vincent, 2000). It is therefore not unreasonable to expect that the laminated structures in Lake J originated from cyanobacteria that had been washed into the lake basin from a terrestrial source. Cyanobacterial tolerances to the harsh arctic environment are enhanced by the relatively low biodiversity of competitors and herbivores, which would otherwise quickly reduce the cyanobacteria stock due to their overall slow growth rate (Quesada *et al*., 1999; Vincent, 2000). Thick microbial mat accumulations in Antarctic lakes, with similar environmental conditions to Devon Island, suggest that Lake J provides a suitable setting for these microorganisms.

Lake J is shallow, and clastic sediment influx appears to be minimal. Cyanobacteria rely on incoming solar radiation as a source of energy, and therefore they can only exist where sunlight can reach. The Arctic is an extreme environment with respect to solar insolation, but similar conditions are experienced in the Antarctic where microbial mats are also known to exist (Parker *et al*., 1981; Hawes *et al*., 2001). Lake J is 15 m deep and during most of the year, ice covers the lake. Imagery shows the complete removal of the surface ice in late summer and therefore it is expected that ice is maintained year round only in relatively cold years. In late May, the ice was 2.0 - 2.2 m thick, and likely represents the maximum thickness during the year. The transmission of light through ice is largely dependent on the clarity of the ice and on the presence of snow cover. For example, on Great Slave Lake with an ice thickness of ~1.5 m, 15 to 25% of photosynthetically active radiation (PAR) received at the ice surface

was transmitted completely through clear ice (Bolsenga *et al*., 1996). A thin (3 cm) snowcover reduced this transmission to less than 1%. Field observations at Lake J in 2004 and 2005 suggest that snowcover on the lake was minimal and large sections of bare clear ice are maintained by strong winds. Vézina and Vincent (1997) showed that polar cyanobacteria species were able to photosynthesize under such limiting conditions.

The limited influx of sediment to Lake J is another reason why microbial mats may persist in the lake. Although a delta in the southwest corner of the lake was visible on aerial photographs, that source of inflow currently appears to be minor due to ice recession. The other sources of meltwater to Lake J are from the surrounding hillslopes as minor overland flow. Wilkinson and Bunting (1975) described the transport of fine (< 40 µm) sediment via a network of rills on an Arctic hillslope which were fed by snowpatches existing late into the summer. Although minor, the observed sediment transport was not negligible and therefore provides a mechanism for the minor seasonal influx of sediment to Lake J. Additionally, due to the low amount of sediment influx to the lake, turbidity is likely to be low and would provide a relatively clear water column for penetration of incoming solar radiation.

Other MISS records

The explicit identification of MISS in the High Arctic has been absent, although there is perhaps indication that similar sequences have been found elsewhere. In Lake DV09 (Gajewski *et al*., 1997), ~100 km SSE of Lake J on Devon Island, finely laminated couplets of organic (“cohesive layer”) and clastic

("grey layer") material were found which were qualitatively similar to the sediments discussed in Lake J. Their work was supported by detailed sedimentological and geochemical analyses. However, the cores were short (max = 22 cm) and little information was provided regarding observed or inferred sedimentary processes. Although the authors identified the organic laminae as bacterial, they did not detail the formative processes in that context. However, based on ^{210}Pb dates, they interpreted the clastic-organic couplets as varves (Gajewski *et al*., 1997).

Lake DV09 is morphologically comparable to Lake J and both share physiographically-similar watersheds with no significant inflows. Similarly, recent sediments from a lake on southwestern Melville Island in the western Canadian Arctic Archipelago are qualitatively similar to the sediments presented in this study and were obtained from a shallow freshwater lake with minor inflows (S. Lamoureux, unpublished data). The morphologic and limnologic characteristics shared by these three lake systems where microbial sedimentary structures have been found provide a limnological context in which modern stromatolites may be found elsewhere in the High Arctic. However, these characteristics, particularly relatively shallow waters (10-15 m) are not commonly sampled for sedimentary records and therefore may have been overlooked. Alternatively, the widespread destructive sampling of organic sediment cores (e.g., Smol *et al*., 2005) may preclude the identification of MISS. Hence, the potential for MISS in freshwater arctic lakes and ponds appears to be positive and underdeveloped, compared to the Antarctic and other settings.

Hypothesized depositional environment

The following scenario is proposed by which cyanobacterial mats and sediment influx interact through the course of a year to ultimately produce a sequence of microbially induced sedimentary structures (Fig. 8). Beginning in winter, persistent darkness, thick lake ice and snow cover reduce the growth of the surface mat though they may be sustained by the accumulation of reserves acquired during the previous summer (Hawes *et al*., 2001). Beginning in mid-February, the sun rises above the horizon and by mid-April the sun remains above the horizon. During this time, photosynthetically active radiation penetrates the lake ice and reaches the lake bottom, allowing the cyanobacteria to photosynthesize and grow (Vézina and Vincent, 1997; Wagner *et al*., 2006). As temperature rises in late spring, snowmelt induced runoff develops and clastic sediment begins to enter the lake and settle onto the mat surface (Type 1 sediment; Fig. 8A). During and after the brief influx of sediment, the cyanobacteria move vertically upward through the sediment by the excretion of EPS, to maintain their surface position and thereby avoid burial by the clastic sediment (Type 2 sediment; Fig. 8B) (Simmons *et al*., 1993; Reid *et al*., 2000). Small and isolated fragments of Type 2 sediment observed in the upper part of the Type 1 sediment suggest that the movement of cyanobacteria begins during sedimentation, although the lack of clastic grains in the Type 2 sediment suggest that the majority of mat formation occurs after clastic sedimentation. In this process, the mat from the previous year is buried, producing the overall MISS. Later in the summer, thinning lake ice and increased PAR at depth leads to the development of a secondary biofilm community (Type 3 sediment; Fig. 8C)

(Hawes *et al*., 2001). At this point, the mat is fully developed and remains until the following spring.

Controls on the progression of this hypothesized seasonal cycle are not well understood. The input of nutrients may be restricted by available inflow from the watershed, which may vary significantly between years (Woo, 1983). Recent work suggests that nutrient flux is dominantly during the spring melt peak and substantially diminished during the summer (Lafrenière and Lamoureux, *in press*). The delivery of sediment and nutrients to the lake is controlled by snow water equivalence in the basin and the timing and intensity of temperature-derived melt (Forbes and Lamoureux, 2005; Cockburn and Lamoureux, *in press*; Lafrenière and Lamoureux, *in press*). It is likely that the influence of water temperature is minimal, as the year-to-year change in temperature at the bottom of the lake is likely small. The exception to this may be in the case of more extensive ice cover removal and lake water warming during the melt season (Oliver, 1964; Heath, 1988). It is also possible that the duration of snow and ice cover on the lake influences microbial growth through control over the amount of PAR reaching the lake bottom as a limitation over the photosynthetic activity of the microbes (Heath, 1988; Vézina and Vincent, 1997). Ongoing studies of the ecology of microbial systems in arctic lakes (e.g. Vincent, 2007), particularly in systems like Lake J where MISS are present, will likely provide further links between ecosystem processes and the sedimentary record. The recognition of these lacustrine ecosystems and sedimentary remains in arctic lakes represents a key opportunity to evaluate contemporary ecosystem function and the potential for paleoenvironmental indicators of microbial community activity.

CONCLUSIONS

Sediments in High Arctic coastal Lake J provided a record of Holocene sediment deposition. Three distinct phases of Holocene deposition were observed and associated with progression from a glaciomarine to lacustrine basin. Chronological evidence suggested that the isolation from marine environment began approximately 6.8-ka BP (5.5-ka cal BP). Subsequent lacustrine sediments were organic-rich and finely laminated, and sedimentological investigations suggested the presence of microbially induced sedimentary structures (MISS). The Lake J sediments strongly resembled those described in Antarctic Dry Valleys lakes, although a similar sediment record has not been previously described in the Arctic.

The microbially induced sedimentary structures in the Lake J record represent a complex interaction between clastic sedimentation and microbial growth. The two types of organic laminae identified are inferred to represent stages in community development, with mobile cyanobacteria developing a mat on the freshly deposited sediment surface and a more developed biofilm forming later in the melt season and perhaps under autumn and winter ice cover. This hypothesized annual cycle provides linkages to microbial ecosystem studies and may permit paleoenvironmental interpretations to be developed from these distinctive lacustrine settings.

ACKNOWLEDGEMENTS

This work was supported by ArcticNet, a Network of Centres of Excellence of Canada, and a Natural Sciences and Engineering Research Council of Canada

Discovery Grant to S.F.L. and Northern Scientific Training Program and Queen's University Graduate Dean's Travel grants to K.J.C. The Polar Continental Shelf Project, Natural Resources Canada, provided logistical field support. This research was supported by Nunavut Research Institute Scientific Research License 0200406R-M. Field assistance from J. Cockburn and D. Fortin and laboratory assistance from J. Tomkins is greatly appreciated.

REFERENCES

Abbott, M.B. and T.W. Stafford, Jr. 1996. Radiocarbon geochemistry of modern and ancient arctic lake systems, Baffin Island, Canada. *Quaternary Research*, **45**: 300-311.

Appleby, P.G. and F. Oldfield. 1978. The calculation of lead-210 dates assuming a constant rate of supply of unsupported ^{210}Pb to the sediment. *Catena*, **5**: 1-8.

Berner, R.A. 1970. Pleistocene sea levels possibly indicated by buried black sediment in the Black Sea. *Nature*, **227**: 700.

Berner, R.A. 1984. Sedimentary pyrite formation: an update. *Geochimica et Cosmochimica Acta*, **48**: 605-615.

Bolsenga, S.J., Evans, M., Vanderploeg, H.A. and D.G. Norton. 1996. PAR transmittance through thick, clear freshwater ice. *Hydrobiologia*, **330**: 227-230.

Bonilla, S., Villeneuve, V. and W.F. Vincent. 2005. Benthic and planktonic algal communities in a High Arctic lake: pigment structure and contrasting responses to nutrient enrichment. *Journal of Phycology*, **41**: 1120-1130.

Boyle, J.F. 1995. A simple closure mechanism for a compact, large-diameter, gravity corer. *Journal of Paleolimnology*, **13**: 85-87.

Chutko, K.J. and S.F. Lamoureux. 2008. Identification of coherent links between interannual sedimentary structures and daily meteorological observations in Arctic proglacial lacustrine varves: potentials and limitations. *Canadian Journal of Earth Sciences*, **45**: 1-13.

Cockburn, J.M.H. and S.F. Lamoureux. In press. Hydroclimate controls over seasonal sediment yield in two adjacent high arctic watersheds, *Hydrological Processes*, doi: 10.1002/hyp.6798.

Dumat, C., Cheshire, M.V., Fraser, A.R., Shand, C.A. and S. Staunton. 1997. The effect of removal of soil organic matter and iron on the adsorption of radiocaesium. *European Journal of Soil Science*, **48**: 675-683.

Dyke, A.S. 1998. Holocene delevelling of Devon Island, Arctic Canada: implications for ice sheet geometry and crustal response. *Canadian Journal of Earth Sciences*, **35**: 885-904.

Dyke, A.S. 1999. Last glacial maximum and deglaciation of Devon Island, arctic Canada: support for an Innutian Ice Sheet. *Quaternary Science Reviews*, **18**: 393-420.

Forbes, A.C. and S.F. Lamoureux. 2005. Climatic controls on streamflow and suspended sediment transport in three large Middle Arctic catchments, Boothia Peninsula, Nunavut, Canada. *Arctic, Antarctic, and Alpine Research*, **37**: 304-315.

Gajewski, K., Hamilton, P.B. and R. McNeely. 1997. A high resolution proxy-climate record from an arctic lake with annually-laminated sediments on Devon Island, Nunavut, Canada. *Journal of Paleolimnology*, **17**: 215-225.

Gerdes, G., Klenke, T. and N. Noffke. 2000. Microbial signatures in peritidal siliciclastic sediments: a catalogue. *Sedimentology*, **47**: 279-308.

Gilbert, R. 1975. Sedimentation in Lillooet Lake, British Columbia. *Canadian Journal of Earth Sciences*, **12**: 1697-1711.

Gilbert, R. 2003. Lacustrine sedimentation. *In*: Middleton, G.V. (ed.). Encyclopedia of Sedimentology and Sedimentary Rocks. Kluwer AP, Dordrecht: 404-408.

Hawes, I. 1989. Filamentous green algae in freshwater streams on Signy Island, Antarctica. *Hydrobiologia*, **172**: 1-18.

Hawes, I., Moorhead, D., Sutherland, D., Schmeling, J. and A.-M. Schwartz. 2001. Benthic primary production in two perennial ice-covered Antarctic lakes: patterns of biomass accumulation with a model of community metabolism. *Antarctic Science*, **13**: 18-27.

Heath, C.W. 1988. Annual primary productivity of an Antarctic continental lake: phytoplankton and benthic algal mat production strategies. *Hydrobiologia*, **165**: 77-87.

Heiri, O., Lotter, A.F., and G. Lemke. 2001. Loss on ignition as a method for estimating organic and carbonate content in sediments: reproducibility and comparability of results. *Journal of Paleolimnology*, **25**: 101-110.

Hermanson, M.H. 1990. ^{210}Pb and ^{137}Cs chronology of sediments from small, shallow Arctic lakes. *Geochimica et Cosmochimica Acta*, **54**: 1443-1451.

Koerner, R.M. 2002. Glaciers of the High Arctic Islands. *In*: Williams R.S. and J.G. Ferrigno (eds.). *Glaciers of the Arctic Islands*. United States Geological Survey Professional Paper 1386-J-1: J111-J146.

King, R.H. 1991. Paleolimnology of a polar oasis, Truelove Lowland, Devon Island, N.W.T., Canada. *Hydrobiologia*, **214**: 317-325.

Krumbein, W.E. 1983. Stromatolites – the challenge of a term in time and space. *Precambrian Research*, **20**: 493-531.

Lafrenière, M. and S.F. Lamoureux. In press. Seasonal dynamics of dissolved nitrogen exports from two High Arctic watersheds, Melville Island, Canada. *Hydrologic Research*.

Lamoureux, S.F. 1994. Embedding unfrozen lake sediments for thin section preparation. *Journal of Paleolimnology*, **10**: 141-146.

Lamoureux, S.F. 1999. Catchment and lake controls over the formation of varves in monomictic Nicolay Lake, Cornwall Island, Nunavut. *Canadian Journal of Earth Sciences*, **36**: 1533-1546.

Lamoureux, S.F. and R.S. Bradley. 1996. A late Holocene varved sediment record of environmental change from northern Ellesmere Island, Canada. *Journal of Paleolimnology*, **16**: 239-255.

Lamoureux, S.F., Gilbert, R. and T. Lewis. 2002. Lacustrine sedimentary environments in High Arctic proglacial Bear Lake, Devon Island, Nunavut, Canada. *Arctic, Antarctic, and Alpine Research*, **34**: 130-141.

Laval, B., Cady, S.L., Pollack, J.C., McKay, C.P., Bird, J.S., Grotzinger, J.P., Ford, D.C. and H.R. Bohm. 2000. Modern freshwater microbialite analogues for ancient dendritic reef structures. *Nature*, **407**: 626-629.

Leemann, A. and Niessen, F. 1994. Varve formation and the climatic record in an Alpine proglacial lake: calibrating annually-laminated sediments against hydrological and meteorological data. *The Holocene*, **4**: 1-8.

Lotter, A.F. 1989. Evidence of annual layering in Holocene sediments of Soppensee, Switzerland. *Aquatic Sciences*, **51**: 19-30.

Marsh, P. and M.-K. Woo. 1981. Snowmelt, glacier melt, and High Arctic streamflow regimes. *Canadian Journal of Earth Sciences*, **18**: 1380-1384.

Mayr, U., de Freitas, T., and B. Beauchamp. 1998. *The Geology of Devon Island North of 76°, Canadian Arctic Archipelago*. Geological Survey of Canada Bulletin 526.

Midwood, A.J. and T.W. Boutton. 1998. Soil carbonate decomposition by acid has little effect on $\delta^{13}C$ of organic matter. *Soil Biology and Biochemistry*, **30**: 1301-1307.

Mikutta, R., Kleber, M., Kaiser, K. and R. Jahn. 2005. Review: organic matter removal from soils using hydrogen peroxide, sodium hypochlorite and disodium peroxodisulfate. *Soil Science Society of America Journal*, **69**: 120-135.

Noffke, N., Gerdes, G., Klenke, T., Krumbein, W.E. 2001. Microbially induced sedimentary structures – a new category within the classification of primary sedimentary structures. *Journal of Sedimentary Research*, **71**: 649-656.

Oliver, D.R. 1964. A limnological investigation of a large arctic lake, Nettiling Lake, Baffin Island. *Arctic*, **17**: 69-83.

Parker, B.C., Simmons Jr., G.M., Love, F.G., Wharton, R.A. and K.G. Seaburg. 1981. Modern stromatolites in Antarctic Dry Valley lakes. *Bioscience*, **31**: 656-661.

Paterson, D.M. and K.S. Black. 2000. Siliciclastic intertidal microbial sediments. *In*: Riding, R. and S. Awramik (eds.). *Microbial Sediments*. Springer-Verlag, Berlin: 217-225.

Pierson, B.K. 1992. Modern mat-building microbial communities: A key to the interpretation of Proterozoic stromatolitic communities - Introduction. *In*: Schopf, J.W. and C. Klein (eds.). *The Paleozoic Biosphere: A Multidisciplinary Study*. Cambridge UP, Cambridge: 247-251.

Priester, J.H., Horst, A.M., Van De Werfhorst, L.C., Saleta, J.L., Mertes, L.A.K. and P.A. Holden. 2007. Enhanced visualization of microbial biofilms by staining and environmental scanning electron microscopy. *Journal of Microbiological Methods*, **68**: 577-587.

Quesada, A., Vincent, W.F. and D.R.S. Lean. 1999. Community and pigment structure of Arctic cyanobacterial assemblages: the occurrence and distribution of UV-absorbing compounds. *FEMS Microbiology Ecology*, **28**: 315-323.

Reid, R.P., Visscher, P.T., Decho, A.W., Stolz, J.F., Bebout, B.M., Dupraz, C., Macintyre, I.G., Paerl, H.W., Pinckney, J.L., Prufert-Bebout, L., Steppe, T.F. and D.J. DesMarais. 2000. The role of microbes in accretion, lamination and early lithification of modern marine stromatolites. *Nature*, **406**: 989-992.

Reimer, P.J., Baillie, M.G.L., Bard, E., Bayliss, A., Beck, J.W., Bertrand, C.J.H., Blackwell, P.G., Buck, C.E., Burr, G.S., Cutler, K.B., Damon, P.E., Edwards, R.L., Fairbanks, R.G., Friedrich, M., Guilderson, T.P., Hogg, A.G., Hughen, K.A., Kromer, B., McCormac, G., Manning, S., Bronk Ramsey, C., Reimer, R.W., Remmele, S., Southon, J.R., Stuiver, M., Talamo, S., Taylor, F.W., van der Plicht, J. and C.E. Weyhenmeyer. 2004.

IntCal04 terrestrial radiocarbon age calibration, 0-26 cal kyr BP. *Radiocarbon*, **46**: 1029-1058.

Retelle, M.J. 1986. Stratigraphy and sedimentology of coastal lacustrine basins, northeastern Ellesmere Island, N.W.T. *Géographie Physique et Quaternaire*, **40**: 117-128.

Rozanov, A.Y. 2005. Bacterial paleontology. *In*: Hoover, R.B., Rozanov, A.Y. and R. Paepe (eds.). *Perspectives in Astrobiology*. NATO Science Series, I: Life and Behavioural Sciences, **366**: 132-145.

Schieber, J. 1999. Microbial mats in terrigenous clastics: the challenge of identification in the rock record. *Palaios*, **14**: 3-12.

Simmons Jr., G.M., Vestal, J.R. and R.A. Wharton Jr. 1993. Environmental regulators of microbial activity in continental Antarctic lakes. *In*: Green, W.J. and E.I. Friedmann (eds.). *Physical and Biogeochemical Processes in Antarctic Lakes*. Antarctic Research Series, 59. American Geophysical Union, Washington D.C.: 165-195.

Smith, D.G. 1998. Vibracoring: a new method for coring deep lakes. *Palaeogeography, Palaeoclimatology, Palaeoecology*, **140**: 433-440.

Smol, J.P., Wolfe, A.P., Birks, H.J.B., Douglas, M.S.V., Jones, V.J, Korhola, A., Pienitz, R., Rühland, K., Sorvari, S., Antoniades, D., Brooks, S.J., Fallu, M.-A., Hughes, M., Keatley, B.E., Laing, T.E., Michelutti, N., Nazarova, L., Nyman, M., Paterson, A.M., Perren, B., Quinlan, R., Rautio, M., Saulnier-Talbot, É, Siitonen, S., Solovieva, N., and J. Weckström. 2005. Climate-driven regime shifts in the biological communities of arctic lakes. *Proceedings of the National Academy of Sciences*, **102**: 4397-4402.

St. Jacques, J.-M., Cumming, B.F. and J.P. Smol. In press. A statistical method for varve verification using seasonal pollen deposition. *Journal of Paleolimnology*.

Tomkins, J.D. and S.F. Lamoureux. 2005. Multiple hydroclimatic controls over recent sedimentation in proglacial Mirror Lake, southern Selwyn Mountains, Northwest Territories. *Canadian Journal of Earth Sciences*, **42**: 1589-1599.

Van Hove, P., Belzile, C., Gibson, J.A.E. and W.F. Vincent. 2006. Coupled landscape-lake evolution in High Arctic Canada. *Canadian Journal of Earth Sciences*, **43**: 533-546.

Vézina, S. and W.F. Vincent. 1997. Arctic cyanobacteria and limnological properties of their environment: Bylot Island, Northwest Territories, Canada (73°N, 80°W). *Polar Biology*, **17**: 523-534.

Vincent, W.F. 2000. Cyanobacterial dominance in the polar regions. *In*: Whitton, B.A. and M. Potts (eds.). *The Ecology of Cyanobacteria*. Kluwer AP, Dordrecht: 321-340.

Vincent, W.F. 2007. Cold tolerance in cyanobacteria and life in the cryosphere. *In*: Seckbach, J (ed.). *Algae and Cyanobacteria in Extreme Environments*. Springer, Heidelberg: 287-301.

Vopel, K. and I. Hawes. 2006. Photosynthetic performance of benthic microbial mats in Lake Hoare, Antarctica. *Limnology and Oceanography*, **51**: 1801-1812.

Wagner, B., Melles, M., Doran, P.T., Kenig, F., Forman, S.L., Pierau, R. and P. Allen. 2006. Glacial and postglacial sedimentation in the Fryxell basin,

Taylor Valley, southern Victoria Land, Antarctica. *Palaeogeography, Palaeoclimatology, Palaeoecology*, **241**: 320-337.

Wharton, Jr., R.A., Lyons, W.B. and D.J. DesMarais. 1993. Stable isotopic biogeochemistry of carbon and nitrogen in a perennially ice-covered Antarctic Lake. *Chemical Geology (Isotope Geoscience Section)*, **107**: 159-172.

Wilderer, P.A. and W.G. Characklis. 1989. Structure and function of biofilms. *In*: Characklis, W.G. and P.A. Wilderer (eds.). *Structure and Function of Biofilms*. Life Science Research Report **46**: 5-17.

Wilkinson, T.J. and B.T. Bunting. 1975. Overland transport of sediment by rill water in a periglacial environment in the Canadian High Arctic. *Geografiska Annaler*, **57A**: 105-116.

Woo, M.-K. 1983. Hydrology of a drainage basin in the Canadian High Arctic. *Annals of the Association of American Geographers*, **73**: 577-596.

Zolitschka, B. 1996. Recent sedimentation in a high arctic lake, northern Ellesmere Island, Canada. *Journal of Paleolimnology*, **16**: 169-186.

Table 1. Median grain size (D_{50}), and percent loss-on-ignition (%LOI) and carbonate content (%$CaCO_3$) for Type 1 and Type 2/3 sediment. All differences are statistically significant at a 95% confidence interval.

	Type 1	Type 2/3 (undifferentiated)
D_{50}	19.3 ± 9.4	13.8 ± 1.2
%LOI	6.3 ± 3.8	15.8 ± 5.8
%$CaCO_3$	33.9 ± 3.2	31.1 ± 2.2

Figure Captions

Figure 1. A) Location of the study site on Colin Archer Peninsula, Devon Island. The Devon Ice Cap (DIC) and Resolute (R) are identified. B) The Archer River basin in the central Colin Archer Peninsula. C) Bathymetry of Lake J, with depth soundings and coring station identified. The lake currently flows into the Archer River. Aerial photographs suggest a past glacier meltwater inflow in the southwest part of the lake. D) Photograph of Lake J surface looking north from coring site.

Figure 2. ^{210}Pb CRS depth-age models (Appleby and Oldfield, 1978) derived from ^{210}Pb activity profile and assume background supported ^{210}Pb of either [1] 0.027 or [2] 0.021 Bq·g^{-1}. Down core ^{210}Pb activity (right panel).

Figure 3. Relative sea level curve for Colin Archer Peninsula, after Dyke (1998).

Figure 4. Composite schematic core log.

Figure 5. Photomicrographs of Lake J thin sections. A) Massive Facies I sediment, 2.33 m, core J2-04. B) Lower Facies II laminated sediment, 2.20 m, core J2-04. C) Upper Facies II laminated sediment, 1.94 m, core J2-04. D) Boundary (arrow) between Facies II laminae and sulphide-rich massive cap, 1.93 m, core J2-04. E) Facies III laminated sediment, 0.60 m, core J2-04. F) Laminated Facies III sediment, demonstrating the typically observed sequence

of three sediment types, 4.5 cm, core J1-04. G) Internally laminated Type-2 sediment, 11.8 cm, core J1-04. H) Individual grain separation in Type-3 sediment, 6.6 cm, core J1-04.

Figure 6. Down-core trends in organic matter (%OM), carbonate content (%$CaCO_3$), organic carbon (%C_{org}), nitrogen (%N), sulphur (%S), and grain size (texture). The three sedimentary facies are shown at right.

Figure 7. Electron microscope images of Lake J sediments. A) Fine silt to fine sand sediment typical of Type-1 sediment (core J1-05, 11.5 cm, 10 kV SEM). B) Clay- and silt-sized particles (core J1-05, 26.5 cm, 10 kV SEM). C) Filamentous material typical of Type-2 sediment (core J1-05, 11.5 cm, 10 kV SEM). D) Filamentous material binding clastic grains (core J1-05, 17.5 cm, 10 kV SEM). E) Mucus material associated with Type-3 sediment (core J1-05, 7.5 cm, 20 kV ESEM). F) Mucus material between clastic layers (core J1-05, 11.5 cm, 10 kV SEM).

Figure 8. Schematic diagram of hypothesized model for annual clastic and organic laminae deposition in Lake J. A) Spring nival melt delivers clastic sediment to the lake which accumulates on the previous sediment. B) As the supply of meltwater diminishes, sedimentation is reduced and mobile cyanobacteria form a primary mat on the sediment surface. C) Later in the summer under reduced or absent ice cover, a secondary bacterial community forms and generates a biofilm layer on the cyanobacterial mat and persists

through to the following spring. Figure not to scale.

Figure 1.

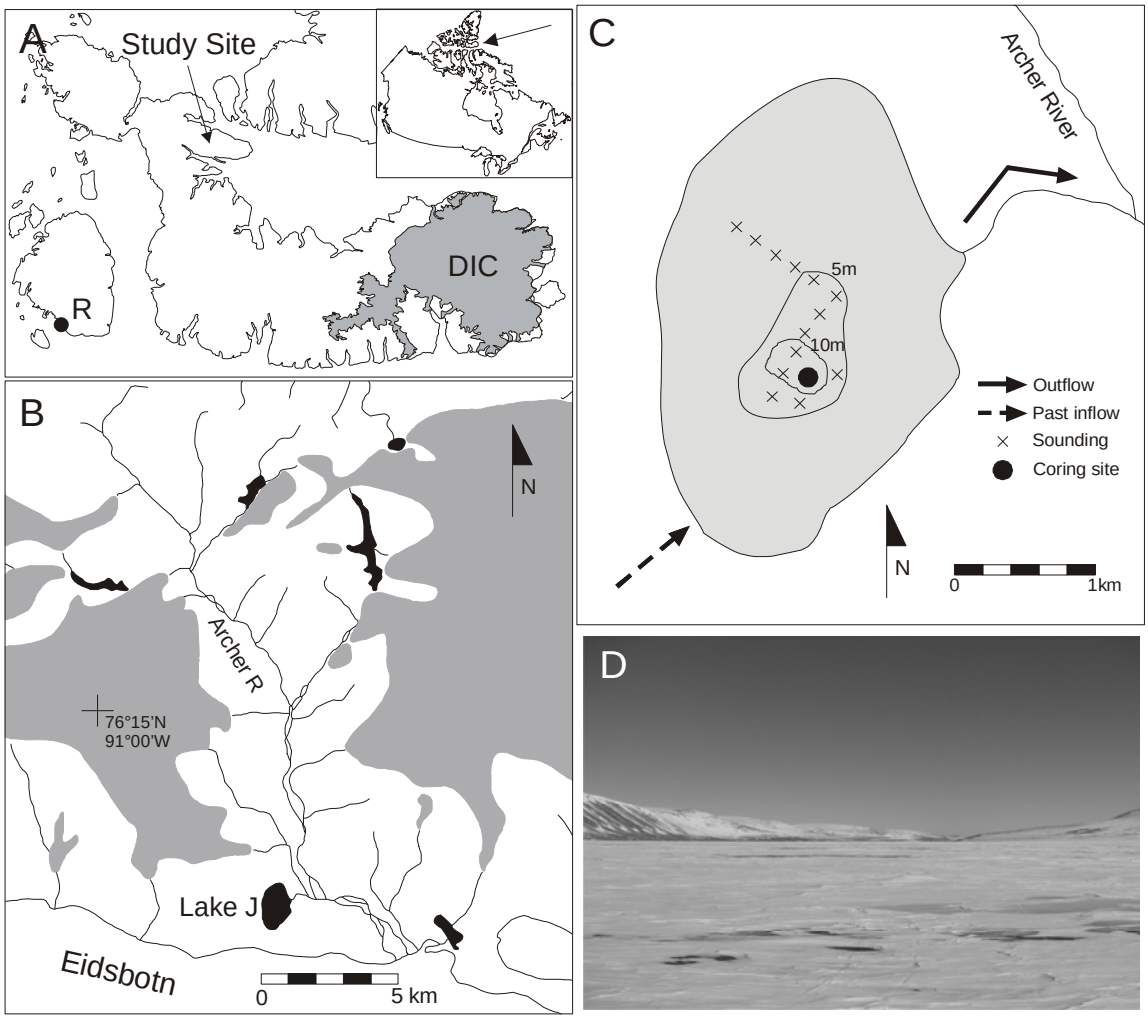
A
Study Site
DIC
R
B
N
Archer R
76°15'N
91°00'W
Lake J
Eidsbotn
0
5 km
C
Archer River
5m
10m
Outflow
Past inflow
Sounding
Coring site
N
0
1km
D

Figure 2.

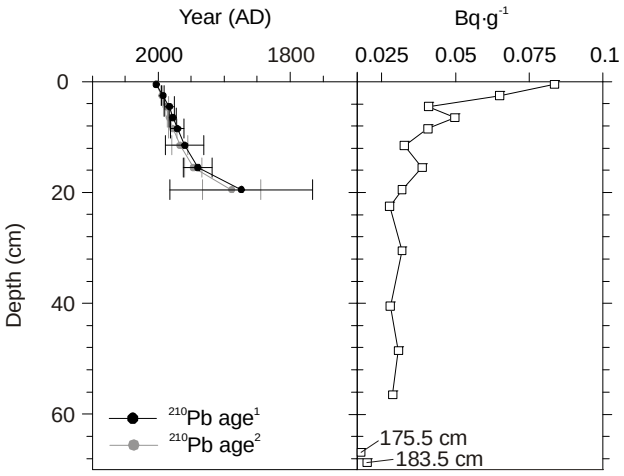
Year (AD)
2000
1800
Bq·g-1
0.025
0.05
0.075
0.1
0
20
40
60
Depth (cm)
210Pb age1
210Pb age2
175.5 cm
183.5 cm

Figure 3.

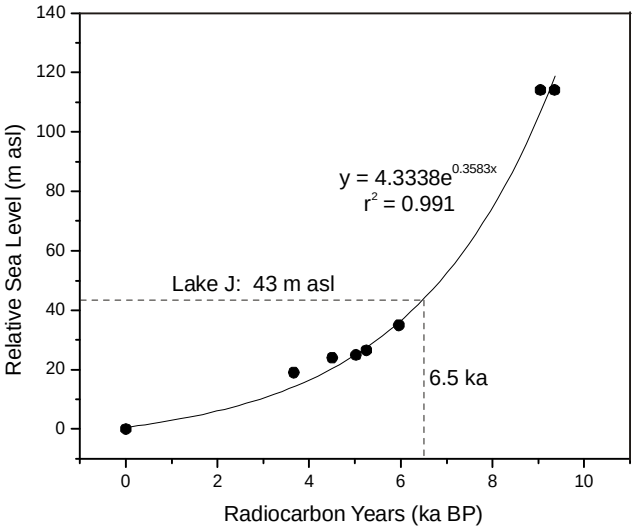
Relative Sea Level (m asl)
Radiocarbon Years (ka BP)
y = 4.3338e^0.3583x
r^2 = 0.991
Lake J: 43 m asl
6.5 ka
0
20
40
60
80
100
120
140
0
2
4
6
8
10

Figure 4.

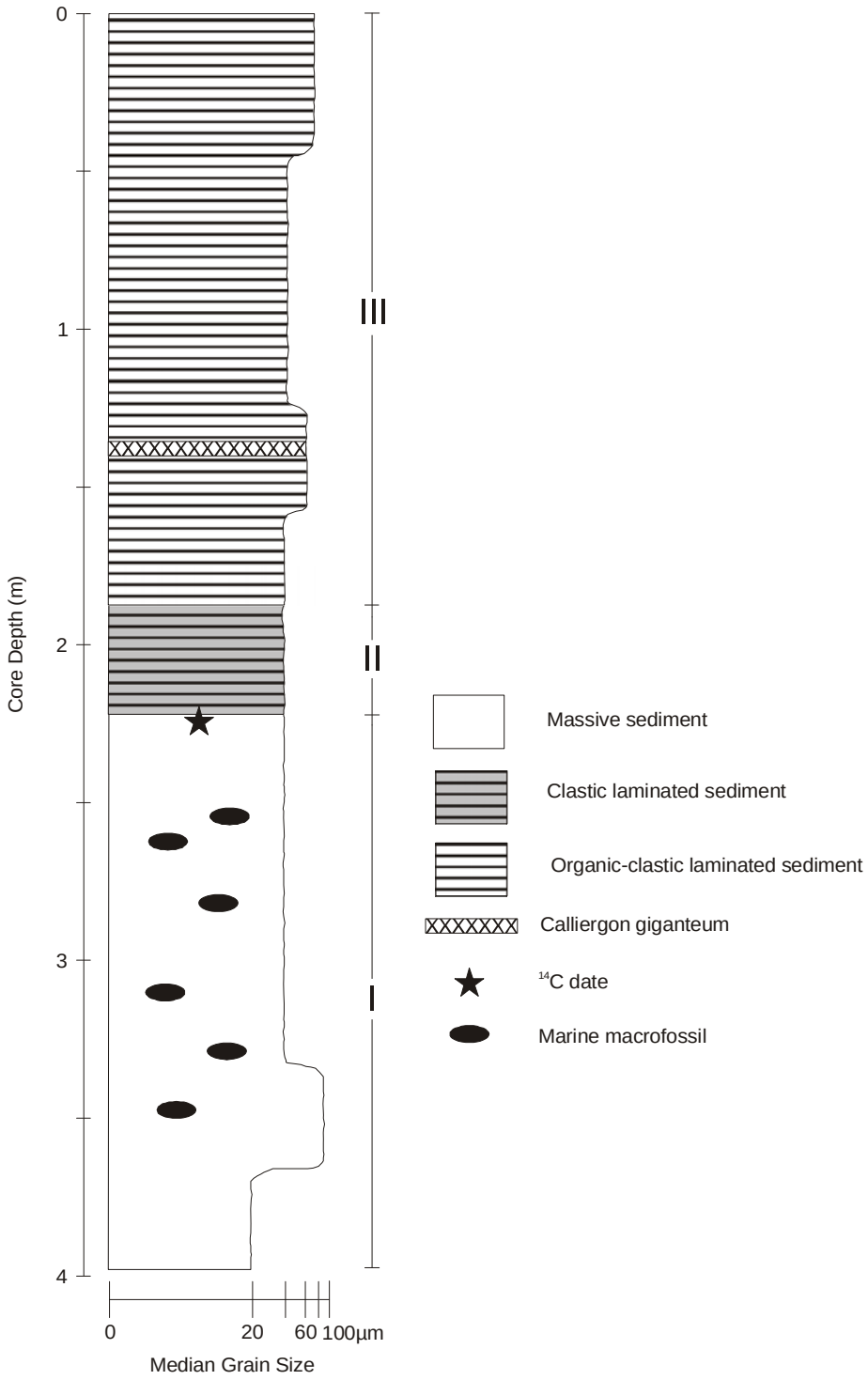
0
1
2
3
4
Core Depth (m)
III
II
I
0
20
60
100µm
Median Grain Size
Massive sediment
Clastic laminated sediment
Organic-clastic laminated sediment
Calliergon giganteum
14C date
Marine macrofossil

Figure 5.

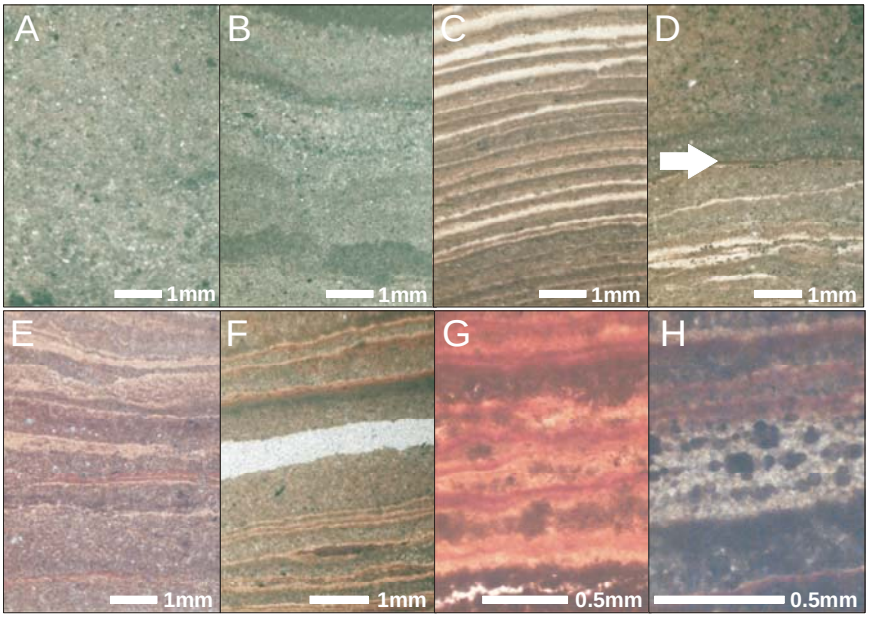

Figure 6.

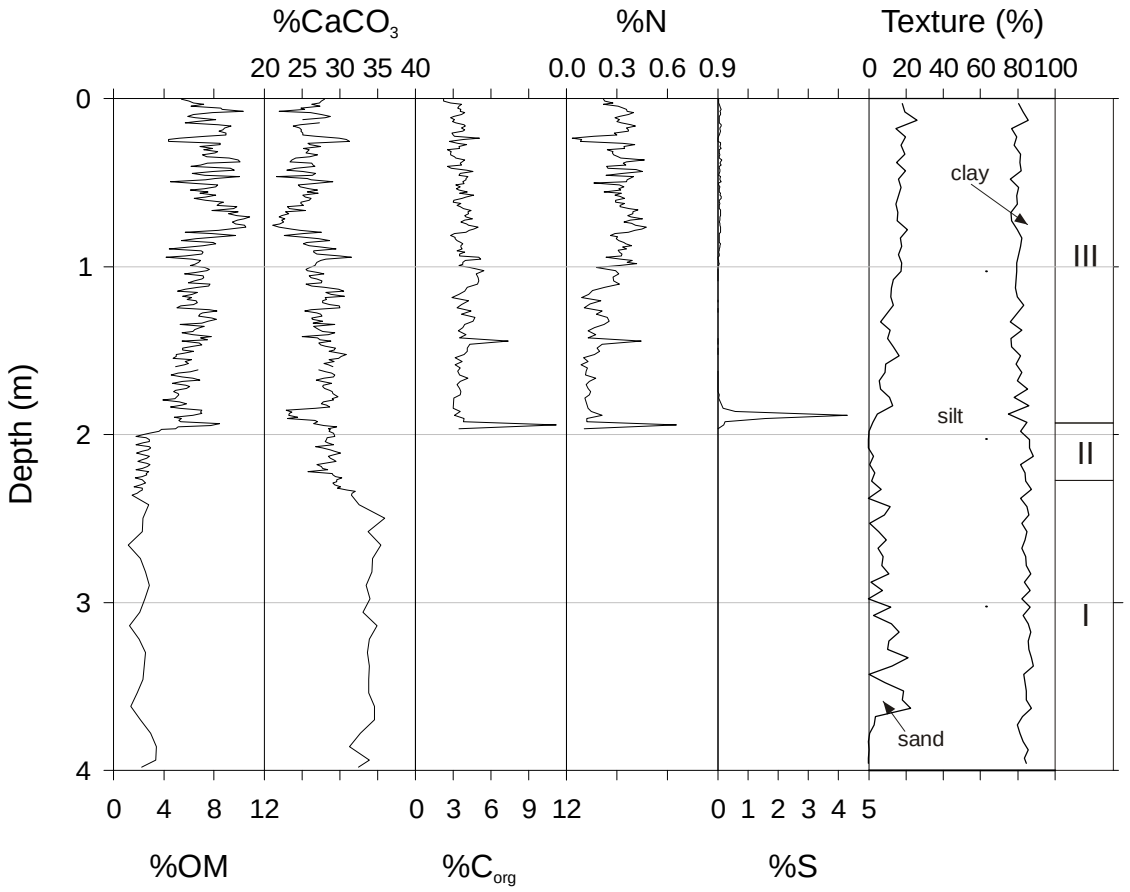
%CaCO3
20 25 30 35 40
%N
0.0 0.3 0.6 0.9
Texture (%)
0 20 40 60 80100
Depth (m)
0
1
2
3
4
clay
silt
sand
III
II
I
0 4 8 12
%OM
0 3 6 9 12
%Corg
0 1 2 3 4 5
%S

Figure 7.

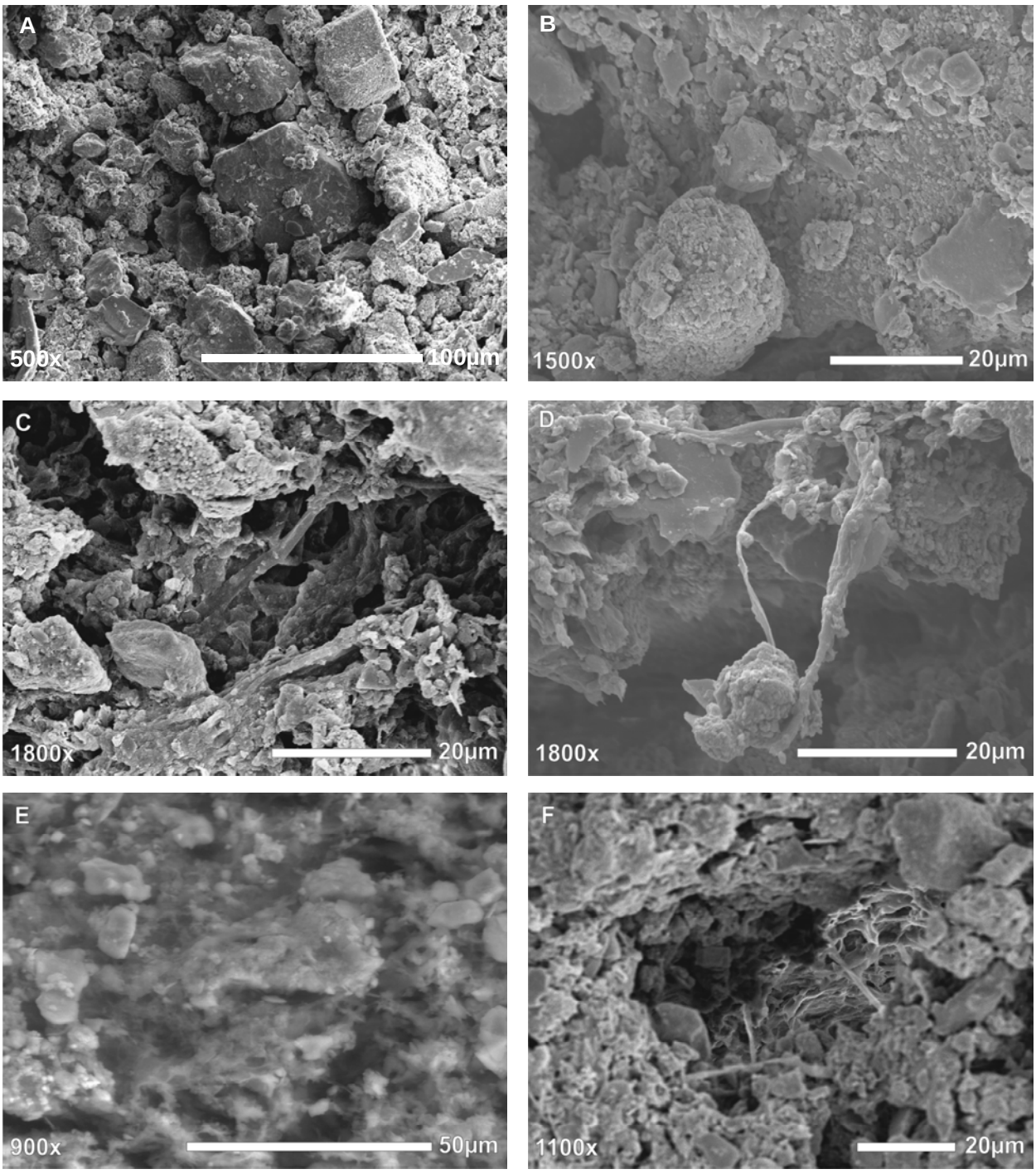
A
500x
100µm
B
1500x
20µm
C
1800x
20µm
D
1800x
20µm
E
900x
50µm
F
1100x
20µm

Figure 8.

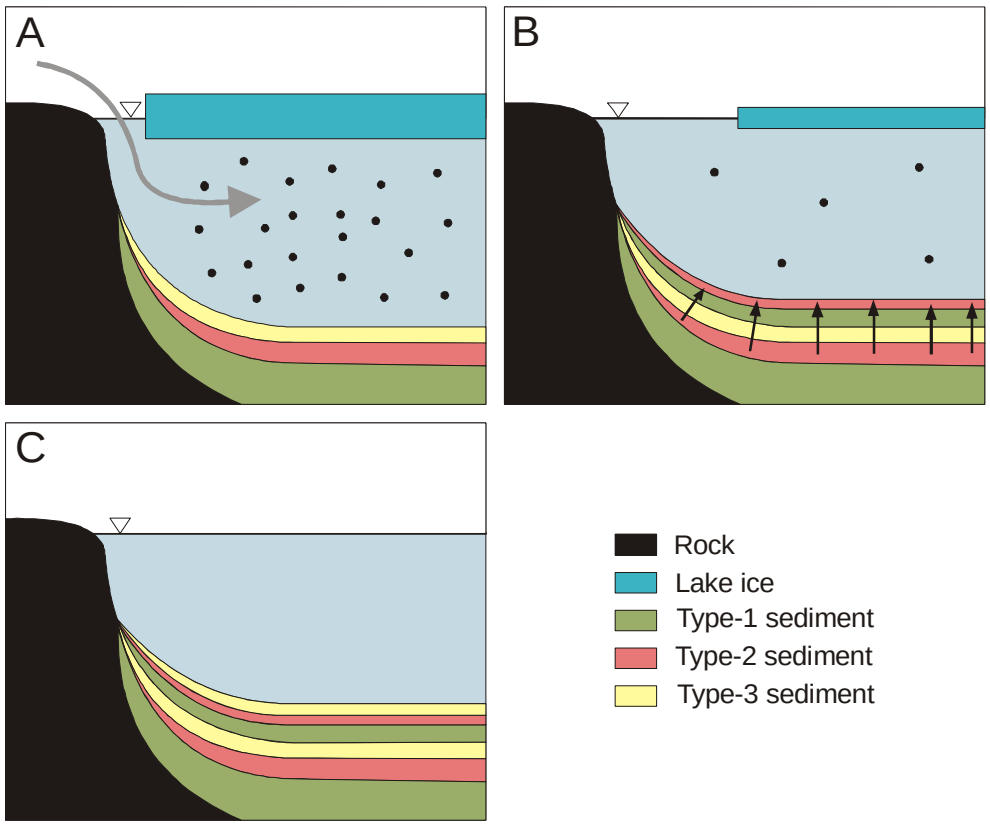
A
B
C
Rock
Lake ice
Type-1 sediment
Type-2 sediment
Type-3 sediment

CHAPTER 5

LACUSTRINE BIOLAMINATED SEDIMENTS FROM A HIGH ARCTIC FRESHWATER LAKE

KRYSTOPHER J. CHUTKO AND SCOTT F. LAMOUREUX

ABSTRACT

A laminated sequence of lacustrine sediment from an Arctic coastal lake was examined for the potential chronological and successional information contained within the record. The laminae are microbially induced sedimentary structures (MISS), the unlithified precursor of stromatolites, and are previously unreported in the Arctic. The annual sequence was interpreted to contain a basal clastic unit, overlain with successive cyanobacterial and extracellular polymeric substance units. The complex succession of laminae and inconclusive dating analysis results provided a challenge for identifying the chronological nature of the sedimentary structures. Statistical (Markov chain) and time series (auto-regressive models) analyses suggested that a plausible, quasi-annual sequence could be identified to provide a context for paleoenvironmental reconstruction. These results provide key recognition of sedimentary structure in recent biolaminated sediments and provide a first step towards the paleoenvironmental evaluation of the unusual geomicrobiological sequence.

INTRODUCTION

Microbially induced sedimentary structures (MISS) are a category of sediment laminae that are produced by the interaction between clastic sediment deposition and microbial (primarily cyanobacterial films and mats) production and growth (Noffke *et al*., 2001). These structures are considered the unlithified precursor of stromatolites (Parker *et al*., 1981; Reid *et al*., 2000), which range in age from Archaen to modern times (Pratt, 2003). Stromatolites have been a focus of research attention as they hold clues to the early evolution of life on Earth (Grotzinger and Knoll, 1999) and microbial mats have been documented in a wide range of environments, including both polar regions where they occur in extreme environmental conditions (Pierson, 1992). However, despite the potential for paleoenvironmental interpretation from these sediments, long records of MISS are absent from the current literature. This work provides the first detailed analysis of a MISS sequence from recent biolaminated sediments to investigate the chronological significance of the laminae and the time series characteristics of the sedimentary components. These results provide primary evidence for the likely presence of a quasi-annual sedimentary sequence and represent a first step towards evaluation of these geomicrobiological structures.

STUDY SITE

Lake J (unofficial name, 76° 11.4’ N, 90° 46.4’ W) is a moderate depth (z_{max} = 15 m), coastal lake (40 m asl) on the glaciated Colin Archer Peninsula, Devon Island, Canadian Arctic Archipelago (Fig. 1). The peninsula is underlain by mid-Devonian limestone (Mayr *et al*., 1998) and overlain by Quaternary glacial

and marine sediments (Dyke, 1998). Lake ice thickness was ~2.2 m thick in late May (2004 and 2005), and the bottom water was fresh (specific conductivity = 284 $\mu S \cdot cm^{-1}$). The 140 ha lake receives inflows of water and sediment from the surrounding hillslopes, primarily during the peak snowmelt period (Marsh and Woo, 1981). Post-glacial emergence of the lake occurred ~5.5 ka BP (Dyke, 1998) and since that time, sediment accumulation has consisted of a complex assemblage of organic and inorganic material (Chutko and Lamoureux, in preparation [4]).

Sediment cores were recovered with a Boyle (1995) corer in May 2004, stored unfrozen and upright, and transported to the laboratory upright. The cores were split lengthwise and sub-samples were prepared as thin sections for sedimentary analysis (Lamoureux, 1994). Thin sections were scanned at 2400 dpi on a Hewlett Packard S20 slide scanner and compiled into stratigraphic position in CorelDRAW X3. Where sedimentary structures were too thin (i.e., < 100 µm), light microscopy (100-200x) was used to identify sedimentary features.

Chronological constraint of the recent sediments was attempted with ^{137}Cs and ^{210}Pb profiles. Overall low levels of activity due to the High Arctic location complicated both methods (e.g., Hermanson, 1990). Results for ^{137}Cs yielded measurable concentrations in the upper 2.0 cm of the core, which had been disturbed by post-extraction transport. Results from ^{210}Pb α-spectroscopy (MyCore Scientific, Deep River, Canada) using the constant rate of supply (CRS) model (Appleby and Oldfield, 1978) were further complicated by highly variable

accumulation rates and uncertainty in the supported ^{210}Pb level (Fig. 2). Radiocarbon analysis was not carried out due to the absence of terrestrial macro-organic material and the abundance of carbonate terrain (Abbott and Stafford, 1996). Therefore, no conclusive or reliable conventional radioisotopic chronology could be applied to the sediment.

STRATIGRAPHIC ANALYSIS

Visual microscopy and related analyses indicated that the sediment was composed of microbially induced sedimentary structures (MISS; Noffke *et al*., 2001; Chutko and Lamoureux, in preparation [4]). The sediment was composed of three types: Type 1 (clastic), Type 2 (laminated organic), and Type 3 (massive organic). Clastic material was primarily composed of medium silt and likely originates from terrestrial runoff and inflow during the short spring snowmelt period. The two organic types were distinguished by colour and textural differences. Conventional scanning and environmental electron microscopy showed that the organic components were a combination of filamentous and mucus-like material, which were inferred to be cyanobacteria and extracellular polymeric substances, respectively (Chutko and Lamoureux, in preparation [4]). The individual laminae were counted, their thickness measured, and identified as Type 1, Type 2, or Type 3, based on the physical characteristics of each type. In total, 2102 laminae were identified in the 37.5 cm surface sediment core (Table 1).

Markov chain analysis was used to identify systematic succession patterns in the sedimentary sequence (Davis, 2002). An embedded Markov chain was

used, as the laminae of the same type did not succeed each other in the sequence. A χ^2 non-parametric test ($\alpha = 0.05$) was used to identify significant successions. First- and second-order analyses showed the dominant and significant presence of a Type 1/Type 2/Type 3 (hereafter 1-2-3) sequence (Table 2). The 1-2-3 sequence comprised 80% of all first-order transitions and 67% of all second-order transitions. Less frequent transitions included a 1-3-1 sequence (15% of second-order transitions), which generally appeared in clusters of thin units that demonstrated fragmented and folded structures (Fig. 3). A 1-2-1 sequence also occurred in clusters (9% of second order transitions), although these were less frequent and did not exhibit folded structures. Other sequence combinations were substantially less common (Table 2) and were irregularly distributed through the record.

After the sequence was split into one of the three sediment types (Fig. 4), the individual series were analyzed for serial correlation. Autocorrelation and partial autocorrelation plots show significant autoregressive behaviour in the Type 2 (AR(1), $\phi_1 = 0.21$) and Type 3 (AR(2), $\phi_1 = 0.18$, $\phi_2 = 0.16$) sedimentary structures. No evidence for significant time series structure was found with the Type 1 sediment. An AR1 and AR2 autoregressive model applied to the Type 2 and 3 series, respectively, produced residuals with no significant serial correlation and indicated that these models were parsimonious. These results suggested that the clastic laminae (Type 1) originated from effectively stochastic events with no statistical dependence on previous deposit thickness. By contrast, the two types of biogenic laminae demonstrated systematic dependence on the thickness

of the previous deposits. Hence, the biogenic laminae properties suggest that formation conditions were controlled, in part, by prior biogenic deposition.

CHRONOLOGAL INTERPRETATION

Although a conventional radioisotopic chronology could not be conclusively assigned to the Lake J sediment, the relatively simple High Arctic hydroclimatic regime provided a conceptual basis for the interpretation of a quasi-annual signal in the biolaminated sedimentary record. Since the lake basin is non-glacial and rainfall amounts in the region are typically low (Marsh and Woo, 1981; Chutko and Lamoureux, 2008 [2]), inputs of meltwater and sediment were generally restricted to the period of nival melt (Forbes and Lamoureux, 2005; Cockburn and Lamoureux, *in press*). This suggests that a clastic layer is likely to be deposited once per year during the primary snow melt period. Based on this assumption, the prominent 1-2-3 succession logically represents an annual sequence where the presence of the Type-1 sediment indicates spring deposition. Sediments from a morphologically comparable lake on Devon Island (Gajewski *et al*., 1997) appear to contain sedimentary components similar to Lake J, although they were not documented in a stratigraphic context. However, that study concluded that the organic-clastic rhythmites were annual structures.

The interpretation of an annual signal is further complicated by the presence of sedimentary sequences that do not follow the predominant 1-2-3 pattern. A heuristic model was developed to systematically define annual rhythmites throughout the record and defined as follows:

1. 1-2-3 represents the typical annual sequence;
2. 1-2 is an annual sequence without the biofilm (3) unit;
3. 1-3 is an annual sequence without the cyanobacteria (2) unit;
4. 2-3 is a rare annual sequence without the clastic (1) unit;
5. 2 is a rare annual sequence without both the clastic (1) and biofilm (3) units.

In rules 2 – 5, missing laminae are interpreted to be the result of a number of environmental conditions that either limit substantial sediment inflow to the lake and/or development of the microbial benthos. These conditions include insufficient meltwater and/or sediment supply to allow clastic sediment deposition (e.g., Braun *et al*., 2000), and delayed or incomplete lake ice removal which limits photosynthetically active radiation (PAR) penetration to the lake bottom or warming of the water column (Heath, 1988).

Application of these rules yielded 837 quasi-annual rhythmites, 57% of which were the idealized 1-2-3 sequence. Although this method considered all the laminae in the record, it did not allow for more complex sequences that may be produced by subannual meteorological, hydrological or microbiological phases. For example, unusual clusters of successive 1-3 units, which often contained contorted and folded laminae (Fig. 3) were one example of a sequence that may represent significant departure from the regular accumulation conditions assumed by the heuristic model. The nature of these clustered 1-3 sequences remains enigmatic, and no rational basis to either omit or include them in the chronology could be demonstrated.

The resultant chronological record showed the strong influence that the Type 1 sediment had on the inferred annual unit thickness (Fig. 5, Table 1). Correlation analysis further demonstrated the importance of the clastic component to overall sedimentation rates (Table 3). Positive outliers were more prevalent in the recent half of the record for all three sediment types. In particular, Type 2 outliers greater than 0.05 mm thickness were essentially absent in the early record (Fig. 5).

An alternative chronological approach considered only the 1-2-3 sequences as quasi-annual rhythmites and assumed that sequences that did not fit this pattern represented subannual units and were added to the preceeding 1-2-3 unit. This approach resulted in 474 inferred quasi-annual units and the number of laminae per unit ranged from three to 29. Although the accuracy of this method cannot be directly tested, it did compare more closely to the modelled ^{210}Pb age profiles (Fig. 2). At 19.5 cm, 171 annual units were found compared to 114-129 years suggested by the ^{210}Pb. However, it is likely that the 171 quasi-annual units represent an underestimate due to the 2.3 cm disturbance at the top of the sediment core.

Collectively, these results indicate the presence of complex sedimentary sequences and the basis for chronological development remains uncertain. Regardless, the persistence of the idealized 1-2-3 sequence strongly suggests the presence of a quasi-annual sedimentary signal.

ARCTIC LACUSTRINE MICROBIALLY INDUCED SEDIMENTARY STRUCTURES

While the identification of the sedimentary organic units as cyanobacteria and biofilm is equivocal, the structures bear a remarkable resemblance to those presented in previous studies. Schieber (1999) described wavy-crinkly laminae and cohesive behaviour as two characteristics of sedimentary structures influenced by microbial activity. Gerdes *et al*. (1993) and Noffke *et al*. (2001) provided detailed descriptions of the formation of MISS and detailed imagery of the structures. In all instances, the Lake J sediments resemble those of the previously reported sedimentary records (Fig. 3). However, identification of MISS records in a stratigraphic context in polar regions has previously not been reported. Gajewski *et al*. (1997) presented sedimentary results from a comparable lake on Devon Island and described the sediment as microbially influenced, although they did not evaluate the sedimentary sequence in detail. Cyanobacteria and microbial mat environments are ubiquitous in the polar regions (Vincent, 2000) and therefore it is reasonable to observe such sedimentary structures, and several cases of sediment records from the Taylor Valley in Antarctica contain biolaminated sediments (Parker *et al*., 1981; Wagner *et al*., 2006). However, our results represent the first detailed documentation of microbially induced sedimentary structure sequence characteristics. These results indicate the need for further integration of microbial studies (e.g., Vincent, 2000) with sedimentary approaches (e.g., Noffke *et al.*, 2001) to fully realize the potential of the sediments for paleoenvironmental studies of microbial activity. The potential of this work represents a complementary and significant step

beyond sedimentary pigment analyses that depend on bulk sampling techniques (e.g., Vézina and Vincent, 1997; Leavitt and Hodgson, 2001).

RECENT ENVIRONMENTAL CHANGES

The inferred chronology in the Lake J record suggests the potential that these sediments have for paleoenvironmental interpretations. The clastic laminae originate from snowmelt-induced runoff, and therefore potentially contain information regarding snowfall and melt processes (Forbes and Lamoureux, 2005; Cockburn and Lamoureux, *in press*). Similarly, the organic units may be in part controlled by availability of photosythetically active radiation at the lake bottom, which is in turn controlled by lake ice thickness (Vopel and Hawes, 2006). Following these interpretations, we speculate that the increased variability in unit thickness and the presence of significant outliers in the upper part of the record is consistent with changes to algal ecosystems in the past 100-150 years that suggest reduced ice cover due to anthropogenic climate warming in the Arctic (Smol *et al*., 2005). However, a more detailed understanding of contemporary environment-microbial interactions and formation processes (e.g., Vézina and Vincent, 1997; Tang and Vincent, 2000) is necessary to elaborate on these observations in the MISS.

CONCLUSIONS

The stratigraphic record of a biolaminated sediment sequence from an Arctic freshwater lake was examined and the temporal and sequence characteristics were evaluated in order to determine the chronological nature of

individual structures and dominant sequence associations. Laminae were defined as Type 1 (clastic), Type 2 (cyanobacteria) or Type 3 (biofilm). The record of clastic and organic laminae demonstrated strong first- and second-order Markovian properties, and a prominent and significant sequence with Type 1/2/3 laminae was observed. Significant serial correlation was evident in the two types of inferred biogenic laminae, while the clastic laminae thickness was stochastic. Inconclusive radiogenic dating due to low radioisotope activities prevented reliable conventional chronological constraint. However, a chronological framework was developed with simple heuristic rules based on physically plausible assessments of laminae formation. This quasi-annual chronology represents a first attempt to develop paleoenvironmental inferences from a record of microbially induced sedimentary structures (MISS). Additional characterization of the biogenic components may reveal further links to contemporary ecological and geomicrobiological processes.

ACKNOWLEDGEMENTS

This work was supported by ArcticNet, a Network of Centres of Excellence of Canada, and a Natural Sciences and Engineering Research Council of Canada Discovery Grant to S.F.L. and Northern Scientific Training Program and Queen's University Graduate Dean's Travel grants to K.J.C. The Polar Continental Shelf Project, Natural Resources Canada, provided logistical field support. This research was supported by Nunavut Research Institute Scientific Research License 0200406R-M. Field assistance by J. Cockburn and laboratory assistance by J. Tomkins is greatly appreciated.

REFERENCES

Abbott, M.B. and T.W. Stafford, Jr. 1996. Radiocarbon geochemistry of modern and ancient arctic lake systems, Baffin Island, Canada. *Quaternary Research*, **45**: 300-311.

Appleby, P.G. and F. Oldfield. 1978. The calculation of lead-210 dates assuming a constant rate of supply of unsupported ^{210}Pb to the sediment. *Catena*, **5**: 1-8.

Boyle, J.F. 1995. A simple closure mechanism for a compact, large-diameter, gravity corer. *Journal of Paleolimnology*, **13**: 85-87.

Braun, C., Hardy, D.R., Bradley, R.B. and M.J. Retelle. 2000. Streamflow and suspended sediment transfer to Lake Sophia, Cornwallis Island, Nunavut, Canada. *Arctic, Antarctic, and Alpine Research*, **32**: 456-465.

Chutko, K.J. and S.F. Lamoureux. 2008. Identification of coherent links between interannual sedimentary structures and daily meteorological observations in Arctic proglacial lacustrine varves: potentials and limitations. *Canadian Journal of Earth Sciences*, **45**: 1-13.

Cockburn , J.M.H. and S.F. Lamoureux. In press. Hydroclimate controls over seasonal sediment yield in two adjacent High Arctic watersheds. *Hydrological Processes*.

Davis, J.C. 2002. *Statistics and data analysis in geology*. John Wiley and Sons, New York.

Dyke, A.S. 1998. Holocene delevelling of Devon Island, Arctic Canada: implications for ice sheet geometry and crustal response. *Canadian Journal of Earth Sciences*, **35**: 885-904.

Forbes, A.C., and Lamoureux, S.F. 2005. Climatic controls on streamflow and suspended sediment transport in three large Middle Arctic catchments, Boothia Peninsula, Nunavut, Canada. *Arctic, Antarctic, and Alpine Research*, **37**: 304-315.

Gajewski, K., Hamilton, P.B. and R. McNeely. 1997. A high resolution proxy-climate record from an arctic lake with annually-laminated sediments on Devon Island, Nunavut, Canada. *Journal of Paleolimnology*, **17**: 215-225.

Gerdes, G., Claes, M., Dunajtschik-Piewak, K., Riege, H., Krumbein, W.E. and H.-E. Reineck. 1993. Contribution of microbial mats to sedimentary surface structures. *Facies*, **29**: 61-74.

Grotzinger, J.P. and A.H. Knoll. 1999. Stromatolites in Precambrian carbonates: evolutionary mileposts or environmental dipsticks. *Annual Review of Earth and Planetary Sciences*, **27**: 313-358.

Heath, C.W. 1988. Annual primary productivity of an Antarctic continental lake: phytoplankton and benthic algal mat production strategies. *Hydrobiologia*, **165**: 77-87.

Hermanson, M.H. 1990. ^{210}Pb and ^{137}Cs chronology of sediments from small, shallow Arctic lakes. *Geochimica et Cosmochimica Acta*, **54**: 1443-1451.

Lamoureux, S.F. 1994. Embedding unfrozen lake sediments for thin section preparation. *Journal of Paleolimnology*, **10**: 141-146.

Leavitt, P.R. and D.A. Hodgson. 2001. Sedimentary pigments. *In*: Smol, J.P., Birks, H.J.B. and W.M. Last (eds.). *Tracking Environmental Change Using Lake Sediments. Volume 3: Terrestrial, Algal, and Siliceous Indicators*. Kluwer AP, Dordrecht: 295-325.

Marsh, P. and M.-K. Woo. 1981. Snowmelt, glacier melt, and High Arctic streamflow regimes. *Canadian Journal of Earth Sciences*, **18**: 1380-1384.

Mayr, U., de Freitas, T., and B. Beauchamp. 1998. *The Geology of Devon Island North of 76°, Canadian Arctic Archipelago*. Geological Survey of Canada Bulletin 526.

Noffke, N., Gerdes, G., Klenke, T., Krumbein, W.E. 2001. Microbially induced sedimentary structures – a new category within the classification of primary sedimentary structures. *Journal of Sedimentary Research*, **71**: 649-656.

Parker, B.C., Simmons Jr., G.M., Love, F.G., Wharton, R.A. and K.G. Seaburg. 1981. Modern stromatolites in Antarctic Dry Valley lakes. *Bioscience*, **31**: 656-661.

Pierson, B.K. 1992. Modern mat-building microbial communities: A key to the interpretation of Proterozoic stromatolitic communities - Introduction. *In*: Schopf, J.W. and C. Klein (eds.). *The Paleozoic Biosphere: A Multidisciplinary Study*. Cambridge UP, Cambridge: 247-251.

Pratt, B.R. 2003. Stromatolites. *In*: Middleton, G.V. (ed.). *Encyclopedia of Sedimentology and Sedimentary Rocks*. Kluwer AP, Dordrecht: 688-690.

Reid, R.P., Visscher, P.T., Decho, A.W., Stolz, J.F., Bebout, B.M., Dupraz, C., Macintyre, I.G., Paerl, H.W., Pinckney, J.L., Prufert-Bebout, L., Steppe, T.F. and D.J. DesMarais. 2000. The role of microbes in accretion, lamination and early lithification of modern marine stromatolites. *Nature*, **406**: 989-992.

Schieber, J. 1999. Microbial mats in terrigenous clastics: the challenge of identification in the rock record. *Palaios*, **14**: 3-12.

Smol, J.P., Wolfe, A.P., Birks, H.J.B., Douglas, M.S.V., Jones, V.J, Korhola, A., Pienitz, R., Rühland, K., Sorvari, S., Antoniades, D., Brooks, S.J., Fallu, M.-A., Hughes, M., Keatley, B.E., Laing, T.E., Michelutti, N., Nazarova, L., Nyman, M., Paterson, A.M., Perren, B., Quinlan, R., Rautio, M., Saulnier-Talbot, É, Siitonen, S., Solovieva, N., and J. Weckström. 2005. Climate-driven regime shifts in the biological communities of arctic lakes. *Proceedings of the National Academy of Sciences*, **102**: 4397-4402.

Tang, E.P.Y. and W.F. Vincent. 2000. Effects of day length and temperature on the growth and photosynthesis of an Arctic cyanobacterium, *Schizothrix calcicola* (Oscillatoriaceae). *European Journal of Phycology*, **35**: 263-272.

Vézina, S. and W.F. Vincent. 1997. Arctic cyanobacteria and limnological properties of their environment: Bylot Island, Northwest Territories, Canada (73°N, 80°W). *Polar Biology*, **17**: 523-534.

Vincent, W.F. 2000. Cyanobacterial dominance in the polar regions. *In*: Whitton, B.A. and M. Potts (eds.). *The Ecology of Cyanobacteria*. Kluwer AP, Dordrecht: 321-340.

Vopel, K. and I. Hawes. 2006. Photosynthetic performance of benthic microbial mats in Lake Hoare, Antarctica. *Limnology and Oceanography*, **51**: 1801-1812.

Wagner, B., Melles, M., Doran, P.T., Kenig, F., Forman, S.L., Pierau, R. and P. Allen. 2006. Glacial and postglacial sedimentation in the Fryxell basin, Taylor Valley, southern Victoria Land, Antarctica. *Palaeogeography, Palaeoclimatology, Palaeoecology*, **241**: 320-337.

Table 1. Summary statistics of laminae counts and thickness measurements.

Unit Type	Number of Units	Mean Thickness (mm)	Standard Deviation	Maximum Thickness (mm)	Minimum Thickness (mm)
Type 1 (clastic)	748	0.355	0.744	8.545	0.004
Type 2 (cyanobacteria)	646	0.045	0.033	0.428	0.006
Type 3 (biofilm/EPS)	708	0.081	0.097	0.841	0.003

Table 2. Observed (A) first- and (B) second-order Markovian transition frequency matrices of the Lake J laminated sequence. A total of 2102 laminae were identified.

A

From \ To	1	2	3	Total
1	0	556	192	748
2	129	0	516	645
3	618	90	0	708
Total	747	646	708	2101

B

From \ To	1	2	3	Total
1-2	80	0	475	555
1-3	139	53	0	192
2-1	0	108	21	129
2-3	479	37	0	516
3-1	0	447	171	618
3-2	49	0	41	90
Total	747	645	708	2100

Table 3. Pearson correlation coefficients between each of the three sediment types and the inferred annual unit derived from the heuristic model. Significant correlations (α = 0.01) are noted in bold.

	Type 1	Type 2	Type 3	Annual Unit
Type 1	1.000			
Type 2	**0.114**	1.000		
Type 3	0.018	**-0.106**	1.000	
Annual Unit	**0.991**	**0.147**	**0.143**	1.000

Figure Captions

Figure 1. Study site. A. Colin Archer Peninsula, Devon Island, Canadian Arctic Archipelago. B. Lake J in the Archer River valley. Dark grey areas indicate plateau ice caps. C. Bathymetry and coring location in Lake J.

Figure 2. ^{210}Pb CRS depth-age models and interpreted MISS chronologies (left panel). The starting years for the MISS chronologies are based on estimated 55 (heuristic model) and 31 (alternative model) year gaps due to the disturbed upper portion of the core, and determined using respective 0.42 and 0.74 mm·a^{-1} accumulation rates. Down core ^{210}Pb activity (right panel). Constant rate of supply (CRS) age models (Appleby and Oldfield, 1978) are derived from ^{210}Pb activity profile and assume background supported ^{210}Pb of either ^{1}0.027 or ^{2}0.021 Bq·g^{-1}.

Figure 3. Thin section photomicrographs of Lake J MISS. A) Typical 1-2-3 sequence, 4.5 cm core depth. B) Type 2 sediment (arrows) exhibiting wavy-crinkly structure, 11.8 cm core depth. C) Type 3 sediment exhibiting microbial grain separation (box), 6.6 cm core depth. D) 1-3-1 sequence showing contorted structures (box), 16.3 cm core depth.

Figure 4. Laminae thickness for the three sediment types. The vertical dashed lines indicate equivalent core depth levels, as the number of laminae of each type was not equal.

Figure 5. Chronological interpretation of the three sediment types and the total annual unit for all laminae based on the 1-2-3 sequence and the heuristics discussed in the text.

Figure 1.

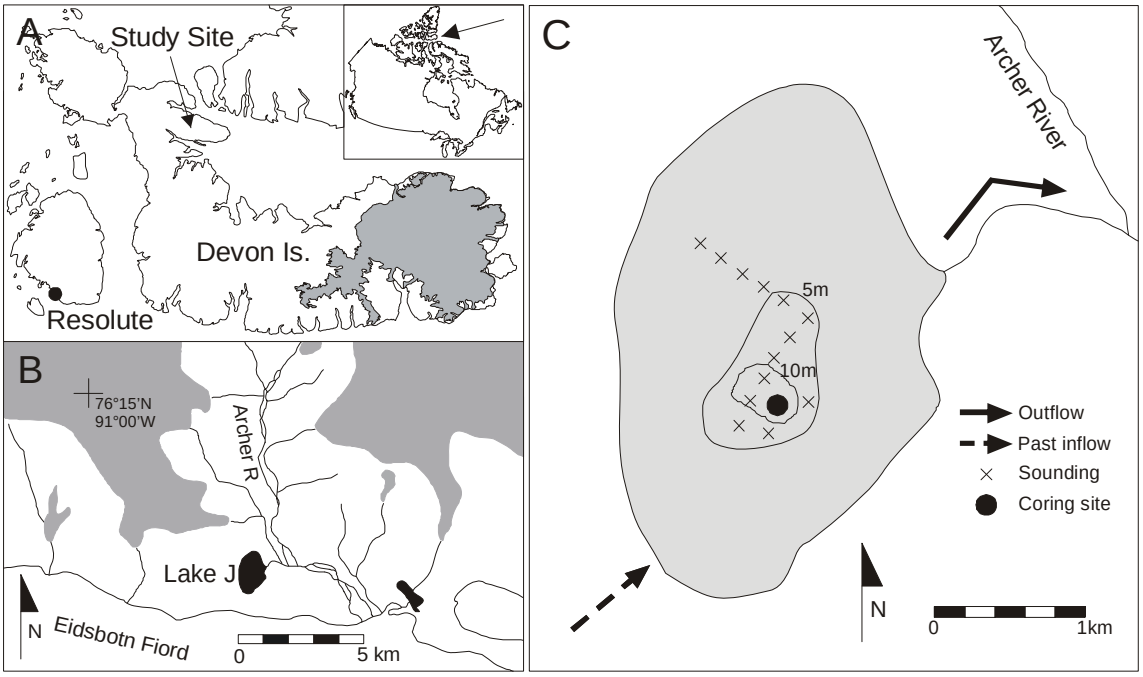
A
Study Site
Devon Is.
Resolute
B
76°15'N
91°00'W
Archer R
Lake J
N
Eidsbotn Fiord
0
5 km
C
Archer River
5m
10m
Outflow
Past inflow
Sounding
Coring site
N
0
1km

Figure 2.

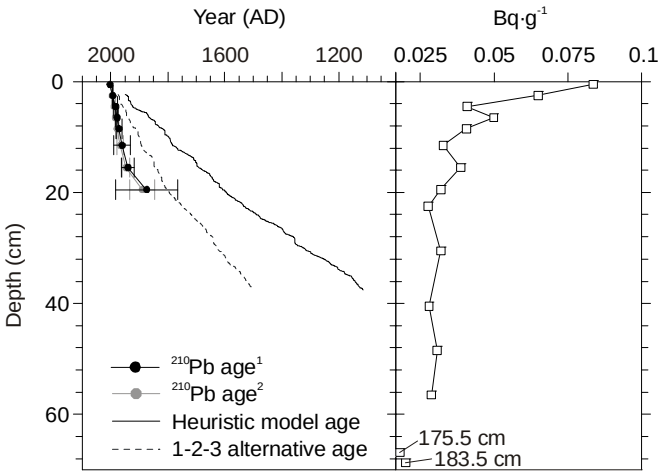
Year (AD)
2000
1600
1200
Bq·g-1
0.025
0.05
0.075
0.1
0
20
40
60
Depth (cm)
210Pb age1
210Pb age2
Heuristic model age
1-2-3 alternative age
175.5 cm
183.5 cm

Figure 3.

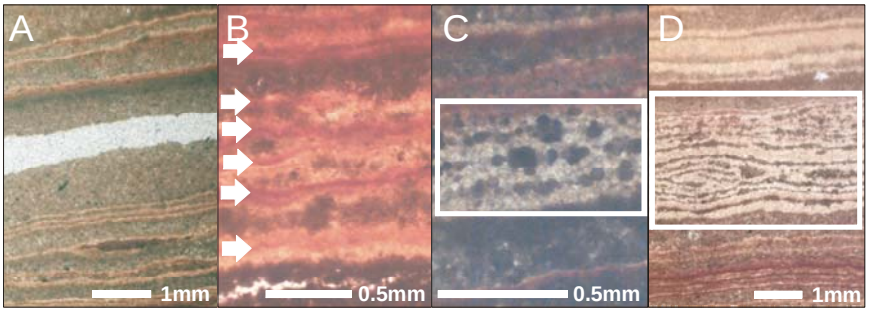

Figure 4.

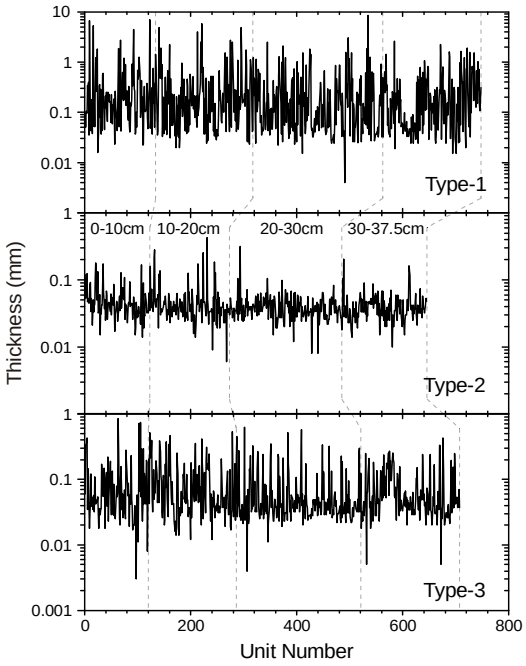
Thickness (mm)
Unit Number
Type-1
Type-2
Type-3
0-10cm
10-20cm
20-30cm
30-37.5cm
10
1
0.1
0.01
1
0.1
0.01
1
0.1
0.01
0.001
0
200
400
600
800

Figure 5.

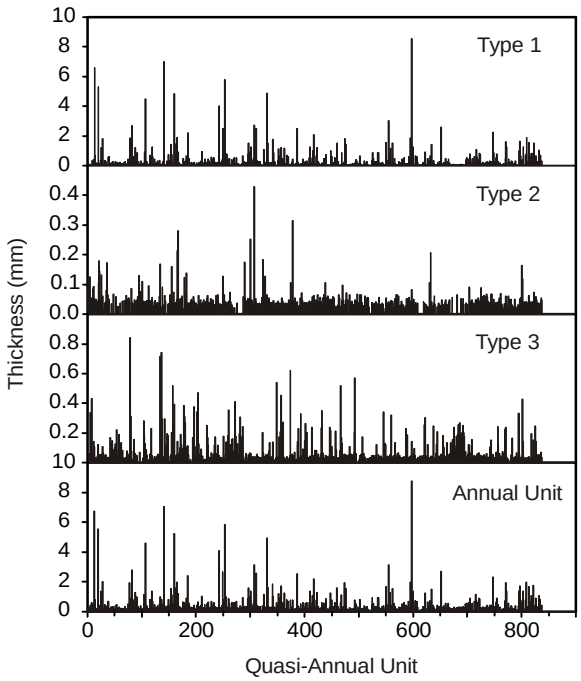
Type 1
Type 2
Type 3
Annual Unit
Thickness (mm)
Quasi-Annual Unit
0
200
400
600
800

CHAPTER 6

GENERAL DISCUSSION AND CONCLUSIONS

Laminated lacustrine sediments have been used for a number of studies of paleoenvironmental change (e.g., Desloges and Gilbert, 1994; Lamoureux and Bradley, 1996; Moore *et al*., 2001). However, many of these studies rely on an inferred simple relationship between the sedimentary structure (i.e., the varve) and one or more broad meteorological forcings (e.g., summer temperature). While these relationships often show statistical significance, they are often weak and do not explain a large proportion of the variance observed between the two records (Hodder *et al*., 2007). Subannual structures, on the other hand, potentially allow for the distinction between different causative factors, such as temperature and rainfall-induced deposition, and therefore produce a more complete representation of the climatic signal contained in the varve (Shaw *et al*., 1978; Leemann and Niessen, 1994; Hambley and Lamoureux, 2006). Where varves are not present, a chronology may be inferred from identifying annual accumulation patterns in the individual sedimentary structures.

Clastic proglacial sediments in Lake R contain complex subannual laminae, which, in some cases, can be attributed directly to short-term weather conditions during the particular melt season. These sedimentary structures showed a rhythmicity that was confirmed to be annual. The subannual laminae were shown to be related to various meteorological events that occurred throughout the year, including early season melt events, small and large glacial

melt events through the melt season, and infrequent large rainfall events that occurred primarily in the late summer. Although a clear varve-meteorology relationship could be shown for a number of years in the record, the relationship was compromised by variable geomorphic controls that influenced the delivery of sediment to the lake bottom. This control affected the effective proximal-distal relationship between the coring station and the sediment inflow, which was reflected in variations in sediment grain size and distribution. These observations demonstrated the value of understanding the controls on sediment deposition, and that relationships between sedimentation and meteorology may not be simple (e.g., Hodder *et al*., 2007).

The varve-meteorology relationship is further complicated by the paucity of long term, continuous weather monitoring stations in the High Arctic. Such monitoring records are needed in order to calibrate the recent varve record and allow for interpretation beyond the measurement period. However, High Arctic weather stations located near sea level are not necessarily representative of the surrounding region, particularly in the central and eastern Arctic which is dominated by plateau and alpine topography. Simplified vertical temperature extrapolation by the use of “typically observed” (e.g., Legates and Willmott, 1990; Glover, 1999; Braithwaite *et al*., 2006) vertical lapse rates (VLRs) does not capture the highly variable vertical lapse rates observed in the High Arctic (Marshall *et al*., 2007).

In particular, summer inversions potentially influence snow and ice melt energy to a great extent. Inversions were seen to occur coincidentally with periods of positive temperatures at sea level, and thereby increased the air

temperature at high elevations. Also, summer inversions were most common between late June and early August, the primary period of melt in the region. Furthermore, increased summer inversion frequency since the late 1980s was coincident with observations of enhanced glacial melt. It is therefore speculated that increased summer inversions, potentially controlled by the occurrence of a Siberian-centred polar vortex, have contributed to the increase in summer melt rates observed in the Arctic since the late 1980s.

While laminated minerogenic sediments often produce records of annual or subannual environmental conditions, biolaminated sediment also hold potential for the development of paleoenvironmental reconstructions. Microbially induced sedimentary structures (MISS) are the result of the interaction between clastic sedimentation and microbial growth and production (Noffke *et al*., 2001), both of which are potentially controlled by processes that occur in the lake and watershed. However, MISS are not easily interpreted, and the bulk of microbial mat research is focused on contemporary biogeochemical processes operating at the mat surface (e.g., Vézina and Vincent, 1997; Bonilla *et al*., 2005) and not necessarily on the formation of annual or subannual sedimentary remains and structures. Long records of polar MISS have been identified in Antarctica (Wagner *et al*., 2006) and potentially in the High Arctic (Gajewski *et al*., 1997), although they have not been discussed in a sedimentary context and only broad environmental interpretations have been made.

Biolaminated sediments in Lake J were described in the context of Holocene lake development as well as the potential for a quasi-annual interpretation of sediment accumulation. The lake record documented changes

in the nature of sediment deposition from open, proglacial marine conditions, followed by a quiescent, emergent marine-lacustrine transition, to isolated, shallow lacustrine conditions with a productive benthic microbial ecosystem which has existed for approximately 5000 years. Although the record of Holocene emergence has been described before for Arctic lakes (Van Hove *et al*., 2007), the remarkable late Holocene MISS record has not been described in the research literature.

However, significant challenges, primarily with radiogenic chronological techniques, precluded the construction of a reliable depth-age model for the MISS record and therefore the laminae could not be readily identified as being varved or quasi-annually laminated. The sedimentary structures did show clear rhythmicity, and Markov chain analyses showed that a prominent pattern of clastic-cyanobacteria-biofilm laminae accumulation was present. Furthermore, the two organic components exhibited significant autoregressive behaviour, while the clastic component exhibited stochastic behaviour. On the basis of these observations, a heuristic model that utilized physically plausible quasi-annual accumulation scenarios was developed. This model allowed the construction of a quasi-annual sediment chronology, potentially from which paleoenvironmental conditions can be interpreted.

Future directions

Recent work has illuminated the importance of subannual laminae in understanding the composition of varves for the purposes of developing paleoenvironmental interpretations (Hambley and Lamoureux, 2006; Cockburn

and Lamoureux, 2007). However, further work is necessary to implement this understanding in an effort to develop detailed reconstructions of past environmental conditions and change.

Sediment structures undergo physical changes as they are progressively buried. For example, compaction of sediments at depth is known to occur, but the structure of the sediment remains, including the presence of subannual laminae (Petterson *et al*., 1993). Therefore there is potential for long sedimentary sequences to contain centennial to millennial-length records of subannual meteorological conditions, where such records can be recovered.

There is also a need to investigate the processes that produce microbially induced sedimentary structures in the High Arctic environment. While such studies have been carried out extensively in tropical and temperate regions (e.g., Gerdes *et al*., 1993; Noffke *et al*., 2001), the Arctic environment likely has specific formative processes. Much research has been focused on the productivity of contemporary Arctic microbial mat ecosystems (Vézina and Vincent, 1997; Bonilla *et al*., 2005), but little of this effort has been directed at understanding the controls on annual growth, burial and diagenetic processes. Although the Arctic hydroclimatic system is often treated as more simple than in other regions, the primary assumption being that most activity occurs during the short Arctic summer, this may not be the case with submerged microbial ecosystems and the interaction between the sedimentological and biological systems is complex and in need of dedicated study. By doing so, it may be possible to extend the links between meteorological observations and clastic sedimentation to include biogenic sediments that will yield a wide range of paleoenvironmental

interpretations. In microbial mat environments, such interpretations would likely contribute towards a refinement of the understanding of the evolution of early life on Earth as well.

References

Bonilla, S., Villeneuve, V. and W.F. Vincent. 2005. Benthic and planktonic algal communities in a High Arctic lake: pigment structure and contrasting responses to nutrient enrichment. *Journal of Phycology*, **41**: 1120-1130.

Braithwaite, R.J., Raper, S.C.B. and K. Chutko. 2006. Accumulation at the equilibrium-line of glaciers inferred from a degree-day model and tested against field observations. *Annals of Glaciology*, **43**: 329-334.

Cockburn, J.M.H. and S.F. Lamoureux. 2007. Century-scale variability in late-summer rainfall events recorded over seven centuries in subannually laminated lacustrine sediments, White Pass, British Columbia. *Quaternary Research*, **67**: 193-203.

Desloges, J.R. and R. Gilbert. 1994. Sediment source and hydroclimatic inferences from glacial lake sediment: the postglacial sedimentary record of Lillooet Lake, British Columbia. *Journal of Hydrology*, **159**: 375-393.

Gajewski, K., Hamilton, P.B. and R. McNeely. 1997. A high resolution proxy-climate record from an arctic lake with annually-laminated sediments on Devon Island, Nunavut, Canada. *Journal of Paleolimnology*, **17**: 215-225.

Gerdes, G., Claes, M., Dunajtschik-Piewak, K., Riege, H., Krumbein, W.E. and H.-E. Reineck. 1993. Contribution of microbial mats to sedimentary surface structures. *Facies*, **29**: 61-74.

Glover, R.W. 1999. Influence of spatial resolution and treatment of orography on GCM estimates of the surface mass balance of the Greenland Ice Sheet. *Journal of Climate*, **12**: 551-563.

Hambley, G.W. and S.F. Lamoureux. 2006. Recent summer climate recorded in complex varved sediments, Nicolay Lake, Cornwall Island, Nunavut, Canada. *Journal of Paleolimnology*, **35**: 629-640.

Hodder, K.R., Gilbert, R. and J.R. Desloges. 2007. Glaciolacustrine varved sediment as an alpine hydroclimatic proxy. *Journal of Paleolimnology*, **38**: 365-394.

Lamoureux, S.F. and R.S. Bradley. 1996. A late Holocene varved sediment record of environmental change from northern Ellesmere Island, Canada. *Journal of Paleolimnology*, **16**: 239-255.

Leemann, A. and F. Niessen. 1994. Varve formation and the climatic record in an Alpine proglacial lake: calibrating annually-laminated sediments against hydrological and meteorological data. *The Holocene*, **4**: 1-8.

Legates, D.R. and C.J. Willmott. 1990. Mean seasonal and spatial variability in global surface air temperature. *Theoretical and Applied Climatology*, **41**: 11-21.

Marshall, S.J., Sharp, M.J., Burgess, D.O. and F.S. Anslow. 2007. Near-surface-temperature lapse rates on the Prince of Wales Icefield, Ellesmere Island, Canada: implications for regional downscaling of temperature. *International Journal of Climatology*, **27**: 385-398.

Moore, J.J., Hughen, K.A., Miller G.J. and J.T. Overpeck. 2001. Little Ice Age recorded in summer temperature reconstruction from varved sediments of Donard Lake, Baffin Island, Canada. *Journal of Paleolimnology*, **25**: 503-517.

Noffke, N., Gerdes, G., Klenke, T., Krumbein, W.E. 2001. Microbially induced sedimentary structures – a new category within the classification of primary sedimentary structures. *Journal of Sedimentary Research*, **71**: 649-656.

Petterson, G., Renberg, I., Geladi, P, Lindberg, A. and F. Lindgren. 1993. Spatial uniformity of sediment accumulation in varved lake sediments in northern Sweden. *Journal of Paleolimnology*, **9**: 195-208.

Shaw, J., Gilbert, R. and J.J.J. Archer. 1978. Proglacial lacustrine sedimentation during winter. *Arctic and Alpine Research*, **10**: 689-699.

Van Hove, P., Belzile, C., Gibson, J.A.E. and W.F. Vincent. 2006. Coupled landscape-lake evolution in High Arctic Canada. *Canadian Journal of Earth Sciences*, **43**: 533-546.

Vézina, S. and W.F. Vincent. 1997. Arctic cyanobacteria and limnological properties of their environment: Bylot Island, Northwest Territories, Canada (73°N, 80°W). *Polar Biology*, **17**: 523-534.

Wagner, B., Melles, M., Doran, P.T., Kenig, F., Forman, S.L., Pierau, R. and P. Allen. 2006. Glacial and postglacial sedimentation in the Fryxell basin, Taylor Valley, southern Victoria Land, Antarctica. *Palaeogeography, Palaeoclimatology, Palaeoecology*, **241**: 320-337.

APPENDICES

APPENDIX I

Melt event plots using an annual vertical lapse rate calculation, 1961-2003. Plots in the left column include a -3 °C ice proximity cooling factor. Daily rainfall ($mm \cdot d^{-1}$) is plotted on the upper x-axis. Melt event intensity (°C) is plotted on the lower x-axis.

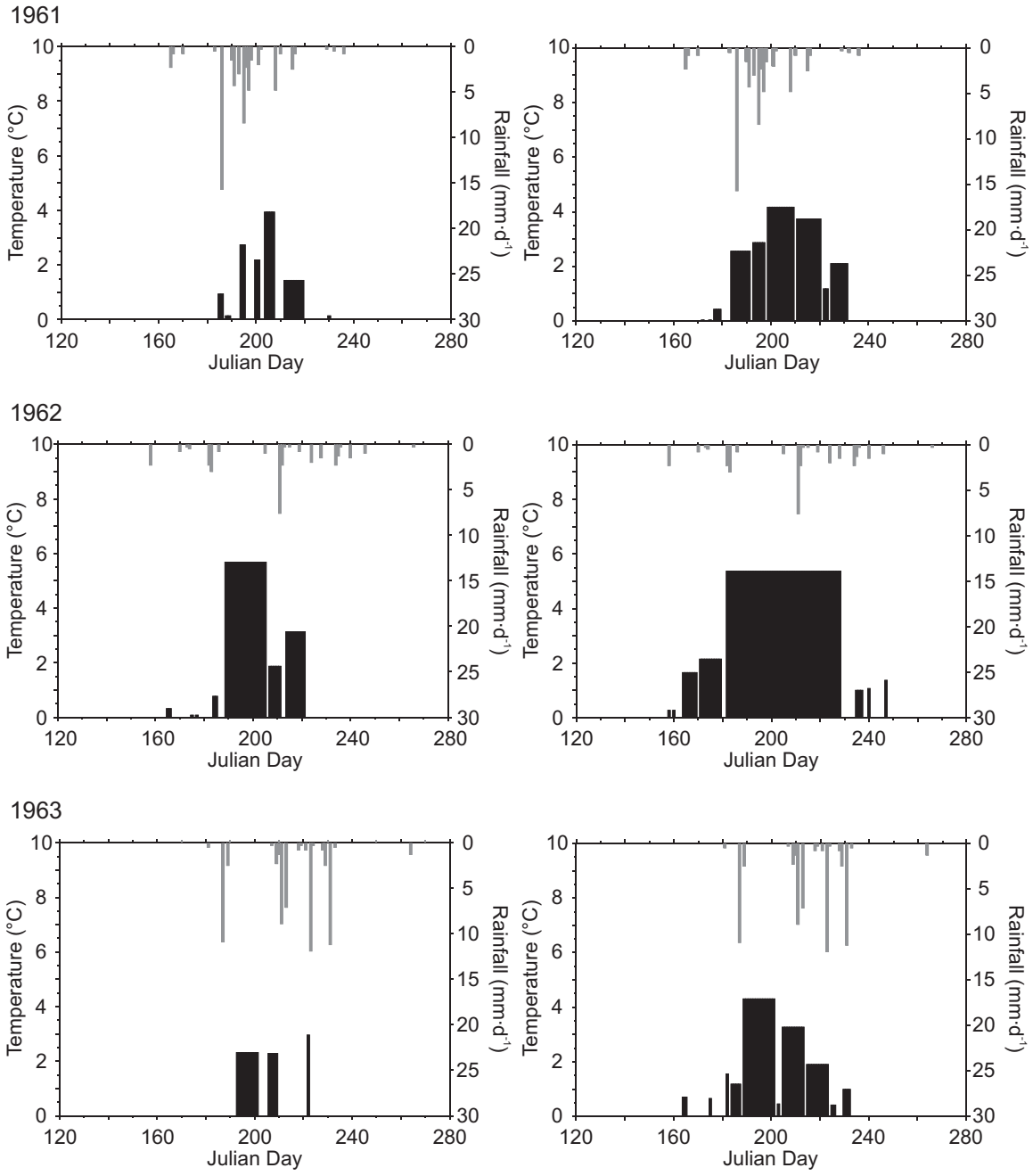

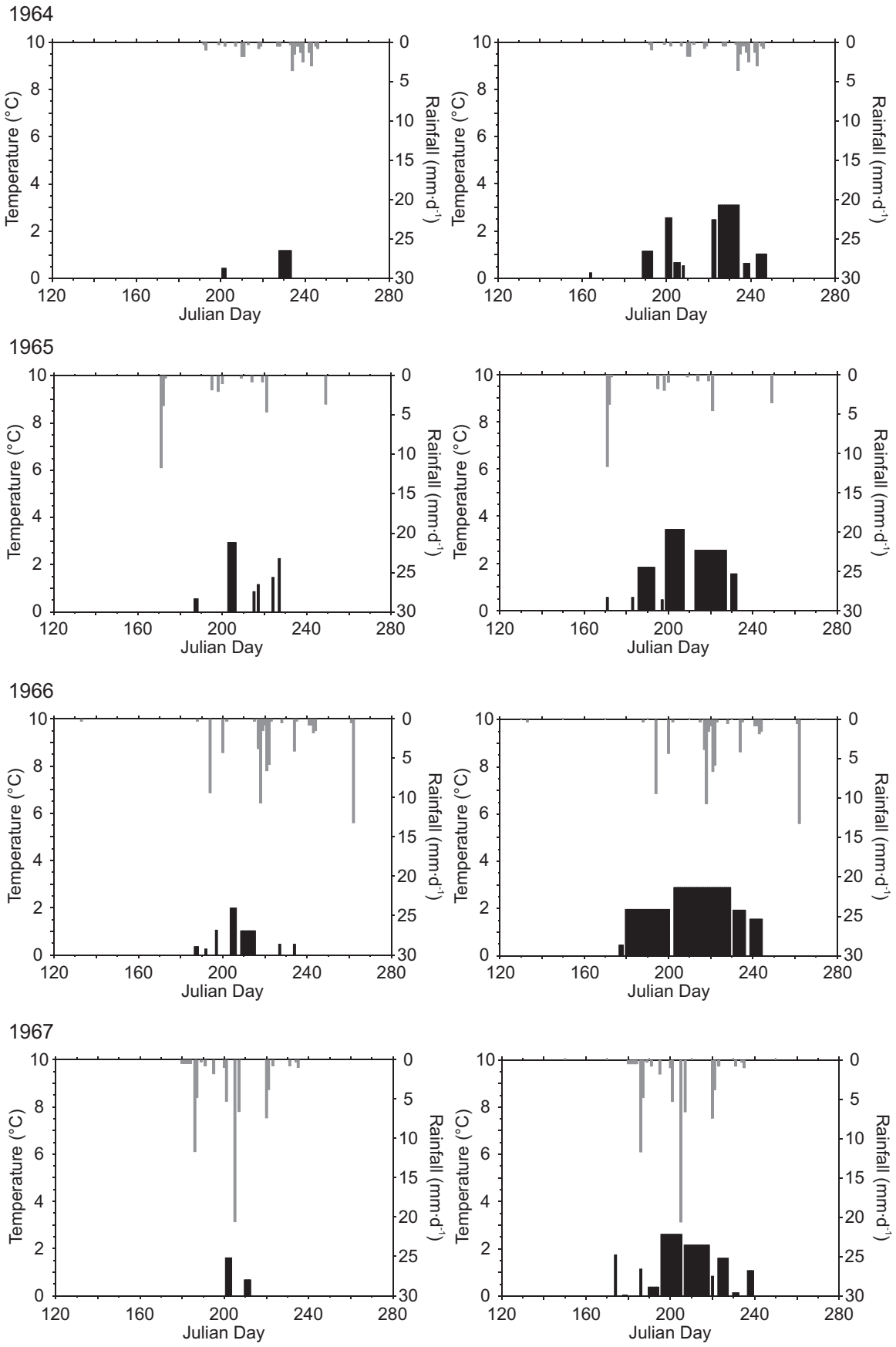
1964
1965
1966
1967
Temperature (°C)
Rainfall (mm·d-1)
Julian Day
120
160
200
240
280
0
2
4
6
8
10
0
5
10
15
20
25
30

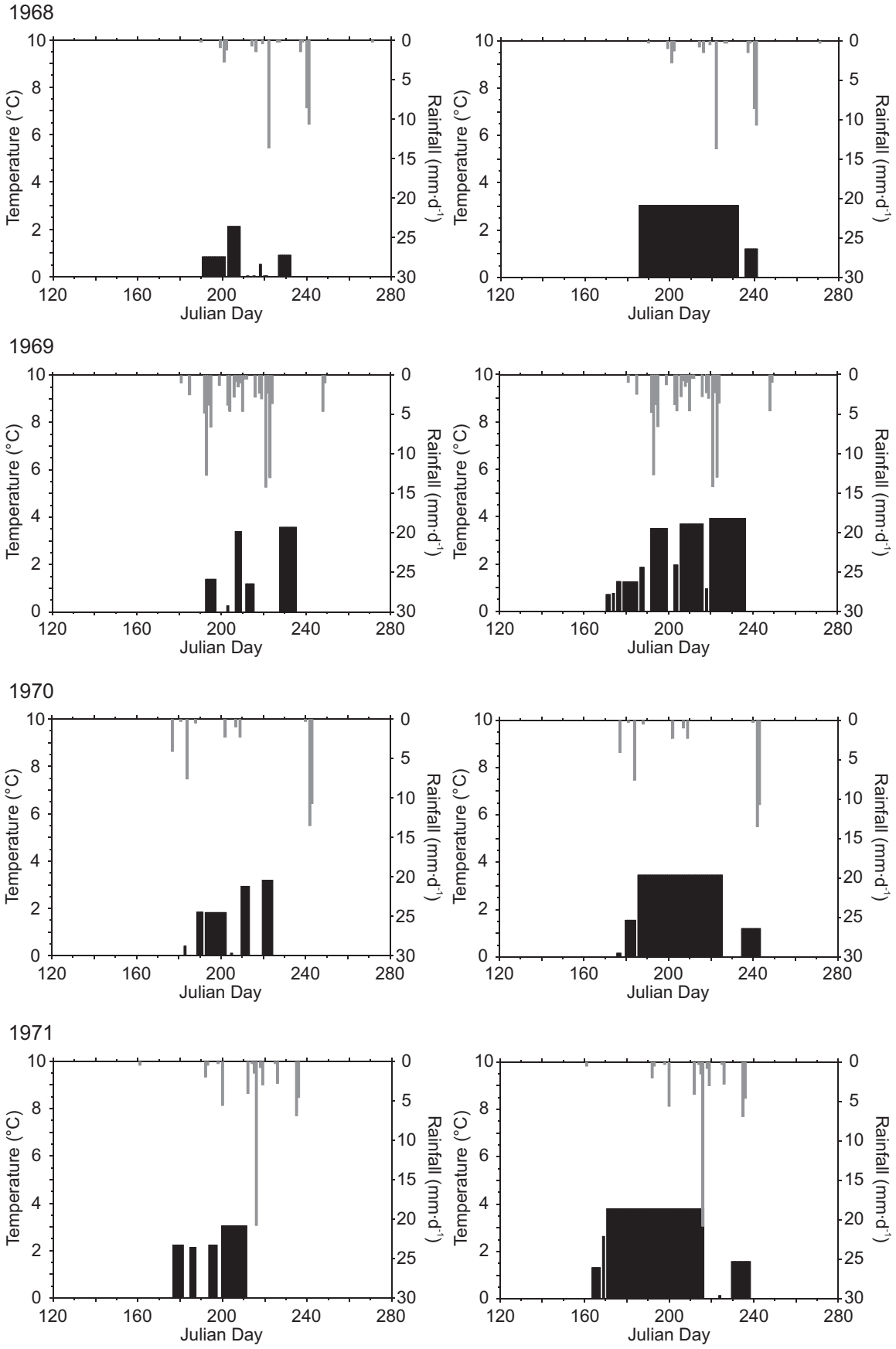
1968
1969
1970
1971
Temperature (°C)
Rainfall (mm·d-1)
Julian Day
120
160
200
240
280
0
2
4
6
8
10
0
5
10
15
20
25
30

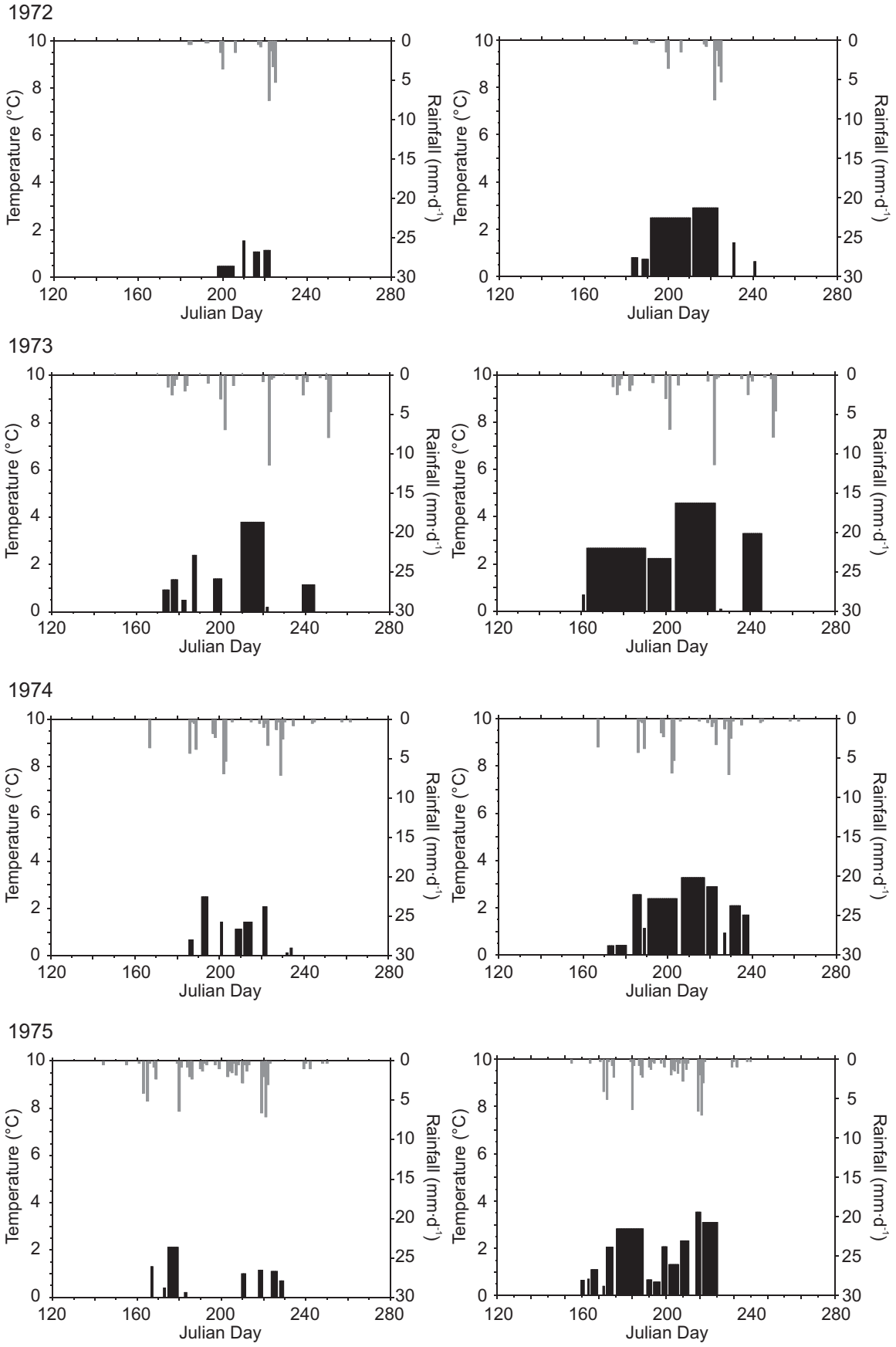
1972
1973
1974
1975
Temperature (°C)
Rainfall (mm·d-1)
Julian Day
120
160
200
240
280
0
2
4
6
8
10
0
5
10
15
20
25
30

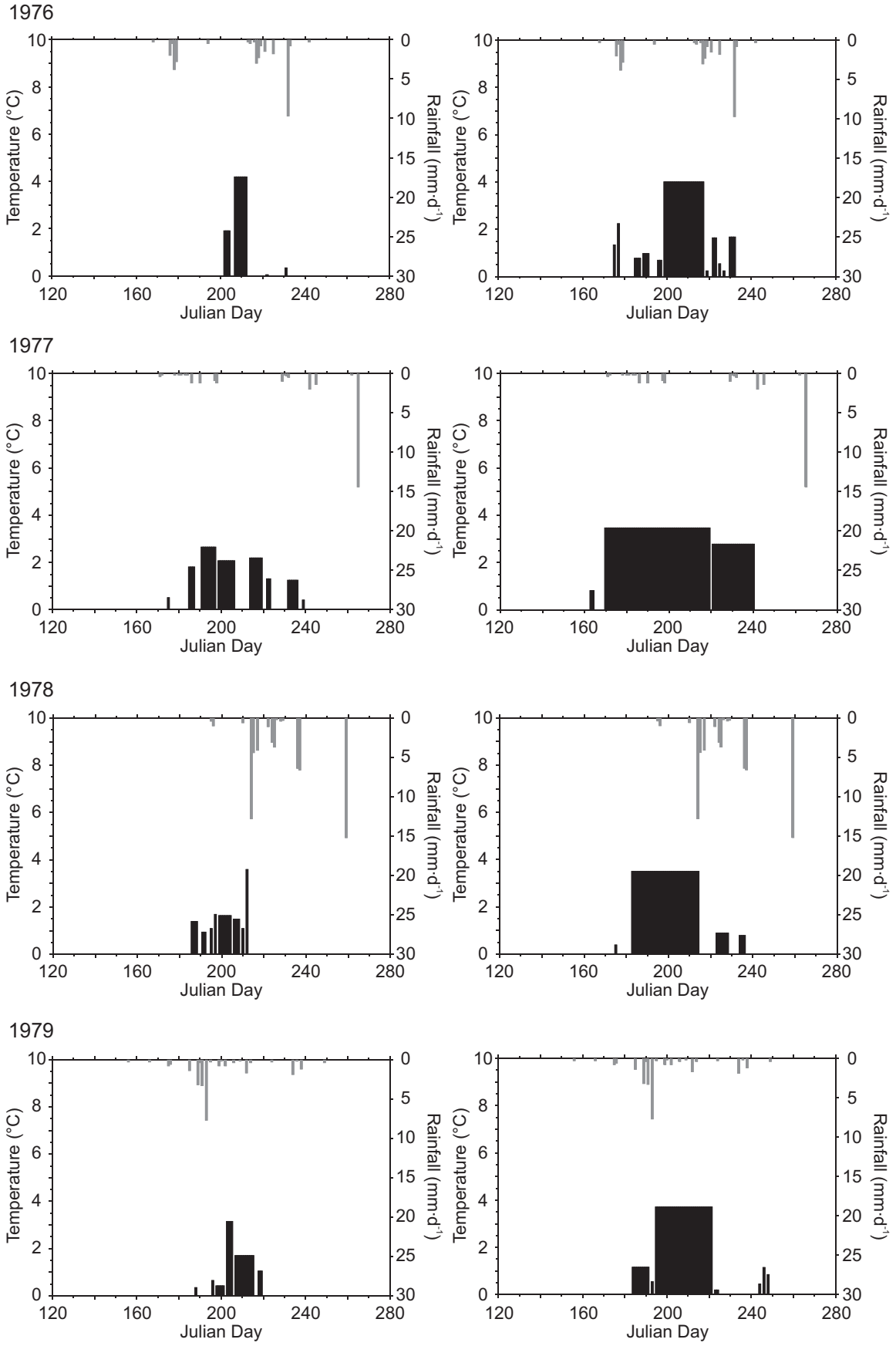
1976
1977
1978
1979
Temperature (°C)
Rainfall (mm·d-1)
Julian Day
120
160
200
240
280
0
2
4
6
8
10
0
5
10
15
20
25
30

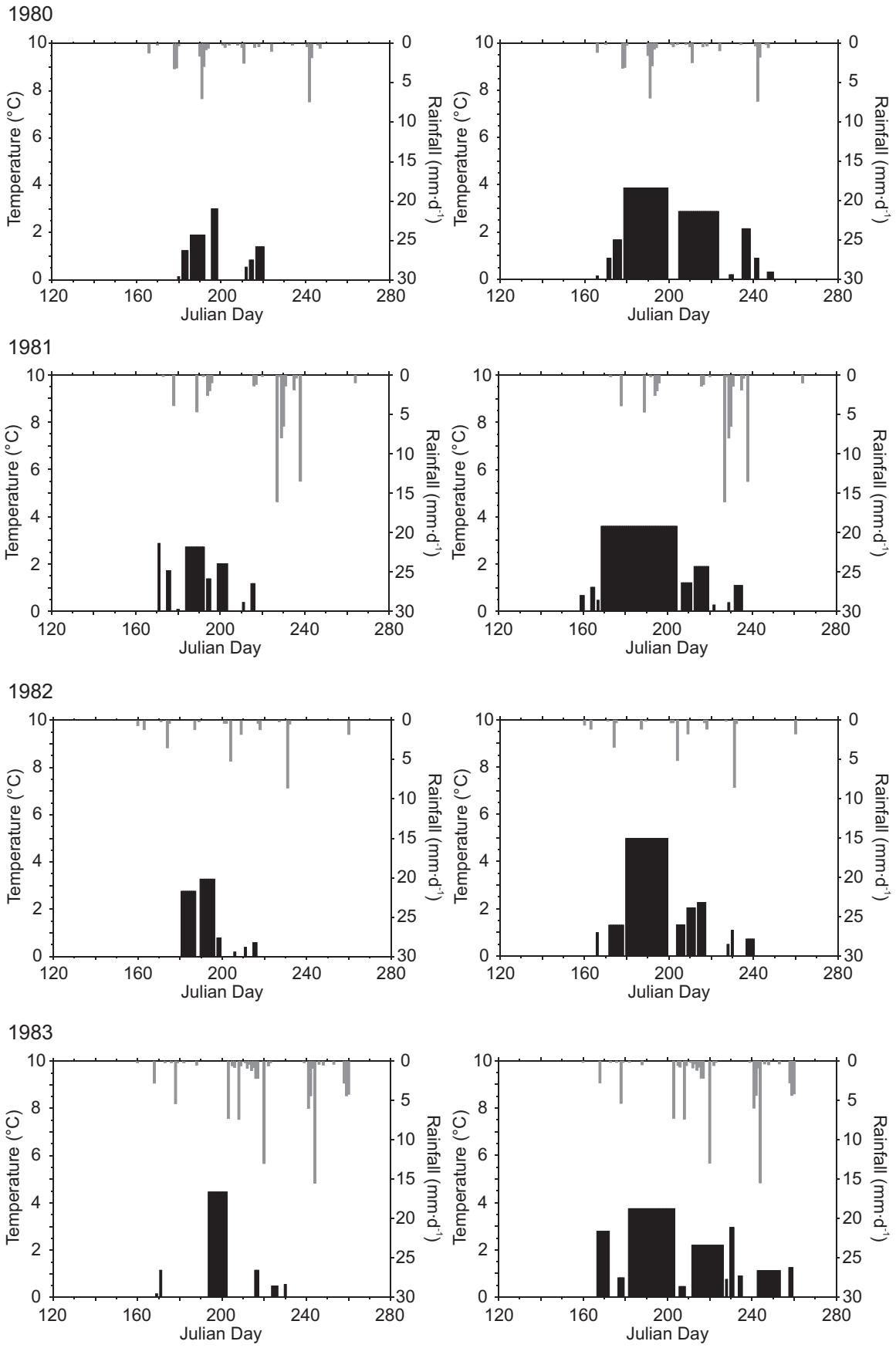
1980
1981
1982
1983
Temperature (°C)
Rainfall (mm·d-1)
Julian Day
120
160
200
240
280
0
2
4
6
8
10
0
5
10
15
20
25
30

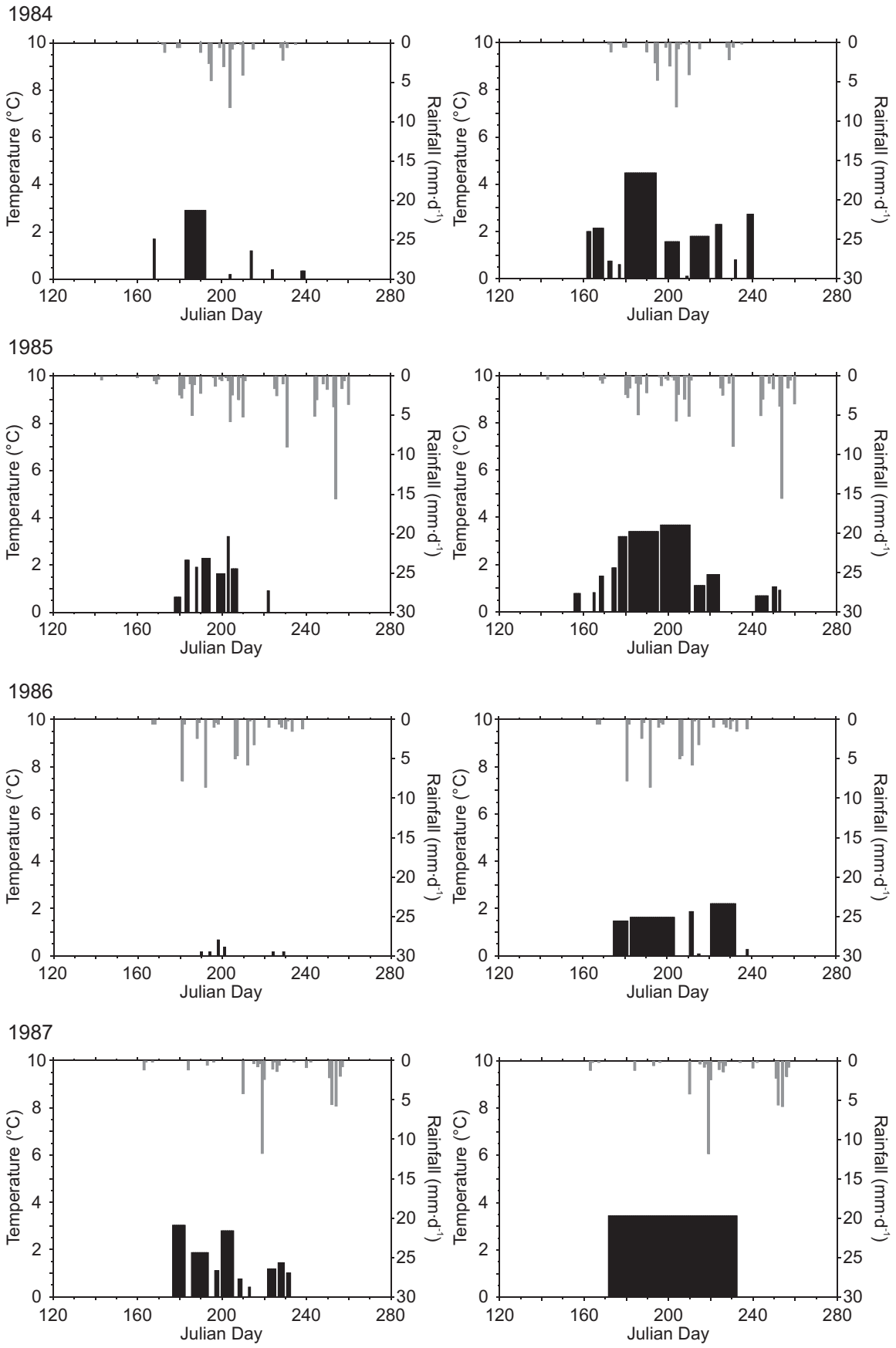
1984
1985
1986
1987
Temperature (°C)
Rainfall (mm·d-1)
Julian Day
120
160
200
240
280
0
2
4
6
8
10
0
5
10
15
20
25
30

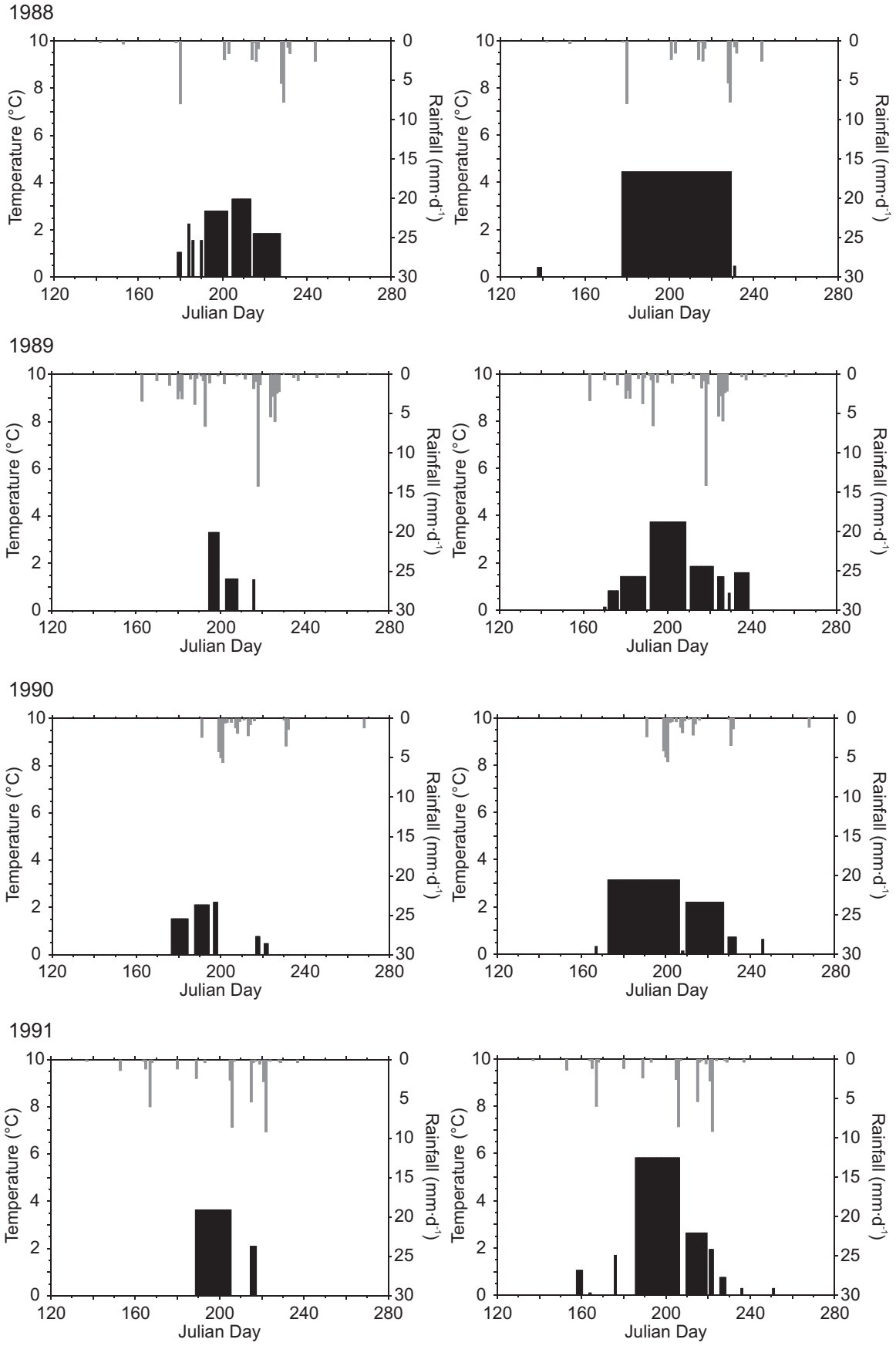
1988
1989
1990
1991
Temperature (°C)
Rainfall (mm·d-1)
Julian Day
120
160
200
240
280
0
2
4
6
8
10
0
5
10
15
20
25
30

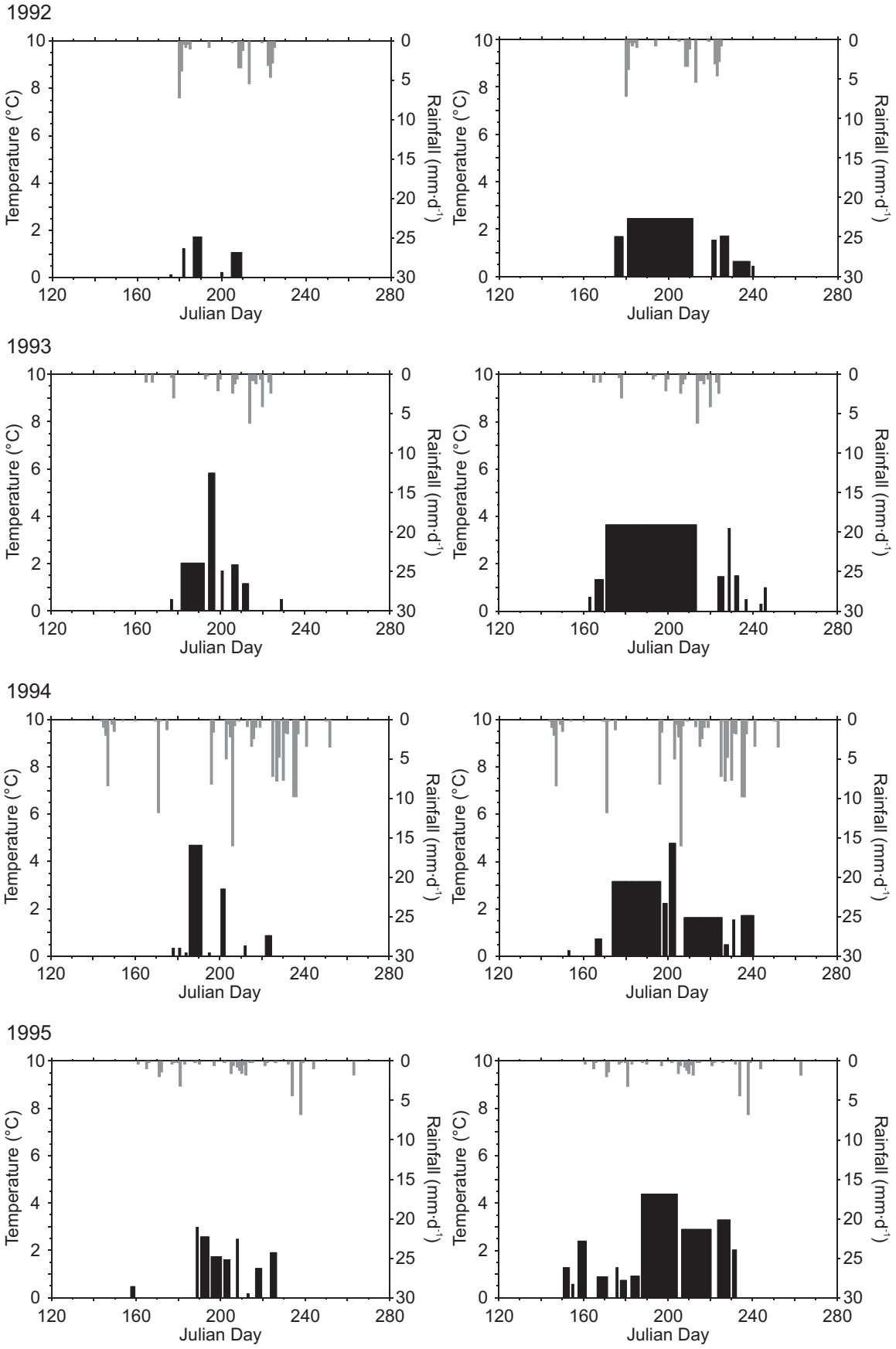
1992
1993
1994
1995
Temperature (°C)
Rainfall (mm·d-1)
Julian Day
0
2
4
6
8
10
0
5
10
15
20
25
30
120
160
200
240
280

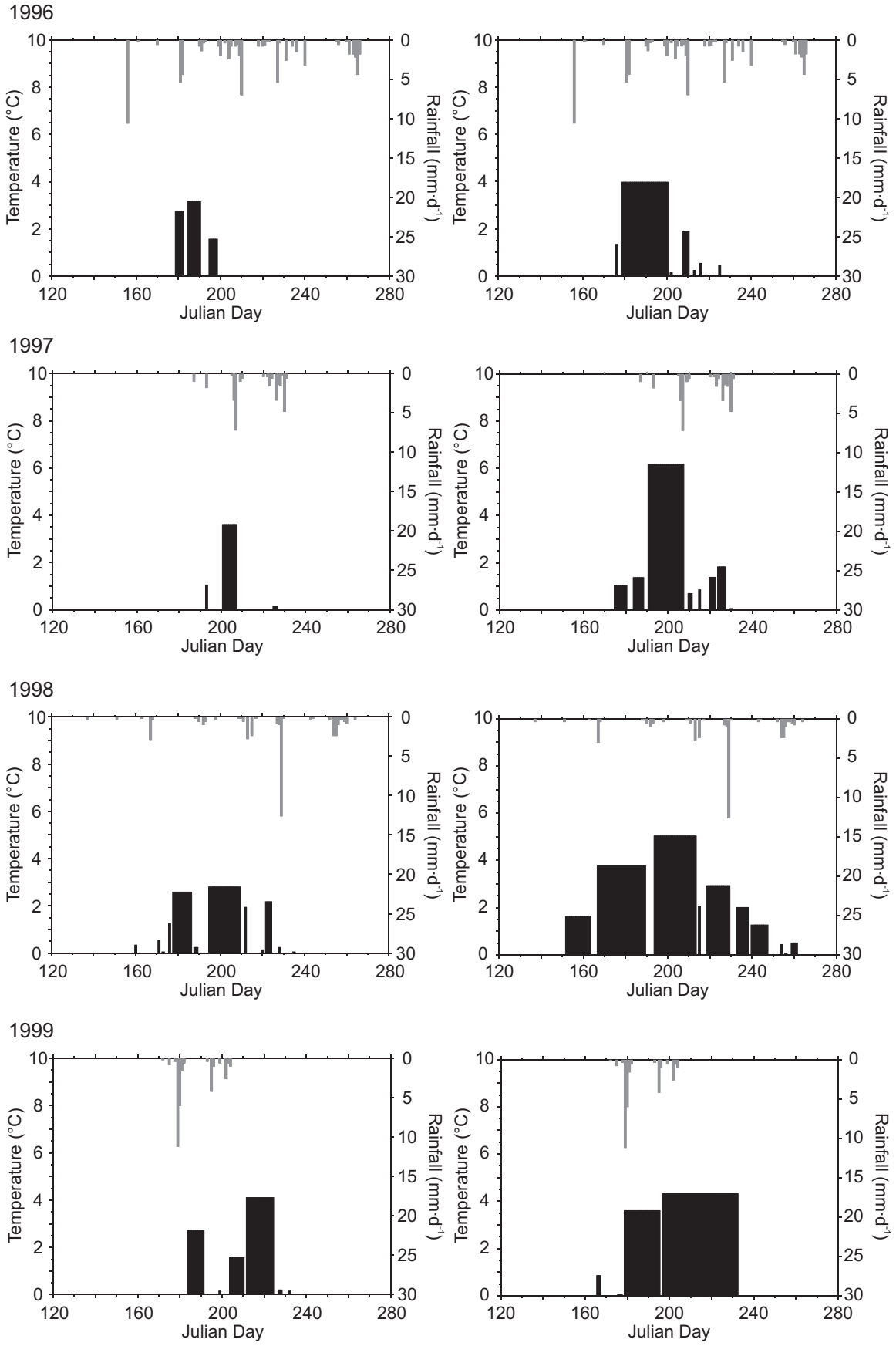
1996
1997
1998
1999
Temperature (°C)
Rainfall (mm·d-1)
Julian Day
120
160
200
240
280
0
2
4
6
8
10
0
5
10
15
20
25
30

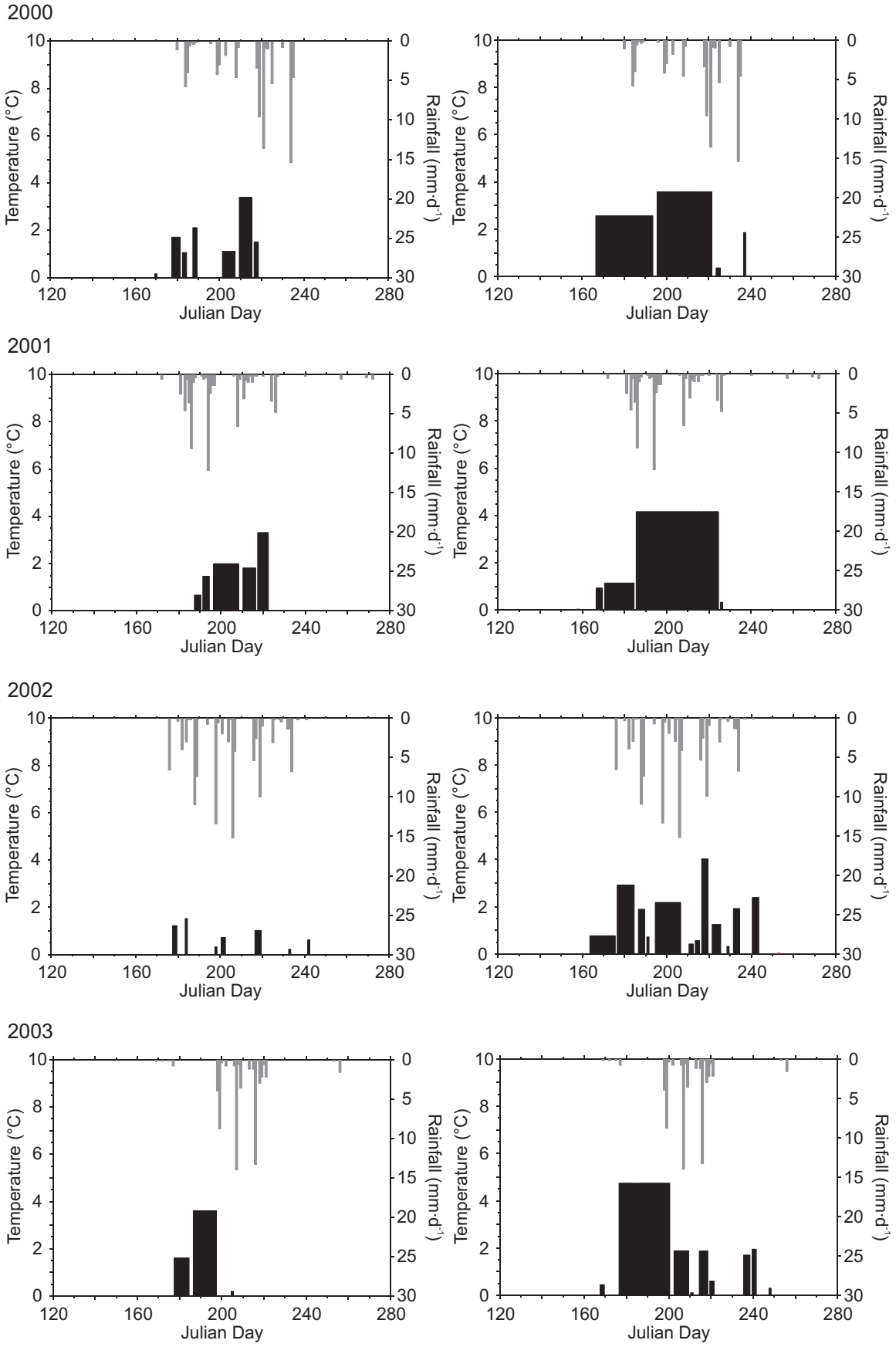
2000
2001
2002
2003
Temperature (°C)
Rainfall (mm·d-1)
Julian Day
120
160
200
240
280
0
2
4
6
8
10
0
5
10
15
20
25
30

APPENDIX II

Melt event plots using a daily vertical lapse rate calculation, 1961-2003. Plots in the left column include a -3 °C ice proximity cooling factor. Daily rainfall ($mm \cdot d^{-1}$) is plotted on the upper x-axis. Melt event intensity (°C) is plotted on the lower x-axis.

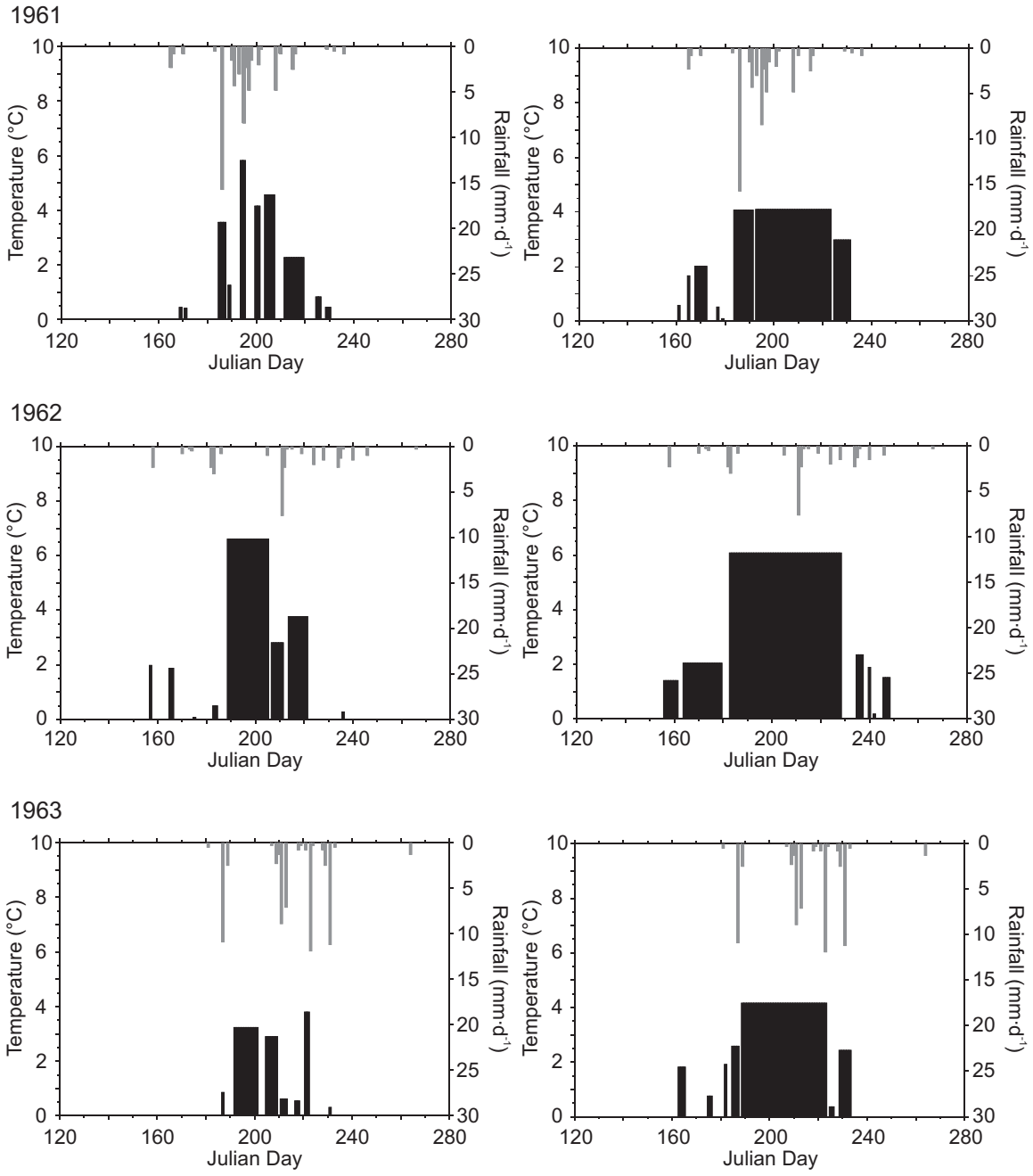

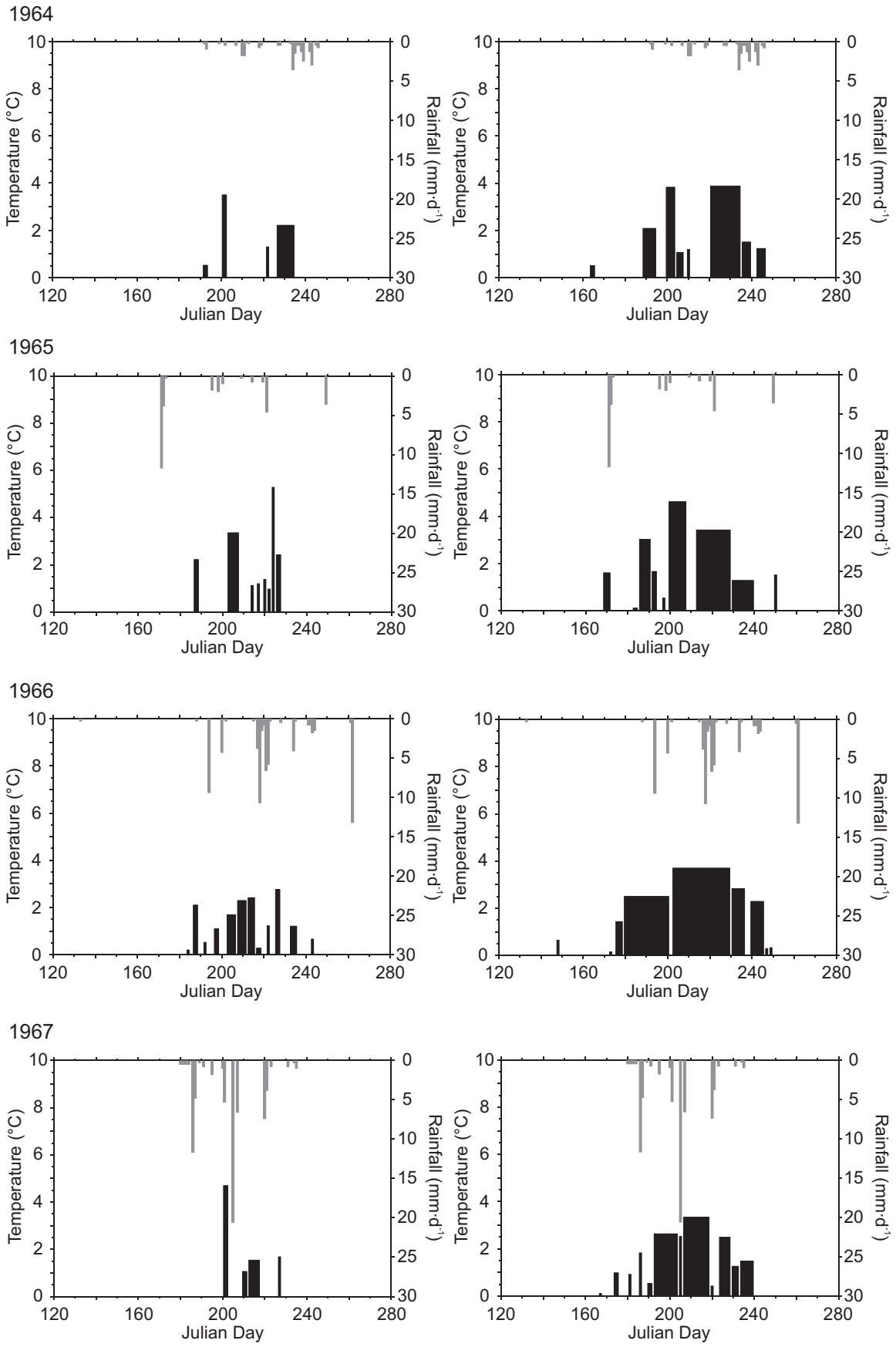
1964
1965
1966
1967
Temperature (°C)
Rainfall (mm·d-1)
Julian Day
120
160
200
240
280
0
2
4
6
8
10
0
5
10
15
20
25
30

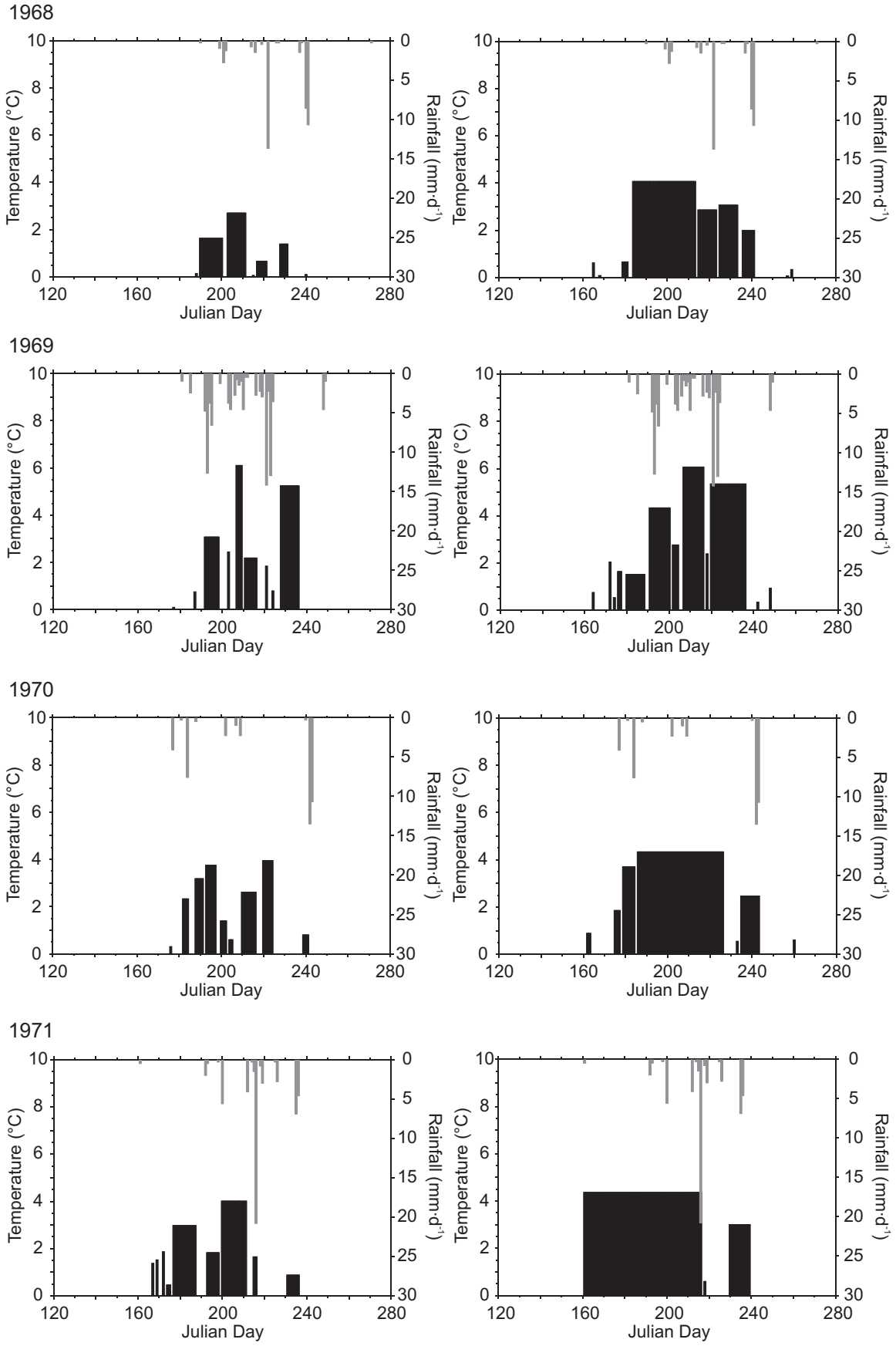
1968
1969
1970
1971
Temperature (°C)
Rainfall (mm·d-1)
Julian Day
120
160
200
240
280
0
2
4
6
8
10
0
5
10
15
20
25
30

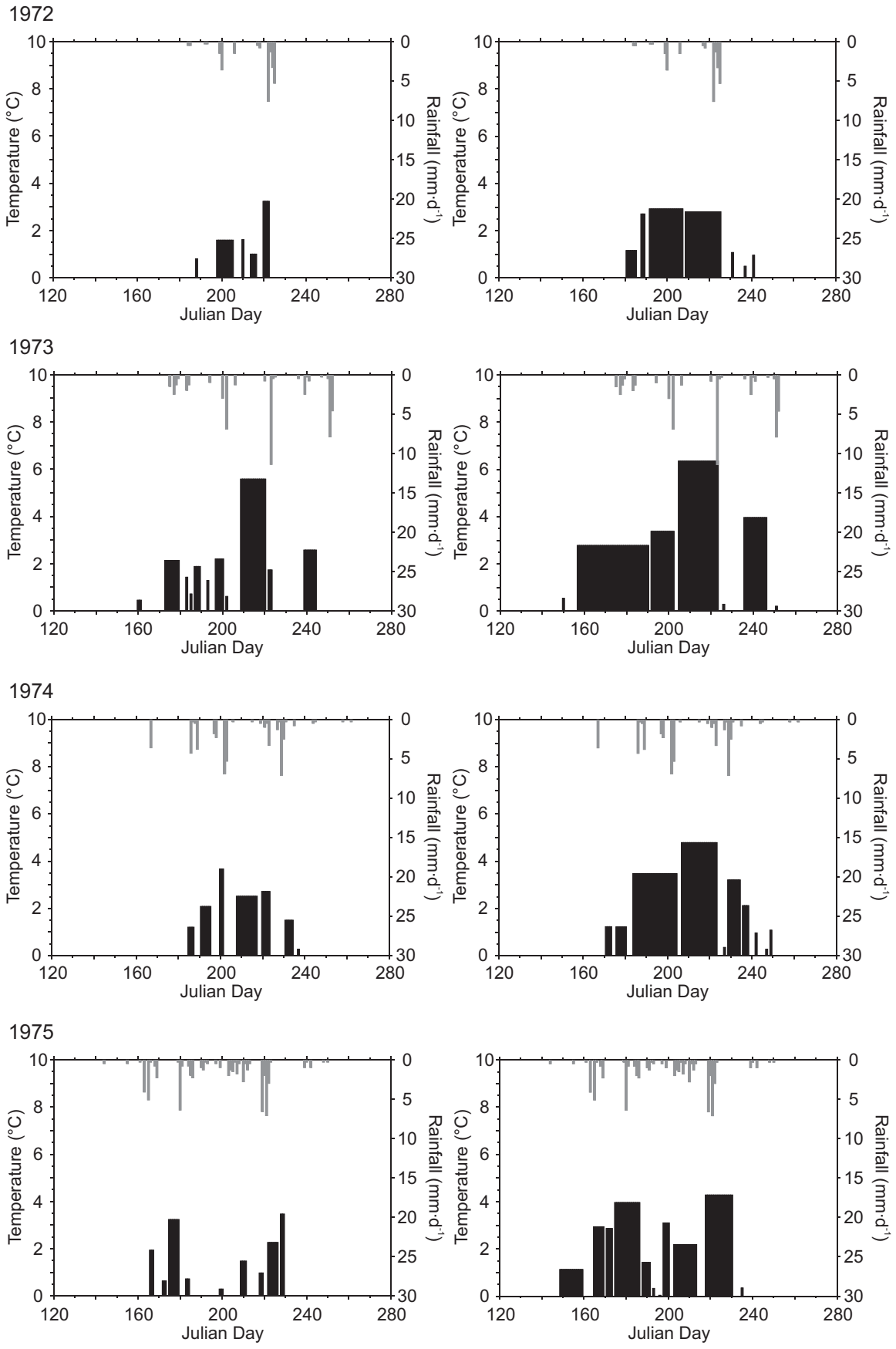
1972
1973
1974
1975
Temperature (°C)
Rainfall (mm·d-1)
Julian Day
0
2
4
6
8
10
0
5
10
15
20
25
30
120
160
200
240
280

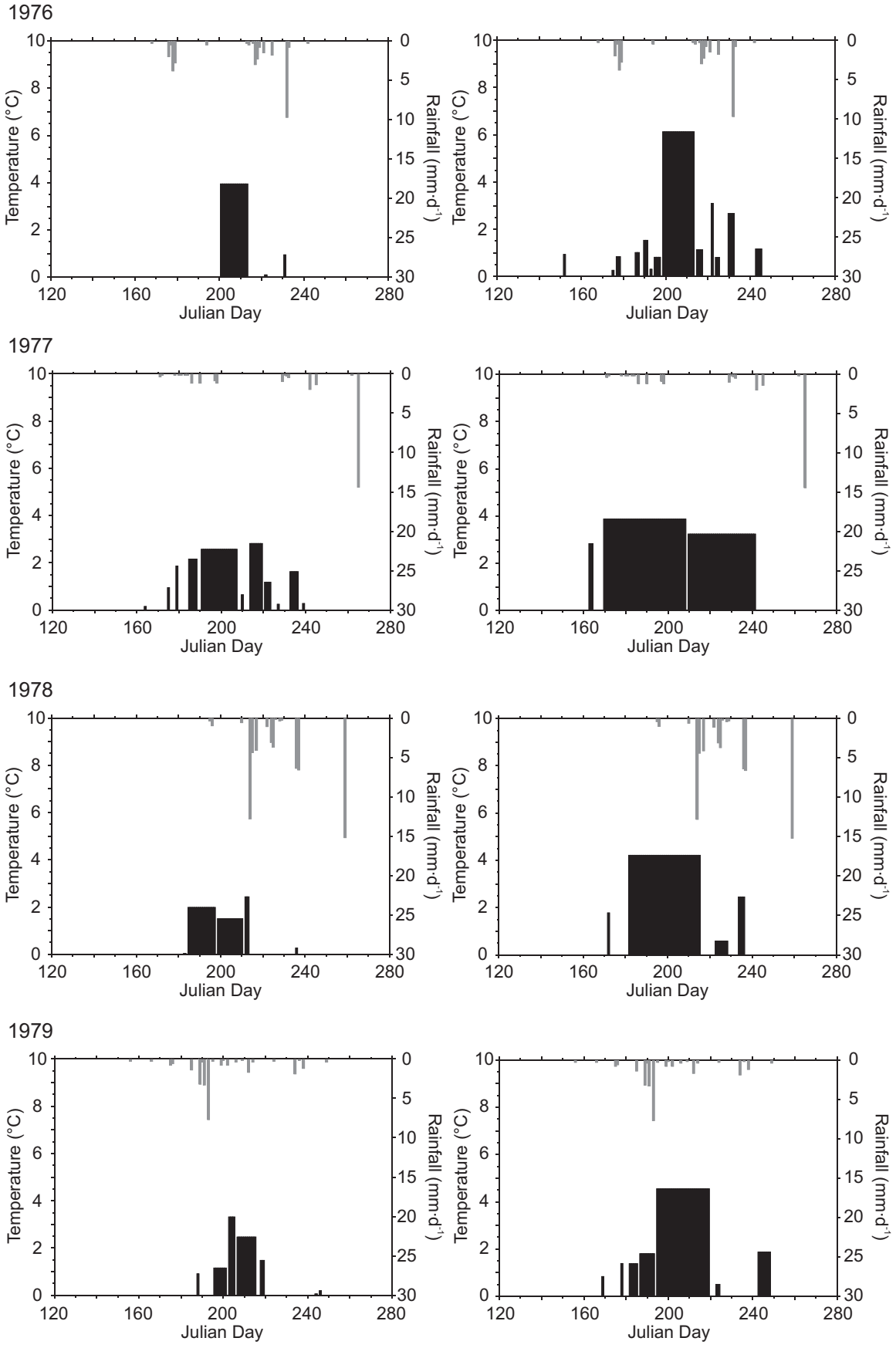
1976
1977
1978
1979
Temperature (°C)
Rainfall (mm·d-1)
Julian Day
120
160
200
240
280
0
2
4
6
8
10
0
5
10
15
20
25
30

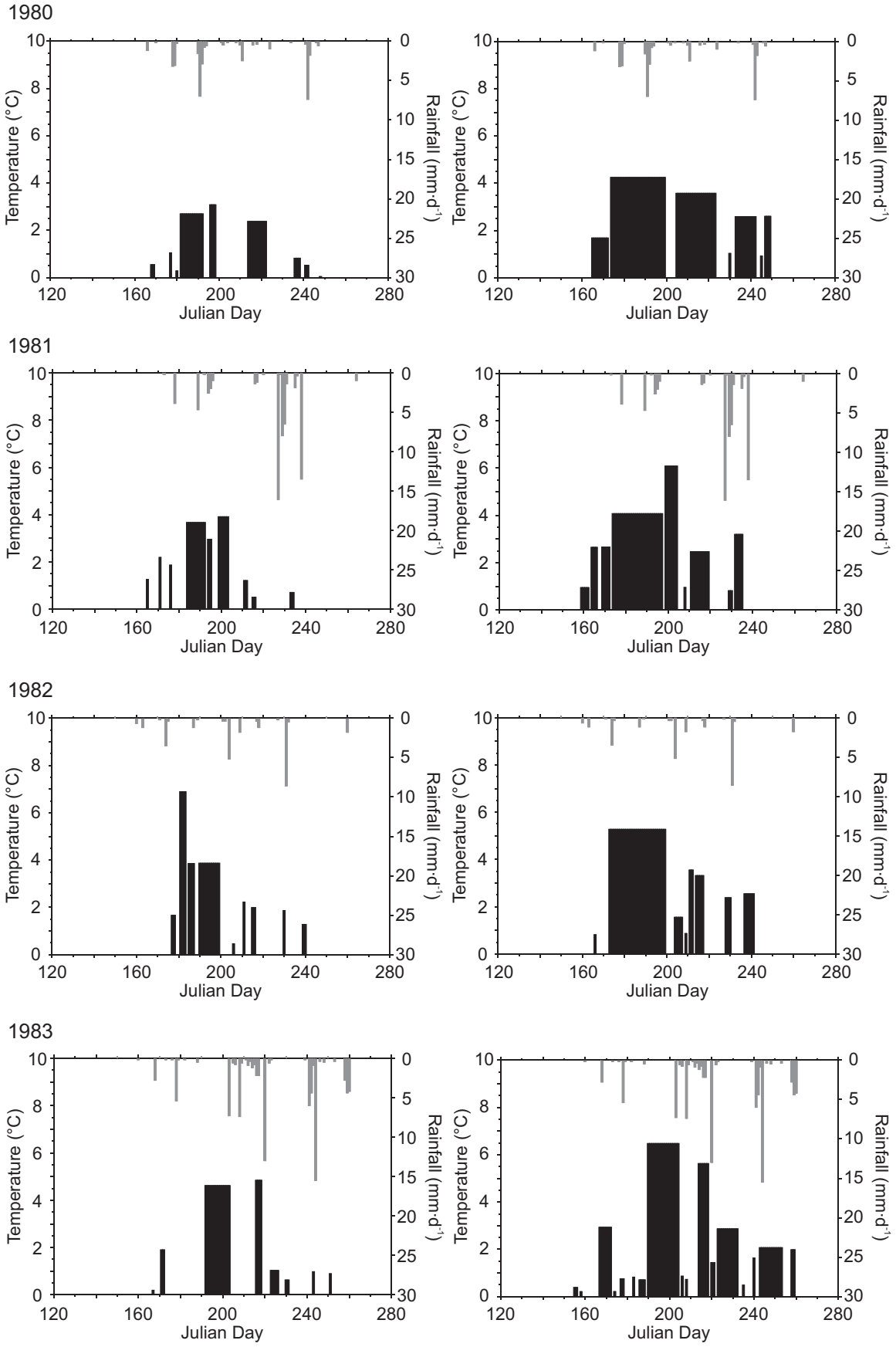
1980
1981
1982
1983
Temperature (°C)
Rainfall (mm·d-1)
Julian Day
0
2
4
6
8
10
0
5
10
15
20
25
30
120
160
200
240
280

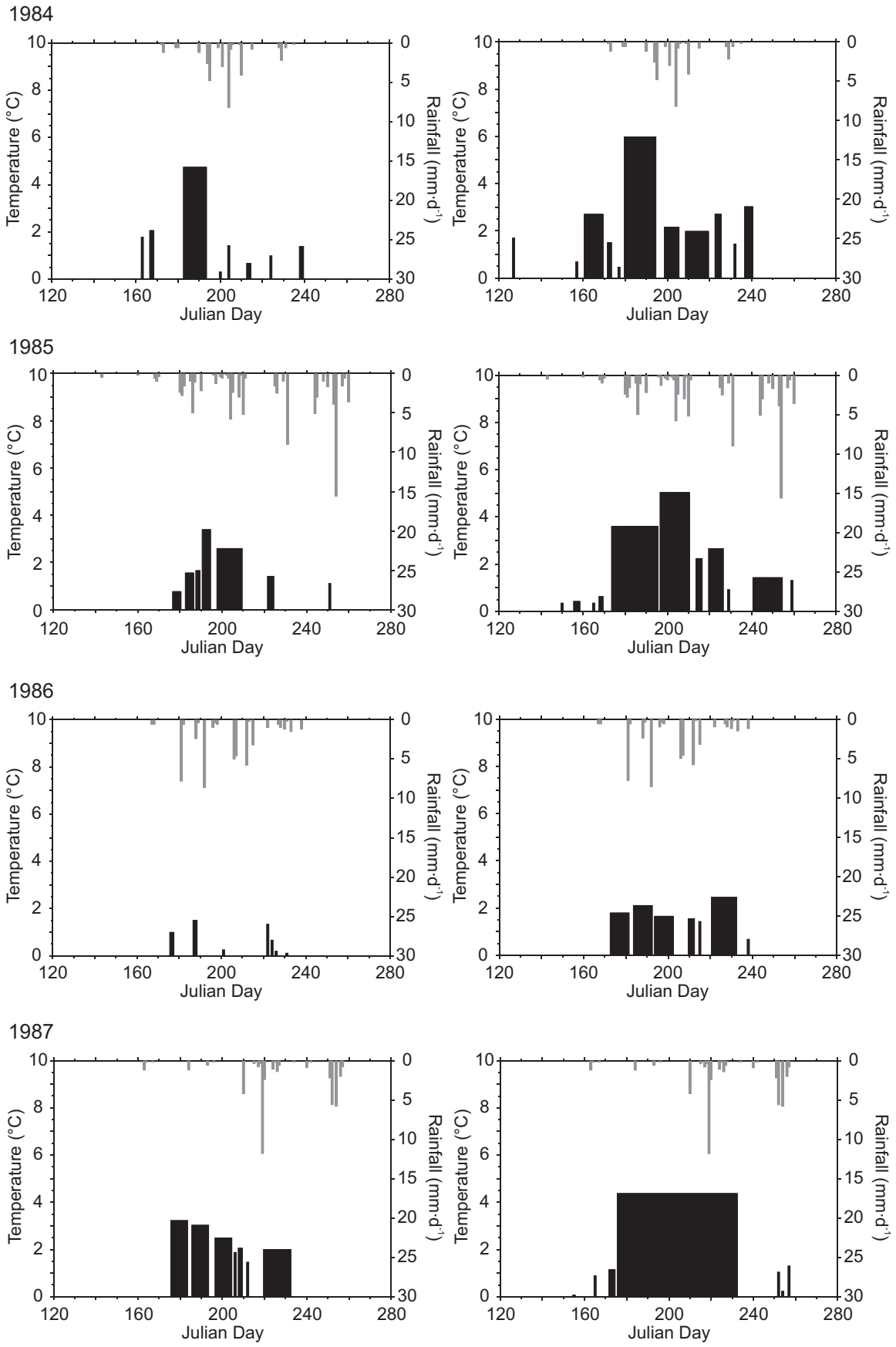
1984
1985
1986
1987
Temperature (°C)
Rainfall (mm·d-1)
Julian Day
120
160
200
240
280
0
2
4
6
8
10
0
5
10
15
20
25
30

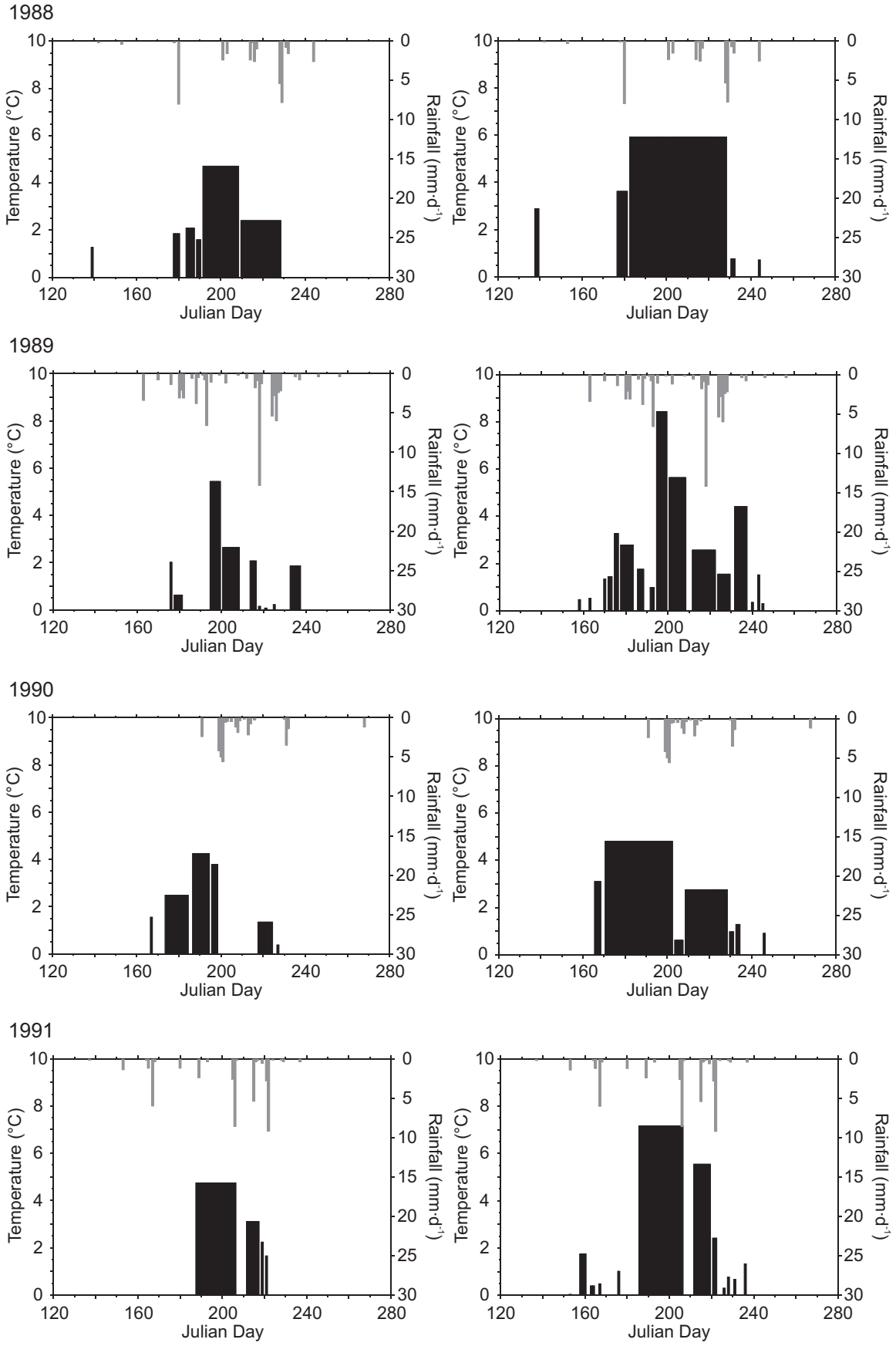
1988
1989
1990
1991
Temperature (°C)
Rainfall (mm·d-1)
Julian Day
0
2
4
6
8
10
0
5
10
15
20
25
30
120
160
200
240
280

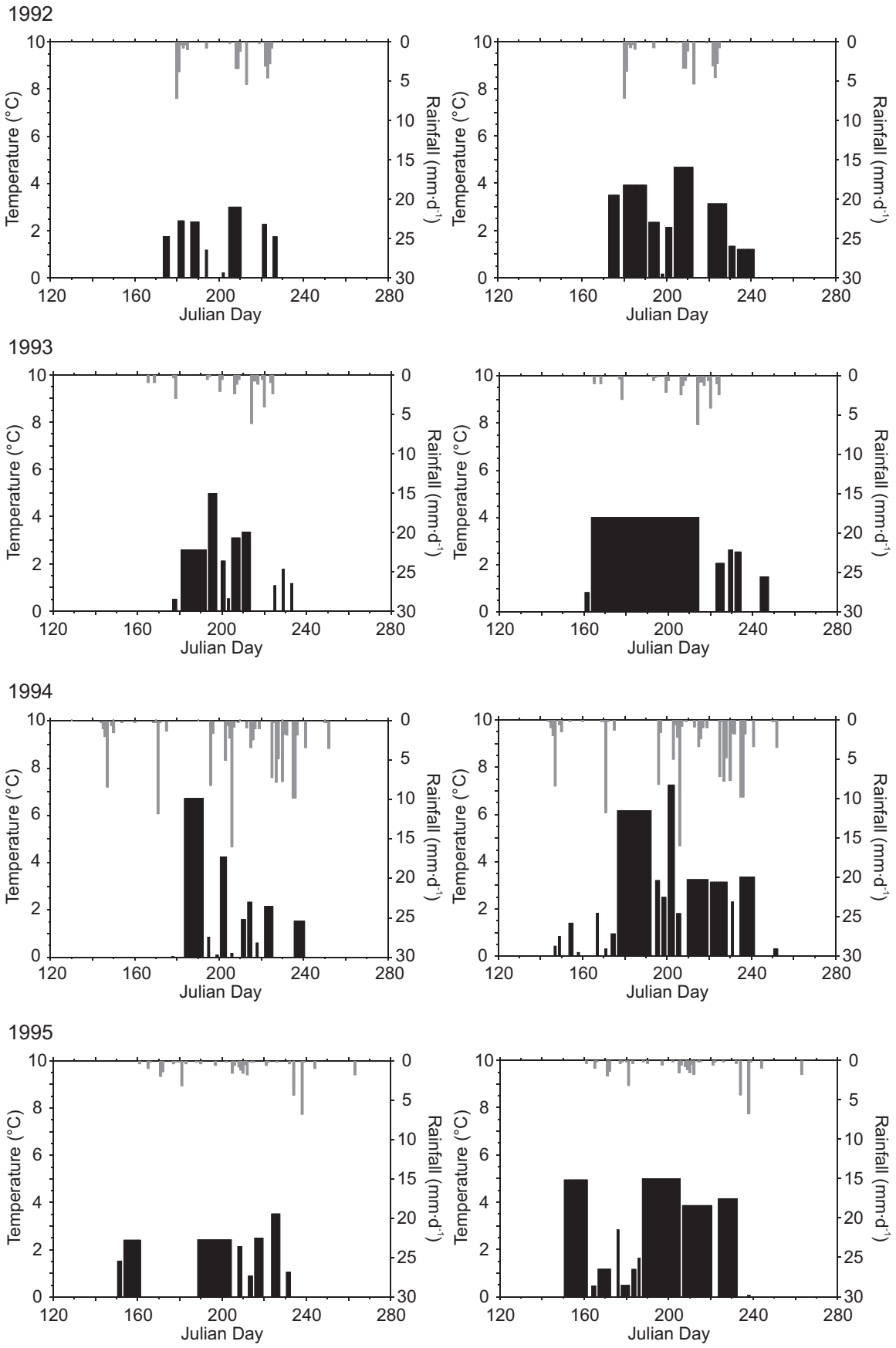
1992
1993
1994
1995
Temperature (°C)
Rainfall (mm·d-1)
Julian Day
120
160
200
240
280
0
2
4
6
8
10
0
5
10
15
20
25
30

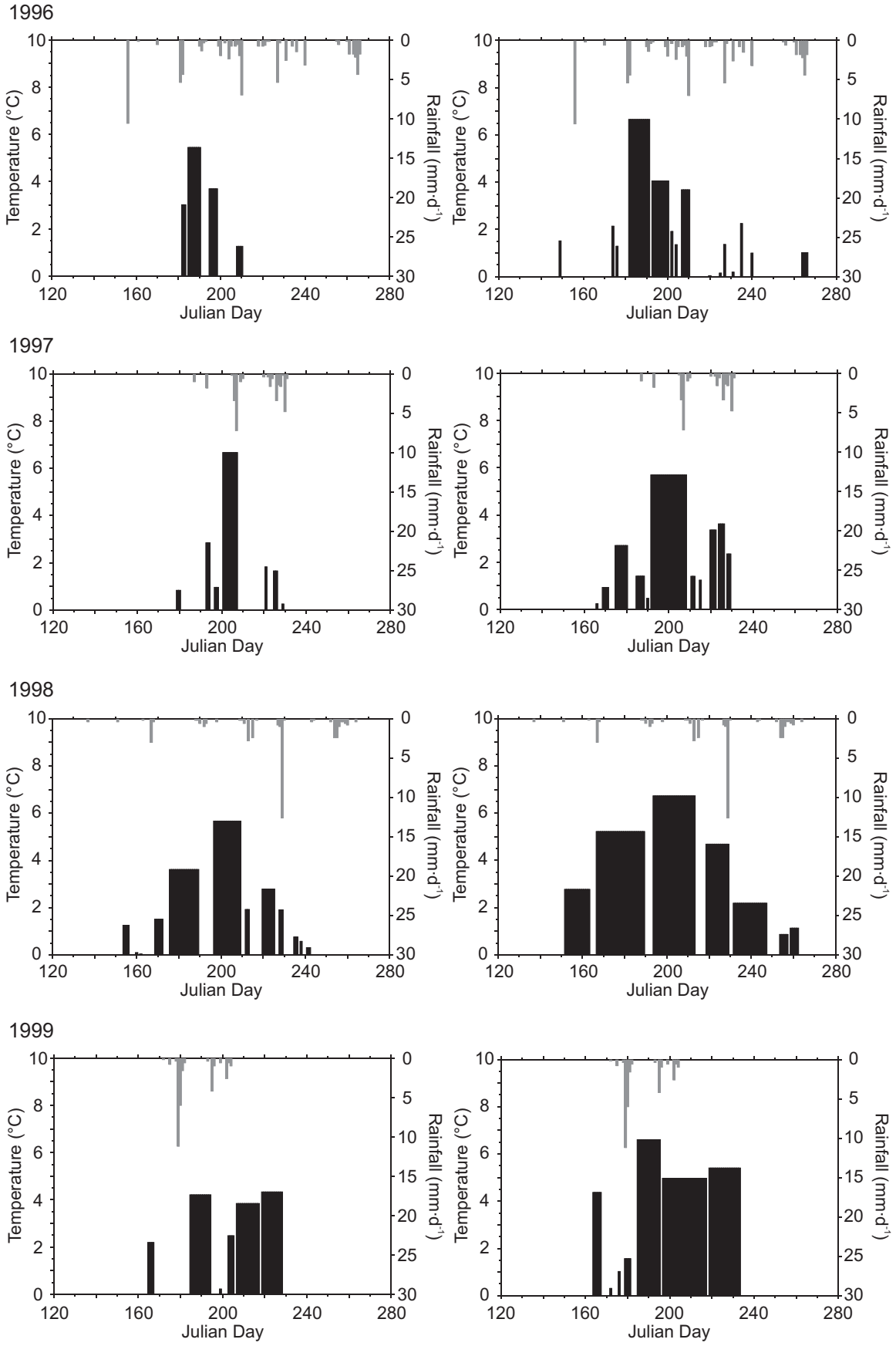
1996
1997
1998
1999
Temperature (°C)
Rainfall (mm·d-1)
Julian Day
120
160
200
240
280
0
2
4
6
8
10
0
5
10
15
20
25
30

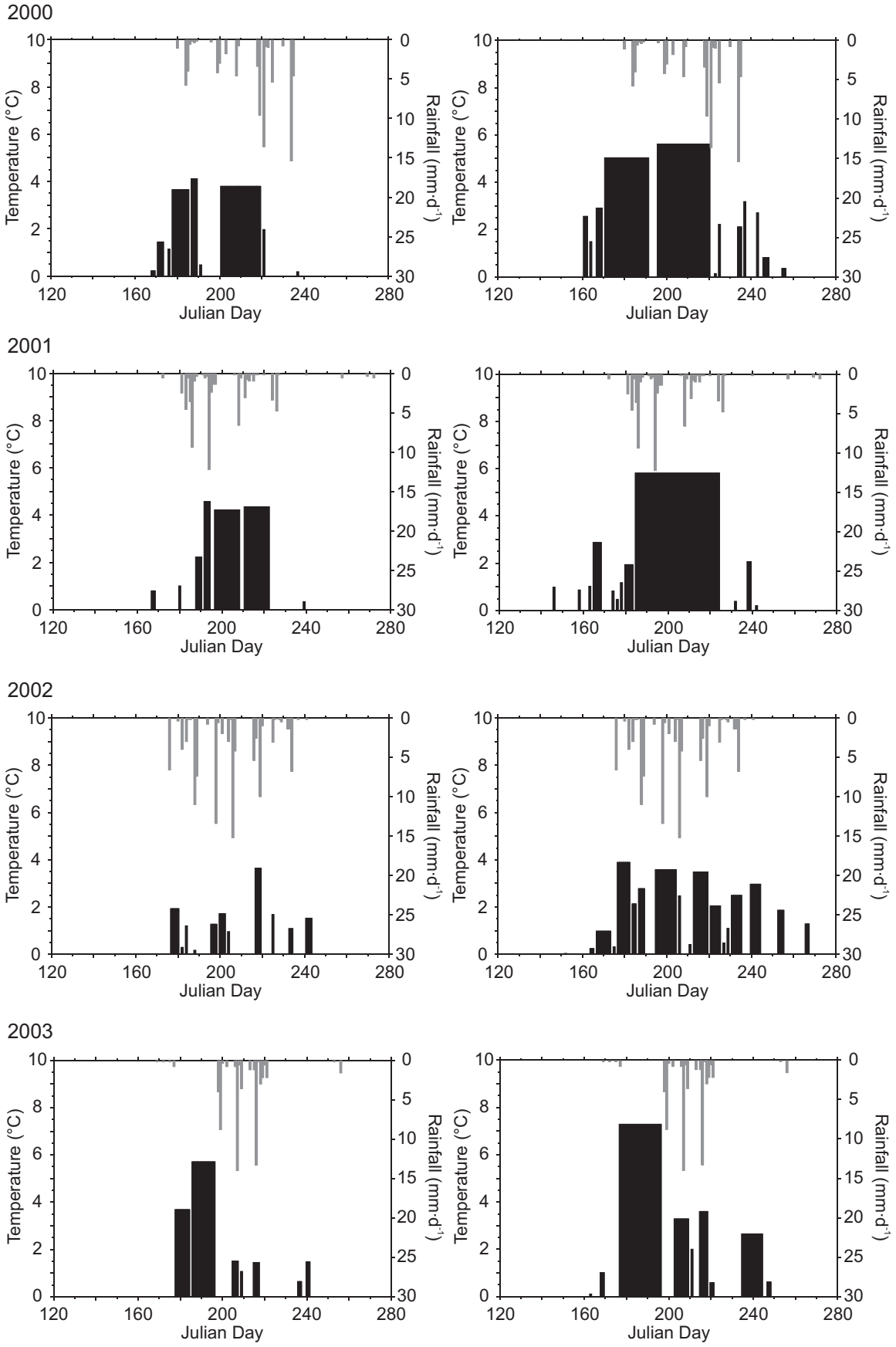
2000
2001
2002
2003
Temperature (°C)
Rainfall (mm·d-1)
Julian Day
120
160
200
240
280
0
2
4
6
8
10
0
5
10
15
20
25
30

APPENDIX III

Scanned varve images (2400dpi) with subannual units marked, 1961-2000. All scale bars are 0.5 mm.

1961

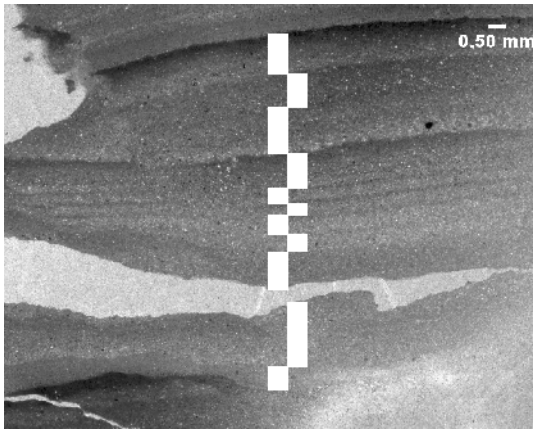

1962

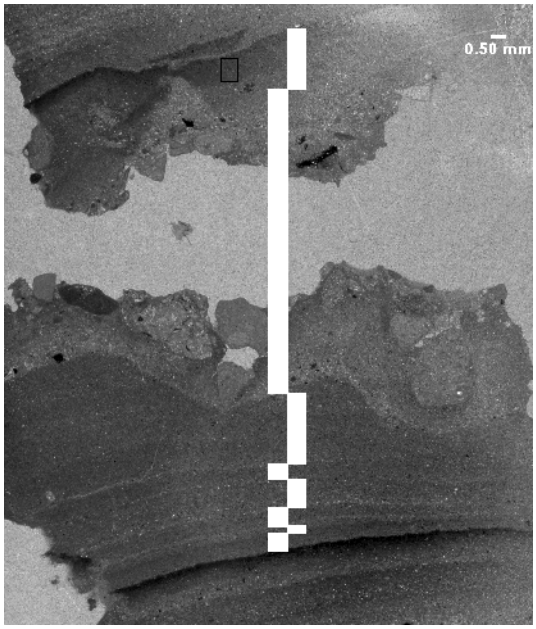

1963

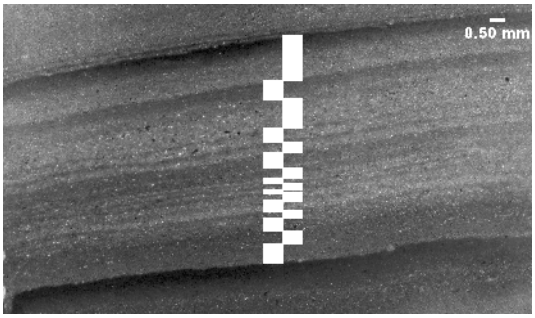

1964

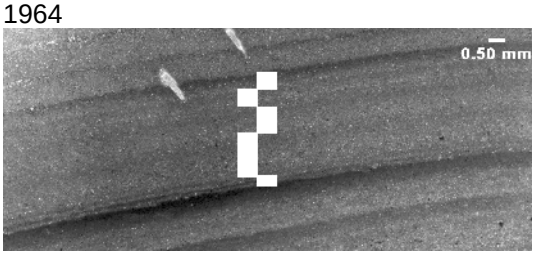

1965

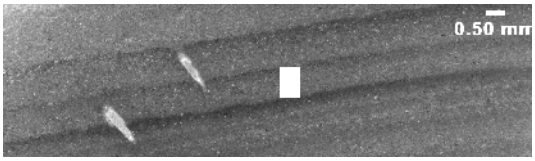

1966

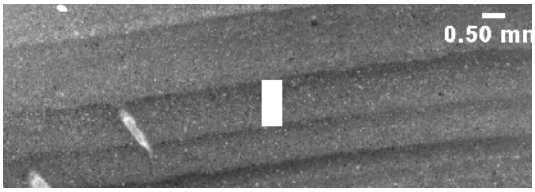

1967

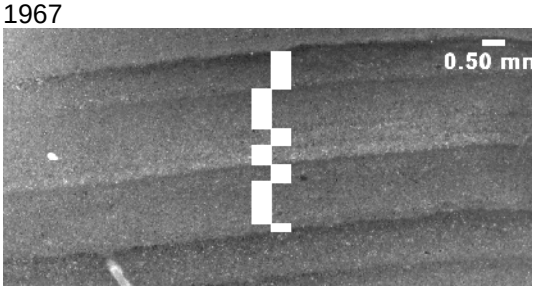

1968

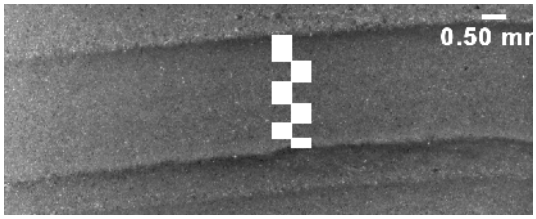

1969

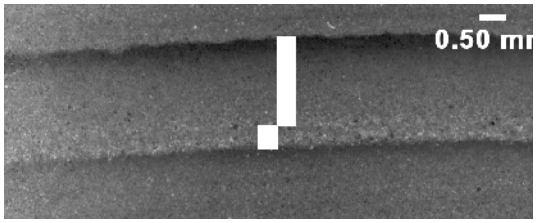

1970

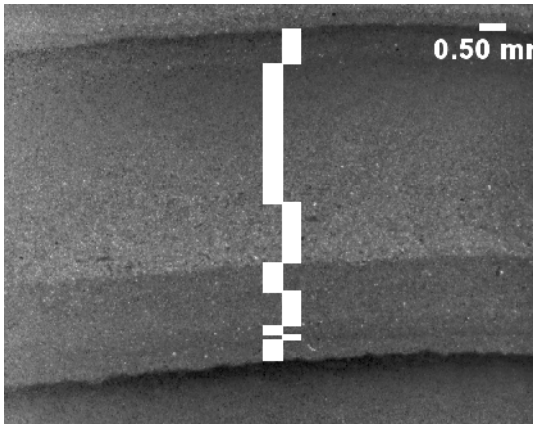

1971

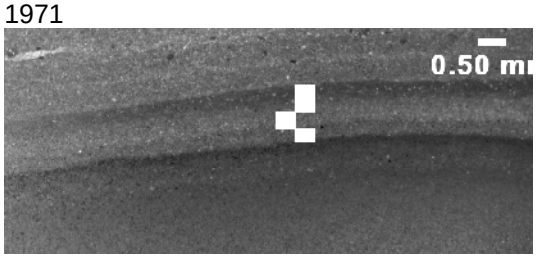

1972

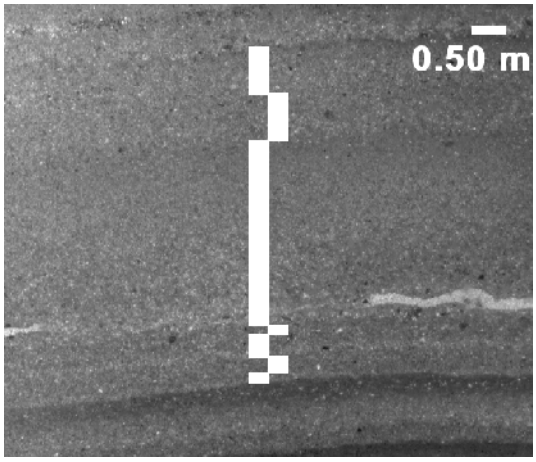

1973

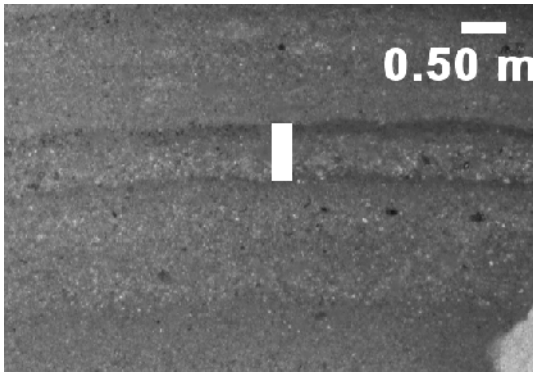

1974

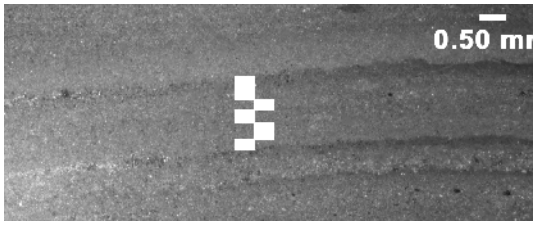

1975

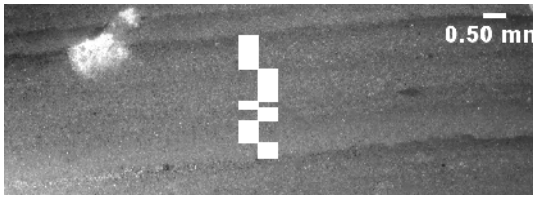

1976

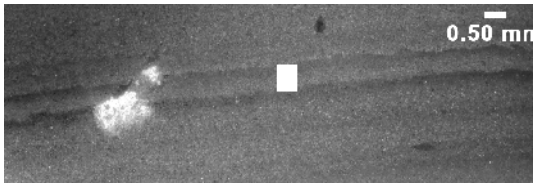

1977

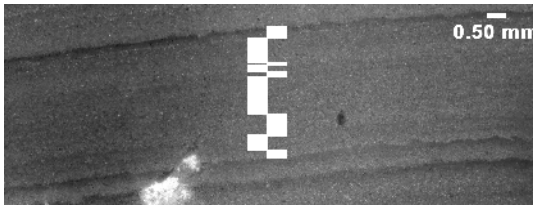

1978

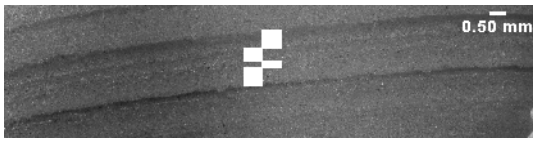

1979

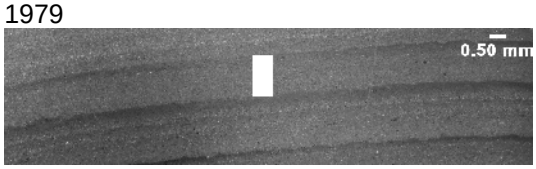

1980

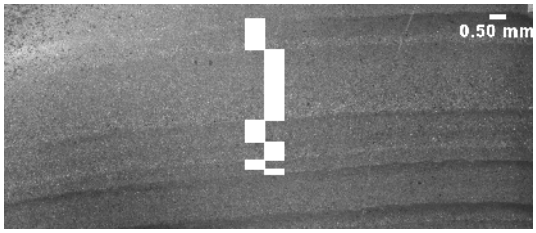

1981

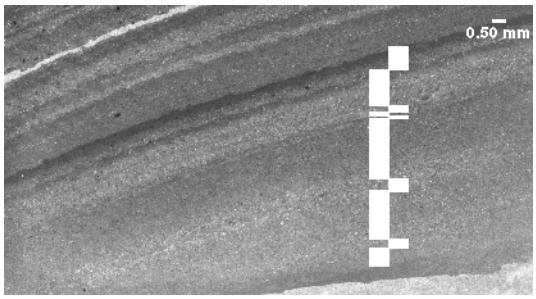

1982

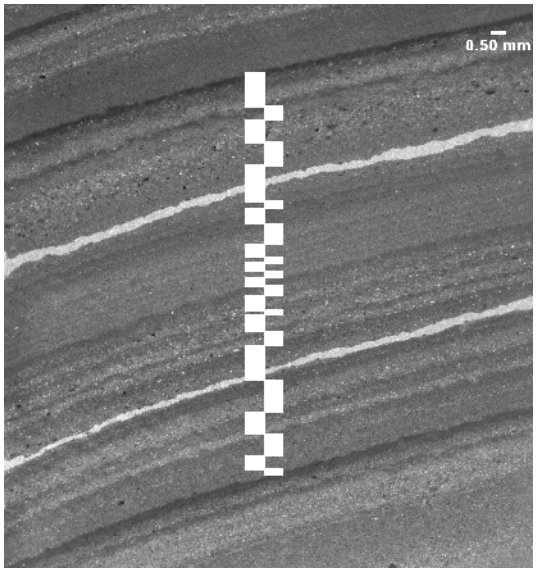

1983

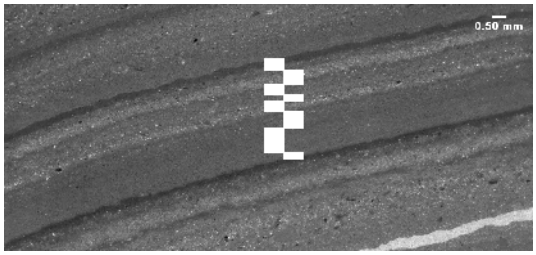

1984

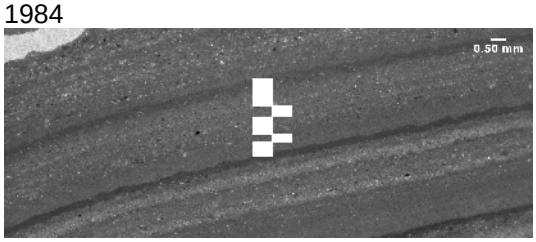

1985

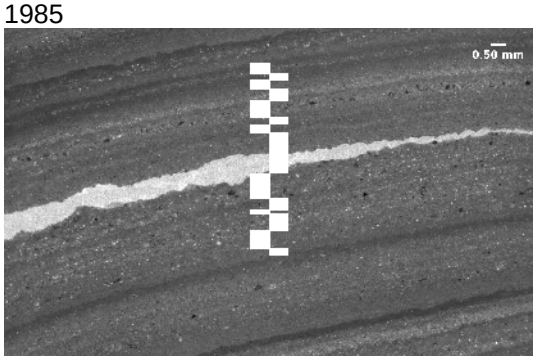

1986

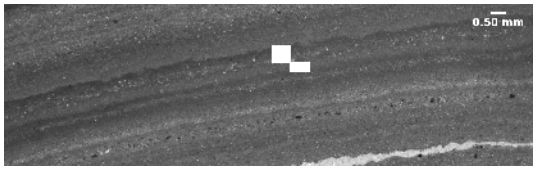

1987

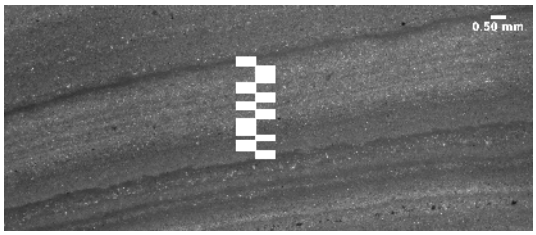

1988

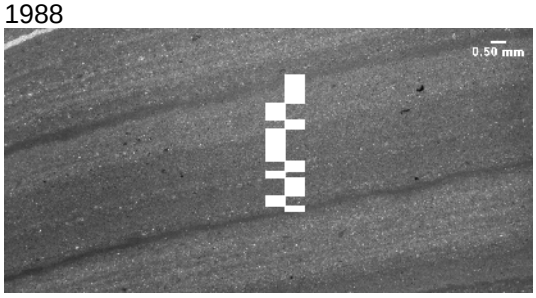

1989

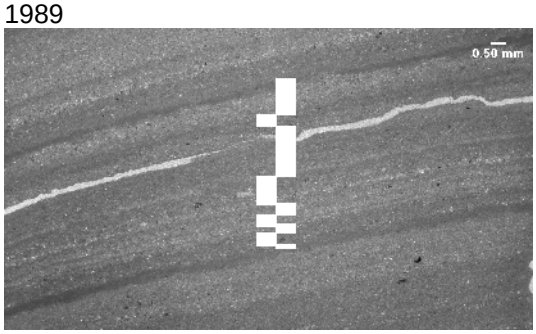

1990

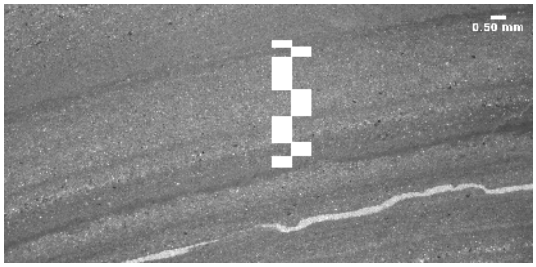

1991

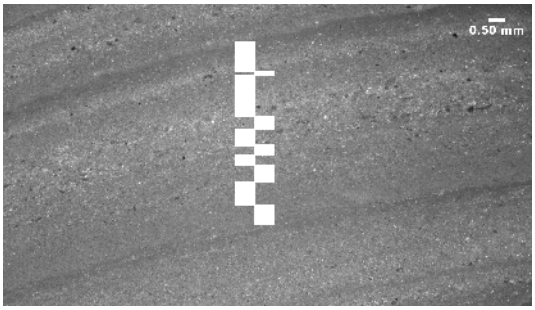

1992

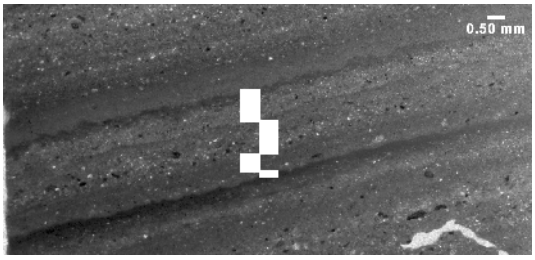

1993

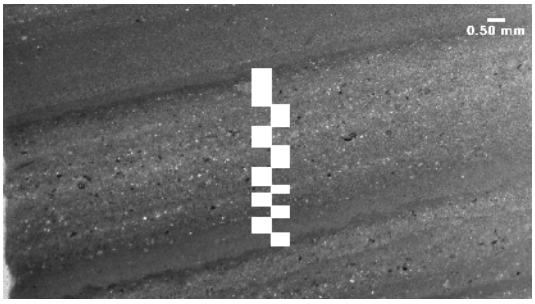

1994

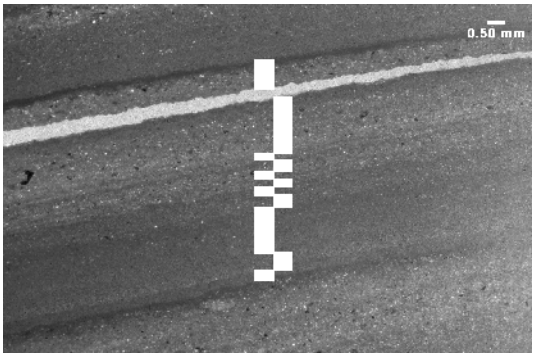

1995

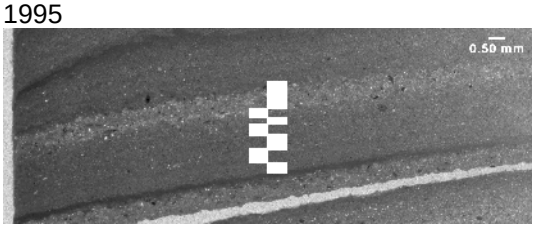

1996

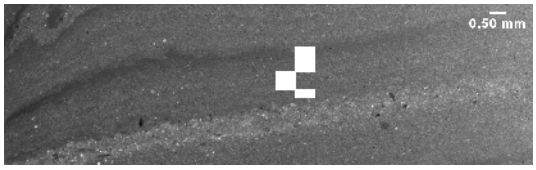

1997

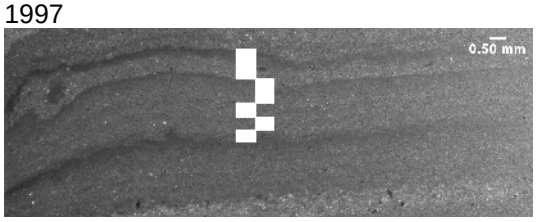

1998

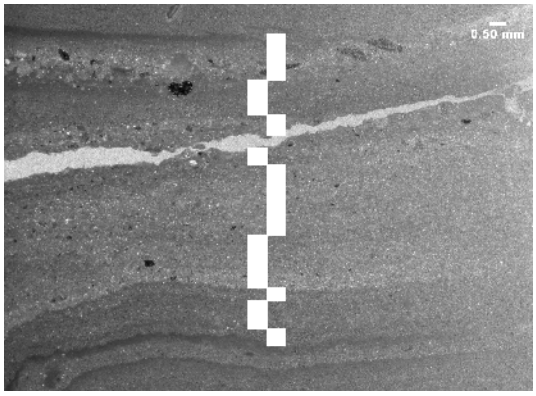

1999

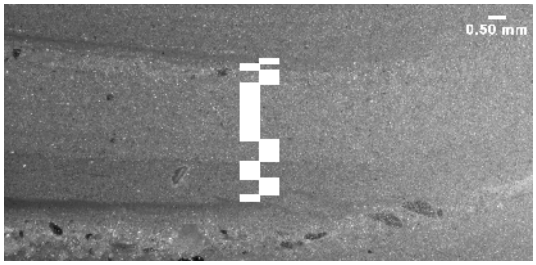

2000

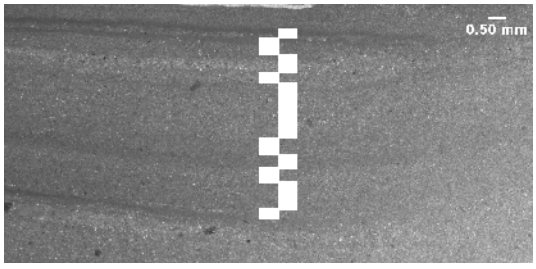

APPENDIX IV

Varve thickness and adjusted annual cumulative melting degree-days, 1959-2003. Varve thickness is the mean of R1-05 and R2-05 (see Chapter 2, Fig. 3). Melting degree-days (MDD) are adjusted for elevation at 300 m asl using an annual mean vertical lapse rate. Varve thickness and MDD ranks are also given, where 1 was the thickest and warmest and 38 the thinnest and coldest, respectively. The difference in ranks (thickness-MDD) was used to identify varves that were thinner or thicker than expected based on the meteorological conditions in the given year. Large positive differences are indicative of meteorological conditions favouring a thick varve but a thin varve was observed. Large negative difference are indicative of meteorological conditions favouring a thin varve but a thick varve was observed. Notes: [1]1959-1962 varves are from R1-05 only. 1963-2000 varves were used in the Chapter 2 analyses. 2001-2003 varves are from R2-05 only. [2]Upper-air temperature measurements are not available before 1961.

Year[1]	Thickness (mm)	Thickness rank	MDD[2]	MDD rank	Difference
1959	9.90	---	---	---	---
1960	12.80	---	---	---	---
1961	9.10	---	39.23	---	---
1962	15.00	---	133.32	---	---
1963	8.48	3	32.94	23	-20
1964	4.14	15	7.94	36	-21
1965	1.08	35	18.60	32	3
1966	1.25	33	16.00	33	0
1967	4.46	12	6.84	37	-25
1968	2.86	23	27.96	26	-3
1969	2.43	27	50.66	11	16
1970	7.15	5	52.04	9	-4
1971	1.21	34	63.16	8	26
1972	5.33	8	11.75	35	-27
1973	0.70	37	66.88	5	32
1974	1.62	31	24.01	30	1
1975	3.08	22	21.50	31	-9
1976	0.64	38	31.24	24	14
1977	3.52	20	63.53	7	13
1978	1.85	29	27.82	27	2
1979	1.43	32	29.60	25	7
1980	4.68	11	35.38	19	-8
1981	7.54	4	46.31	12	-8
1982	12.66	1	45.60	14	-13
1983	3.64	18	45.75	13	5
1984	2.56	25	33.30	22	3
1985	5.59	6	33.59	21	-15
1986	0.96	36	1.72	38	-2
1987	3.30	21	65.14	6	15
1988	3.72	17	91.90	1	16
1989	4.31	14	25.94	29	-15
1990	3.60	19	33.82	20	-1
1991	5.22	9	68.10	4	5
1992	2.23	28	13.86	34	-6
1993	3.85	16	51.77	10	6
1994	5.49	7	37.84	17	-10
1995	2.73	24	39.71	16	8
1996	1.62	30	36.16	18	12

Year[1]	Thickness (mm)	Thickness rank	MDD[2]	MDD rank	Difference
1997	2.55	26	26.60	28	-2
1998	9.27	2	76.78	3	-1
1999	4.37	13	86.80	2	11
2000	4.99	10	43.38	15	-5
2001	3.98	---	57.77	---	---
2002	2.01	---	9.62	---	---
2003	1.24	---	51.20	---	---

APPENDIX V

Total melting degree-days calculated using the annual mean (AMM) and daily calculation (DCM) derived vertical lapse rates rates, with and without a –3 °C ice proximity cooling factor, 1961-2003.

Year	With Ice Cooling Factor		Without Ice Cooling Factor	
	AMM (MDD)	DCM (MDD)	AMM (MDD)	DCM (MDD)
1961	39.23	71.56	136.44	193.42
1962	133.32	193.59	287.43	334.67
1963	32.94	58.51	115.20	175.16
1964	7.94	27.00	59.19	98.47
1965	18.60	35.99	90.28	130.08
1966	16.00	41.88	141.10	188.63
1967	6.84	20.87	69.32	102.78
1968	27.96	51.53	150.36	190.52
1969	50.66	106.07	157.28	227.73
1970	52.04	84.61	157.06	230.87
1971	63.16	106.30	197.14	275.23
1972	11.75	27.97	88.67	108.30
1973	66.88	120.33	216.61	297.25
1974	24.01	63.78	114.96	192.86
1975	21.50	48.08	128.70	178.75
1976	31.24	52.43	95.68	122.22
1977	63.53	83.48	230.42	260.59
1978	27.82	49.07	120.28	155.89
1979	29.60	43.19	112.85	146.37
1980	35.38	66.33	155.82	227.57
1981	46.31	68.74	157.83	194.29
1982	45.60	85.39	136.64	190.74
1983	45.75	81.27	159.15	210.62
1984	33.30	64.81	127.20	178.15
1985	33.59	62.52	143.75	200.35
1986	1.72	7.53	74.98	86.08
1987	65.14	103.30	209.91	256.28
1988	91.90	144.07	232.45	298.23
1989	25.94	68.77	120.87	189.35
1990	33.82	84.08	149.98	226.27
1991	68.10	112.66	160.27	210.28
1992	13.86	49.60	97.80	162.76
1993	51.77	86.55	176.52	233.33
1994	37.84	99.12	136.26	227.47
1995	39.71	93.29	164.30	252.24
1996	36.16	57.29	95.74	130.00
1997	26.60	61.40	93.85	151.77
1998	76.78	161.40	265.14	382.50
1999	86.80	141.96	218.45	281.60
2000	43.38	122.31	165.16	282.78
2001	57.77	126.32	181.34	262.07
2002	9.62	38.74	97.40	154.18
2003	51.20	102.82	145.90	216.30

APPENDIX VI

Calculated May 1 – September 30 average daily vertical lapse rates, 0 – 5000 m asl, and estimated temperature difference at 300 m asl, 1961-2004.

Year	Coeff (°C·m^{-1})	Constant (T @ z_0)	r^2	T @ 300 m asl
1961	-0.0046	5.2019	0.6476	-1.37
1962	-0.0048	5.4960	0.8014	-1.43
1963	-0.0051	3.8275	0.8997	-1.54
1964	-0.0039	2.0174	0.6209	-1.17
1965	-0.0048	3.1102	0.8433	-1.44
1966	-0.0042	4.8375	0.8733	-1.25
1967	-0.0045	1.8057	0.9082	-1.36
1968	-0.0049	4.8027	0.8206	-1.48
1969	-0.0041	4.5168	0.6969	-1.24
1970	-0.0046	7.0644	0.7783	-1.39
1971	-0.0052	6.1462	0.9275	-1.56
1972	-0.0036	3.4202	0.7949	-1.07
1973	-0.0044	4.5685	0.8803	-1.31
1974	-0.0046	5.2157	0.8424	-1.37
1975	-0.0043	3.2070	0.8054	-1.30
1976	-0.0039	1.6235	0.8693	-1.16
1977	-0.0046	6.0636	0.8944	-1.39
1978	-0.0047	6.6138	0.8392	-1.41
1979	-0.0038	3.4906	0.7919	-1.15
1980	-0.0055	6.9822	0.9498	-1.66
1981	-0.0048	7.5644	0.8934	-1.43
1982	-0.0050	8.7687	0.8276	-1.51
1983	-0.0042	5.0223	0.7218	-1.25
1984	-0.0047	8.6063	0.8421	-1.40
1985	-0.0050	6.9042	0.7702	-1.49
1986	-0.0038	3.3647	0.8392	-1.13
1987	-0.0050	7.2977	0.8065	-1.49
1988	-0.0045	7.9151	0.8012	-1.35
1989	-0.0040	2.7332	0.7541	-1.19
1990	-0.0046	8.0335	0.8205	-1.38
1991	-0.0044	5.0089	0.5205	-1.31
1992	-0.0049	5.4780	0.8977	-1.47
1993	-0.0050	7.1007	0.8960	-1.51
1994	-0.0049	8.8941	0.7011	-1.46
1995	-0.0048	4.7475	0.7925	-1.43
1996	-0.0049	8.5543	0.8209	-1.46
1997	-0.0052	3.7629	0.8555	-1.55
1998	-0.0049	6.3471	0.6928	-1.46
1999	-0.0048	9.2874	0.8946	-1.45
2000	-0.0045	5.5722	0.6671	-1.34
2001	-0.0046	6.1819	0.8508	-1.37
2002	-0.0046	2.8233	0.7373	-1.38
2003	-0.0053	10.5130	0.9383	-1.60
2004	-0.0045	4.9788	0.6921	-1.35

APPENDIX VII

Vertical lapse rate (°C·km^{-1}) between surface measurement and first measurement above 300 m asl at Resolute, 1961-2003. Measurement altitudes varied annually and are described in Chapter 3. Mean daily radiosonde measurements are shown in grey. The 9-day running mean is shown in black. Positive VLRs are indicative of thermal inversion conditions.

1961

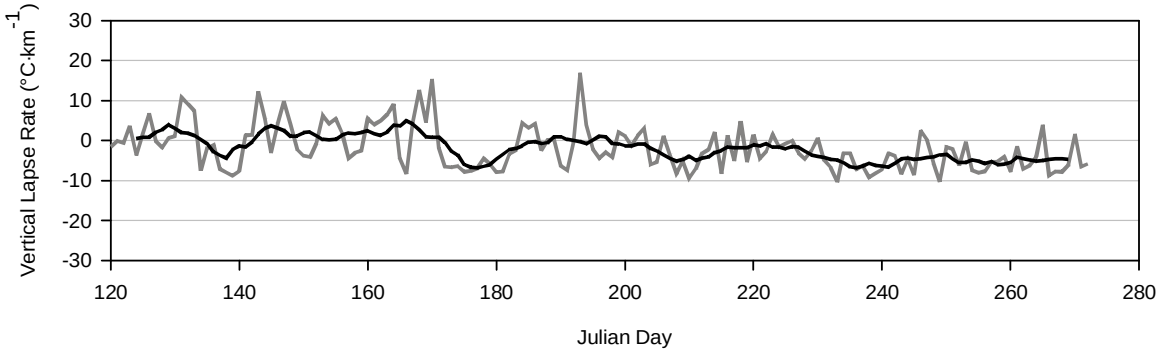

1962

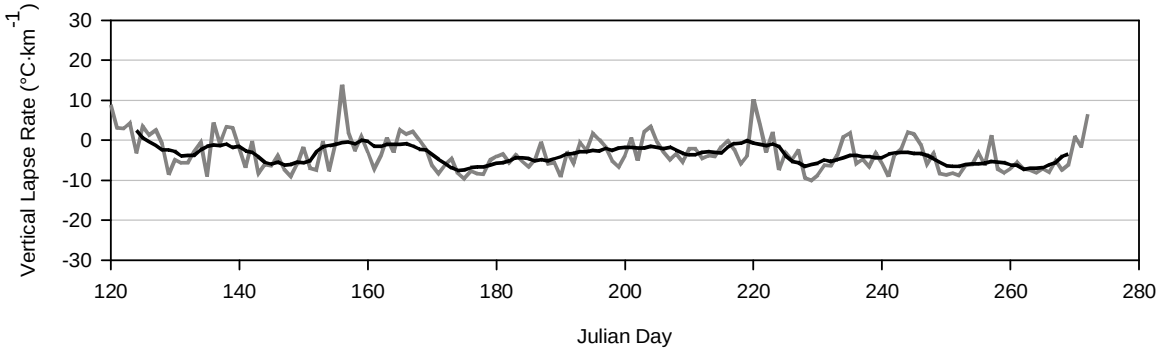

1963

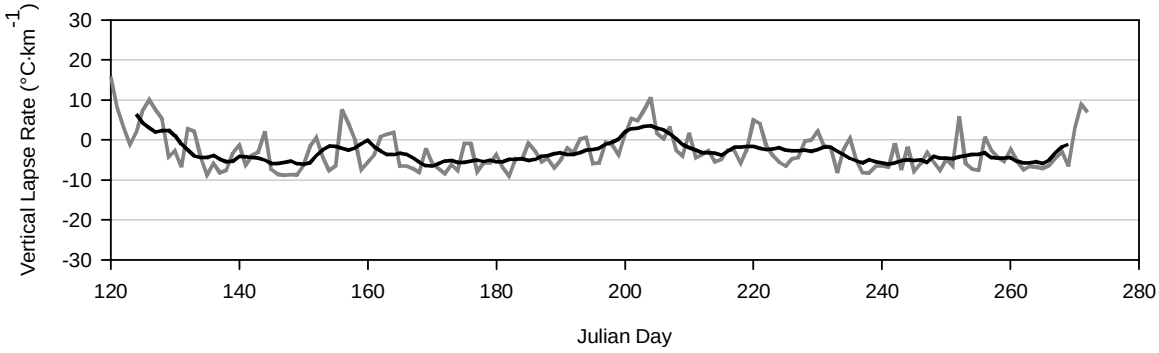

1964

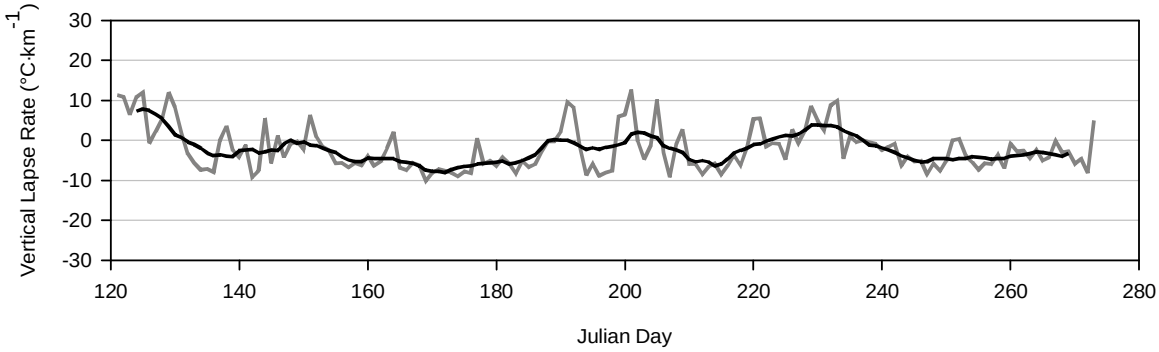

1965

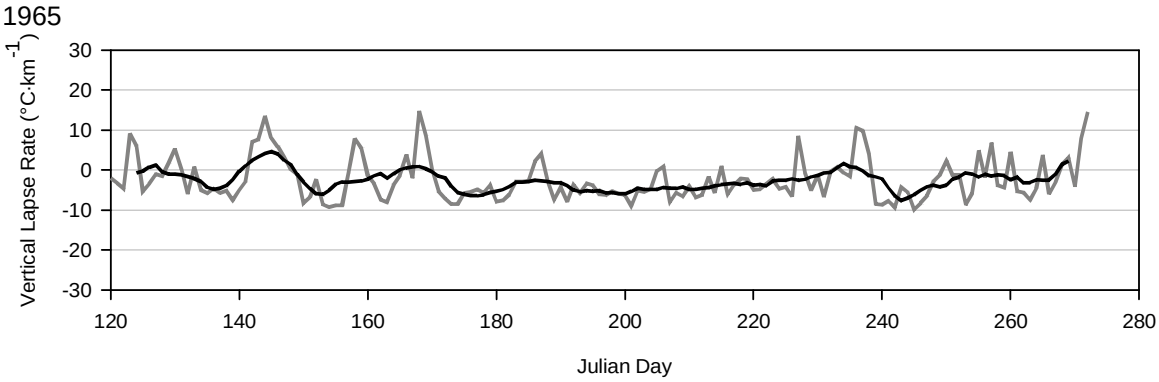

1966

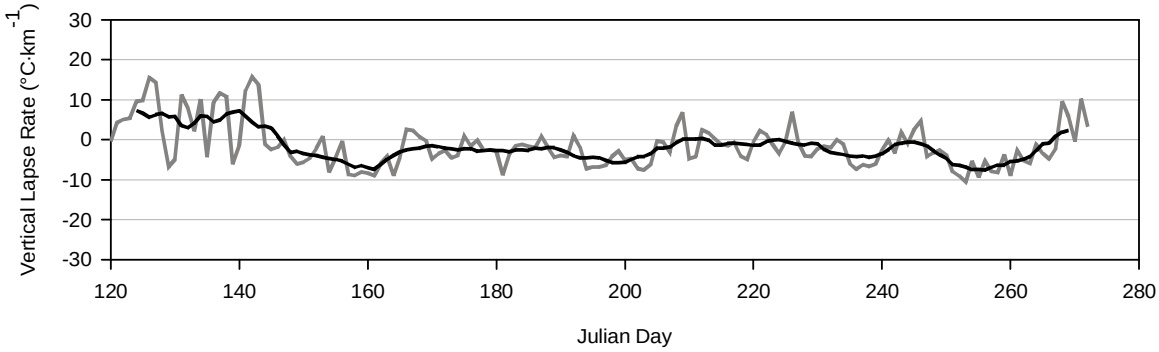

1967

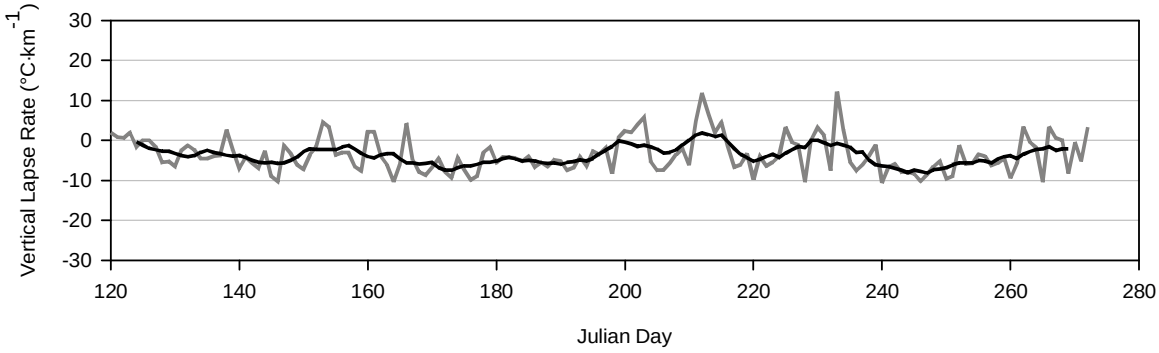

1968

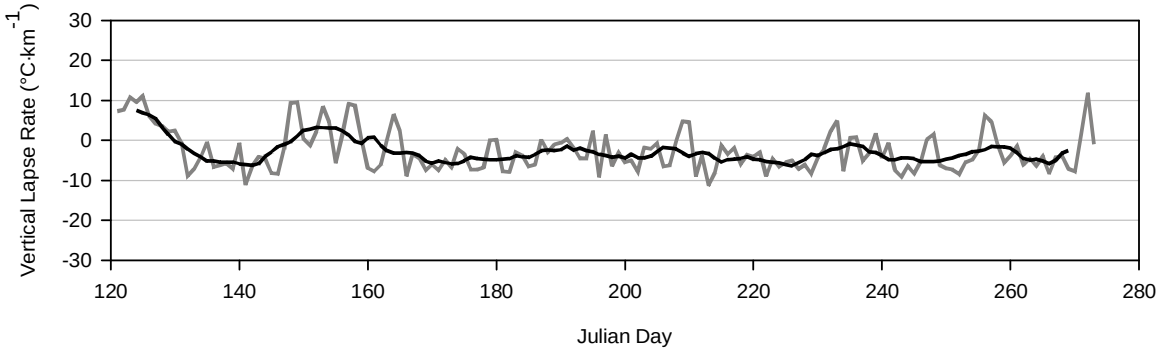

1969

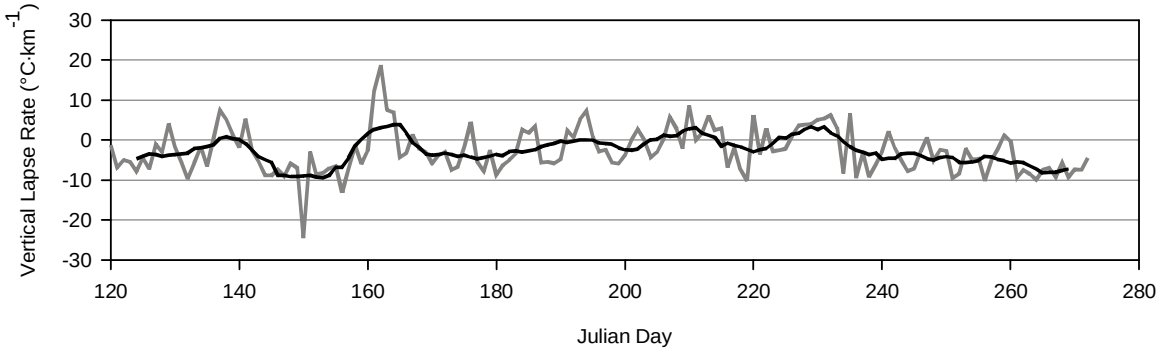

1970

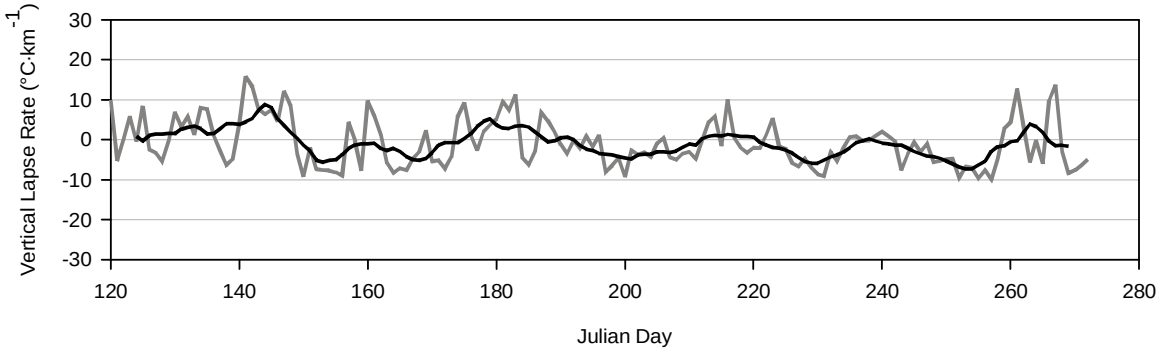

1971

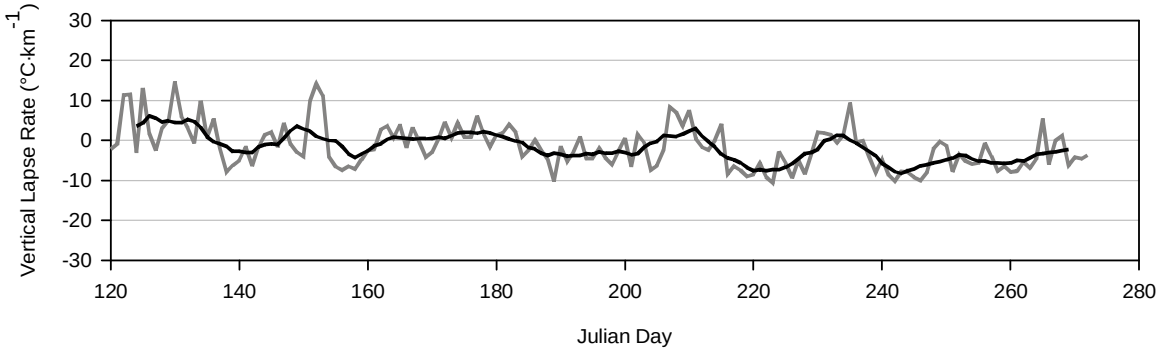

1972

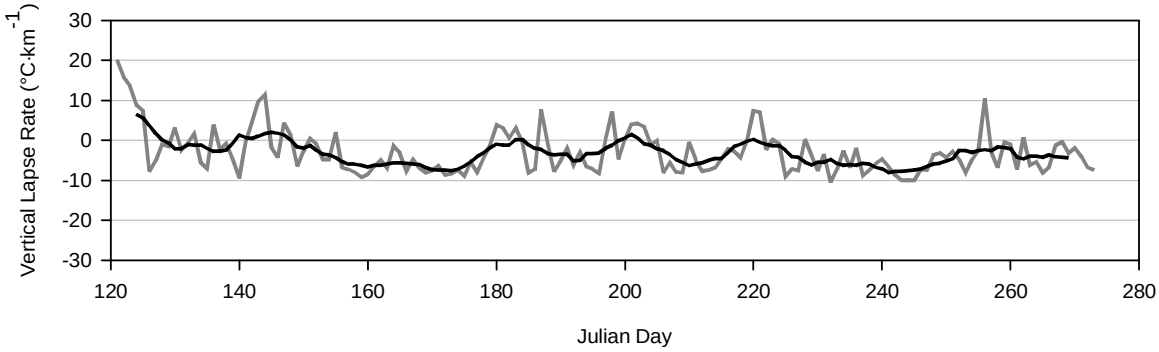

1973

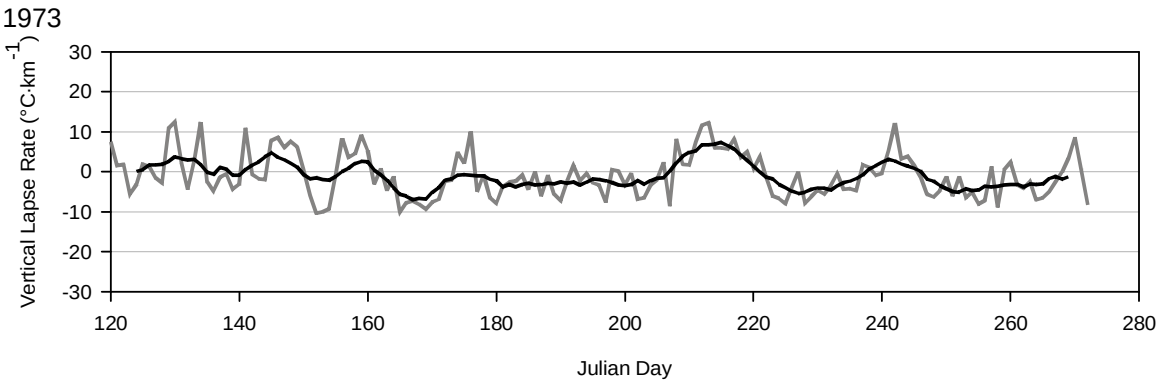

1974

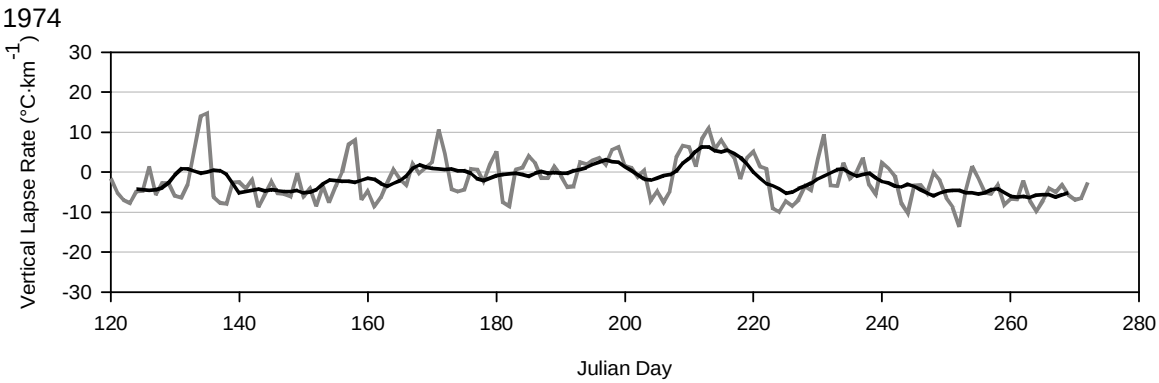

1975

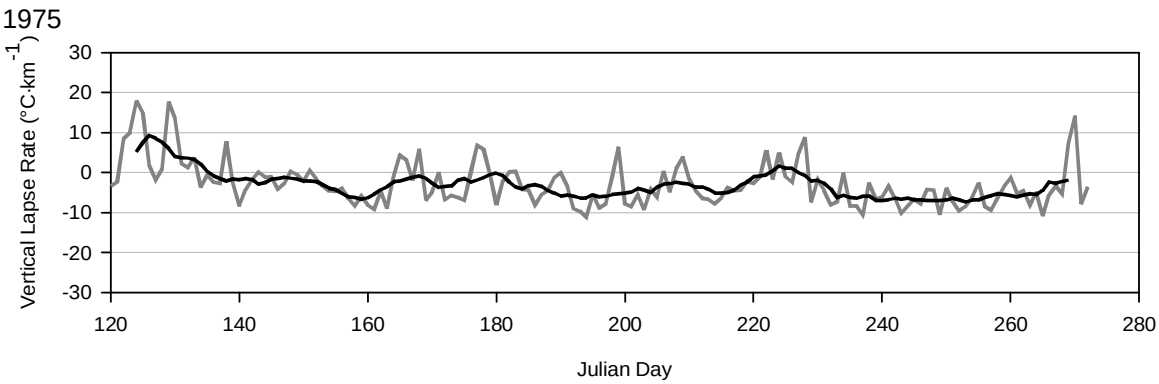

1976

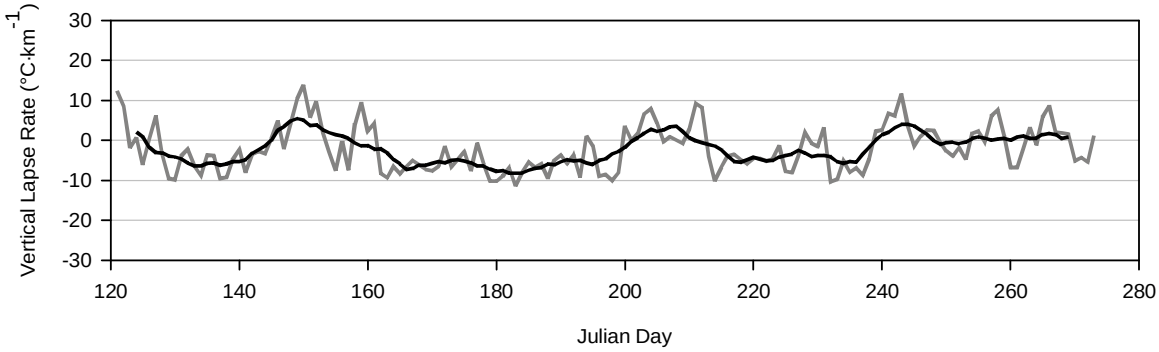

1977

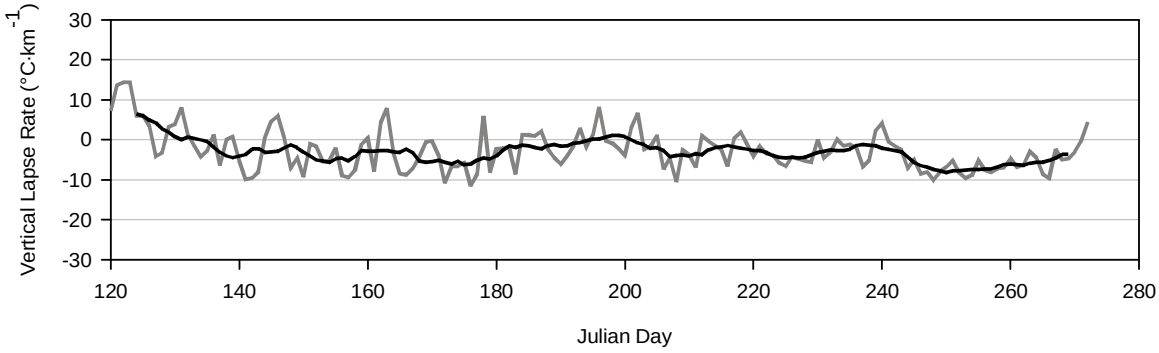

1978

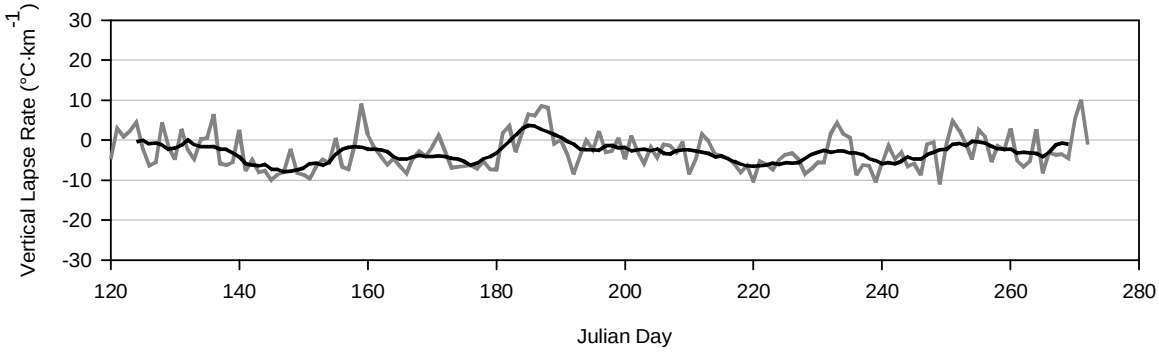

1979

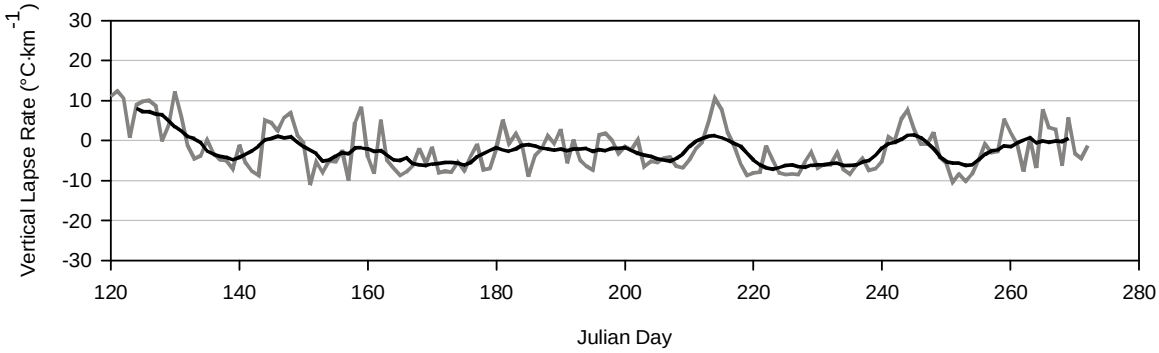

1980

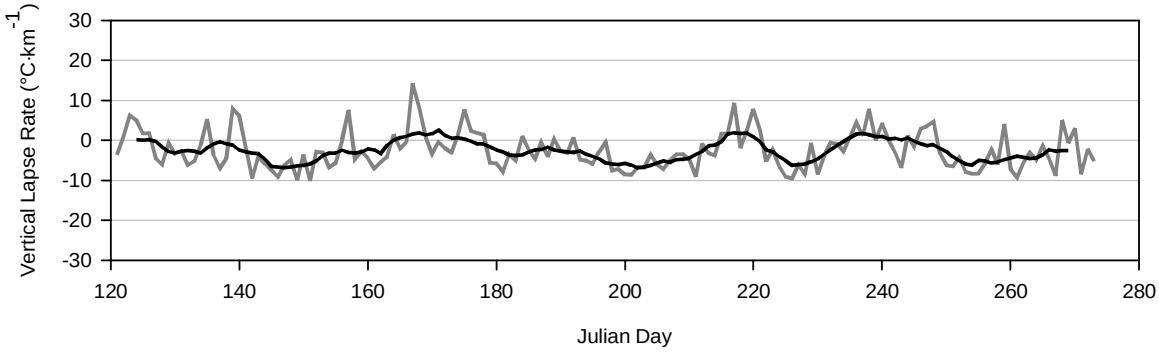

1981

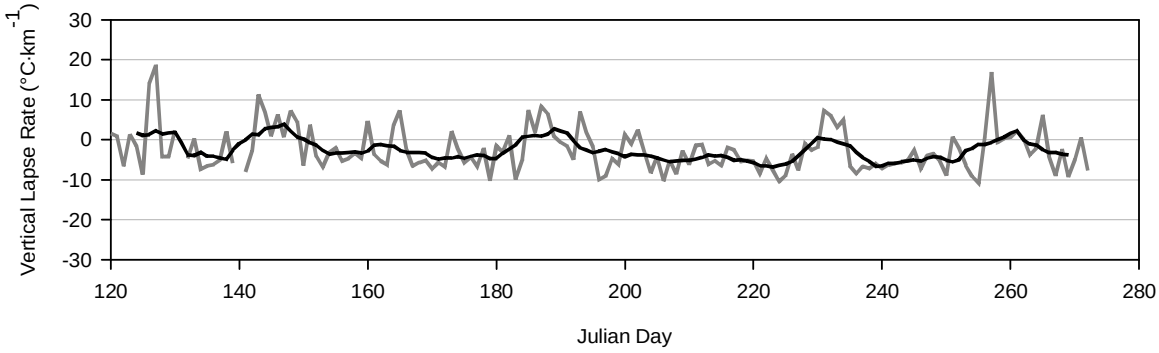

1982

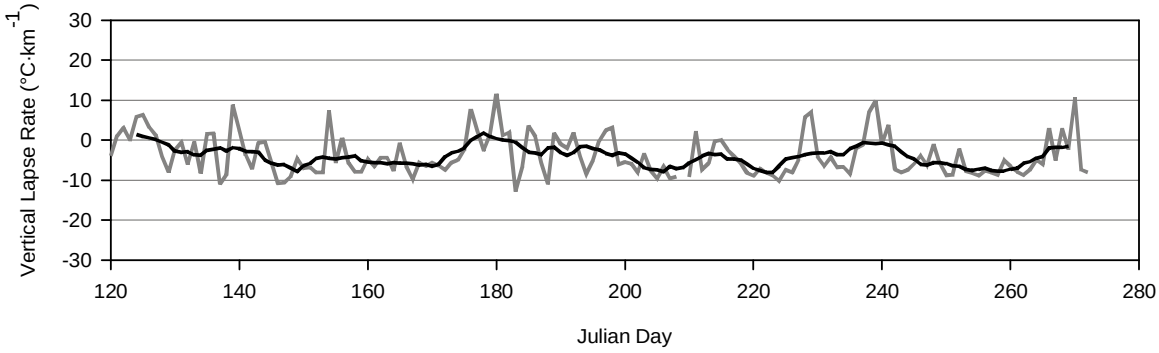

1983

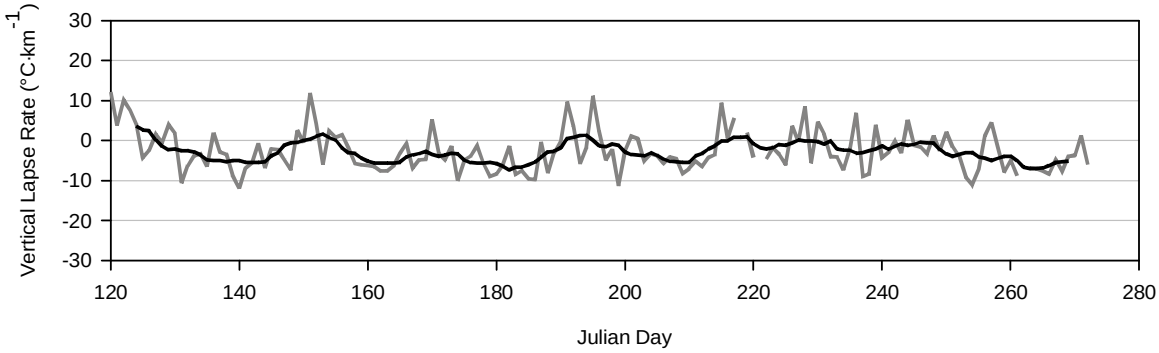

1984

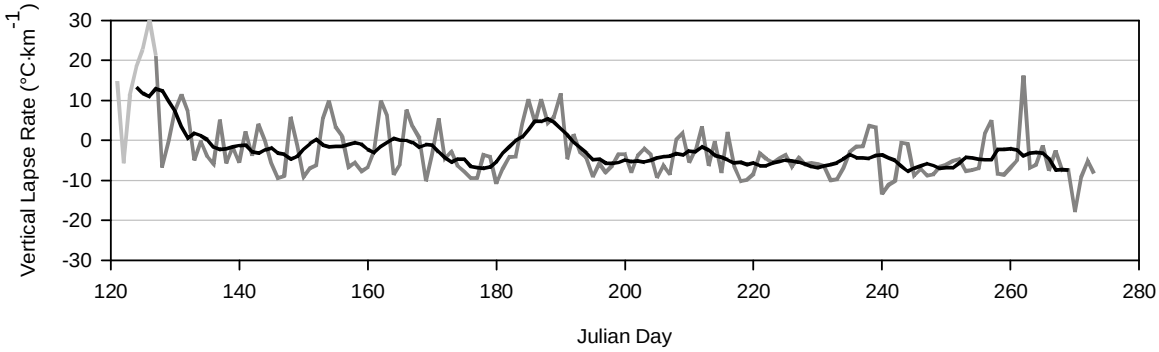

1985

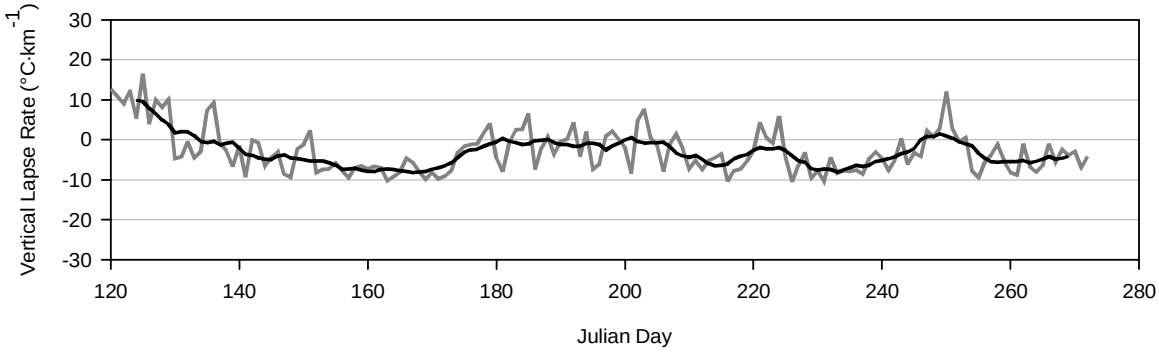

1986

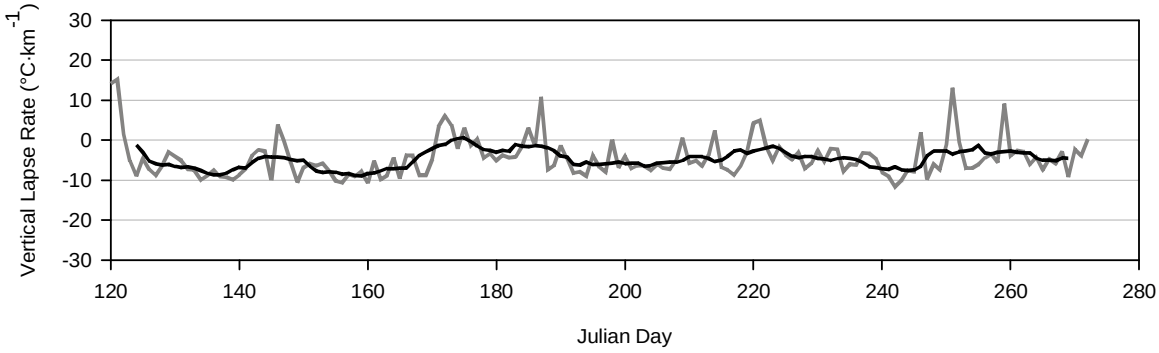

1987

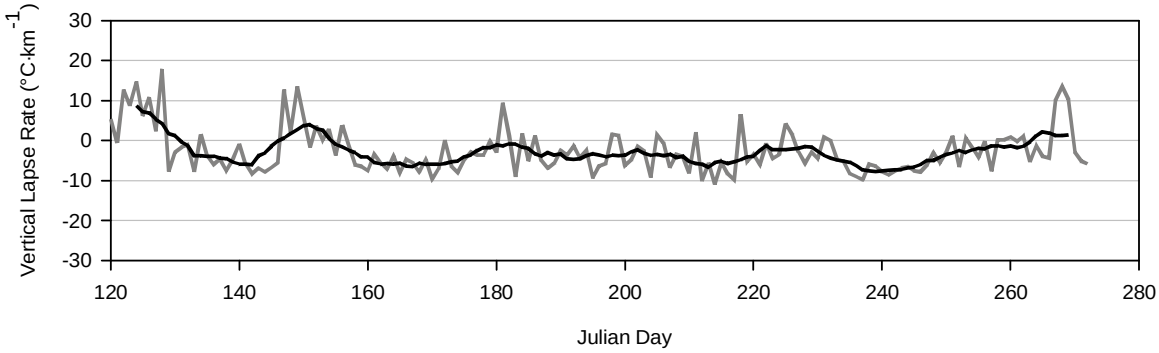

1988

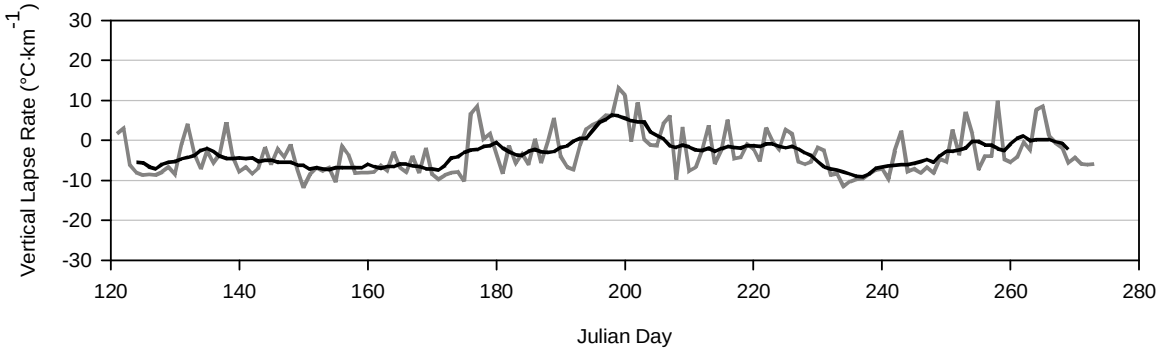

1989

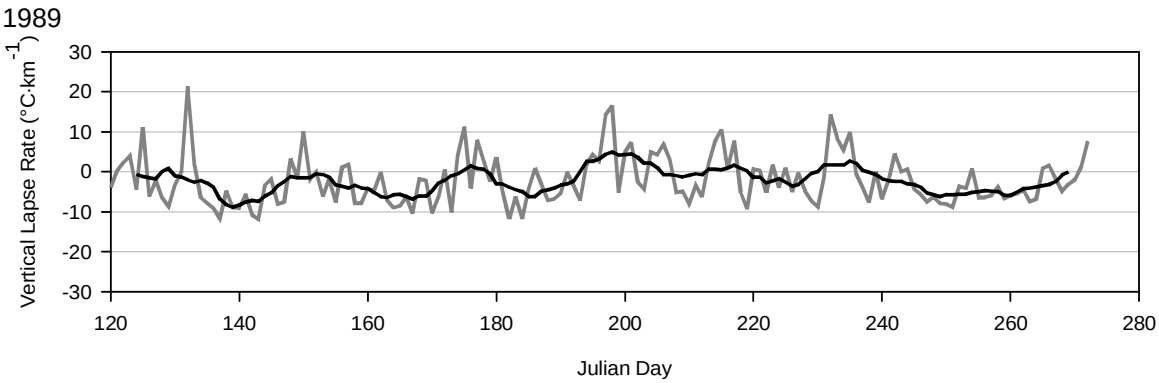

1990

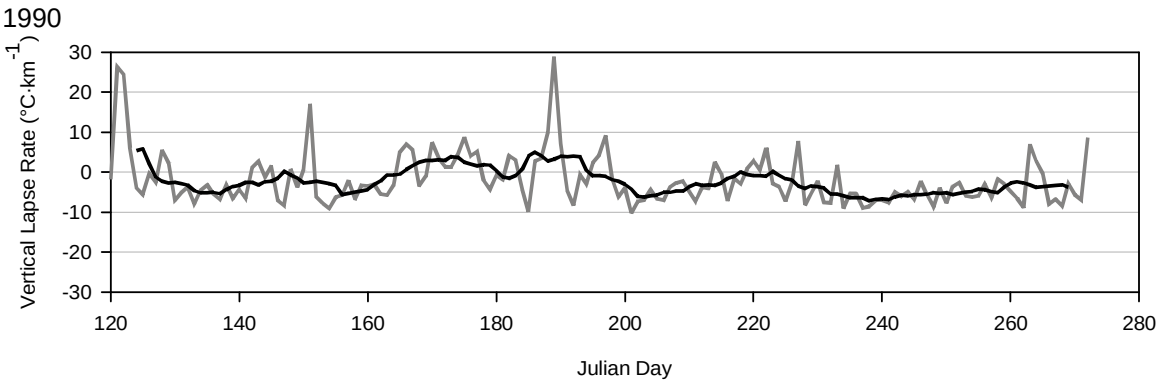

1991

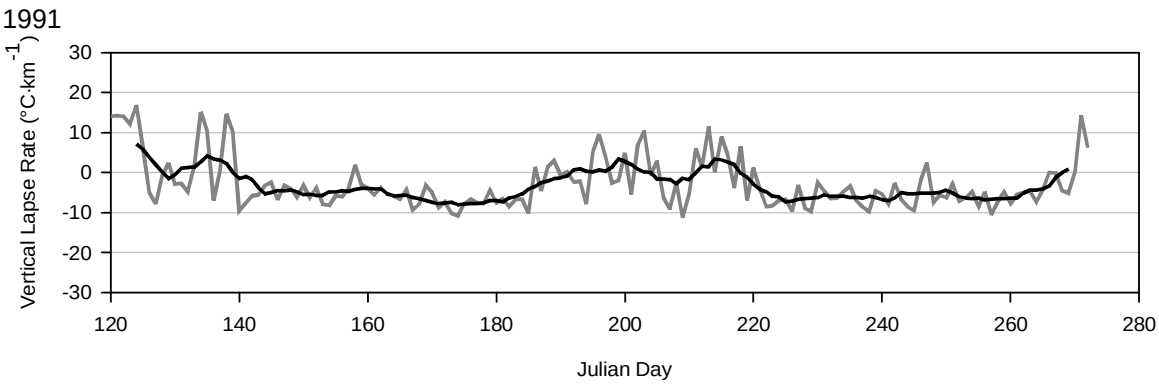

1992

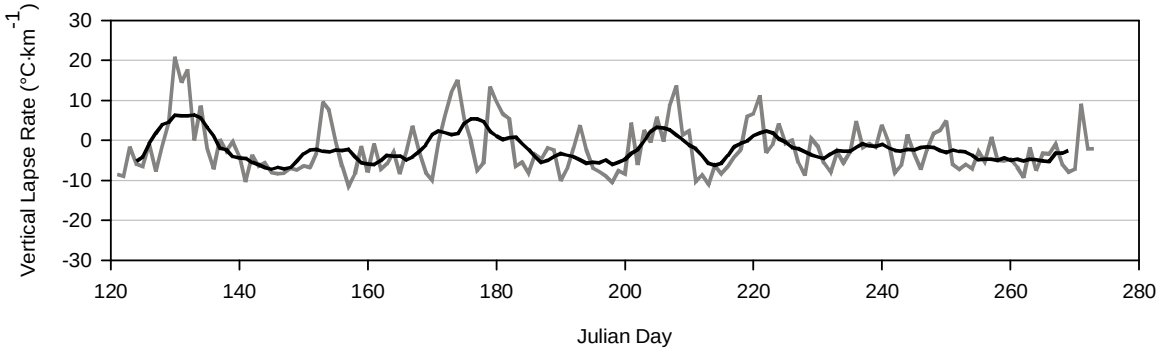

1993

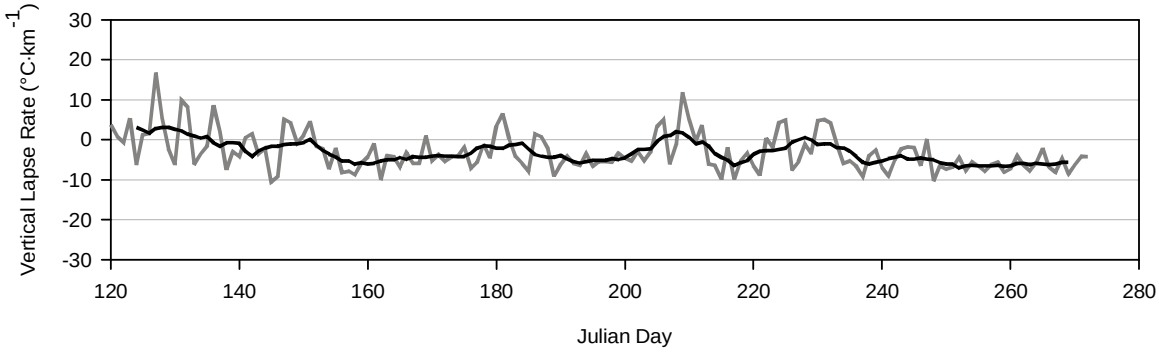

1994

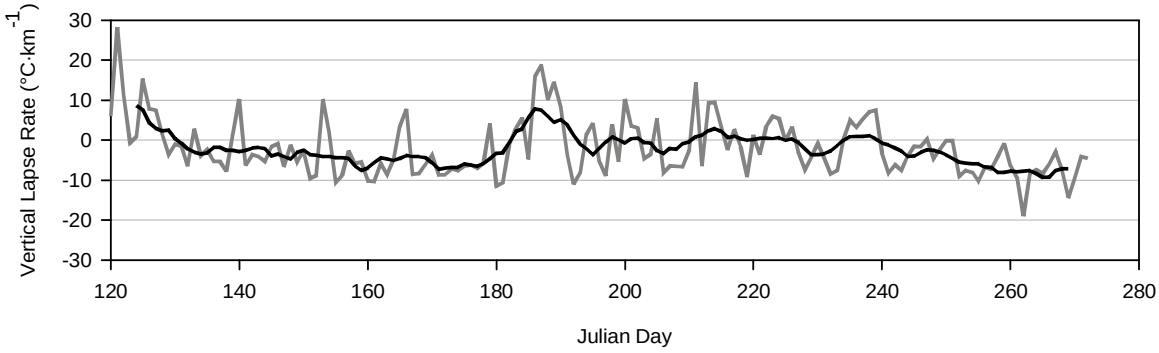

1995

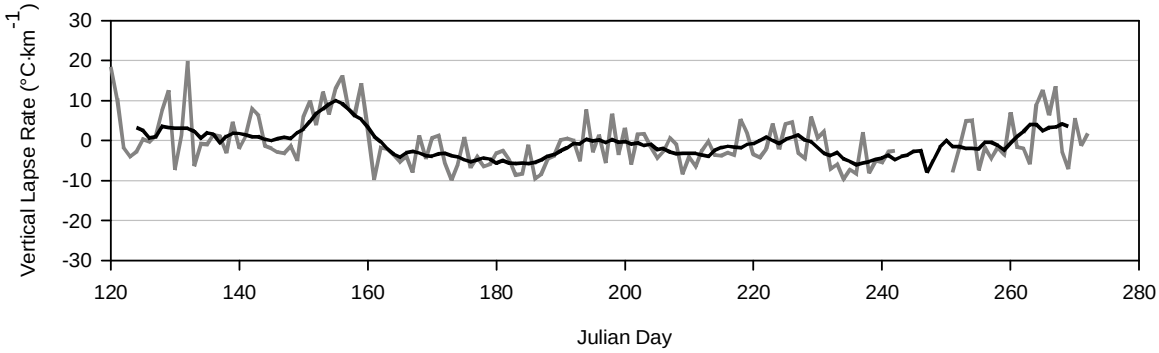

1996

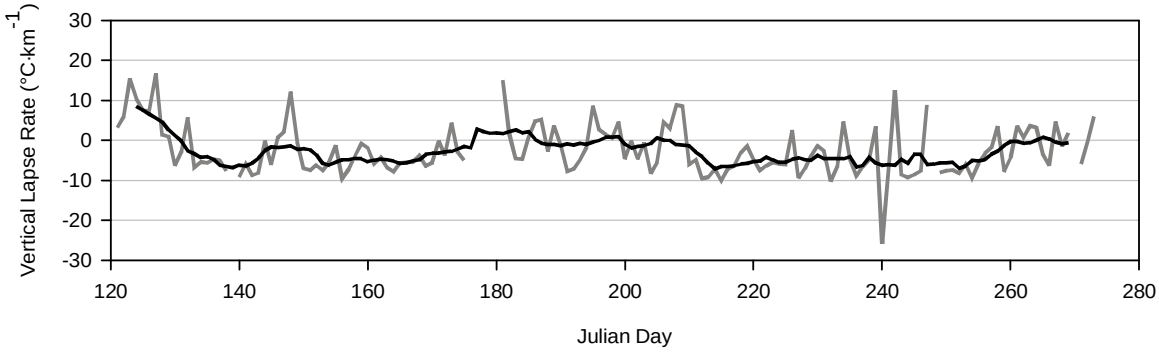

1997

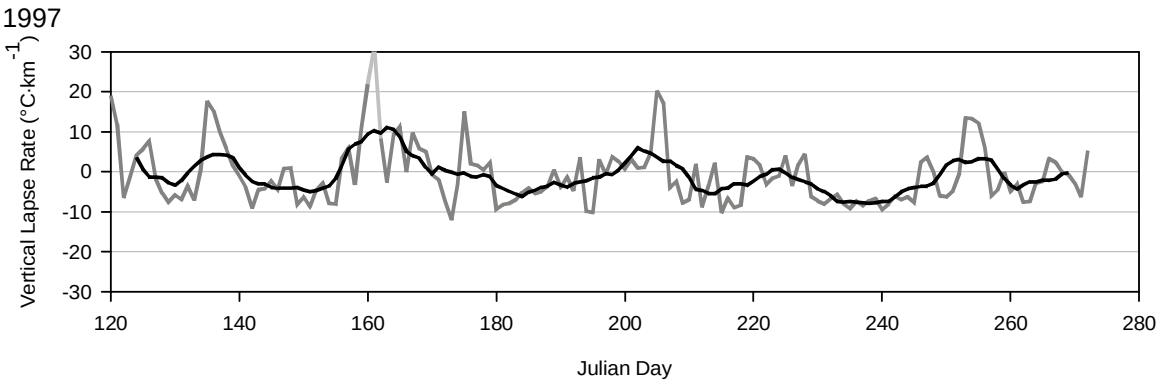

1998

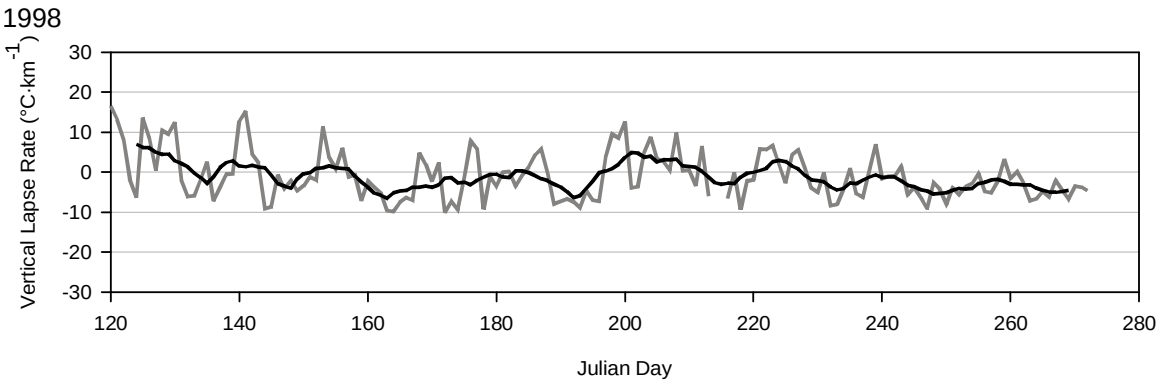

1999

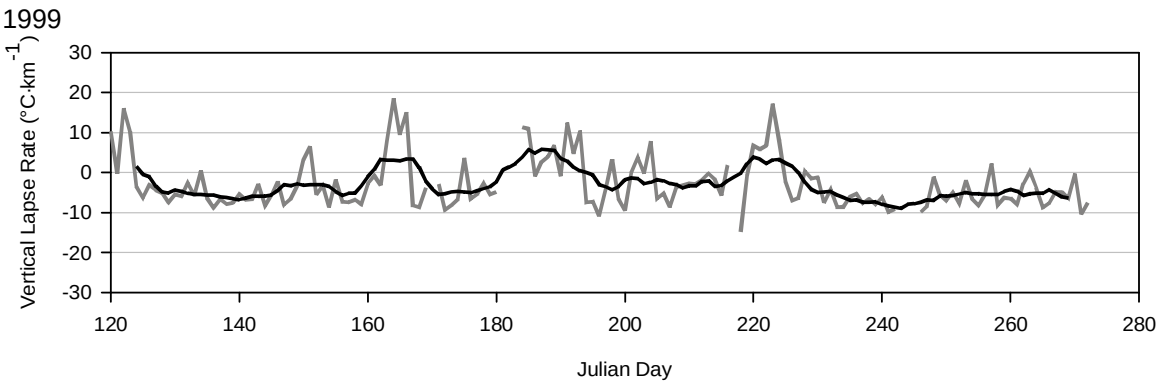

2000

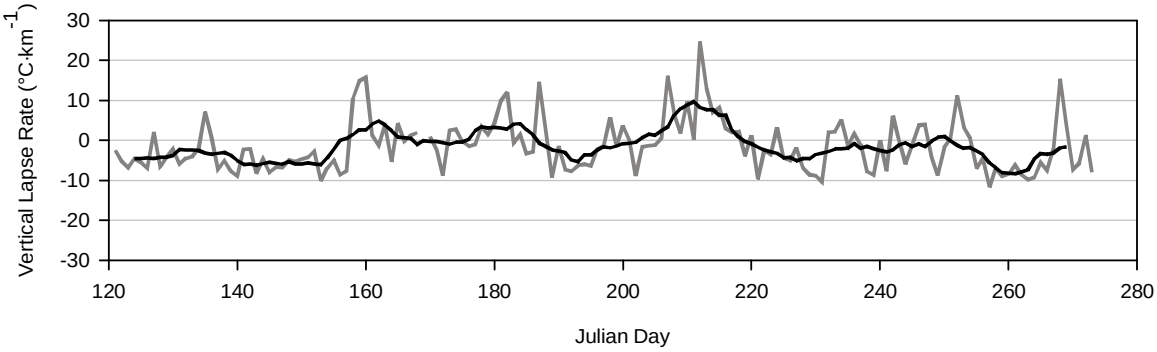

2001

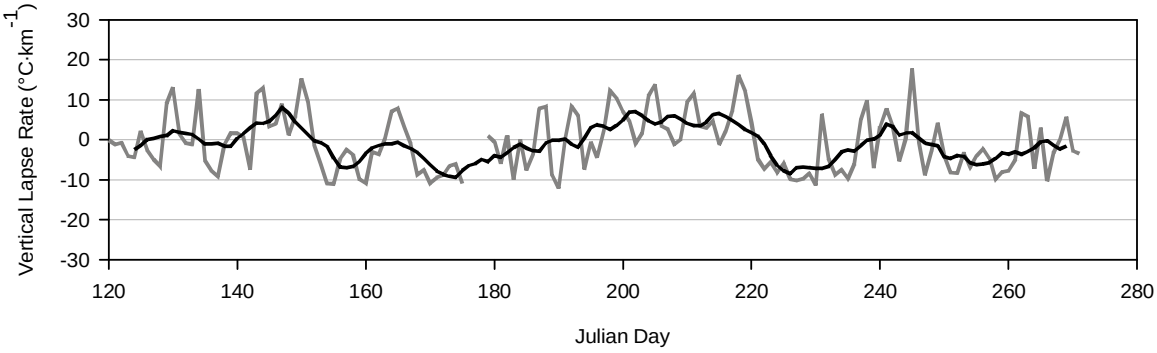

2002

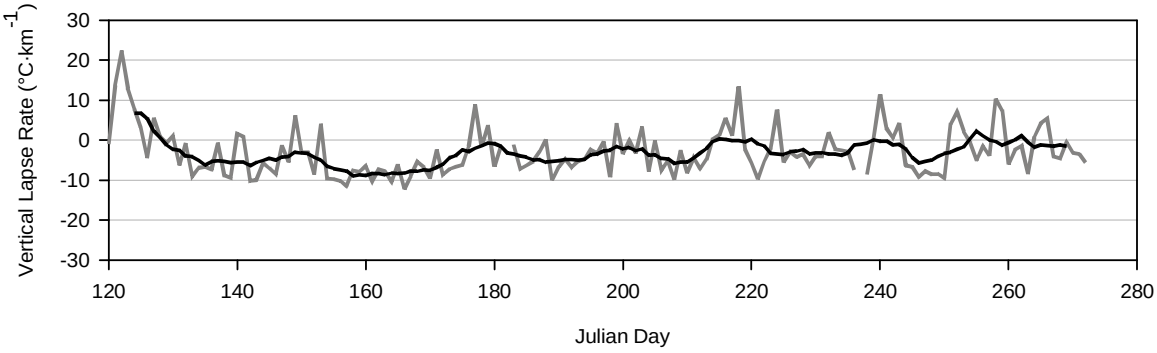

2003

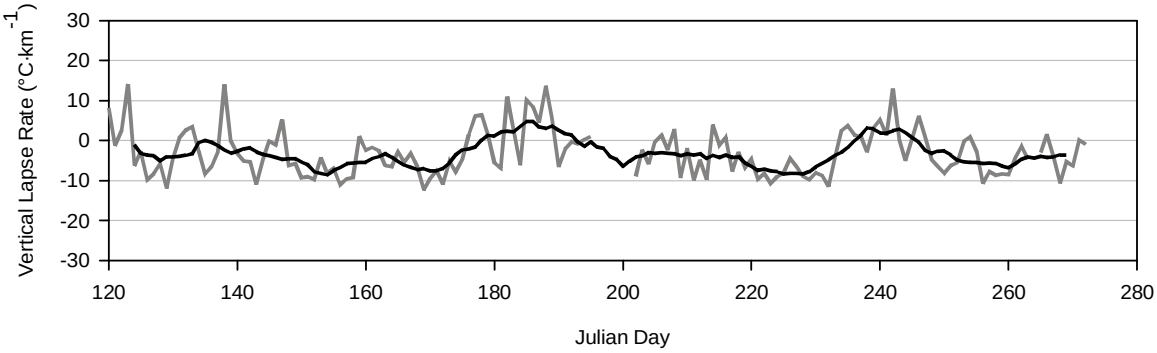

APPENDIX VIII

Mean, median and modal grain size for core R1-05. Samples were pretreated with hydrogen peroxide and sodium hexametaphosphate and analyzed with sonication three times for 60 seconds each. Values shown below are from the third analysis run.

Sample Midpoint (cm)	Mean (μm)	Median (μm)	Mode (μm)
0.5	8.89	10.67	13.61
1.5	8.27	9.82	13.61
2.5	7.07	8.21	23.81
3.5	5.76	6.85	11.29
4.5	8.56	9.84	28.70
5.5	8.41	9.95	26.14
6.5	8.68	10.26	13.61
7.5	9.30	11.35	14.94
8.5	8.58	10.32	13.61
9.5	8.31	9.74	23.81
10.5	8.95	10.73	13.61
11.5	9.28	11.37	14.94
12.5	7.67	8.96	26.14
13.5	9.13	11.00	13.61
14.5	8.49	10.24	13.61
15.5	8.81	10.66	13.61
16.5	8.98	10.92	14.94
17.5	8.23	9.75	23.81
18.5	8.23	9.54	12.40
19.5	8.73	10.64	13.61
20.5	8.73	10.64	13.61
21.5	8.67	10.62	13.61
22.5	6.93	7.99	10.29
23.5	6.43	7.29	23.81
24.5	8.13	9.61	12.40
25.5	7.28	8.55	11.29
26.5	7.32	8.44	11.29
27.5	7.90	9.05	11.29
28.5	8.02	9.21	11.29
29.5	8.89	10.51	13.61
30.5	8.06	9.57	12.40
31.5	7.58	9.36	12.40
32.5	6.19	6.95	8.54
33.5	6.25	7.17	10.29
34.5	6.69	7.53	9.37
35.5	9.69	12.23	16.40
36.5	7.61	9.08	23.81
37.5	9.61	11.84	28.70
38.5	8.65	10.14	28.70
39.5	8.78	10.20	28.70
40.5	8.82	10.34	26.14
41.5	8.96	9.66	9.37
42.5	9.65	11.62	28.70
43.5	7.83	8.84	10.29
44.5	8.72	9.84	11.29
45.5	7.57	8.86	12.40
46.5	7.53	8.86	21.69
47.5	7.09	8.47	12.40
48.5	8.32	9.32	10.29
49.5	7.36	8.55	11.29
50.5	7.43	8.66	11.29
51.5	7.39	8.86	12.40
52.5	7.95	9.54	26.14
53.5	9.32	11.51	28.70
54.5	9.76	12.13	28.70
55.5	9.40	11.52	28.70
56.5	8.19	9.72	13.61
57.5	7.21	8.52	11.29
58.5	8.30	10.01	13.61
59.5	8.04	9.60	12.40
60.5	6.57	7.85	10.29
61.5	7.25	8.88	12.40
62.5	9.24	11.50	28.70
63.5	9.64	11.74	14.94
64.5	8.28	9.82	12.40
65.5	7.28	8.63	11.29
66.5	6.51	7.73	10.29
67.5	7.75	9.22	12.40
68.5	9.23	11.43	14.94
69.5	10.08	12.37	34.58
70.5	7.97	9.45	11.29
71.5	9.50	12.17	28.70
72.5	12.28	16.43	31.50
73.5	10.74	14.08	28.70
74.5	9.83	12.39	14.94
75.5	7.83	9.71	13.61
76.5	9.26	11.67	14.94
77.5	8.74	10.65	13.61
78.5	7.53	9.17	12.40
79.5	7.56	9.37	12.40
80.5	8.99	11.29	14.94
81.5	10.10	12.79	28.70
82.5	7.52	9.05	11.29
83.5	5.48	6.43	9.37
84.5	5.55	6.31	8.54
85.5	8.31	10.01	26.14
86.5	10.73	13.57	31.50
87.5	11.52	14.61	34.58
88.5	9.45	11.02	13.61
89.5	7.08	8.07	10.29

Sample Midpoint (cm)	Mean (µm)	Median (µm)	Mode (µm)
90.5	7.25	8.32	10.29
91.5	7.41	8.28	10.29
92.5	6.77	7.90	10.29
93.5	7.45	8.41	26.14
94.5	7.97	9.11	26.14
95.5	6.86	7.77	9.37
96.5	6.64	8.06	11.29
97.5	8.51	10.55	26.14
98.5	11.83	15.32	34.58
99.5	13.45	19.04	31.50
100.5	15.21	21.12	31.50
101.5	11.98	15.47	26.14
102.5	11.15	14.48	21.69
103.5	9.97	12.46	16.40
104.5	11.64	14.59	34.58
105.5	12.13	15.34	34.58
106.5	12.50	16.34	34.58
107.5	11.51	14.37	34.58
108.5	9.06	10.69	12.40
109.5	7.76	9.51	12.40
110.5	7.23	8.76	13.61
111.5	10.57	13.23	31.50
112.5	8.22	9.35	28.70
113.5	8.12	9.65	12.40
114.5	10.91	13.66	31.50
115.5	9.48	11.40	28.70
116.5	5.37	5.94	7.78
117.5	6.71	7.21	8.54
118.5	8.61	10.46	13.61
119.5	8.60	10.62	26.14
120.5	6.57	7.92	11.29
121.5	6.87	7.99	10.29
122.5	7.44	8.76	11.29
123.5	6.83	7.90	10.29
124.5	7.51	8.79	11.29
125.5	6.82	8.03	11.29
126.5	5.54	6.30	7.78
127.5	5.63	6.19	7.08
128.5	6.90	7.82	9.37
129.5	6.28	7.19	8.54
130.5	5.85	6.74	8.54
131.5	6.01	6.78	8.54
132.5	6.45	7.03	8.54
133.5	9.58	10.84	34.58
134.5	8.62	9.61	11.29
135.5	8.97	11.03	19.76
136.5	13.41	17.82	31.50
137.5	11.83	15.35	34.58
138.5	6.54	7.31	9.37
139.5	5.88	6.58	9.37
140.5	5.89	6.55	8.54
141.5	7.67	9.01	12.40
142.5	11.44	14.02	18.00
143.5	14.80	19.88	34.58
144.5	12.00	14.48	34.58
145.5	8.66	10.31	12.40
146.5	7.02	8.43	11.29
147.5	8.09	9.50	12.40
148.5	9.81	10.76	37.97
149.5	8.68	10.31	12.40
150.5	8.14	9.62	12.40
151.5	6.59	7.76	11.29
152.5	11.61	14.37	34.58
153.5	10.82	12.99	31.50
154.5	7.76	9.19	12.40
155.5	7.59	8.62	11.29
156.5	8.27	9.83	12.40
157.5	7.97	9.41	12.40
158.5	9.87	11.52	28.70
159.5	9.19	10.69	26.14
160.5	8.67	10.31	13.61
161.5	9.42	11.17	34.58
162.5	13.88	16.71	41.68
163.5	18.29	24.32	50.22
164.5	14.91	18.85	41.68
165.5	14.62	18.08	45.75
166.5	14.74	18.09	45.75
167.5	10.98	12.05	37.97
168.5	5.52	6.07	8.54
169.5	8.15	8.79	34.58
170.5	13.04	15.56	45.75
171.5	14.55	18.66	41.68
172.5	9.82	10.56	31.50
173.5	12.62	14.78	41.68
174.5	12.30	13.64	50.22
175.5	14.63	17.10	26.14
176.5	13.43	16.74	34.58
177.5	17.88	22.73	34.58
178.5	13.93	14.85	34.58
179.5	12.52	14.09	45.75
180.5	12.18	13.92	14.94
181.5	10.47	12.33	13.61
182.5	11.90	13.85	16.40
183.5	7.95	9.13	11.29
184.5	7.41	8.54	11.29
185.5	8.31	9.41	28.70
186.5	8.40	9.04	26.14
187.5	9.20	10.50	28.70
188.5	9.74	11.18	28.70
189.5	9.76	11.20	28.70
190.5	10.85	12.98	16.40
191.5	6.96	7.57	8.54
192.5	7.33	8.02	9.37
193.5	7.23	8.01	9.37
194.5	8.32	9.14	10.29
195.5	9.63	10.03	9.37
196.5	9.69	11.26	31.50
197.5	9.56	11.24	28.70

Sample Midpoint (cm)	Mean (µm)	Median (µm)	Mode (µm)
198.5	9.87	11.83	28.70
199.5	8.39	9.81	12.40
200.5	9.44	11.18	28.70
201.5	9.59	11.40	28.70
202.5	9.74	11.28	28.70
203.5	8.89	10.21	26.14
204.5	8.86	10.09	11.29
205.5	10.82	13.31	31.50
206.5	8.59	10.12	12.40
207.5	6.22	7.20	11.29
208.5	6.28	7.02	8.54
209.5	7.45	8.37	9.37
210.5	7.84	8.51	9.37
211.5	6.88	7.50	8.54
212.5	6.92	7.64	8.54
213.5	7.45	8.41	10.29
214.5	7.09	7.92	9.37
215.5	7.88	8.73	9.37
216.5	6.80	7.65	8.54
217.5	7.03	7.92	9.37
218.5	5.21	5.78	7.08
219.5	7.27	7.81	8.54
220.5	7.20	7.59	7.78
221.5	6.38	6.82	7.78
222.5	6.73	7.47	8.54
223.5	7.53	8.37	9.37
224.5	8.07	8.92	9.37
225.5	8.08	8.58	8.54
226.5	9.20	10.53	26.14
227.5	8.80	10.30	28.70
228.5	7.90	8.97	10.29
229.5	8.10	9.25	10.29
230.5	8.13	9.56	11.29
231.5	7.11	8.21	10.29
232.5	6.72	7.75	9.37
233.5	6.12	7.10	8.54

APPENDIX IX

Mean, median and modal grain size for core R2-05. Samples were pretreated with hydrogen peroxide and sodium hexametaphosphate and analyzed with sonication three times for 60 seconds each. Values shown below are from the third analysis run.

Sample Midpoint (cm)	Mean (μm)	Median (μm)	Mode (μm)
0.5	7.40	8.64	28.70
1.5	8.02	9.75	12.40
2.5	8.19	10.05	12.40
3.5	8.09	9.90	12.40
4.5	8.77	10.69	13.61
5.5	9.15	10.98	13.61
6.5	8.97	10.60	12.40
7.5	9.25	10.81	12.40
8.5	9.41	10.90	12.40
9.5	9.32	11.25	13.61
10.5	9.61	11.71	13.61
11.5	10.11	12.19	14.94
12.5	9.64	11.42	13.61
13.5	9.96	12.08	14.94
14.5	9.21	11.31	13.61
15.5	10.38	12.47	14.94
16.5	10.31	12.22	13.61
17.5	9.43	11.18	13.61
18.5	7.71	9.04	11.29
19.5	9.06	10.41	12.40
20.5	9.16	10.36	12.40
21.5	8.54	9.49	11.29
22.5	8.44	9.38	11.29
23.5	8.46	9.08	10.29
24.5	10.40	11.25	12.40
25.5	9.55	10.95	12.40
26.5	10.25	10.63	11.29
27.5	10.84	11.28	12.40
28.5	10.84	10.71	10.29
29.5	9.01	9.81	11.29
30.5	9.76	11.32	16.40
31.5	10.95	12.47	23.81
32.5	9.96	10.67	37.97
33.5	11.95	14.23	23.81
34.5	9.62	11.34	13.61
35.5	8.81	10.03	12.40
36.5	8.07	9.36	12.40
37.5	8.52	9.43	11.29
38.5	7.65	8.68	11.29
39.5	7.97	8.98	11.29
40.5	9.09	10.20	12.40
41.5	9.55	11.35	14.94
42.5	10.83	12.95	23.81
43.5	9.18	10.84	13.61
44.5	9.43	10.73	12.40
45.5	9.42	10.50	11.29
46.5	9.51	10.23	9.37
47.5	8.23	9.37	11.29
48.5	9.14	10.27	12.40
49.5	12.17	13.64	13.61
50.5	8.95	9.89	11.29
51.5	7.75	8.86	11.29
52.5	9.38	10.94	13.61
53.5	10.62	11.96	12.40
54.5	10.74	12.76	14.94
55.5	12.27	15.61	21.69
56.5	11.00	13.31	19.76
57.5	9.65	11.71	14.94
58.5	10.03	11.99	14.94
59.5	10.89	12.47	13.61
60.5	8.75	10.40	12.40
61.5	11.40	13.07	13.61
62.5	9.91	11.85	14.94
63.5	8.34	9.51	11.29
64.5	8.04	9.18	11.29
65.5	9.53	11.08	13.61
66.5	21.67	28.43	80.07
67.5	14.74	16.29	34.58
68.5	15.19	16.56	34.58
69.5	9.93	11.08	12.40
70.5	11.48	12.38	12.40
71.5	9.21	10.28	11.29
72.5	12.86	12.69	10.29
73.5	9.27	10.70	13.61
74.5	8.71	10.13	12.40
75.5	7.49	8.67	10.29
76.5	14.25	14.73	12.40
77.5	18.06	21.30	37.97
78.5	17.62	21.53	31.50
79.5	20.02	23.44	26.17
80.5	19.26	22.59	23.81
81.5	15.11	18.09	21.69
82.5	13.34	16.00	21.69
83.5	18.29	20.92	26.14
84.5	15.36	17.31	23.81
85.5	16.76	19.15	23.81
86.5	13.71	16.90	23.81
87.5	20.03	22.67	116.30
88.5	19.94	23.28	87.90
89.5	15.21	16.24	13.61

Sample Midpoint (cm)	Mean (µm)	Median (µm)	Mode (µm)
90.5	18.45	21.34	96.49
91.5	18.90	23.66	87.90
92.5	17.90	20.42	96.49
93.5	16.06	17.57	80.07
94.5	18.40	20.23	96.49
95.5	18.01	21.13	80.07
96.5	17.76	20.36	34.58
97.5	12.93	137.4	11.29
98.5	11.30	11.75	11.29
99.5	12.72	13.17	11.29
100.5	12.63	13.45	13.61
101.5	15.64	16.54	14.94
102.5	19.07	21.19	96.49
103.5	20.33	25.47	80.07
104.5	16.40	17.11	13.61
105.5	11.19	12.04	12.40
106.5	7.74	9.02	11.29
107.5	11.77	11.76	11.29
108.5	8.20	9.03	10.29
109.5	7.58	8.44	10.29
110.5	10.04	9.79	10.29
111.5	---	---	---
112.5	10.83	11.77	12.40
113.5	8.58	10.00	12.40
114.5	12.19	12.57	11.29
115.5	15.33	15.03	12.40
116.5	10.12	10.37	10.29
117.5	8.42	9.09	10.29
118.5	10.98	11.08	10.29
119.5	13.35	13.38	10.29
120.5	16.75	20.18	66.44
121.5	17.59	19.61	72.94
122.5	17.30	17.73	80.07
123.5	17.29	18.30	16.40
124.5	22.40	25.37	23.81
125.5	20.42	25.55	66.44
126.5	18.74	23.04	72.94
127.5	6.00	7.01	10.29
128.5	7.87	9.60	23.81
129.5	9.83	12.33	26.14
130.5	8.93	10.97	26.14
131.5	7.65	8.63	18.00
132.5	8.81	10.45	23.81
133.5	7.71	9.10	12.40
134.5	6.08	7.07	9.37
135.5	6.64	7.65	10.29
136.5	7.17	8.16	19.76
137.5	5.56	6.04	19.76
138.5	8.27	9.84	12.40
139.5	7.44	9.02	12.40
140.5	6.77	8.10	11.29
141.5	6.46	7.57	19.76
142.5	7.49	8.87	21.69
143.5	7.69	8.98	19.76
144.5	7.78	9.50	19.76
145.5	6.76	7.83	10.29
146.5	6.54	7.53	9.37
147.5	6.26	7.07	8.54
148.5	6.07	6.86	8.54
149.5	6.79	7.93	10.29
150.5	7.89	9.41	12.40
151.5	7.40	8.66	19.76
152.5	5.78	6.47	21.69
153.5	6.15	6.75	7.78
154.5	8.10	9.52	23.81
155.5	8.52	10.07	23.81
156.5	11.05	12.35	41.68
157.5	6.86	7.73	16.40
158.5	8.95	10.71	31.50
159.5	8.22	9.53	23.81
160.5	8.17	9.02	23.81
161.5	7.79	8.49	23.81
162.5	8.78	9.61	10.29
163.5	6.62	7.29	8.54
164.5	5.63	6.48	8.54
165.5	4.83	5.19	5.88
166.5	5.89	6.64	7.78
167.5	9.70	12.26	26.14

APPENDIX X

Mean, median and modal grain size for core R4-05. Samples were pretreated with hydrogen peroxide and sodium hexametaphosphate and analyzed with sonication three times for 60 seconds each. Values shown below are from the third analysis run.

Sample Midpoint (cm)	Mean (μm)	Median (μm)	Mode (μm)
0.5	9.73	13.03	23.81
1.5	9.97	12.99	23.81
2.5	11.07	14.93	23.81
3.5	---	---	---
4.5	8.60	9.62	23.81
5.5	9.60	12.44	23.81
6.5	9.08	11.51	21.69
7.5	9.93	13.29	23.81
8.5	8.83	10.28	23.81
9.5	10.40	14.05	23.81
10.5	8.82	11.44	21.69
11.5	10.20	13.98	23.81
12.5	14.34	16.61	26.14
13.5	42.79	63.50	153.80
14.5	8.92	11.22	23.81
15.5	10.85	14.85	26.14
16.5	19.59	23.12	23.81
17.5	10.40	13.94	23.81
18.5	9.71	12.84	23.81
19.5	10.68	14.37	26.14
20.5	10.31	13.84	23.81
21.5	10.82	14.68	26.14
22.5	9.95	13.36	23.81
23.5	10.70	14.01	26.14
24.5	---	---	---
25.5	11.32	15.63	26.14
26.5	11.85	16.49	28.70
27.5	16.54	20.04	26.14
28.5	11.68	15.68	28.70
29.5	10.46	13.95	26.14
30.5	16.63	20.74	28.70
31.5	20.38	26.29	34.58
32.5	11.05	14.59	28.70
33.5	12.22	17.08	28.70
34.5	12.18	16.79	28.70
35.5	12.50	17.08	31.50
36.5	18.85	21.10	31.50
37.5	13.28	17.05	31.50
38.5	10.66	14.00	26.14
39.5	10.55	13.93	26.14
40.5	10.61	14.20	26.14
41.5	10.11	13.11	26.14
42.5	11.00	14.45	28.70
43.5	16.60	21.20	28.70
44.5	9.51	12.67	21.69
45.5	17.43	19.90	23.81
46.5	11.06	15.52	26.14
47.5	17.26	21.97	28.70
48.5	10.19	13.98	23.81
49.5	10.76	14.34	26.14
50.5	10.23	13.37	26.14
51.5	19.36	3.82	31.50
52.5	23.11	28.83	34.58
53.5	12.80	18.38	28.70
54.5	11.06	15.63	26.14
55.5	8.54	11.06	21.69
56.5	15.59	18.24	21.69
57.5	16.93	16.00	16.89
58.5	9.40	12.35	21.69
59.5	9.99	13.38	21.69
60.5	10.62	14.55	23.81
61.5	9.91	13.49	23.81
62.5	17.77	22.43	28.70
63.5	11.37	15.79	26.14
64.5	11.43	15.98	28.70
65.5	12.12	17.02	28.70
66.5	11.72	16.10	26.14
67.5	11.92	16.64	26.14
68.5	11.82	15.58	23.81
69.5	10.57	13.78	18.00
70.5	9.21	11.68	14.94
71.5	8.84	11.05	14.94
72.5	8.81	11.05	13.61
73.5	9.50	11.79	14.94
74.5	9.97	12.82	16.40
75.5	8.87	11.35	14.94
76.5	7.90	9.83	13.61
77.5	8.85	10.91	13.61
78.5	9.12	11.64	14.94
79.5	8.36	10.35	13.61
80.5	12.46	16.57	28.70
81.5	10.89	13.70	16.40
82.5	9.70	12.01	14.94
83.5	9.97	12.94	16.40
84.5	11.50	15.30	31.50
85.5	9.63	12.23	16.40
86.5	8.28	10.35	14.94
87.5	9.05	11.33	14.94
88.5	9.5	11.84	14.94
89.5	8.83	11.15	14.94

Sample Midpoint (cm)	Mean (µm)	Median (µm)	Mode (µm)
90.5	6.89	8.08	11.29
91.5	8.59	10.56	13.61
92.5	6.87	8.10	11.29
93.5	6.89	7.91	10.29
94.5	6.63	7.85	10.29
95.5	7.08	8.31	10.29
96.5	6.98	8.15	10.29
97.5	---	---	---
98.5	6.39	7.37	10.29
99.5	6.94	8.19	10.90
100.5	7.07	8.28	10.29
101.5	6.15	7.08	9.37
102.5	6.45	6.97	9.37
103.5	7.32	7.88	8.54
104.5	6.96	7.60	8.54
105.5	6.85	7.44	8.54
106.5	7.40	8.19	9.37
107.5	---	---	---
108.5	8.12	8.78	10.29
109.5	7.98	8.49	9.37
110.5	9.33	10.06	11.29
111.5	7.94	9.01	11.29
112.5	7.39	7.99	9.37
113.5	6.72	7.27	8.54
114.5	6.51	7.27	9.37
115.5	6.72	7.6.	9.37
116.5	7.17	7.81	9.37
117.5	6.52	7.14	8.54
118.5	7.03	7.47	8.54
119.5	6.52	7.20	8.54
120.5	6.50	7.30	8.54
121.5	6.55	7.05	7.78
122.5	6.66	7.11	7.78
123.5	6.35	6.77	7.78
124.5	6.92	7.38	7.78
125.5	6.50	7.04	7.78
126.5	8.21	9.49	11.29
127.5	8.00	9.22	11.29
128.5	8.53	9.64	11.29
129.5	8.81	10.25	12.40
130.5	7.15	7.84	9.37
131.5	6.78	7.62	9.37
132.5	6.90	7.62	9.37
133.5	6.80	7.45	8.54
134.5	7.25	8.44	11.29
135.5	8.16	9.52	12.40
136.5	8.12	9.16	11.29
137.5	7.71	8.37	9.37
138.5	7.12	8.01	10.29
139.5	6.98	7.77	9.37
140.5	8.50	9.54	11.29
141.5	7.06	8.04	10.29
142.5	7.45	8.51	11.29
143.5	8.21	9.06	10.29
144.5	7.66	8.51	11.29
145.5	9.33	11.16	14.94
146.5	11.11	13.64	18.00
147.5	10.95	13.37	16.40
148.5	9.79	11.64	14.94
149.5	9.60	11.13	13.61
150.5	10.26	12.66	16.40
151.5	10.66	12.84	16.40
152.5	10.29	12.82	16.40
153.5	9.29	11.64	16.40
154.5	9.53	12.08	16.40
155.5	9.79	12.21	16.40
156.5	11.31	14.27	18.00
157.5	9.62	11.68	14.94
158.5	8.74	10.38	13.61
159.5	9.80	11.50	16.40
160.5	10.59	13.17	18.00
161.5	10.79	13.29	16.40
162.5	8.95	11.07	14.94
163.5	10.77	13.93	19.76
164.5	11.83	14.79	19.76
165.5	9.98	12.65	16.40
166.5	11.13	13.01	14.94
167.5	14.15	18.73	34.58
168.5	12.57	15.63	21.69
169.5	11.60	14.66	19.76
170.5	10.35	12.97	18.00
171.5	11.72	15.20	26.14
172.5	12.28	15.08	19.76
173.5	6.42	7.21	10.29
174.5	10.57	12.82	19.76
175.5	13.38	17.69	31.50
176.5	16.43	22.90	37.97
177.5	14.61	20.28	41.68
178.5	14.47	19.65	37.97
179.5	13.57	17.57	23.81
180.5	13.09	17.45	28.70
181.5	15.96	20.99	26.14
182.5	12.48	16.33	21.69
183.5	13.37	17.55	28.70
184.5	12.06	15.40	19.76
185.5	10.59	13.07	16.40
186.5	11.14	13.07	14.94
187.5	9.54	11.19	14.94
188.5	10.09	12.60	31.50
189.5	13.15	17.76	31.50
190.5	13.07	18.02	31.50
191.5	14.68	18.85	26.14
192.5	12.94	17.21	26.14
193.5	13.13	17.77	31.50
194.5	13.53	18.55	31.50
195.5	13.50	18.05	31.50
196.5	13.65	18.43	31.50
197.5	13.04	17.40	31.50

Sample Midpoint (cm)	Mean (µm)	Median (µm)	Mode (µm)
198.5	11.9	15.39	31.50
199.5	11.39	14.23	18.00
200.5	11.49	14.39	18.00
201.5	11.72	14.97	19.76
202.5	11.20	14.44	19.76
203.5	13.09	17.35	34.58
204.5	13.01	17.36	34.58
205.5	14.16	18.53	26.14
206.5	13.00	16.85	21.69
207.5	13.09	16.96	21.69
208.5	14.38	19.16	26.14
209.5	14.38	19.28	34.58
210.5	11.36	14.18	18.00
211.5	11.26	13.82	18.00
212.5	10.83	13.39	16.40
213.5	9.67	11.85	16.40
214.5	11.61	13.69	14.94
215.5	13.53	17.22	41.68
216.5	13.54	16.92	23.81
217.5	15.39	19.59	26.14
218.5	13.79	16.83	50.22
219.5	12.46	15.52	45.75
220.5	13.68	16.57	28.70
221.5	13.87	16.60	55.13
222.5	13.03	15.34	50.22
223.5	12.12	13.82	45.75
224.5	9.33	11.15	14.94
225.5	9.72	11.96	14.94
226.5	9.43	10.53	12.40
227.5	10.44	11.98	13.61
228.5	11.00	12.98	14.94
229.5	10.74	12.49	14.94
230.5	10.90	12.60	14.94
231.5	11.21	12.67	14.94
232.5	10.83	12.51	14.94
233.5	10.08	11.42	13.61
234.5	10.96	13.09	14.94
235.5	11.55	13.63	14.94
236.5	10.08	12.44	14.94

APPENDIX XI

Mean, median and modal grain size for core J2-04. Samples were pretreated with hydrogen peroxide and sodium hexametaphosphate and analyzed with sonication three times for 60 seconds each. Values shown below are from the third analysis run.

Sample Midpoint (cm)	Mean (μm)	Median (μm)	Mode (μm)
5.0	16.47	18.80	31.50
10.0	17.88	22.42	41.68
15.0	21.34	26.89	66.44
20.0	13.82	15.91	34.58
25.0	16.78	21.04	55.13
30.0	15.33	17.60	50.22
35.0	17.68	22.93	55.13
40.0	15.56	18.41	31.50
45.0	18.49	22.78	45.75
50.0	13.87	16.26	50.22
55.0	16.51	19.95	34.58
60.0	15.53	18.64	34.58
65.0	15.48	18.72	41.68
70.0	14.62	18.91	45.75
75.0	14.40	17.44	45.75
80.0	17.59	21.63	41.68
85.0	17.07	21.04	41.68
90.0	17.05	20.63	45.75
95.0	16.07	19.28	41.68
100.0	16.42	20.68	41.68
105.0	15.43	18.88	55.13
110.0	14.56	18.46	41.68
115.0	13.95	17.17	41.68
120.0	13.67	15.45	37.97
125.0	16.22	21.13	37.97
130.0	---	---	---
135.0	12.09	14.89	50.22
140.0	15.52	20.43	37.97
145.0	13.03	16.58	34.58
150.0	13.46	16.29	72.94
155.0	15.20	16.68	72.94
160.0	12.71	13.83	34.58
165.0	13.09	13.82	10.29
170.0	11.22	11.29	9.37
175.0	12.34	12.26	11.29
180.0	13.28	15.51	45.75
185.0	15.21	16.33	12.40
190.0	10.35	10.94	28.70
195.0	13.79	16.78	23.81
196.0	11.13	14.01	37.97
197.0	12.50	15.16	31.50
198.0	12.01	14.85	41.68
199.0	11.41	13.89	37.97
200.0	13.14	17.45	41.68
201.0	12.19	16.42	41.68
202.0	14.04	18.63	37.97
203.0	12.47	15.56	34.58
204.0	13.52	17.00	21.69
205.0	13.15	16.42	34.58
206.0	12.92	16.12	34.58
207.0	12.77	15.81	19.76
208.0	11.45	14.10	18.00
209.0	12.88	15.88	19.76
210.0	12.93	15.95	19.76
211.0	12.55	15.07	18.00
212.0	14.96	18.64	23.81
213.0	13.78	17.5	50.22
214.0	12.88	15.43	19.76
215.0	15.78	19.49	50.22
216.0	11.81	14.00	16.40
217.0	13.77	18.73	45.75
218.0	11.73	14.50	18.00
219.0	10.02	12.45	16.40
220.0	13.09	17.20	45.75
221.0	11.61	15.17	41.68
222.0	14.08	17.15	21.69
223.0	15.99	18.86	21.69
224.0	14.72	17.63	21.69
225.0	13.55	16.67	26.14
226.0	13.65	16.68	19.76
227.0	10.65	12.78	16.40
228.0	12.07	14.22	14.94
229.0	14.05	17.16	19.76
230.0	14.24	19.26	28.70
234.0	15.20	18.06	28.70
238.0	13.99	19.00	28.70
240.0	11.75	15.10	34.58
242.0	14.39	18.63	28.70
246.0	16.13	20.63	28.70
248.0	13.34	17.41	41.68
250.0	16.11	20.92	28.70
254.0	12.56	16.24	41.68
258.0	14.66	18.45	28.70
262.0	17.50	23.83	41.68
264.0	14.43	18.42	31.50
266.0	15.88	21.19	34.58
270.0	14.25	19.34	34.58
274.0	15.66	20.91	31.50
278.0	14.43	19.31	34.58
280.0	14.77	18.31	31.50

Sample Midpoint (cm)	Mean (µm)	Median (µm)	Mode (µm)
282.0	14.11	18.55	26.14
286.0	17.87	23.16	28.70
288.0	13.62	17.77	28.70
290.0	14.64	20.47	37.97
294.0	15.50	20.66	28.70
296.0	16.15	20.77	31.50
298.0	14.43	19.96	37.97
300.0	12.23	16.22	34.58
302.0	14.66	18.56	28.70
304.0	13.70	17.32	28.70
306.0	17.49	22.25	34.58
310.0	13.42	17.13	28.70
312.0	20.04	24.44	31.50
314.0	16.03	19.25	28.70
318.0	14.63	17.81	26.14
320.0	17.96	21.17	28.70
322.0	16.30	19.68	26.14
326.0	15.72	18.73	26.14
328.0	18.11	21.15	28.70
330.0	15.31	18.13	23.81
332.0	18.36	22.20	28.70
334.0	17.43	21.35	28.70
336.0	19.81	23.93	96.49
338.0	17.17	19.88	28.70
342.0	15.89	18.50	26.14

Sample Midpoint (cm)	Mean (µm)	Median (µm)	Mode (µm)
344.0	18.35	21.87	34.58
346.0	12.22	14.67	23.81
348.0	25.00	33.01	96.49
350.0	14.39	17.17	31.50
352.0	17.13	21.02	80.07
353.0	15.32	18.82	60.52
356.0	17.65	21.62	87.90
358.0	17.01	20.20	80.07
362.0	15.84	17.90	87.90
364.0	23.29	30.45	105.90
366.0	20.16	24.99	87.90
370.0	12.85	15.80	26.14
372.0	14.15	17.17	21.69
374.0	11.61	13.80	18.00
376.0	11.03	13.32	16.40
378.0	11.18	13.29	19.76
382.0	10.38	12.36	14.94
384.0	10.02	12.48	18.00
386.0	10.44	12.35	14.94
390.0	12.16	14.21	19.76
392.0	11.22	13.20	19.76
394.0	11.47	14.16	28.70
396.0	12.33	15.76	21.69
398.0	12.09	15.14	19.76

APPENDIX XII

Markov chain analysis, results and statistical tests for core J1-04.

Embedded Markov chain sequence

Top
212321212323232132121213213213213213212132121321321321321213213213213213213
213213213213212132132132313131323131313231313132313131323131313231313231
313132121321212312121232313131321321321321321321321321321321321212121232121212
121213213213132132132132121212132121321321323213213213213213213213213213213213
321213213213213213213232132321321321323231313131321212121321321321321321321
321313132121321231321213213213232132313231321313231313213213213213213123
121212131232131321321323213213213213212132132132132132132121231321321321321
213213213213213213213213212121321321313213213213213131321321312313213213123
123132131321313213213213213213213213213213213213213131321313131313131313
131313132132121212132132121321313213212132132121321321321321321213131213213212
313213213212121232323131213213213213213213212321312132132132132132121121
321321323132321321321321321313213213213213213213213213212321321321321213213132
132132132121321231321321213212131313213213213213213213213213213213213213123
212313213213213213213213213213212132132132132123132132132132132132132131321
321321321321321321321232132132132321323213132132132123132132132132132132132
132132123132313213213213213213213213213213213213131313213213213132131313213
131321321321212121212132132132132123123132132132132121213213213213213131313
132132131321232132123132132321321232132132132132123131313213213213213213213
321231321321321321213232132121321321321321313231313213213213213213212312132
132132132131321321321213213213132132132132132131321321321321321321313131313
131313132132131323132123123132132121321323213212313213213212313131321321321321
321321321321321321321232132132132132132313213213213213131313213131313131313
131321313131313131321313213213213131313213213123131213132132121323123123132132
321321321321321321321321321321321321232313213213213213213213213213213213213213
321313213213213213213213212321232132132132132132323213213232132313232132132132121
213213213213212132121212123132132132132132132132131312323232132132132132121
321321313212132132132132132132132132132132132132132132132132132132132132132132132
312312313213213213213213213

First-order Markov chain analysis

Observed transition frequency matrix:

From \ To	1	2	3	Total
1	0	556	192	748
2	129	0	516	645
3	618	90	0	708
Total	747	646	708	2101

Observed transition probability matrix:

From \ To	1	2	3	Total
1	0.000	0.743	0.257	1.000
2	0.200	0.000	0.800	1.000
3	0.873	0.127	0.000	1.000
Total	1.073	0.870	1.057	1.000

Observed marginal probability vector:

1	0.356
2	0.307
3	0.337

Estimated transition frequency matrix (from Davis, 2002)

Step 1: Initial estimate of transition frequency matrix, with 1000 inserted in each diagonal position

From \ To	1	2	3	Total
1	1000	556	192	1748
2	129	1000	516	1645
3	618	90	1000	1708
Total	1747	1646	1708	5101

Step 2: Estimate of transition probabilities of diagonal elements

From \ To	1	2	3	Total
1	0.343			0.343
2		0.323		0.323
3			0.335	0.335
Total	0.343	0.323	0.335	1.000

Step 3: Second estimate of transition frequency matrix using new diagonal elements. Process is repeated until the estimated transitional frequencies along the diagonal do not change between iterations.

1.

From \ To	1	2	3	Total
1	559	556	192	1347
2	129	530	516	1175
3	618	90	572	1280
Total	1346	1176	1280	3802

2.

From \ To	1	2	3	Total
1	462	556	192	1210
2	129	379	516	1024
3	618	90	429	1137
Total	1209	1025	1137	3370

3.

From \ To	1	2	3	Total
1	414	556	192	1162
2	129	330	516	975
3	618	90	381	1089
Total	1161	976	1089	3226

4.

From \ To	1	2	3	Total
1	398	556	192	1146
2	129	315	516	960
3	618	90	364	1072
Total	1145	961	1072	3178

5.

From \ To	1	2	3	Total
1	393	556	192	1141
2	129	309	516	954
3	618	90	359	1067
Total	1140	955	1067	3162

6.

From \ To	1	2	3	Total
1	391	556	192	1139
2	129	308	516	953
3	618	90	357	1065
Total	1138	954	1065	3157

7.

From \ To	1	2	3	Total
1	390	556	192	1138
2	129	307	516	952
3	618	90	357	1065
Total	1137	953	1065	3155

8.

From \ To	1	2	3	Total
1	390	556	192	1138
2	129	307	516	952
3	618	90	356	1064
Total	1137	953	1064	3154

Expected marginal probability vector:

1	0.361
2	0.302
3	0.337

Expected probability matrix for all transitions:

From \ To	1	2	3	Total
1	0.130	0.109	0.122	0.361
2	0.109	0.091	0.102	0.302
3	0.122	0.102	0.114	0.338
Total	0.361	0.302	0.338	1.000

Expected transition frequency matrix:

From \ To	1	2	3	Total
1	411	344	384	1138
2	344	287	321	952
3	384	321	359	1064
Total	1138	952	1064	3154

The off-diagonal elements are the expected frequencies of transitions within the Lake J embedded sequence, assuming independence between successive states.

Statistical significance is tested with a χ^2 non-parametric test:

$$\chi^2 = \frac{(O-E)^2}{E}$$

where *O* and *E* are the observed and expected transition frequencies, respectively. The test has $v = (m-1)^2 - m$ degrees of freedom, where *m* is the number of states ($m = 3$, $v = 1$). The critical

value of χ^2 for 1 degree of freedom and an $\alpha = 0.01$ level of significance is 6.63. The test statistic of χ^2 is 788.6, therefore the successive laminae in the Lake J sediment are not independent.

Second-order Markov chain analysis

Observed transition frequency matrix:

From \ To	1	2	3	Total
1-2	80	0	475	555
1-3	139	53	0	192
2-1	0	108	21	129
2-3	479	37	0	516
3-1	0	447	171	618
3-2	49	0	41	90
Total	747	645	708	2100

Observed transition probability matrix:

From \ To	1	2	3	Total
1-2	0.144	0.000	0.856	1.000
1-3	0.724	0.276	0.000	1.000
2-1	0.000	0.837	0.163	1.000
2-3	0.928	0.072	0.000	1.000
3-1	0.000	0.723	0.277	1.000
3-2	0.544	0.000	0.456	1.000
Total	2.340	1.908	1.752	1.000

Observed marginal probability vector:

1-2	0.264
1-3	0.091
2-1	0.061
2-3	0.246
3-1	0.294
3-2	0.043

Estimated transition frequency matrix (from Davis, 2002)

Step 1: Initial estimate of transition frequency matrix, with 1000 inserted in each diagonal position

From \ To	1	2	3	Total
1-2	80	1000	475	1555
1-3	139	53	1000	1192
2-1	1000	108	21	1129
2-3	479	37	1000	1516
3-1	1000	447	171	1618
3-2	49	1000	41	1090
Total	2747	2645	2708	8100

Step 2: Estimate of transition probabilities of diagonal elements

From \ To	1	2	3	Total
1-2		0.192		0.192
1-3			0.147	0.147
2-1	0.139			0.139
2-3			0.187	0.187
3-1	0.200			0.200
3-2		0.135		0.135
Total	0.339	0.327	0.334	1.000

Step 3: Second estimate of transition frequency matrix using new diagonal elements. Process is repeated until the estimated transitional frequencies along the diagonal do not change between iterations.

1.

From \ To	1	2	3	Total
1-2	80	299	475	854
1-3	139	53	175	367
2-1	157	108	21	286
2-3	479	37	284	800
3-1	323	447	171	941
3-2	49	147	41	237
Total	1228	1090	1167	3485

2.

From \ To	1	2	3	Total
1-2	80	164	475	719
1-3	139	53	54	246
2-1	40	108	21	169
2-3	479	37	150	666
3-1	188	447	171	806
3-2	49	32	41	122
Total	975	841	912	2727

3.

From \ To	1	2	3	Total
1-2	80	138	475	693
1-3	139	53	36	228
2-1	24	108	21	153
2-3	479	37	125	641
3-1	161	447	171	779
3-2	49	16	41	106
Total	932	799	869	2600

4.

From \ To	1	2	3	Total
1-2	80	133	475	688
1-3	139	53	34	226
2-1	21	108	21	150
2-3	479	37	120	636
3-1	156	447	171	774
3-2	49	14	41	104
Total	924	792	861	2578

5.

From \ To	1	2	3	Total
1-2	80	132	475	687
1-3	139	53	33	225
2-1	21	108	21	150
2-3	479	37	119	635
3-1	155	447	171	773
3-2	49	14	41	104
Total	922	791	860	2574

6.

From \ To	1	2	3	Total
1-2	80	132	475	687
1-3	139	53	33	225
2-1	21	108	21	150
2-3	479	37	119	635
3-1	154	447	171	772
3-2	49	14	41	104
Total	921	791	860	2573

Expected marginal probability vector:

1-2	0.267
1-3	0.087
2-1	0.058
2-3	0.247
3-1	0.300
3-2	0.040

Expected probability matrix for all transitions:

From \ To	1-2	1-3	2-1	2-3	3-1	3-2	Total
1-2	0.071	0.023	0.016	0.066	0.080	0.011	0.267
1-3	0.023	0.008	0.005	0.022	0.026	0.004	0.087
2-1	0.016	0.005	0.003	0.014	0.017	0.002	0.058
2-3	0.066	0.022	0.014	0.061	0.074	0.010	0.247
3-1	0.080	0.026	0.017	0.074	0.090	0.012	0.300
3-2	0.011	0.004	0.002	0.010	0.012	0.002	0.040
Total	0.267	0.087	0.058	0.247	0.040	0.040	1.000

Expected transition frequency matrix:

From \ To	1-2	1-3	2-1	2-3	3-1	3-2	Total
1-2	183	60	**40**	**169**	206	28	687
1-3	60	20	13	56	**68**	**9**	225
2-1	**40**	**13**	9	37	45	6	150
2-3	169	56	37	157	**191**	**26**	635
3-1	**206**	**68**	45	191	232	31	772
3-2	28	9	**6**	**26**	31	4	104
Total	687	225	150	635	772	104	2573

The boldface elements are the expected frequencies of transitions within the Lake J embedded sequence, assuming independence between successive states.

Statistical significance is tested with a χ^2 non-parametric test:

$$\chi^2 = \frac{(O-E)^2}{E}$$

where *O* and *E* are the observed and expected transition frequencies, respectively. The test has $v = (m-1)^2 - m$ degrees of freedom, where *m* is the number of states ($m = 3$, $v = 1$). The critical value of χ^2 for 1 degree of freedom and an $\alpha = 0.01$ level of significance is 6.63. The test statistic of χ^2 is 2193.2, therefore the successive laminae in the Lake J sediment are not independent.